





This is to certify that the  
thesis entitled

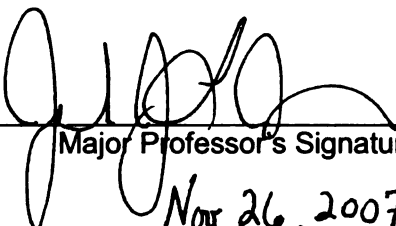
THE ROLE OF HIF1 $\alpha$  SIGNALING IN METAL-INDUCED  
TOXICITY

presented by

Ajith Vengellur

has been accepted towards fulfillment  
of the requirements for the

\_\_\_\_ Ph.D \_\_\_\_ degree in \_\_\_\_ GENETICS \_\_\_\_

\_\_\_\_\_  
  
Major Professor's Signature  
\_\_\_\_\_  
Nov 26, 2007

Date

**PLACE IN RETURN BOX** to remove this checkout from your record.  
**TO AVOID FINES** return on or before date due.  
**MAY BE RECALLED** with earlier due date if requested.

<b>DATE DUE</b>	<b>DATE DUE</b>	<b>DATE DUE</b>

**THE ROLE OF HIF1 $\alpha$  SIGNALING IN METAL-INDUCED TOXICITY**

**By**

**Ajith Vengellur**

**A DISSERTATION**

**Submitted to  
Michigan State University  
in partial fulfillment of the requirements  
for the degree of**

**DOCTOR OF PHILOSOPHY**

**GENETICS**

**2007**

## **ABSTRACT**

### **THE ROLE OF HIF1 $\alpha$ SIGNALING IN METAL-INDUCED TOXICITY**

**By**

**Ajith Vengellur**

Oxygen is critical for all aerobic organisms and they have well developed cell signaling systems in place to maintain homeostasis under oxygen deprivation. Hypoxia inducible factor 1 $\alpha$  (HIF1 $\alpha$ ) is the major transcription factor that mediates the cellular response to hypoxia in higher eukaryotes. HIF1 $\alpha$  protein undergoes proteolytic degradation under normoxia by the concerted activity of HIF prolyl hydroxylase (PHD) that modifies HIF1 $\alpha$  and the Von hippel-lindaeu (VHL) protein that recognizes the hydroxyproline and instigates HIF1 $\alpha$ 's 26s proteasome dependent proteolysis. PHDs require oxygen and 2-oxoglutarate as substrates and iron and ascorbate as cofactors. Divalent metals such as cobalt and nickel and iron chelator desferoxamine act as hypoxia mimic by inhibiting PHDs. Global gene expression profiling in Hep3B cells revealed that cobalt, desferoxamine and hypoxia modulate the expression a battery of common genes. We hypothesized that divalent metal ions may cause toxicity to cells by their ability to aberrantly activate HIF1 signaling under normoxia. Using wild type and HIF1 $\alpha$  null mouse embryonic fibroblasts, we showed that cobalt and hypoxia treatments induce similar HIF1 $\alpha$  dependent gene expression patterns (i.e. cobalt exposure includes 'signature hypoxia genes'). For example, cobalt exposure

leads to elevated levels of genes with characterized hypoxia response elements, including many glycolytic enzymes, glucose transporters and the pro-death factors, NIX and BNip3. BNIP3 expression was only observed in the wild type cells and its increase had functional significance, leading to caspase-independent cytotoxicity. Moreover, shRNA that specifically reduced the levels of BNIP3 within the cell were shown to be protective against cobalt-induced cell damage. In contrast, cadmium treatment does not stabilize HIF1 $\alpha$  protein and is more toxic to HIF1 $\alpha$  null cells compared to wild type cells, and cadmium exposure induces apoptotic cell death characterized by chromatin condensation and caspase-3 activity. Cadmium treatment also causes increased oxidative stress, and cadmium induced toxicity could be prevented by co-treatment with N-acetyl cysteine and melatonin. The increased susceptibility of HIF1 $\alpha$  -/- cells to cadmium-induced damage could be due, in part, to the fact that these null cells had elevated levels of ROS in the untreated condition and a compromised ROS scavenging system. Taken together, our results suggest that cobalt-induced cell damage is promoted through HIF1 $\alpha$  stabilization, and subsequent transcriptional activation of BNip3 gene and cadmium-induced cytotoxicity is due to ROS generation and the compromised nature of the ROS scavenging system in the HIF1 $\alpha$  -/- cells. This study suggests that HIF1 signaling is an important factor in the underlying pathology of injuries seen in workers exposed to metals, such as cobalt and cadmium, and understanding this connection is critical to our ability to cope with these injuries.

**DEDICATION**

**To My Teachers**

## **ACKNOWLEDGEMENTS**

From the beginning of my graduate school life I have been fortunate to have a great many number of people who taught me very valuable lessons both scientific and personal. First and foremost I want to acknowledge Dr. John LaPres, my mentor who guided me to the completion of my PhD. He has taught me to think logically and positively even when things are going tough. I will be always grateful to him for the freedom he bestowed upon me while planning and executing experiments. I would like to thank my guidance committee members Dr. David Arnosti, Dr. Robert Roth and Dr. Tim Zacharewski for their valuable comments and advice during the course of my work. It has certainly helped me to tackle scientific problems in creative ways. I would also like to thank Dr. John Wang and, Dr. Ron Patterson for scientific advice, Dr. Louis King of the MSU flow cytometry facility and members of the Genomic Technology Support Facility for technical support. Dr. Helmut Bertrand, Dr. Barb Sears and Jeannine Lee of the Genetics program made my life easy in dealing with academic requirements. I would like to thank Genetics program and MSU graduate school for financial support.

I would also like to thank present and past members of LaPres lab; Barbara Woods, Eric Jerks, KangAe Lee, Dorothy Tappenden, Yogesh Saini, Scott Lynn, Jeremy Lynd, Steve Proper and Andrea MacFadden as well as Zacharewski lab members; Darrell Boverhof, Ed Dere, Josh Kwekel, Lyle Burgoon, Cora Fong and Jeremy Burt who made my stay in East Lansing very pleasant and

memorable. I am grateful to Fraker lab members; Joe Frentzel and Jim Mann as well as Roth lab members; Dr. Jane Maddox, Dr. Umesh Hanumegowda, Dr. Bryan Copple and Dr. Jesus Olivero-Verbal for assisting me in running various assays. Finally I would like to thank my family and all my friends at MSU and beyond.

## TABLE OF CONTENTS

LIST OF TABLES.....	x
LIST OF FIGURES.....	xii
INTRODUCTION.....	1
I. Metals.....	1
I.A. History.....	1
I.B. Metal Ions in Biological Systems.....	2
I.C. Transition Metals.....	3
I.D. Cobalt.....	8
I.D.1. Occurrence.....	8
I.D.2. Exposure.....	9
I.D.3. Biological Functions.....	9
I.D.4. Toxicity.....	10
I.E. Cadmium.....	12
I.E.1. Occurrence.....	12
I.E.2. Exposure.....	12
I.E.3. Biological Function and Toxicity.....	13
I.F. Molecular Effects of Transition Metal Exposure.....	15
I.F.1. Effects on Metal Ion Transport and Metalloproteins.....	15
I.F.2. Metal-induced ROS and Biomolecule Damage.....	16
I.F.3. Metal-induced Changes in Gene Expression and Signaling Pathways.....	17
II. Hypoxia.....	20
II.A. Hypoxic Signaling.....	21
II.A.1. Physiological Changes to Hypoxia.....	22
II.A.2. Tissue Responses to Hypoxia.....	23
II.A.3. Cellular Responses to Hypoxia.....	25
II.B. Hypoxia Inducible Factors (HIFs).....	27
II.B.1. Regulation of Hypoxia Inducible Factors.....	28
II.B.1.a. Transcriptional and Translational Regulation of HIF.....	30
II.B.1.b. Post-translational Regulation of HIF.....	30
II.B.2. Regulation of Gene Expression by HIF1 $\alpha$ .....	35
II.B.2.a. Survival Response.....	36
II.B.2.b. Cell Death Response.....	37
II.C. Role of Hypoxic Signaling in Human Diseases.....	38
III. Reactive Oxygen Species.....	41
III.A. Source of Reactive Oxygen Species (ROS).....	42
III.A.1. Mitochondria.....	42
III.A.2. Transition Metals.....	45
III.A.3. Hypoxia and Hypoxia Reperfusion.....	47
III.A.4. Extra-mitochondrial Sources.....	47

III.B. Protection against ROS.....	48
IV. Hypothesis and Specific Aims.....	49
References.....	53
CHAPTER 1 – Gene Expression Profiling of Hypoxia Signaling in Human Hepatocellular Carcinoma Cells.....	72
Abstract.....	73
Introduction.....	74
Materials and Methods.....	75
Results.....	79
Discussion.....	93
Acknowledgements.....	101
References.....	102
CHAPTER 2 – Gene Expression Profiling of the Hypoxia Signaling Pathway in Hypoxia Inducible Factor 1 $\alpha$ Null Mouse Embryonic Fibroblasts.....	105
Abstract.....	106
Introduction.....	107
Materials and Methods.....	108
Results.....	116
Discussion.....	135
Acknowledgements.....	142
References.....	143
Appendix.....	147
CHAPTER 3 – The Role of Hypoxia Inducible Factor 1 $\alpha$ in Cobalt Chloride Induced Cell Death in Mouse Embryonic Fibroblasts.....	154
Abstract.....	155
Introduction.....	156
Materials and Methods.....	158
Results.....	163
Discussion.....	176
Acknowledgements.....	180
References.....	181
CHAPTER 4 – The Role of HIF1 $\alpha$ in Metal-Induced Toxicity in Mouse Embryonic Fibroblasts.....	185
Abstract.....	186
Introduction.....	188
Materials and Methods.....	188
Results.....	194
Discussion.....	211
Acknowledgements.....	217
References.....	218

SUMMARY AND DISCUSSION..... 221

## LIST OF TABLES

### INTRODUCTION

<u>Table 1: Metalloproteins in Organisms.....</u>	5
---	---

### CHAPTER 1

<u>Table 2: Primers used in qRT-PCR.....</u>	80
--	----

<u>Table 3: Top 20 Hypoxia Up and Down-regulated Probe Sets.....</u>	82
--	----

<u>Table 4: The 62 Probe Sets Representing the Overlap Between all Four Treatments.....</u>	85
---	----

<u>Table 5: Top 20 up and Down-regulated Genes Specific to Hypoxia (1% O<sub>2</sub>) Exposure.....</u>	91
---	----

<u>Table 6: Top 20 up and Down-regulated Genes Specific to CoCl<sub>2</sub> (100μM) Exposure.....</u>	92
---	----

<u>Table 7: Top 20 up and Down-regulated Genes Specific to Deferoxamine (100μM) Exposure.....</u>	94
---	----

<u>Table 8: Top 20 up and Down-regulated Genes Specific to NiCl<sub>2</sub> (100μM) Exposure.....</u>	95
---	----

### CHAPTER 2

<u>Table 9: Primers for Microarray Production and RT-PCR.....</u>	111
---	-----

<u>Table 10: Significantly influenced Genes in WT Cells Treated with Hypoxia or Cobalt.....</u>	122
---	-----

### CHAPTER 2 APPENDIX

<u>Table 11: Genes Significantly Influenced by Cobalt and Hypoxia in HIF1α -/- Cells.....</u>	148
---	-----

<u>Table 12: Genes Significantly Influenced by Cobalt and Hypoxia in Wild Type and HIF1α -/- Cells.....</u>	150
---	-----

<u>Table 13: Genes Significantly Influenced by Cobalt in Wild Type and HIF1α -/- Cells.....</u>	151
---	-----

<b><u>Table 14:</u> Comparison of Genes in Table 2 with those Presented in Jiang et. al Ref. 36.....</b>	<b>152</b>
--	------------

**CHAPTER 3**

<b><u>Table 15:</u> qRT-PCR Primers.....</b>	<b>161</b>
--	------------

**CHAPTER 4**

<b><u>Table 16:</u> qRT-PCR Primers.....</b>	<b>191</b>
--	------------

<b><u>Table 17:</u> shRNA Sequences.....</b>	<b>191</b>
--	------------

## LIST OF FIGURES

### INTRODUCTION

<b>Figure 1: Fenton Reaction.....</b>	<b>7</b>
<b>Figure 2: Graphical representation of HIF1<math>\alpha</math> Protein.....</b>	<b>29</b>
<b>Figure 3: HIF1<math>\alpha</math> and Hypoxia Signaling.....</b>	<b>33</b>
<b>Figure 4: Sites of ROS Production in Mitochondria.....</b>	<b>44</b>

### CHAPTER 1

<b>Figure 5: Venn Diagrams Representing Genes whose Expression was Significantly Influenced by Treatment.....</b>	<b>83</b>
<b>Figure 6: qRT-PCR Verification of 12 Genes.....</b>	<b>88</b>
<b>Figure 7: Analytical Comparison of qRT-PCR and Microarray Data.....</b>	<b>89</b>

### CHAPTER 2

<b>Figure 8: Experimental Design of Loop.....</b>	<b>112</b>
<b>Figure 9: HIF1<math>\alpha</math> Western Blot.....</b>	<b>117</b>
<b>Figure 10: Hierarchical Cluster Diagram of Entire Data Set .....</b>	<b>119</b>
<b>Figure 11: Analysis of CoCl<sub>2</sub> and Hypoxia Treatments in Wild Type Cells.....</b>	<b>121</b>
<b>Figure 12: Venn Diagrams of Various Combinations of Cell Types and Treatments.....</b>	<b>126</b>
<b>Figure 13: Glycolytic Enzyme Cluster.....</b>	<b>129</b>
<b>Figure 14: Comparison of Microarray and rRT-PCR Results.....</b>	<b>131</b>
<b>Figure 15: Time Course Analysis of the PHDs by rRT-PCR.....</b>	<b>134</b>

<b><u>Figure 16:</u> Analysis of the Basal Levels of GST-<math>\mu</math>, SOD1, SOD2 and Catalase by rRT-PCR.....</b>	<b>136</b>
<b><u>Figure 17:</u> Transient Transfection of Hep3B Cells.....</b>	<b>137</b>
<b>CHAPTER 3</b>	
<b><u>Figure 18:</u> Growth Curve.....</b>	<b>164</b>
<b><u>Figure 19:</u> Dose Response and Time Course Analysis of CoCl<sub>2</sub>-induced Cytotoxicity.....</b>	<b>165</b>
<b><u>Figure 20:</u> qRT-PCR Data for BNip3 and BNip3L .....</b>	<b>167</b>
<b><u>Figure 21:</u> qRT-PCR Data for BNip3 Expression under CoCl<sub>2</sub> and Hypoxia Time Course in Wild Type Cells.....</b>	<b>169</b>
<b><u>Figure 22:</u> BNIP3 and BNIP3L (NIX) Western Blot.....</b>	<b>171</b>
<b><u>Figure 23:</u> Cell Morphology.....</b>	<b>173</b>
<b><u>Figure 24:</u> Caspase-3 Assay.....</b>	<b>175</b>
<b>CHAPTER 4</b>	
<b><u>Figure 25:</u> Cytotoxicity of CoCl<sub>2</sub> and CdCl<sub>2</sub> to MEFs.....</b>	<b>195</b>
<b><u>Figure 26:</u> Characterization of Cadmium-induced Cell Death.....</b>	<b>197</b>
<b><u>Figure 27:</u> Hypoxia Signaling and Cytotoxicity to CoCl<sub>2</sub> and CdCl<sub>2</sub>.....</b>	<b>198</b>
<b><u>Figure 28:</u> Oxidative Stress in CoCl<sub>2</sub> and CdCl<sub>2</sub> mediated Cytotoxicity.....</b>	<b>203</b>
<b><u>Figure 29:</u> Expression and Activity of Superoxide Dismutases.....</b>	<b>209</b>
<b><u>Figure 30:</u> Cellular Glutathione Levels under CoCl<sub>2</sub> and CdCl<sub>2</sub> Treatments.....</b>	<b>212</b>

(Images in this dissertation are presented in color)

## INTRODUCTION

### I. Metals

#### I.A. History

The earliest form of life is thought to have evolved on the face of earth approximately four billion years ago from a pre-biotic soup, rich in various chemical nutrients (1). Current theory suggests that RNA molecules were produced in the early days by random chemical reactions. These RNA's later acquired the ability to perform catalysis and self replication and were possibly enclosed in micelles leading to the origin of the early life form (2). It is also thought that the catalytic activity of RNA was dependent on the presence of divalent cations (3). As time passed, organisms evolved into more complex life forms through multiple cycles of mutation and natural selection. Even as DNA rose in prominence and the major role of catalysts were taken over by proteins, the role of divalent cations in facilitating various chemical reactions was conserved (4).

Meanwhile, the process of evolution and natural selection lead to the creation of advanced life forms like vertebrates and subsequently mammals such as *Homo sapiens* that require certain metals as essential nutrients. It was not until the late Stone Age, approximately 8000 B.C. that the use of metal or rather metal rich mineral rocks were first introduced as tools for hunting (5). Metals, such as gold and silver, which occur more or less in the pure form, were the first to be used along with rocks rich in copper. The Bronze Age, which occurred around 3500

B.C., began a new age with the production of tools for farming and hunting thus ushering in the new era of metallurgy.

It took a further two millennia for the advent of the Iron Age when iron tools and steel production began in earnest. By this time people began combining different metals and minerals to produce alloys with distinct properties. The discovery of new metals and alloys heralded an era where human civilization was pushed to new heights by the introduction of advanced tools that took advantage of the strength and malleability of these new materials (6). Many new metals, such as cobalt, cadmium, uranium were discovered after the advent of the new field of chemistry and advances in metallurgy. By this time the exploitation of natural resources by mining and further refining had created enormous global industries, fostering advances in many fields such as aerospace and atomic energy. This also resulted in increased exposure of worker, as well as, the general population, to various potentially toxic metals and minerals.

### **I.B. Metal Ions in Biological systems**

Metals ions are associated with almost one third of all enzymes and are essential for their activity (7). A metal's ability to rapidly transfer electrons facilitates enzyme catalyzed reaction and without the metal a metalloenzyme's activity is drastically reduced. Since metals ions are generally positively charged and act as electrophiles, they can operate as a buffer system facilitating reduction/oxidation (redox) reactions (8, 9). In addition, metals are essential for

maintaining pH in cells via their role in ion transport, and play equally critical roles in cellular energy production via their role in the electron transport chain (ETC) (10). Most organisms employ coupled oxidoreductase systems for the production of energy, a process known as oxidative phosphorylation. In higher life forms, the ETC employs a variety of metalloproteins to transfer electrons obtained through oxidation of carbons to oxygen, producing ATP and water. The metalloproteins of the ETC utilize the energy produced as the electrons move through the ETC to transport  $H^+$  ions across the inner-membrane of the mitochondria. This process is coupled to energy production by ATP synthase (also known as Complex V) that utilizes the membrane potential to drive the production of ATP. Therefore, metals are essential to energy production and thus life of a cell.

Nevertheless, not all metal ions are utilized by living things. Many of the heavy metals (i.e. metals that are heavier than the rare earth metals), such as mercury and arsenic are not employed by cells and are generally toxic to most life forms (11). Even metals that play an essential role in supporting life the levels are maintained within a strict limit. Any change in the homeostasis of these metals is detrimental to the cells. They can have adverse reactions with cellular components such as proteins, lipids and nucleic acids (9).

### **I.C. Transition Metals**

In chemistry, a metal (Greek: Metallon) is an element that readily forms ions (cations). The metals are one of the three groups of elements, along with the metalloids and nonmetals, each distinguished by their ionization and bonding properties. The transition metals are distinguished by the number and distribution of electrons in their outer two shells and include metals such as iron, zinc, manganese, molybdenum, nickel, cobalt, and cadmium. The properties inherent in the distribution of these electrons, accord these metals certain features, such as high tensile strength and different oxidation states.

Metals, such as iron, calcium, and zinc, play critical roles in major biological processes at molecular level (12). Among all these metals, iron has a central metabolic role as it facilitates many critical cellular processes, such as oxygen transport (e.g. hemoglobin and myoglobin) and energy production (e.g. ETC). Evolution of complex life forms, such as vertebrates, was made possible by the ability to deliver oxygen to distant tissues, an iron dependent process (13). Moreover, the evolution of the electron transport chain, a system that requires iron and copper, increased the efficiency of energy production. Zinc, another essential nutrient, plays a major role as a prosthetic group for various enzymes and associates with many transcriptional factors (Table 1). Calcium plays a major role in various intercellular signaling processes and along with magnesium and sodium, plays a central role in regulating cellular pH levels and neural signaling (14). Because of the major role played by these metals, they are

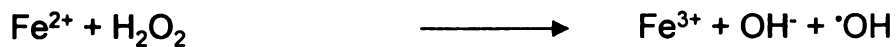
<b>Table 1: Metalloproteins in Organisms</b>		
<b>Metal</b>	<b>Class</b>	<b>Protein</b>
Iron - Heme	Oxygen Transport	Hemoglobin
	Cytochromes	Cytochrome C
	Cytochrome Peroxidases	Horseradish peroxidase
	Cytochrome P-450	Cytochrome P-450
	Oxygenases	Heme Oxygenase
	Oxido-Reductases	Cytochrome c oxidase
Iron – Non-Heme	Iron-Sulfur Clusters	Rubredoxin
	Mononuclear Iron Proteins	Fe-SOD
	Dinuclear Iron Proteins	Ribonucleotide Reductase
	Iron Storage	Ferritin
	Iron Transport	Transferrin
Nickel		Urease
		Nickel-Iron Hydrogenases
		Peptide Deformylase
Selenium	Peroxidase	Glutathione peroxidase
Manganese		Mn-Superoxide Dismutase
		Arginase
		Aminopeptidase P
Cobalt		Glutamate Mutase
		Methylmalonyl CoA Mutase
		Methionine Synthase
Vanadium		Vanadium Haloperoxidase
Molybdenum / Tungsten		Nitrogenase
		Aldehyde Oxidoreductase
		CO Dehydrogenase
Copper	Type1 Copper Proteins	Plastocyanin
	Type-2 Copper Enzymes	Cu-Zn Superoxide Dismutase
	Type-3 Copper Enzymes	Hemocyanin
	Binuclear Copper	Binuclear Copper A
	Multicopper enzymes	Ascorbate oxidase
	Copper storage	Copper Metallothionein
Zinc	Oxidoreductases	
	Transferases	Protein prenyltransferase
	Hydrolases: Ester bonds	5'-Nucleotidase
	Hydrolases: Peptide bonds	Matrix metalloproteinase
	Other Hydrolases	GTP Cyclohydrolase 1
	Lyases	Carbonic Anhydrase
	Zinc-Fingers	RING Domain proteins
	Zinc Storage	Metallothioneins
	Other Zinc proteins	Insulin
Calcium	EF-H and Ca <sup>2+</sup> binding	Calmodulin
	EGF-Domains	
	GLA Domains	
	C2-Like Domains	
Magnesium	Chlorophyll	Mg-protoporphyrin IX chelatase
	ATPases	Mg(2+) transport ATPase,
	Transporters	Magnesium transporter protein 1

considered as essential nutrients, however; under various conditions, these metals can also become toxic and aberrantly influence cellular function.

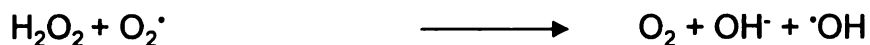
The reactive nature of these metal ions is essential for their biological activity and is also responsible for cellular damage following exposure to excess metal levels. These metals tend to react with acids and other functional groups, forming various adducts, and tend to undergo oxidation reactions producing various reactive species (15). Several metals, such as iron and cobalt, are capable of undergoing Fenton-like reactions (Figure 1). Fenton-like reactions lead to the production of reactive oxygen species (ROS) when the metal reacts with hydrogen peroxide, producing extremely reactive hydroxyl radicals. These hydroxyl radicals can begin a cascade of chemical reactions producing other types of ROS within the cell, causing cellular damage (16).

Belonging to the same class of periodic table, transition metals have similar chemical properties and valence states. Because of this, it is important for the cells to regulate the levels of various metals so as to prevent them from inhibiting each other's chemical function. An increase in exposure to metals such as cobalt and nickel which are essential for the function of many enzymes and proteins but are not considered essential nutrient, may lead to the disruption of metal ion homeostasis (17). Many proteins that contain co-coordinately bonded metal ions such as non-heme iron and zinc at their catalytic site are prone to replacement by nickel and cobalt ions because of their similarity in charge and

### **Fenton Reaction**



### **Haber-Weiss Reaction**



### **Fenton-like Reaction of Metals**

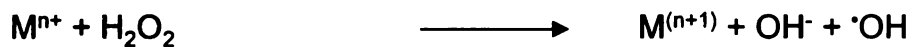


### **Figure 1. Fenton Reaction**

Iron, Cobalt, Nickel, Copper and Manganese can be oxidized by  $\text{H}_2\text{O}_2$  producing hydroxyl anion and hydroxyl radicals. The oxidized metal ions gets reduced by superoxide anion. This can lead to a continuous cycle of ROS production.

size (18). Moreover, metals such as cadmium and arsenic can bind to proteins, forming adducts that can disrupt normal cellular processes (19).

## **I.D. Cobalt**

### **I.D.1.Occurrence**

Cobalt is a magnetic element with ferrous-like properties. It occurs as arsenides, oxides and sulfides in nature and its introduction into manufactured goods began in Egypt and Persia in second century B.C. as a dye for pottery. Later, Leonardo Da Vinci used cobalt for its bright color in oil paints. The actual element was isolated by the Swedish chemist, George Brandt in the early 18<sup>th</sup> century and T.O. Bergman identified it as an element in 1780 (20). The first cobalt-containing permanent magnetic alloy, called alnico, was developed in 1930. Cobalt is usually not seen in the free form and exists as ores with other metals such as copper, silver and nickel. The main cobalt ores are cobaltite and glaucodot ((Co,Fe)AsS), erythrite ((Co<sub>3</sub>(AsO<sub>4</sub>)<sub>2</sub>·8H<sub>2</sub>O)), and skutterudite ((Co,Ni,Fe)As<sub>3</sub>) and the main producers are Democratic Republic of Congo, China, and Russia. The radioactive form of the element, <sup>60</sup>Co, was used to irradiate food stuffs and in radiotherapy. Industrial application of cobalt, in high-speed drills and cutting tools as a hard metal in combination with tungsten was started in 20<sup>th</sup> century. Today it is primarily used in the production of superalloys, corrosion resistant alloys, high speed steels, magnets, wear resistant coatings and various metallurgical applications.

### **I.D.2. Exposure**

Cobaltous minerals are primarily found mixed with silver and other minerals of copper, iron, lead, nickel. Cobalt metal is usually produced during the refining of copper or nickel (20). Metal refinery workers and those involved in the production of certain alloys, such as tungsten carbide, are at the greatest risk for cobalt-induced toxicity, however, the general public has become increasingly at risk of cobalt exposure by various mechanisms.

Cobalt is present in air as a result of natural processes, such as erosion, volcanic eruptions, and by various human actions, such as the burning of fossil fuels, sewage sludge, and phosphate fertilizer (21). Being a rare trace element, cobalt content of soils, especially the one derived from sandstone, limestone etc., are inadequate to support basic biological demand. Diet is the main source of exposure for the general population and the average daily intake ranges from 5-45  $\mu\text{g}$ . People with high dietary intake of sea foods, cocoa, bran and molasses ingest more cobalt, as these foods have a higher natural content of this metal. In addition, certain organ meats, especially liver, and fat tissues have high cobalt content (22). Generally, the concentration of cobalt in the drinking water is low (less than  $5\mu\text{g/L}$ ) (20). Cigarette smokers are at an increased risk for cobalt-induced injury, primarily because tobacco smoke contains 0.3-2.3mg Co/kg dry weight (23).

### **I.D.3. Biological Functions**

Cobalt is essential for the production of vitamin B<sub>12</sub> (also known as cobalamin), which is required for the synthesis of methionine and the metabolism of purines and folates (24). The deficiency of cobalt leads to pernicious anemia. Humans cannot synthesize vitamin B<sub>12</sub>; “they” must obtain it through diet. Cobalt is also associated with the regulation of a number of cofactors such as acetyl coenzyme A and enzymes such as lipoprotein lipase (25). Cobalt was used in mid 20th century for the treatment of anemia because of its ability to induce the production of erythropoietin, the red blood cell stimulating factor (26, 27).

#### **I.D.4. Toxicity**

Most cobalt toxicity occurs in an occupational setting, as exposure to the general public is usually rare. Even as cobalt was being used to treat anemic patients, its excessive uptake was reported to cause thyroid failure and goiter (28). In European and Canadian breweries cobalt was used to reduce the effect of soap residues on foam formation in beer production. Brewery workers who drank cases of beers showed symptoms of pericardial effusion, elevated hemoglobin levels and congestive heart failure (29). Post-mortem histology showed myocardial fiber degeneration, increased vacuolation and interstitial edema and extensive damage to mitochondria. In Andean mining communities in South America, polycythemia was seen in miners with excessive levels of serum cobalt (30).

Cobalt exposure leads to a variety of effects. Cobalt is a known allergen and causes allergic dermatitis (31). Acute exposure to high levels of cobalt through inhalation in humans results in respiratory problems such as decrease in ventilatory function, congestion, edema and hemorrhage of the lung. Chronic exposure to cobalt through inhalation leads to respiratory irritation, wheezing, asthma, pneumonia and fibrosis (20). During the World War II, severe pulmonary problems were reported among workers exposed to hard metal particles. Exposure to cobalt dust among diamond polishing workers was reported to cause pneumoconiosis, which was mostly the result of exposure to both tungsten and cobalt. This disease is characterized by intense alveolitis and in the end stage, pulmonary fibrosis. Pneumoconiosis rarely occurs because of cobalt alone and usually is a combined effect with other metals such as tungsten (25).

Other effects of cobalt exposure include cardiovascular damage such as cardiac myopathy, as well as congestion of the liver, kidneys and conjunctiva, and immunological effects. In humans, gastrointestinal effects such as vomiting, diarrhea, liver injury and allergic dermatitis were also reported in case of oral exposure to cobalt (32). There have been no reports of reproductive toxicity of cobalt in either oral or inhalational exposure (33). Although cobalt has been shown to be weakly mutagenic in bacterial systems, conclusive evidence of cobalt genotoxicity in mammals has not been reported (34).

## **I.E. Cadmium**

### **I.E.1. Occurrence**

Pure cadmium is a silvery white, lustrous, soft and ductile metal, which is rare in nature and occurs mostly as inorganic compounds, as organo-cadmium compounds are extremely unstable (35). It is generally seen with other metal ores, most often zinc sulfide, which is called greenockite or cadmium blende (36). Cadmium occurs in small quantities in air, water and soil and is produced as a by-product of the refinement of other metals, as cadmium concentration is not high enough in minerals for a dedicated process. Although known for many years, the industrial use of cadmium began in 1930s and has steadily risen with approximately 20,000 tons produced annually by the end of twentieth century. The general consumption of cadmium has increased as the use of Ni-Cd batteries in electronics has risen. Although cadmium had been used in pigments, PVC stabilizers and, electroplating, consumption for these purposes is decreasing rapidly (37).

### **I.E.2. Exposure**

Cadmium is released into the biosphere by both natural and anthropogenic activities, including volcanoes and weathering of rock. Each plays a major role in the global cadmium cycle but those processes do not result in elevated environmental levels. The main sources of emission into the atmosphere are volcanoes, sea spray, and forest fires (38). The major source of cadmium by human activity results from the mining of cadmium-containing minerals such as

zinc ores, coal and lime. Significant environmental release of cadmium also occurs in countries where extensive waste incineration is performed (38).

Land filling of discarded products and, contaminated waste are major sources of cadmium in the soil. Recently, the use of treated sewage sludge as fertilizer for crops has resulted in an increase in soil contamination (39). These activities are leading to the accumulation of cadmium in the top soil and ground water. Apart from atmospheric deposition, domestic waste water, non-ferrous metal smelting and refining and manufacturing of chemicals and metals have contributed to the localized environmental release of cadmium.

### **I.E.3. Biological Function and Toxicity**

Cadmium is not known to have any endogenous functional role in the animal system, however; in plants it has been shown that sub-toxic levels of cadmium can block the viral invasion of nutrient transport system (40). Cadmium and its compounds are relatively water soluble and mobile in soil, making it more bioavailable and increasing its bioaccumulation in plants, microbes and marine organisms.

In animals, cadmium concentrates in the internal organs such as kidney and liver, and in the body cadmium levels usually increase with age, as only a small proportion of the body burden of cadmium is excreted through urine and feces (41). The acceptable daily intake of cadmium should not exceed 0.4-0.5 mg/week according to WHO guidelines (42). Chronic cadmium exposure leads

to a variety of toxic effects including kidney damage and lung emphysema, in a variety of organisms including birds and mammals (43). Cadmium exposure can also lead to bone loss due to its ability to impair the metabolism of calcium and vitamin D.

In humans where cadmium exposure can occur through food, water and cigarette smoke, the renal accumulation of cadmium results in kidney dysfunction. This renal toxicity leads to impaired re-absorption of proteins, glucose and amino acids (44). In Japan, a syndrome called itai-itai has been associated with chronic cadmium exposure in humans. The affected individuals, mostly elderly women, experience softening of bones (osteomalacia), lumbar pain, myalgia and spontaneous fractures with skeletal deformation (45). Occupational cadmium exposure can lead to a variety of lung changes, including chronic obstructive airway disease and cancer (43). In addition, workers exposed to high cadmium levels are at an increased risk of prostate cancer (46). Interestingly, zinc is antagonistic to cadmium-induced toxicity and has been shown to reduce the toxic effects of cadmium exposure, such as damage to ovaries and testes, hypertension etc. (47).

Although there has been no report of teratogenic effects in the human population exposed to cadmium, effects are reported in rats administered with 1.25mg/kg cadmium (48). This may be due to the fact that cadmium inhibits the placental transport of zinc. Cadmium has also been shown to produce sarcomas at the

sites of injection and interstitial tumors in the testes of rats (49). Even though inhalation of cadmium chloride has resulted in primary lung cancer in rats (50) gastrointestinal exposure did not produce any tumors (51).

### **I.F. Molecular Effects of Transition Metal Exposure**

The essential role that various metals play in sustaining life processes at the cellular level means that maintenance of intracellular concentrations of these metals is vital. Exposure to toxic doses of essential metals or other non-essential metals can result in perturbations to homeostasis of these elements and lead to cellular dysfunction. The changes at the molecular level upon metal exposure can be grouped into three categories – inhibition of function or transport of nutrient metal ions within the cell, generation of reactive oxygen species and resulting damage to biomolecules, and changes in gene expression.

#### **I.F.1. Effects on metal ion transport and metalloproteins**

Divalent non-ferrous metal insult can disturb iron homeostasis by disrupting the transport of iron, as well as inhibiting iron metalloproteins and enzymes. For example, increased cadmium levels in the diet can decrease the uptake of iron due to competitive binding of cadmium to ferritin, an iron storage protein (52). Similarly cadmium can interfere with calcium metabolism, resulting in hypercalciurea and osteoporosis (53). Metals such as lead and mercury, can also interfere with neurotransmitter signaling by disturbing the calcium and sodium transporters in the plasma membrane of neurons and muscle cells (54).

Many metalloenzymes, such as exopeptidases, arginase, keto acid carboxylases, and phosphatases do not show absolute metal specificity and may be activated by many different metals (12). Divalent transition metals, such as cobalt, nickel and cadmium, activate mammalian alkaline phosphatase, a metalloenzyme that has magnesium at its catalytic center (55). In contrast, increased levels of cellular zinc can inhibit cytochrome c oxidase, an important component of the electron transport chain that utilizes copper for enzymatic function, impairing cellular energy production (56). Mercury and copper ions also inhibit rat liver arginase (57).

#### **I.F.2. Metal-induced ROS and biomolecule damage**

Other major cellular endpoints of metal insult are the production of various reactive radicals and depletion of the cellular antioxidant pool. Most redox active transition metals produce ROS through Fenton-like reactions. These reactions produce highly reactive hydrogen peroxide and hydroxyl radicals that in turn react with the surrounding proteins, nucleic acids and lipids, resulting in their oxidation (21). The oxidized products will be non-functional and are subsequently degraded. High levels of ROS production cause massive cellular damage, ultimately leading to cell death (see section III. p.41).

Metals such as arsenic, mercury and cadmium, have electron-sharing affinities that result in the formation of covalent attachments, especially with sulfhydryl groups of proteins (58). For example, arsenic can inhibit the pyruvate

dehydrogenase complex by covalently linking to the active sulfur residue of the lipoic acid covalently attached to E2 subunit, rendering the complex inactive (59). Cadmium is known to bind covalently the sulfhydryl group of glutathione, thus depleting the cellular antioxidant reserves (60). Mercury interacts with many proteins, including albumins, forming S-Hg-S bonds (61). Lead also forms mercaptides with protein SH groups and less stable complexes with other aminoacid side chains (62).

### **I.F.3. Metal-induced changes in gene expression and signaling pathways**

As described earlier, all living organisms utilize the diverse substitution and redox properties of transition metals in a variety of regulatory functions. Metals and metalloproteins also influence the expression of a wide range of genes (63). These genes encode proteins meant for metal detoxification, uptake, storage, transport and homeostasis, as well as various other metabolic pathways. Metal-induced changes in gene expression may be triggered by processes involving a specific metal ion acting as a sensor, changes in the cellular redox status or oxidative stress, and aberrant activity and regulation of various metalloproteins and their downstream effectors (63). Many times one or more of these factors together cause changes in gene expression.

A change in intracellular or extracellular metal concentrations may activate a metal ion sensor, causing downstream changes in expression of genes involved in an adaptive response. For example, heme containing proteins play an

important role in sensing the changes in iron concentration, influencing the expression of genes involved in iron and heme homeostasis (64). Similarly an increase in the level of copper ions causes a copper ion binding regulatory protein, ACE1, to bind to the 5' end of the promoter of metallothionein gene and increase its expression in the yeast, *Candida glabrata* (65). Metallothioneins in turn act as a detoxifier by transporting the excess copper ions out of the cell. In most cases such adaptive responses are not harmful for the cells.

By regulating the activity of various redox sensitive transcription factors, metals can cause gene expression changes and activate various signaling pathways. NF- $\kappa$ B is an important redox sensitive transcription factor that is affected by metal exposure and resulting oxidative stress. Critical cysteine residues in the DNA binding region of NF- $\kappa$ B protein that binds zinc are sensitive to ROS. Alternatively, metals such as cadmium and copper interfere with the DNA binding activity of NF- $\kappa$ B (66, 67). Nickel and cobalt ions, however, have a positive effect on the DNA binding ability of NF- $\kappa$ B (68). Another important transcription factor, AP1, is induced by certain metals. For example, arsenic, vanadium, chromium, nickel, cadmium, lead, cobalt and iron are known to activate AP-1 in a variety of cells. It is thought that AP-1 activation upon metal exposure is mediated by the activity of several protein kinase signaling pathways that are activated by the oxidative stress (69). p53 is another critical protein that is affected by metal-induced oxidative stress. Inorganic arsenic, chromium (VI) and nickel have been shown to induce p53 expression (69).

Metal transcription factor 1 (MTF1) is a protein whose activity is induced by zinc ions and oxidative stress. MTF1 regulates the expression of detoxifying genes such as metallothioneins. Exposure to zinc, cobalt and various other metals result in the expression of metallothioneins, which are major proteins involved in metal detoxification (70). Cadmium also increases metallothionein expression but the mechanism is thought to be MTF1-independent. In case of all metals, metallothioneins act as transporters and storage proteins to limit the free metal concentration within the cell. For example, cadmium is bound by metallothionein inside the body and transported to the kidney for elimination (71). Most metal exposures also lead to changes in the expression of a large number of genes through unknown mechanisms. Cadmium exposure causes the expression of heat shock chaperone proteins, DNA repair enzymes, p53, c-fos, etc. (72-76).

Since the early 1950s, ferrous-like metals such as cobalt, have been known to induce the expression of erythropoietin and was used to treat anemia (77). Later, cobalt and nickel were shown to induce a wide variety of genes involved in angiogenesis, such as vascular endothelial factor (VEGF), and glycolysis, such as hexokinase and pyruvate kinase (78, 79). The ability of these metals to alter this wide expression pattern changes lies with their ability to influence the activity of the transcription factor, hypoxia inducible factor 1 $\alpha$  (HIF1 $\alpha$ ).

Cobalt and nickel are known to stabilize HIF1 $\alpha$ , causing the expression of a large number of genes in the hypoxia signaling pathway. HIF1 $\alpha$  protein function is tightly regulated by a family of non-heme iron-containing dioxygenases called, prolyl hydroxylase domain containing enzymes (PHDs), which hydroxylate and target HIF1 $\alpha$  for proteosomal degradation under normoxia (see section II.B.1.b p.30). Cobalt and nickel interfere with the ability of PHDs to hydroxylate HIFs and thus cause aberrant stabilization and activity of the transcription factor. This ability of metals such as cobalt and nickel, to influence PHD activity has three possible explanations. First, cobalt and nickel might replace the non-covalently held iron atom from the PHDs rendering them catalytically inactive. Second, metal-induced ROS production might affect the redox status of iron that is critical for hydroxylase activity. Finally, it has also been reported that cobalt and nickel can chelate ascorbic acid, an essential cofactor for PHD activity, in the cell (80). It is probable that each of these plays a role in the regulation of PHDs and ultimately influences HIF1 $\alpha$  signaling. For these reason, the ferrous-like metals are considered “hypoxia mimics”.

## **II. Hypoxia**

When life started approximately 4 billion years ago, the world is thought to have had a reducing atmosphere. The passage of time led to the advent of photosynthetic organisms that utilized water and carbon dioxide to produce energy. The principal by-product of this process was oxygen, which began to accumulate in the atmosphere. The reducing atmosphere gradually changed into

an oxidizing one and in modern times, a majority of life forms use aerobic pathways as a means to produce the energy necessary to sustain life (81). The process of oxidative phosphorylation, the source of greater than 95% of the adenosine triphosphate (ATP) produced in a cell, requires molecular oxygen as a final electron acceptor. Without this final step, ATP generation is inhibited and a cell's survival potential is compromised. The ability to sense and cope with changes in available oxygen, therefore, is critical for life (81). Most of the higher organisms have evolved elaborate sensing mechanism to cope with decreases in available oxygen, a condition known as hypoxia.

## **II.A. Hypoxic Signaling**

Hypoxia compromises a cell's ability to produce ATP through oxidative phosphorylation and perform enzymatic reactions that require oxygen, such as hydroxylations. All aerobic life forms, therefore, have evolved unique pathways to respond to changes in oxygen partial pressure (82). The molecular components sense the oxygen tension, transduce the signal to various effectors for facilitating adaptive responses, and promote the physiological and molecular processes associated with these components. The various processes in the hypoxic signaling pathway can be loosely classified, into three groups: physiological changes that occur at an organismal level, coordinated changes that happen at the tissue level, and molecular changes that occur at cellular level.

### **II.A.1. Physiological Changes to Hypoxia**

All multicellular organisms have elaborate systems in place for the delivery of nutrients to metabolically active tissues and cells. In the presence of hypoxia, these systems respond to adapt to maintain balance. In higher organisms, hypoxia leads to a rapid modulation of pulmonary ventilation, perfusion, and blood circulation to optimize the supply of oxygen to tissues. This process is directed by carotid bodies (specialized chemoreceptor cells in the arterial system), neuroepithelial bodies in the airway, and vascular smooth muscle cells (83).

In the presence of decreased oxygen tension, peripheral blood vessels dilate to allow greater blood volume and thus maximum oxygen supply, to be delivered to the peripheral tissues. Hypoxic-mediated vasodilatation in oxygen-deprived tissues is a fast process, mediated by potassium ATP channels of vascular smooth muscle cells. These channels open upon a decrease in ATP levels, a condition that occurs under hypoxic conditions (84). It is also thought that  $\text{Ca}^{2+}$  channels are involved in this process. Hypoxic vasodilation is highly activated in the blood vessels of tissues with a high metabolic load, such as the heart and brain (85). Conversely, pulmonary vasculature constricts to limit the amount of blood being delivered to poorly ventilated regions, matching ventilation to perfusion (86). The hypoxia-induced pulmonary vasoconstriction is also a fast response, mediated by the rapid constriction of vascular smooth muscle cells and is initiated by the depolarization resulting from the inhibition of several  $\text{K}^+$

channels (87). The depolarization activates voltage gated  $\text{Ca}^{2+}$  channels leading to increase in cytosolic  $\text{Ca}^{2+}$  and causes myocyte constriction (85).

On exposure to low  $\text{pO}_2$ , airway neuroepithelial bodies and carotid bodies create cardiorespiratory adjustments through chemosensory fibers (88). Carotid bodies that reside in the carotid arteries are highly vascularized organs that contain type1 glomus cells. These glomus cells contain neurotransmitters, catecholamines and acetylcholine and are in synaptic contact with efferent sensory fibers of the carotid sinus nerve. Membrane  $\text{K}^+$  channels in these cells are inhibited by low  $\text{pO}_2$ , leading to membrane depolarization and  $\text{Ca}^{2+}$  influx through voltage gated  $\text{Ca}^{2+}$  channels (82). The resulting increased calcium concentration leads to neurotransmitter release and activation of sensory fibers.

Neuroepithelial bodies are located in airway bifurcations and comprise neuron derived cells that synapse with branches of afferent and efferent neurons and transmit signals to brain respiratory centers through the release of neurotransmitters such as serotonin (89). The activation process is similar to one that is seen in carotid bodies but the individual channel proteins may vary. The actual oxygen sensor in both carotid bodies and neuroepithelial bodies are thought to be a heme-containing protein, associated closely with oxygen sensitive potassium channel.

## **II.A.2. Tissue responses to Hypoxia**

An important aspect of tissue hypoxia is the increase in angiogenesis. This is mediated by the activity of various pro-angiogenic factors, most importantly vascular endothelial growth factor (VEGF), which mediates the growth of blood vessels to hypoxic regions (90). VEGF promotes cell division of endothelial cells forming new capillaries which supply oxygenated blood to hypoxic tissues (91). Another adaptive response to hypoxia is the production of erythropoietin (EPO) which increases the oxygen carrying capacity of the blood by promoting red blood cell formation (92). Erythropoietin is produced by the kidney and liver and is released into the blood which promotes the formation of erythrocytes from their progenitor cells (93). Together these two changes lead to an increase in oxygen supply to hypoxic tissues.

Chronic hypoxia also leads to vascular remodeling by the release of vasoactive substances. Endothelial cells release vasoconstrictors, growth factors, matrix modifying proteins and adhesion molecules under chronic hypoxia (94). Platelet derived growth factor (PDGF), platelet activating factor (PAF), endothelin, leukotrienes, serotonin etc., are produced, leading to increased proliferation (95-98). Hypoxia increases the production of cytokines such as interleukin-1 (IL-1) and IL-6 mRNA levels (99). The increased production of cell adhesion molecules such as intracellular adhesion molecule (ICAM)-1 and vascular adhesion molecule (VCAM)-1 on endothelial cells along with IL-1 and IL-6 release provide prothrombotic and proinflammatory interactions with circulating cells, facilitating the recruitment and migration of progenitor cells into vessel wall (100, 101).

Matrix metalloproteinases, MMP-9 and MMP-3, enzymes involved in remodeling of extracellular matrix facilitating cell invasion, are also induced by hypoxia promoting vascular remodeling of hypoxic tissues (102).

### **II.A.3. Cellular Responses to hypoxia**

Oxygen is essential for the survival of cells due to its central role as an acceptor of the electrons in the electron transport chain (ETC). The ETC is coupled to ATP synthase, the enzyme responsible for generating ATP through oxidative phosphorylation. ATP is critical for all energy-requiring cellular processes including protein synthesis, DNA replication, metabolic pathways, and maintenance of intracellular pH. Among these, intracellular pH maintenance by ATP-dependent  $\text{Na}^+/\text{K}^+$  ATPase consumes 20-80% of cell's resting stage metabolic output (83). When there is a steep drop in ATP levels, these ATPase pumps fail, leading to membrane depolarization and  $\text{Ca}^{2+}$  influx through voltage gated calcium channels. The rapid rise in intracellular  $\text{Ca}^{2+}$  and subsequent activation of calcium dependent phospholipases and proteases leads to cellular swelling and necrotic cell death (103). Even a transient lack of oxygen, therefore, forces cells to undergo molecular adaptation to cope with a drop in energy levels.

At the cellular level, reductions in ATP levels lead to adaptive response to hypoxia. This is achieved mainly by maximizing the energy production, as well as decreasing the energy consuming processes. Protein, RNA, and DNA synthesis are inhibited almost immediately and ion motive ATPases that perform

$\text{Na}^+/\text{K}^+$  transport and  $\text{Ca}^{2+}$  cycling are favored, as they are essential to maintain a favorable intracellular environment (104). This phenomenon, known as oxygen conformance, involves regulatory mechanisms, including translational arrest (105). Cells show differences in their susceptibility to cell death depending on their electric activity. Electrically active cells, such as neurons, have high ion motive ATPase activity that utilizes 80% of cellular ATP, and are more susceptible to hypoxic cell death than skeletal muscle cells (106).

Under normal oxygen tension oxidative phosphorylation is the major source of cellular ATP. Under hypoxia, cells switch to anaerobic glycolysis, a less efficient source of ATP for the oxygen-starved cells. The increase in glycolysis is achieved by increases in the production and activity of several glycolytic enzymes. Phosphofruktokinase, a major regulator of carbon flux through glycolysis, is allosterically activated by ADP and AMP and is inhibited by ATP, thus deciding the glycolytic rate (107). Phosphofruktokinase-2 (PFK-2) is another important allosteric enzyme involved in regulating the glycolytic pathway. This enzyme is activated by phosphorylation by the AMP-activated protein kinase (AMPK). PFK-2 stimulates the production of fructose-2, 6-bisphosphate, a critical activator of glycolysis, thus increasing the ATP production capacity of the hypoxic cell (108). The transcript level of PFK-2 is also increased under hypoxia (109). AMPK also regulates other pathways that help the cell cope with the loss in oxygen-dependent ATP production, such as glucose uptake controlled by translocation of various glucose transporter (GLUT) proteins to the cell

membrane, the tricarboxylic acid cycle and respiratory chain (110) In addition, AMPK inhibits anabolic pathways such as fatty acid, triglyceride and sterol synthesis, as well as the expression of enzymes involved in fatty acid and gluconeogenesis pathways (111-113).

It can be seen that many of these adaptive responses are dependent on transcriptional activation of genes. Cells undergoing hypoxia show regulated expression of several genes involved in various adaptive responses such as increased glycolysis and angiogenesis (114). How cells sense the lack of oxygen had been a point of contention for quite some time until the discovery of hypoxia inducible factor 1 alpha (HIF1 $\alpha$ ), a transcription factor that is regulated by oxygen tension (115). This transcription factor mediates the transcriptional regulation of a library of genes involved in the cellular and physiological response to tissue hypoxia (116). Although there may be other transcription factors regulated by hypoxia, HIF1 $\alpha$  remains the most important, regulating a large majority of hypoxic gene expression.

## **II.B. Hypoxia Inducible Factors**

The hypoxia inducible factors (HIFs), which include HIF1 $\alpha$ , HIF2 $\alpha$ , HIF3 $\alpha$ , aryl hydrocarbon receptor nuclear translocator - ARNT (also known as HIF1 $\beta$ ) and ARNT2, control the cellular response to hypoxia in mammals (117). All five HIF proteins belong to the basic-Helix-Loop-Helix (bHLH) containing PER-ARNT-SIM (PAS) domain super-family. PAS domains are also found in other transcription

factors involved in circadian regulation and xenobiotic metabolism (118-120). The HIF $\alpha$ s dimerize with ARNT or ARNT2 to form a hetero-dimeric transcription factor. HIF1, a dimer of HIF1 $\alpha$  and ARNT, is the most widely studied hypoxia signaling factor. HIF1 $\alpha$  and ARNT are essential for normal development, as the HIF1 $\alpha$  and ARNT null alleles are embryonic lethal due to vascularization defects (121, 122).

The predominant role that HIF1 $\alpha$  plays in the cellular response to hypoxia makes it the target of intense investigation. Besides its bHLH-PAS domains, the transcription factor also contains a transcriptional activation domain (TAD) towards the carboxy terminus. The TAD is divided into two separate functional regions, the more N-terminal portion, N-TAD and the more C-terminal, C-TAD (Figure 2). The bHLH acts as a contact surface for DNA and a primary interaction surface between HIF1 $\alpha$  and ARNT or ARNT2. The PAS domain of HIF1 $\alpha$  is a secondary dimerization surface thought to provide specificity to the HIF1 $\alpha$ :ARNT interaction (123-125). Finally, HIF1 $\alpha$  contains an oxygen-dependent degradation domain (ODD) that is responsible for regulating the protein's stability under varying oxygen tensions.

### **II.B.1. Regulation of Hypoxia Inducible Factors**

HIF1 $\alpha$  expression and function is translationally and post-translationally regulated. ARNT is constitutively expressed protein and is not known to play a major role in the regulation of HIF1 activity. Under normal oxygen tension, HIF1 $\alpha$

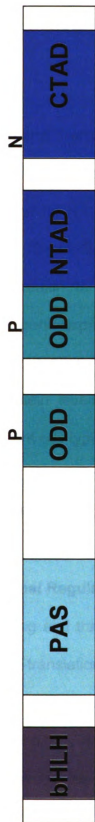


**Figure 2. Graphical representation of the HIF1 $\alpha$  protein:** The various domains are : bHLH – basic Helix-Loop-Helix, PAS- Per-Sim-Armt , ODD- Oxygen dependant degradation , NTAD and CTAD- N-terminal and C-terminal Transcriptional Activation Domain respectively. P and N are the Proline and Asparagine residues that are hydroxylated during normoxia by HIF prolyl hydroxylases (PHDs) and Factor Inhibiting HIF (FIH) respectively.

mRNA is constitutively expressed, translated and the protein is quickly targeted for proteasome-mediated degradation by an ubiquitin-dependent process (126-128).

### **II.B.1.a. Transcriptional and Translational Regulation of HIF**

In almost all cell types, hypoxia leads to HIF1 $\alpha$  protein stabilization whereas there is no change in the mRNA levels. A variety of other factors, such as epidermal growth factor, fibroblast growth factor 2, insulin, insulin like growth factor 1 and 2, and interleukin 1 $\alpha$  induce the expression of HIF1 $\alpha$ , HIF1 DNA binding and HIF1 target gene expression under normoxic conditions (129-131). This is mostly through phosphoinositide-3 kinase (PI3K) signaling pathway, which increases the protein levels of HIF1 $\alpha$  by increased translation. This response varies in different cell types (132, 133). Inhibition of mammalian target of rapamycin kinase (mTOR), a kinase that works downstream of PI3K and AKT, reduces the expression of HIF1 $\alpha$  (134).

### **II.B.1.b. Post-Translational Regulation of Hypoxia Inducible Factors**

HIF1 $\alpha$ -dependent signaling and transcriptional activity is primarily regulated via protein stability and post-translational modifications. Originally, it was thought that this process required a heme containing protein, since HIF1 $\alpha$  stability can be influenced by carbon monoxide, iron-like metals and iron chelators (135, 136). Recently, the signaling mechanism controlling HIF1 $\alpha$  stability has come to light.

It involves motifs within the ODD, ubiquitination and various post-translational modifying enzymes.

The degradation of HIF1 $\alpha$  requires the two ODD motifs found in the carboxy terminus of protein (Figure 2) (127). These ODD motifs each contain a proline residue that, when hydroxylated, creates a binding surface for the Von Hippel Lindau (VHL) tumor suppressor protein. Upon binding HIF1 $\alpha$ , VHL recruits the necessary ubiquitination machinery required for tagging the transcription factor for degradation. In fact, these ODDs can render non-homologous proteins labile in the presence of oxygen (127). The hydroxylation of the conserved prolines in the ODD are performed by a family of non-heme iron-dependent hydroxylases.

The family of prolyl hydroxylase domain containing proteins (PHDs) that modify HIF1 $\alpha$  was first identified in *C. elegans* and later shown to have three mammalian homologs (137, 138). The three hydroxylase family members (PHD1-3) are iron and  $\alpha$ -ketoglutarate ( $\alpha$ -KG) dependent enzymes that utilize oxygen as a co-substrate (139). PHDs hydroxylate prolines within an LXXLAP motif (i.e. human HIF1 $\alpha$  residues 402 and 564 and mouse HIF1 $\alpha$  residues 402 and 577 (137, 138, 140). These enzymes also require ascorbate to maintain proper function. During the reaction cycle, the  $\alpha$ -KG is decarboxylated to yield succinate and the oxygen is transferred to the proline. The involvement of TCA cycle intermediates (i.e.  $\alpha$ -KG and succinate) directly links HIF1 $\alpha$  stability to the metabolic state of the cell. This link led researchers to hypothesize that hypoxia

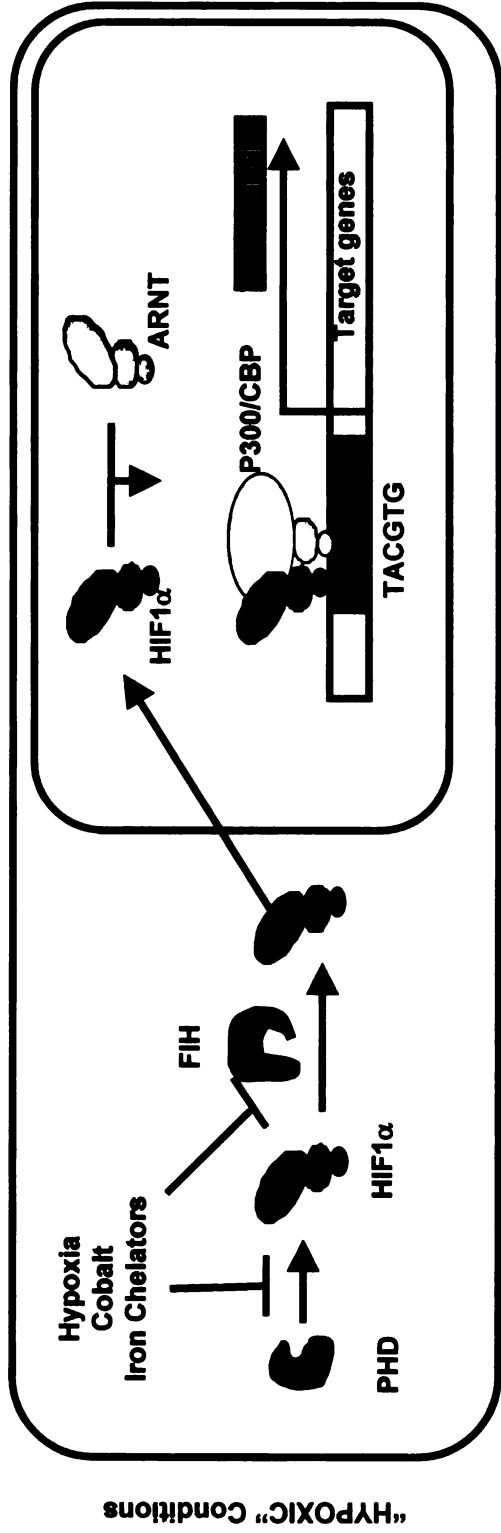
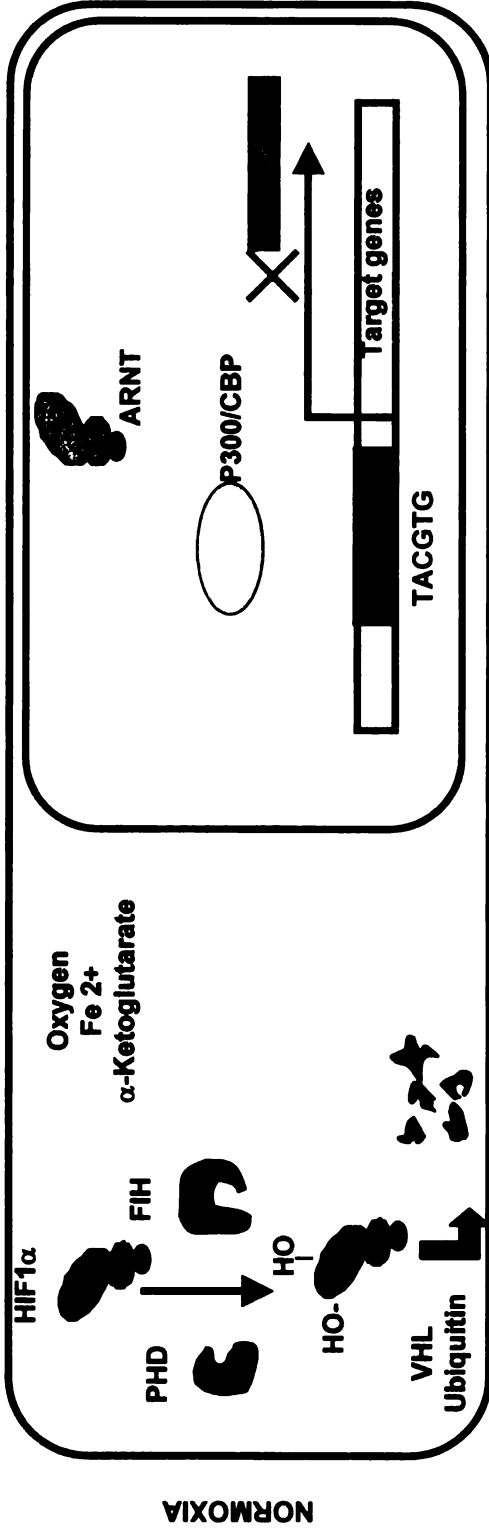
signaling is involved in cancer that develops in families that carry mutations in genes such as succinate dehydrogenase and fumarate hydratase. VHL can only interact with HIF1 $\alpha$  and direct its degradation after HIF1 $\alpha$  is hydroxylated. Under hypoxic conditions, the PHDs are unable to hydroxylate the cytoplasmic HIFs (141). The unmodified HIFs are stabilized and signaled by an unknown mechanism to translocate to the nucleus, where they are free to form dimers with ARNT or ARNT2 (128, 142). The HIF:ARNT heterodimers bind DNA at sequence specific sites termed hypoxia response elements (HREs) of target genes (143) (Figure 3).

HIF1 $\alpha$  is also functionally regulated by hydroxylation. Hypoxic conditions promote the ability of the CTAD of HIF1 $\alpha$  to interact with the transcriptional co-activator, p300 (144, 145). Hydroxylation of a conserved asparagine (residue 803 in hHIF1 $\alpha$  and 813 in mHIF1  $\alpha$ ) in the CTAD inhibits the interaction between CTAD and p300, preventing the recruitment of the basal transcription machinery under normoxic conditions (145-147). HIF asparaginyl hydroxylase also known as factor inhibiting HIF1 (FIH1). This enzyme requires oxygen and  $\alpha$ -KG as substrates and Fe<sup>2+</sup> as a co-factor. Its reaction mechanism is similar to the PHDs, and FIH can also be inhibited by iron chelators, Co<sup>2+</sup> and hypoxia (140, 148-150). Tight control of the HIF transcriptional response under hypoxia is achieved by the dual hydroxylation steps, coupled with difference in K<sub>m</sub> values for O<sub>2</sub> of the PHDs and FIH. PHDs that hydroxylate prolines, causing proteosomal degradation have a higher K<sub>m</sub> value for O<sub>2</sub> than the asparagine hydroxylase, FIH

**Figure 3. HIF1 $\alpha$  and Hypoxia Signaling.**

Prolyl hydroxylase (PHD) is capable of modifying conserved residues in HIF1 $\alpha$  that leads to its VHL-dependent ubiquitination and degradation. PHD requires O<sub>2</sub> and  $\alpha$ -KG as substrate and Fe<sup>2+</sup> as a cofactor. Under hypoxia or in the presence of iron chelators or divalent metals like cobalt and nickel, PHDs are not active, leading to HIF1 $\alpha$  stabilization, nuclear translocation, dimerization with ARNT, and ultimately, transcriptional activation of hypoxia responsive genes. Another oxygen and Fe dependent enzyme FIH hydroxylates a conserved asparagine residue located in the transcriptional activation domain (TAD) under normoxia preventing the interaction between HIF1 $\alpha$  and coactivator CBP/p300 molecule.

# Hypoxia Signal Transduction



(151). The difference in these two enzymes allows the HIF1 $\alpha$  protein to be stable at moderate hypoxia while transcriptionally active only at severe hypoxia.

Studies indicate that HIFs undergo other covalent modifications, such as phosphorylation. P42, AKT and MAP kinases were found to phosphorylate HIF1 $\alpha$  and regulate its activity (152-154). Recently Mylonis et. al. showed that serine-641 and serine-643 of human HIF1 $\alpha$  were targets of phosphorylation by MAP kinase, which promotes the nuclear accumulation of the protein (155). It was also shown that treatment with MAPK inhibitors can inhibit both nuclear accumulation and transcriptional activity of HIF1 $\alpha$ .

In addition to hydroxylation and phosphorylation it has been reported that in mammalian cells ARD1, an acetyl transferase, modifies a lysine (residue 532 in hHIF1  $\alpha$ ) in the ODD of HIF1  $\alpha$ . This modification is thought to enhance the interaction between HIF1 $\alpha$  and VHL and leads to augment HIF1 $\alpha$  ubiquitination (156). Recent reports, however, suggest that the effect of ARD1 on HIF1 $\alpha$  are cell type-specific and its overall role in hypoxia-mediated gene transcription requires further clarification (157, 158).

### **II.B.2. Regulation of gene expression by HIF1 $\alpha$**

Since the discovery of HIF1 $\alpha$  as the transcriptional factor that binds to the promoter of erythropoietin genes, a large number of genes have been found to be directly regulated by HIF1 $\alpha$  (159). Under hypoxic conditions HIF1 $\alpha$  protein

that escapes proteolytic cleavage enters the nucleus, binds ARNT and contact DNA at HREs. This assembly helps in the recruitment of transcriptional mediators such as CBP/p300, which in turn recruits the basal transcriptional machinery (147). The library of genes influenced by HIF1 is varied and can be categorized into survival response or cell death response groups.

### **II.B.2.a. Survival Response**

Under hypoxia, the stabilized HIF1 $\alpha$  protein rapidly induces the expression of genes that increase the oxygen availability to cells such as erythropoietin (EPO) that promotes erythropoiesis. It also induce vascularization by expressing vascular endothelial growth factor (VEGF) (160). In general these genes, along with others such as adrenomedullin, (161), IGF2, a potent mitogen (162) and carbonic anhydrase, a regulator of intracellular pH (163), promote cell survival under hypoxic stress. In addition, HIF1 plays a central role in the switch from aerobic to anaerobic metabolism during hypoxic stress by promoting the expression of glycolytic enzymes, such as hexokinase, enolase1, glyceraldehyde phosphate dehydrogenase (GAPDH), lactate dehydrogenase  $\alpha$  (LDH $\alpha$ ), and phosphoglycerate kinase1 (PGK1) (79). This switch to glycolytic centered energy production is further facilitated by the increased expression of various glucose transporters such as glut-1 (164). HIF1 $\alpha$  also plays a major role in growth and development by promoting cell division by upregulating cyclinG2, TGF $\alpha$  and IGF2, as well as wound healing through increased expression of

extracellular matrix proteins such as prolyl-4-hydroxylase  $\alpha$  (P4H $\alpha$ ), matrix metalloprotease 2 (MMP2), and plasminogen activator inhibitor1(PAI1) (165).

### **II.B.2.b. Cell death response**

Among more than 70 genes that are HRE:HIF1 regulated, a majority of them have a role in promoting cell survival under hypoxia. HIF1 $\alpha$ , however, also regulates the expression of a battery of genes involved in the promotion of cell death, such as BCL2/adenovirus E1B 19kDa interacting protein 3 (BNip3), BNip3-like (BNip3L) and RTP801 (166, 167). BNIP3 and BNIP3L are BH3-domain containing proteins that associate with the mitochondrial outer membrane and can cause the membrane pore to open, leading to loss of membrane potential and cell death in a necrotic manner (168). In primary cardiac myocytes BNIP3 is also known to induce apoptotic cell death under severe hypoxia (169). The necrotic cell death requires a decreased cellular pH when tested in vitro and interestingly, chronic and severe hypoxia can produce tissue acidity (170). Intracellular acidity is also linked to genetic mutations leading to an increased risk of cellular transformation. The expression of BNIP3 may be a method to eliminate potential pre-malignant cells by forcing them to undergo cell death (171).

RTP801 was seen to be regulated in a cell-specific manner by HIF1 $\alpha$  in an ischemic animal model (167). In non-dividing neuron-like cells, RTP801 expression caused cell death, while in MCF7 cells, RT801 showed cellular

protection against glucose deprivation or hypoxia when it was expressed prior to the incident. So by regulating a mix of adaptation and cell death promoting genes, HIF1 $\alpha$  may play an important role in the survival of the organism.

The role of HIF1 $\alpha$  in maintaining the balance between survival and cell death is a critical step that is misregulated in various human diseases and toxic insults. In various solid tumors, the rapid growth of tumor cells and resulting hypoxia favors an adaptive response that might promote even faster tumor growth. Similarly in solid tumors, necrosis of hypoxic regions leads to accumulation of inflammatory immune cells leading to conditions favorable for genetic instability (172-174). Various divalent metals such as cobalt and nickel exposure can also lead to abnormal regulation of hypoxic balance between cell survival and cell death.

### **II.C. Role of hypoxic signaling in human diseases**

In higher organisms, hypoxia resulting from localized or global deficiency in oxygen can lead to life-threatening complications. Organs that have a high metabolic rate, such as the brain and heart, are extremely susceptible to hypoxia-induced damage. For example, the pathological complications of stroke (cerebral ischemia) and heart infarction (myocardial ischemia) are largely due to hypoxia-induced and reperfusion injuries. The influx of oxygen upon tissue reoxygenation after hypoxia produces reactive oxygen species that interact with proteins and lipids, causing cellular damage (175). In addition, hypoxia and HIF1 $\alpha$  signaling play a central role in cellular transformation and tumorigenesis.

The brain offers a special case, given its high energy use and dependence on proper blood flow to supply the nutrients adequately to maintain this high energy production. Stroke-induced damage to the brain in which, the brain stem, hippocampus and cerebral cortex are most susceptible, can cause irreversible brain injury, brain cell death, paralysis and death (176). Even reperfusion, which is required to protect the brain tissues, causes cell death as it produces reactive oxygen species leading to inflammatory cell infiltration (177). In case of a short, not so severe exposure to hypoxia, a reversible phenomenon, called “penumbra”, occurs and is characterized by suppression of protein synthesis and spontaneous electrical activity (176). Brief ischemic injuries are usually reversible and do not cause necrotic cell death and usually lead to a process called stunning (178).

Obstructions in coronary arteries can lead to severe incidents of ischemia. These prolonged ischemic instances can cause necrotic cell death spreading from subendocardium to subepicardium (179). Immediately after the ischemic insult, cells shift to glycolysis for energy production (See section II.A.3 p.25). This shift to anaerobic metabolism increases the production of lactate within the cell and leads to cellular acidosis and edema. Intracellular  $\text{Ca}^{2+}$  also increases and finally leads to cell necrosis (180). Reperfusion is essential to save the cardiac myocytes but leads to reperfusion injury; very similar to what happens to brain cells. The reestablishment of blood flow delivers a burst of oxygen to the

affected tissue and the resulting rapid production of reactive oxygen species can lead to further alterations in  $\text{Ca}^{2+}$  homeostasis. This disruption in  $\text{Ca}^{2+}$  homeostasis can cause the myocardium to lose its contractile function for a short period (181).

Hypoxia and HIF1 $\alpha$  are essential in tumorigenesis (121, 182). HIF1 $\alpha$  is a positive factor in solid tumor growth. In a tumor transplant model, HIF1 $\alpha$  null cells fail to produce tumor. Many human cancers show aberrant HIF1 $\alpha$  protein and hypoxia-mediated transcription (183). The increases in HIF1 $\alpha$  signaling might be the result of the loss of tumor suppressor proteins, such as VHL, or the hypoxic environment inside solid tumor tissues (183, 184). As tumors grow larger than 1 mm<sup>3</sup>, hypoxic regions appear inside the tumor due to an inability of the tumor to maintain adequate vascularization. HIF1 $\alpha$  induces the expression of glycolytic genes and growth factors, such as VEGF, to enable the tumor to maintain ATP production and to re-establish blood flow to the hypoxic region of the tumor, respectively (83). HIF1 $\alpha$  also increases the expression of genes involved in extracellular modification, causing increased metastatic potential (185). Furthermore, in glioblastomas, HIF1 $\alpha$  is overexpressed in viable cells surrounding the areas of necrosis, suggesting that it might be promoting cell survival (186).

Increased expression of HIF1 $\alpha$  has also been shown to be associated with aggressive forms of cancer. Increased intracellular levels of HIF1 $\alpha$  protein are

associated with poor prognosis and resistance to therapy in the case of head and neck tumor, ovarian cancer and esophageal cancer (187, 188). Ryan et al showed that tumor growth and angiogenesis were highly reduced by the loss of HIF1 $\alpha$  (121). HIF1 $\alpha$  is also known to induce multi-drug resistance protein 1 and P-glycoprotein under hypoxia and might play a role in tumor resistance to chemotherapy (189). Radiation therapy is used to treat many tumors and primarily works by promoting the production of ROS. The increased oxidative stress upon radiation causes DNA strand breaks and ultimately the death of the cancer cell. Under hypoxic conditions, ROS production is inhibited and studies have shown that many primary tumors with high levels of HIF1 $\alpha$  expression show increased radiation resistance (183).

### **III. Reactive Oxygen Species**

It is important for a cell's survival to maintain a reducing environment since cells utilize selective oxidation steps to derive energy for running various biological processes. At the same time, the oxidation step necessitates the presence of oxidizing agents such as molecular oxygen. Oxygen is a potent oxidant with two unpaired electrons and can react with various cellular components such as proteins, lipids, nucleic acids. It can also react with transition metals and can produce reactive oxygen species (ROS) which include singlet oxygen ( $O_2^{\bullet}$ ), hydroxyl radicals ( $OH^{\bullet}$ ), and superoxide anions ( $O_2^{\bullet-}$ ). Generally these molecules are highly reactive and easily diffusible (190). Hydrogen peroxide ( $H_2O_2$ ) is another species which is highly reactive but has no unpaired electron

and can be produced from these reactive oxygen species. An important source of ROS is the mitochondrion, which maintains the apparatus for oxidative phosphorylation. This paradox of oxygen as a necessary evil has forced cells to maintain mechanisms to protect themselves from the harmful effects of ROS while utilizing oxygen for energy production. Some time during evolution organisms began using these byproducts of aerobic life as messengers for biological signaling, as well as weapons against hostile invaders (191). Antioxidant enzymes such as superoxide dismutases, as well as antioxidant molecules like ascorbic acid and glutathione are main components of the host defense against cellular ROS damage (192).

### **III.A. Sources of Reactive Oxygen Species (ROS)**

Reactive oxygen species are produced in every cell either through enzymatic or random chemical reactions (193). The major sources of reactive oxygen species are mitochondria and transition metal oxidation. There are also other cytoplasmic enzymes that produce ROS while utilizing oxygen as a substrate for other chemical reactions. The sources of ROS can be classified as mitochondrial, transition metal reactions, hypoxia and hypoxia reperfusion, and extra-mitochondrial sources.

#### **III.A.1. Mitochondria**

Electrons derived from NADH and FADH<sub>2</sub>, synthesized primarily during the TCA cycle, flow through the mitochondrial ETC, terminating with the transfer of 4

electrons to an oxygen atom, producing water. As these electrons travel through the ETC, the energy is used to pump protons into the inter-membrane space of the mitochondria, creating a membrane potential of approximately 200 mV. This membrane potential is coupled to the production of ATP via ATP synthase (also known as Complex V). The oxidation steps are not always complete, leading to the production of superoxide anions (194). Complex 1 and 3 of the ETC, located in the mitochondrial inner-membrane are the major sites of ROS production (195) (Figure 4). Ubisemiquinones at these sites transfer the electrons to oxygen, generating superoxide. Superoxide dismutases in the mitochondria or cytoplasm inactivate superoxide producing  $H_2O_2$ , which may in turn be detoxified by glutathione peroxidase. Any  $H_2O_2$  that escapes detoxification might cause downstream cell signaling or react with cellular components causing damage (196). Hydroxyl radicals might also be formed from superoxide through Haber-Weiss reaction or from  $H_2O_2$  by Fenton reaction (Figure 1). Hydroxyl radicals are very reactive and cause extensive damage to nucleotides (197).  $H_2O_2$  on the other hand, is known to be involved in cell signaling pathways acting as a long range second messenger as it can easily diffuse through the membranes (198). Complex II of the electron transport chain may also produce superoxide when the enzyme is damaged by oxidative stress or aging (199). Recent data suggests that sites other than electron transport chain may produce ROS within the mitochondria (200). For example, alpha ketoglutarate dehydrogenase, a TCA cycle enzyme has been shown to produce  $H_2O_2$  in isolated brain mitochondria. Reduced flavins in other flavoprotein enzymes may also produce superoxide

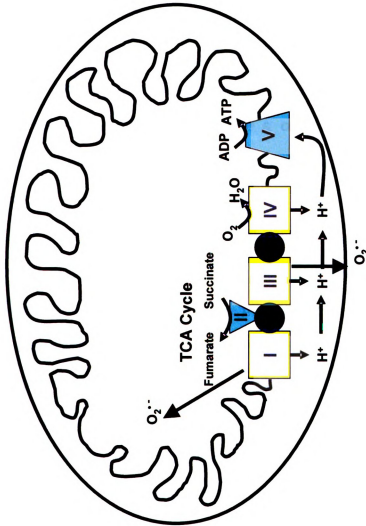


**Figure 4. Sites of ROS production in Mitochondria**

The electron transport chain (Complexes I-IV) couples the flow of electrons to the movement of protons across the inner membrane of the mitochondria. One byproduct of this series of electron transfers is the production of superoxides at complex I and III because of incomplete reduction of oxygen atom. Superoxide generated at complex I escapes into inner mitochondrial space and the one produced by complex III escapes into inter-membrane space and eventually into cytosol.

(199). Monoaminoxidase, an enzyme bound to the outer mitochondrial membrane that oxidizes biogenic amines may also produce  $H_2O_2$  (201).

### **III.A.2. Transition Metals**

Many transition metals are known to produce reactive oxygen species through Fenton like or Haber-Weiss reactions (15) (Figure 1). Redox active metals such as iron, cobalt, and nickel, produce superoxide and hydroxyl radical by reacting with molecular oxygen. Redox inactive metals such as lead, arsenic, mercury and cadmium are thought to deplete a cell's sulfhydryl antioxidant reserves, causing oxidative damage, as well as bonding with the sulfhydryl group of other proteins (19).

The redox state of the cell is generally thought to be highly coupled with the iron redox state. Iron homeostasis is maintained by regulating the absorption, transport and storage of iron through specific iron binding proteins (202). Free iron can readily participate in one electron transport reactions, producing hydroxyl radicals through Fenton-like reactions and these radicals can go on to cause lipid peroxidation and oxidative damage of proteins and DNA (21). This also causes the production of a variety of other ROS species by the decomposing peroxides. The superoxide insult can further increase the free form of iron by the release of iron from binding proteins such as ferritin.

Cobalt ions can form hydroxyl radicals by reacting with endogenous  $H_2O_2$ , causing oxidative damage to cells (15). Cobalt metal particles are also able to produce hydroxyl radicals by reacting with dissolved oxygen in the presence of superoxide dismutase in EPR spin trapping experiments (203). Surprisingly, *in vitro* systems have demonstrated that  $Co^{2+}$  can produce hydroxyl radicals using Fenton reaction, in the presence of low molecular weight chelators such as glutathione and anserine (203). Nickel produces much lower levels of ROS. Both cobalt and nickel's ability to produce ROS are thought to play a critical role in their ability to act as hypoxia mimic (204). Data suggests that  $NiCl_2$  and  $NiS_2$  can produce ROS. Nickel is also shown to deplete GSH, as well as have pro-oxidant effect when present along with GSH (205). Nickel-induced oxidative stress has been linked to DNA damage and cellular transformation.

Although cadmium does not produce significant levels of ROS directly, it is thought to produce oxidative stress indirectly (19). Through a slow reduction, cellular glutathione forms a complex with hexavalent chromium and yields  $Cr(V)$ , which can bind DNA or produce ROS by a Fenton-like reaction (206).  $Cr(V)$  may be further reduced by cellular antioxidants such as ascorbic acid and glutathione producing  $Cr(IV)$  and  $Cr(III)$  that are capable of producing ROS (207). Cells utilize the glutathione/glutathione peroxidase system as a scavenger of intracellular oxygen radicals. Cadmium treatment increased the cellular GSH levels at moderate doses, however; GSH levels were depleted at high doses of the metal, presumably due to the oxidative load (208). Cadmium can also inhibit

the activity of SOD and increase the levels of lipid peroxidation in treated animals (209). Low concentrations of cadmium treatment in human-hamster hybrid cells caused the attenuation of the removal of H<sub>2</sub>O<sub>2</sub>, suggesting the inhibition of peroxide-scavenging enzymes (210).

### **III.A.3. Hypoxia and Hypoxia Reperfusion**

Cells might experience a lack of oxygen for various reasons, most notably due to a blockage in blood vessels (ischemia). As described above (section II.C. p38.), this can have disastrous consequences in case of brain, heart and other organs. ROS production under ischemia is a paradox. While ROS production is suppressed in tissues such as neurons during ischemia, its production increases in heart, lung and skeletal muscle (211). Damage to the mitochondria increases the ROS production during ischemia because decreased flux through ETC coupled with damage to the complexes leads to electron leakage and oxyradical formation (212). Studies with rotenone and antimycin A showed that complex 3 is the primary site of ROS production during hypoxic stress (213). Although a restoration of blood (oxygen) supply is essential for the survival of the organism, the sudden arrival of oxygen also produces a burst of reactive oxygen species, presumably due to inability of the scavenging system to keep up with the sudden burst in oxygen supply. The restoration of blood flow can result in reperfusion injury of organs (175).

### **III.A.4. Extramitochondrial Sources**

Various cellular reactions produce ROS as byproducts. Monooxygenases, cytochrome P-450 (CYP) enzymes are multi-enzyme systems found in the endoplasmic reticulum and include FAD/FMN containing NADPH-cytochrome P450 reductase. Enzymes of this CYP superfamily are involved in biotransformation reactions of xenobiotics and endogenous compounds, such as steroids. The enzymes perform substrate oxidation reactions in an  $O_2$  and NADPH-dependent manner (214). CYP enzymes produce superoxide and  $H_2O_2$  during the oxidation reaction by the accidental release of electrons by the flavins in the NADPH:P450 enzyme (215). Another important source of ROS is peroxisomes, which play a major role as antioxidants, primarily scavenging cytosolic  $H_2O_2$ . Aged peroxisomes lose catalase activity thus becoming a source of ROS, as the balance between production and removal is shifted to the production side (216). The peroxisomal flavin oxidases that are involved in  $\beta$ -oxidation reactions of fatty acids can produce  $H_2O_2$ . Xanthine oxidase, responsible for catalyzing the 1 electron reduction of molecular  $O_2$  using hypoxanthine, xanthine and NADH, is a major source of ROS (217). NADPH oxidases are important source of superoxides in activated macrophages, neutrophils, and endothelial cells (218). The ROS species are used to destroy invading pathogens by the activated immune cells and for signaling vascular remodeling by endothelial cells.

### **III.B. Protection against ROS**

Cells have a well developed system in place to deal with ROS that includes antioxidant enzymes, such as glutathione peroxidase and superoxide dismutase, as well as small antioxidant molecules derived from dietary intake of fruits and vegetables , such as ascorbate and tocopherol (219, 220). This defense system primarily includes six classes of molecules as described by Beckman and Ames (221): These include (i) enzymatic scavengers of ROS such as superoxide dismutases that convert superoxide into  $H_2O_2$ , catalases that convert  $H_2O_2$  into water and  $O_2$ , and glutathione peroxidase that decompose  $H_2O_2$  to water; (ii) ascorbate, urate and glutathione that act as hydrophilic ROS scavengers; (iii) tocopherols, flavonoids, carotenoids and ubiquinol that work in the hydrophobic environment; (iv) enzymes (e.g. GSH reductase, dehydroascorbate reductase) that play a critical role in the recycling of small antioxidant molecules and maintenance of thiol groups of proteins (e.g thioredoxin reductase) under oxidative stress; (v) enzymes that generate reducing equivalents such as glucose-6-phosphate dehydrogenase and help to maintain the appropriate cellular environment by replenishing NADPH levels and (vi) various transcription factors and other proteins such as NF- $\kappa$ B, MTF-1, NRF-2 that promote an adaptive response to an ROS insult. Various components of the antioxidant pathways act in parallel as different antioxidants have similar roles. In addition, they are highly co-operative. For example, SOD and glutathione peroxidase work in tandem to convert superoxide into water and  $O_2$ .

#### **IV. Hypothesis and Specific Aims:**

In daily life we are exposed to metals that are ubiquitous in our environment and, once internalized, can influence HIF1 activity through direct PHD inhibition or indirectly via ROS generation. The aberrant HIF1 activity can disrupt the normal balance established by hypoxia signaling between cell death and adaptation, resulting in cellular damage. Moreover, metal-induced ROS generation might have other cellular consequences outside of HIF1 modulation that also influence cell viability. The published literature overviewed earlier and our own experiments suggest that divalent metal-ions, such as cobalt and nickel, can mimic hypoxia to the extent that there is a significant overlap between the mRNA expression profiles of hypoxia and cobalt chloride-treated mouse embryonic fibroblast cells (MEFs). Understanding how metals, including both hypoxia-mimics (i.e. cobalt and nickel) and non-hypoxia mimics (i.e cadmium) influence cell function and viability, and determining the role that the hypoxia signaling cascade plays in this process has led me to the following hypothesis and specific aims:

**Hypothesis: cobalt and similar divalent metals cause toxicity in MEFs by virtue of their ability to interfere with hypoxic signaling.**

The four chapters in this dissertation focus on testing the above hypothesis with the following specific aims.

**A) Characterize the global gene expression profiles under hypoxic conditions and upon exposure to 'hypoxia mimics'.**

- 1) Determine the global expression changes under hypoxia, cobalt chloride, and desferoxamine treatments using Hep3B cells
- 2) Characterize the extent of overlap in gene expression profiles between hypoxia, cobalt chloride, and desferoxamine treatments.

**B) Characterize the HIF1 $\alpha$ -dependent gene expression profiles following hypoxia and cobalt chloride treatments using wild type and HIF1 $\alpha$  -/- mouse embryonic fibroblasts.**

- 1) Characterize hypoxia mediated gene expression changes in MEFs.
- 2) Determine the HIF1 $\alpha$  -dependent gene expression changes upon hypoxia and CoCl<sub>2</sub> treatment
- 3) Identify shared genes between hypoxia and cobalt treated MEFs with the goal of identifying possible mechanism of action for metal-induced toxicity

**C) Elucidate the role of HIF1 $\alpha$  in mediating cobalt induced toxicity in MEFs.**

- 1) Determine the time course and dose response to CoCl<sub>2</sub> mediated toxicity in wild type and HIF1 $\alpha$  -/- cells.
- 2) Determine the changes in mRNA and protein levels of cytotoxic genes in CoCl<sub>2</sub> treated wild type and HIF1 $\alpha$  -/- cells.
- 3) Characterize the morphological changes associated with CoCl<sub>2</sub> induced cell death in wild type and HIF1 $\alpha$  -/- cells.

**D) Determine the mechanism(s) underlying the difference in toxicity to cobalt chloride and cadmium chloride in wild type and HIF1 $\alpha$  -/- mouse embryonic fibroblasts.**

- 1) Characterize the cytotoxicity to CoCl<sub>2</sub> and CdCl<sub>2</sub> treatment in wild type and HIF1 $\alpha$  -/- MEFs.
- 2) Determine the changes in the cell morphology to CoCl<sub>2</sub> and CdCl<sub>2</sub> treatment in wild type and HIF1 $\alpha$  -/- MEFs.
- 3) Characterize the role of BNip3 in CoCl<sub>2</sub> and CdCl<sub>2</sub> induced toxicity in wild type and HIF1 $\alpha$  -/- MEFs.
- 4) Determine the levels of oxidative stress in CoCl<sub>2</sub> and CdCl<sub>2</sub> mediated toxicity and HIF1 $\alpha$  -/- MEFs.
- 5) Characterize the levels of ROS scavenger enzyme function under CoCl<sub>2</sub> and CdCl<sub>2</sub> treatment in wild type and HIF1 $\alpha$  -/- MEFs.
- 6) Determine the levels of cellular antioxidants in CoCl<sub>2</sub> and CdCl<sub>2</sub> treated wild type and HIF1 $\alpha$  -/- MEFs.

## References

1. Shapiro, R. Small molecule interactions were central to the origin of life. *Q Rev Biol*, **81**: 105-125, 2006.
2. Bartel, D. P. and Unrau, P. J. Constructing an RNA world. *Trends Cell Biol*, **9**: M9-M13, 1999.
3. Muller, U. F. Re-creating an RNA world. *Cell Mol Life Sci*, **63**: 1278-1293, 2006.
4. Cohen, P., Schelling, D. L., and Stark, M. J. Remarkable similarities between yeast and mammalian protein phosphatases. *FEBS Lett*, **250**: 601-606, 1989.
5. Parr, G. J. *Man, Metals and Modern Magic*, 3rd edition, Vol. 1, p. 238. Cleveland, OH: American Society for Metals, 1967.
6. Aitchison, A. *A History of Metals*, 1 edition, Vol. 2, p. 343. New York: Interscience Publishers, Inc., 1960.
7. Glusker, J. P. Structural aspects of metal liganding to functional groups in proteins. *Adv Protein Chem*, **42**: 1-76, 1991.
8. Baker, J. O. Metal-buffered systems. *Methods Enzymol*, **158**: 33-55, 1988.
9. Nelson, N. Metal ion transporters and homeostasis. *Embo J*, **18**: 4361-4371, 1999.
10. Nord, E. P., Brown, S. E., and Crandall, E. D. Characterization of Na<sup>+</sup>-H<sup>+</sup> antiport in type II alveolar epithelial cells. *Am J Physiol*, **252**: C490-498, 1987.
11. Waalkes, M. P., Coogan, T. P., and Barter, R. A. Toxicological principles of metal carcinogenesis with special emphasis on cadmium. *Crit Rev Toxicol*, **22**: 175-201, 1992.
12. Lehninger, A. L. Role of metal ions in enzyme systems. *Physiol Rev*, **30**: 393-429, 1950.
13. Clementi, M. E., Condo, S. G., Castagnola, M., and Giardina, B. Hemoglobin function under extreme life conditions. *Eur J Biochem*, **223**: 309-317, 1994.

14. Strickholm, A. and Clark, H. R. Ionic permeability of K, Na, and Cl in crayfish nerve. Regulation by membrane fixed charges and pH. *Biophys J*, 19: 29-48, 1977.
15. Stohs, S. J. and Bagchi, D. Oxidative mechanisms in the toxicity of metal ions. *Free Radic Biol Med*, 18: 321-336, 1995.
16. Hamai, D., Bondy, S. C., Becaria, A., and Campbell, A. The chemistry of transition metals in relation to their potential role in neurodegenerative processes. *Curr Top Med Chem*, 1: 541-551, 2001.
17. Ho, V. T. and Bunn, H. F. Effects of transition metals on the expression of the erythropoietin gene: further evidence that the oxygen sensor is a heme protein. *Biochem. Biophys. Res. Comm.*, 223: 175-180, 1996.
18. Hartwig, A. Carcinogenicity of metal compounds: possible role of DNA repair inhibition. *Toxicol Lett*, 102-103: 235-239, 1998.
19. Ercal, N., Gurer-Orhan, H., and Aykin-Burns, N. Toxic metals and oxidative stress part I: mechanisms involved in metal-induced oxidative damage. *Curr Top Med Chem*, 1: 529-539, 2001.
20. Barceloux, D. G. Cobalt. *J Toxicol Clin Toxicol*, 37: 201-206, 1999.
21. Valko, M., Morris, H., and Cronin, M. T. Metals, toxicity and oxidative stress. *Curr Med Chem*, 12: 1161-1208, 2005.
22. Cobb, A. G. and Schmalzreid, T. P. The clinical significance of metal ion release from cobalt-chromium metal-on-metal hip joint arthroplasty. *Proc Inst Mech Eng [H]*, 220: 385-398, 2006.
23. Wehner, A. P., Busch, R. H., Olson, R. J., and Craig, D. K. Chronic inhalation of cobalt oxide and cigarette smoke by hamsters. *Am Ind Hyg Assoc J*, 38: 338-346, 1977.
24. Stangl, G. I., Schwarz, F. J., Jahn, B., and Kirchgessner, M. Cobalt-deficiency-induced hyperhomocysteinaemia and oxidative status of cattle. *Br J Nutr*, 83: 3-6, 2000.
25. Lison, D. Human toxicity of cobalt-containing dust and experimental studies on the mechanism of interstitial lung disease (hard metal disease). *Critical Reviews in Toxicology*, 26: 585-616, 1996.
26. Brown, T. E. and Meineke, H. A. Presence of an active erythropoietic factor (erythropoietin) in plasma of rats after prolonged cobalt therapy. *Proc Soc Exp Biol Med*, 99: 435-437, 1958.

27. Goldwasser, E., Jacobson, L. O., Fried, W., and Plzak, L. F. Studies on erythropoiesis. V. The effect of cobalt on the production of erythropoietin. *Blood*, 13: 55-60, 1958.
28. Kriss, J. P., Carnes, W. H., and Gross, R. T. Hypothyroidism and thyroid hyperplasia in patients treated with cobalt. *J Am Med Assoc*, 157: 117-121, 1955.
29. Centeno, J. A., Pestaner, J. P., Mullick, F. G., and Virmani, R. An analytical comparison of cobalt cardiomyopathy and idiopathic dilated cardiomyopathy. *Biol Trace Elem Res*, 55: 21-30, 1996.
30. Jefferson, J. A., Escudero, E., Hurtado, M. E., Pando, J., Tapia, R., Swenson, E. R., Prchal, J., Schreiner, G. F., Schoene, R. B., Hurtado, A., and Johnson, R. J. Excessive erythrocytosis, chronic mountain sickness, and serum cobalt levels. *Lancet*, 359: 407-408, 2002.
31. Fischer, T. and Rystedt, I. Cobalt allergy in hard metal workers. *Contact Dermatitis*, 9: 115-121, 1983.
32. Lauwerys, R. and Lison, D. Health risks associated with cobalt exposure--an overview. *Sci Total Environ*, 150: 1-6, 1994.
33. Paternain, J. L., Domingo, J. L., and Corbella, J. Developmental toxicity of cobalt in the rat. *J Toxicol Environ Health*, 24: 193-200, 1988.
34. Bucher, J. R., Hailey, J. R., Roycroft, J. R., Haseman, J. K., Sills, R. C., Grumbein, S. L., Mellick, P. W., and Chou, B. J. Inhalation toxicity and carcinogenicity studies of cobalt sulfate. *Toxicol Sci*, 49: 56-67., 1999.
35. Nordberg, G. F., Goyer, R. A., and Clarkson, T. W. Impact of effects of acid precipitation on toxicity of metals. *Environ Health Perspect*, 63: 169-180, 1985.
36. Sonke, J. E., Hoogewerff, J. A., van der Laan, S. R., and Vangronsveld, J. A chemical and mineralogical reconstruction of Zn-smelter emissions in the Kempen region (Belgium), based on organic pool sediment cores. *Sci Total Environ*, 292: 101-119, 2002.
37. Hiscock, S. A. Trends in the uses of cadmium (1970-1979). *Ecotoxicol Environ Saf*, 7: 25-32, 1983.
38. Nriagu, J. O. Global inventory of natural and anthropogenic emissions of trace metals to the atmosphere. *Nature*, 279: 409-411, 1979.
39. Davis, R. D. Cadmium - a complex environmental problem. Part II. Cadmium in sludges used as fertilizer. *Experientia*, 40: 117-126, 1984.

40. Carr, J. P. and Murphy, A. M. Cadmium blocks viral invasion in plants. *Nat Cell Biol*, 4: E167-168, 2002.
41. Friberg, L. [Medical effects of toxic metals in the environment]. *Lakartidningen*, 80: 1707-1713, 1983.
42. Karpliuk, I. A., Volkova, N. A., Popov, V. I., and Stepanova, E. N. [Substantiation of daily permissible levels of cadmium intake with food]. *Vopr Pitan* 70-73, 1987.
43. Stanescu, D., Veriter, C., Frans, A., Goncette, L., Roels, H., Lauwerys, R., and Basseur, L. Effects on lung of chronic occupational exposure to cadmium. *Scand J Respir Dis*, 58: 289-303, 1977.
44. Lee, J. S. and White, K. L. A review of the health effects of cadmium. *Am J Ind Med*, 1: 307-317, 1980.
45. Ishizaki, A. and Funkushima, M. [Studies on "Itai-itai" disease (Review)]. *Nippon Eiseigaku Zasshi*, 23: 271-285, 1968.
46. Piscator, M. Role of cadmium in carcinogenesis with special reference to cancer of the prostate. *Environ Health Perspect*, 40: 107-120, 1981.
47. Liu, X. Y., Jin, T. Y., Nordberg, G. F., Rannar, S., Sjostrom, M., and Zhou, Y. A multivariate study of protective effects of Zn and Cu against nephrotoxicity induced by cadmium metallothionein in rats. *Toxicol Appl Pharmacol*, 114: 239-245, 1992.
48. Chernoff, N. Teratogenic effects of cadmium in rats. *Teratology*, 8: 29-32, 1973.
49. Heath, J. C. and Daniel, M. R. The Production of Malignant Tumours by Cadmium in the Rat. *Br J Cancer*, 18: 124-129, 1964.
50. Oberdorster, G. Airborne cadmium and carcinogenesis of the respiratory tract. *Scand J Work Environ Health*, 12: 523-537, 1986.
51. Waalkes, M. P. Cadmium carcinogenesis in review. *J Inorg Biochem*, 79: 241-244., 2000.
52. Huebers, H. A., Huebers, E., Csiba, E., Rummel, W., and Finch, C. A. The cadmium effect on iron absorption. *Am J Clin Nutr*, 45: 1007-1012, 1987.
53. Watanabe, M., Shiroishi, K., Nishino, H., Shinmura, T., Murase, H., Shoji, T., Naruse, Y., and Kagamimori, S. An experimental study on the long-term effect of cadmium in mice fed cadmium-polluted rice with special reference to the effect of repeated reproductive cycles. *Environ Res*, 40: 25-46, 1986.

54. Binah, O., Meiri, U., and Rahamimoff, H. The effects of HgCl<sub>2</sub> and mersalyl on mechanisms regulating intracellular calcium and transmitter release. *Eur J Pharmacol*, 51: 453-457, 1978.
55. Chen, Q. X., Zheng, W. Z., Lin, J. Y., Shi, Y., Xie, W. Z., and Zhou, H. M. Effect of metal ions on the activity of green crab (*Scylla serrata*) alkaline phosphatase. *Int J Biochem Cell Biol*, 32: 879-885, 2000.
56. Kuznetsova, S. S., Azarkina, N. V., Vygodina, T. V., Siletsky, S. A., and Konstantinov, A. A. Zinc ions as cytochrome C oxidase inhibitors: two sites of action. *Biochemistry (Mosc)*, 70: 128-136, 2005.
57. Tormanen, C. D. Inhibition of rat liver and kidney arginase by cadmium ion. *J Enzyme Inhib Med Chem*, 21: 119-123, 2006.
58. Bondy, S. C., Guo-Ross, S. X., and Truong, A. T. Promotion of transition metal-induced reactive oxygen species formation by beta-amyloid. *Brain Res*, 799: 91-96, 1998.
59. Hu, Y., Su, L., and Snow, E. T. Arsenic toxicity is enzyme specific and its effects on ligation are not caused by the direct inhibition of DNA repair enzymes. *Mutat Res*, 408: 203-218, 1998.
60. Im, J. Y., Paik, S. G., and Han, P. L. Cadmium-induced astroglial death proceeds via glutathione depletion. *J Neurosci Res*, 83: 301-308, 2006.
61. Hughes, W. L. and Dintzis, H. M. Crystallization of the Mercury Dimers of Human and Bovine Mercaptalbumin. *J Biol Chem*, 239: 845-849, 1964.
62. Vallee, B. L. and Ulmer, D. D. Biochemical effects of mercury, cadmium, and lead. *Annu Rev Biochem*, 41: 91-128, 1972.
63. O'Halloran, T. V. Transition metals in control of gene expression. *Science*, 261: 715-725, 1993.
64. Pimstone, N. R., Engel, P., Tenhunen, R., Seitz, P. T., Marver, H. S., and Schmid, R. Inducible heme oxygenase in the kidney: a model for the homeostatic control of hemoglobin catabolism. *J Clin Invest*, 50: 2042-2050, 1971.
65. Zhou, P. and Thiele, D. J. Rapid transcriptional autoregulation of a yeast metalloregulatory transcription factor is essential for high-level copper detoxification. *Genes Dev*, 7: 1824-1835, 1993.
66. Hainaut, P. and Milner, J. A structural role for metal ions in the "wild-type" conformation of the tumor suppressor protein p53. *Cancer Res*, 53: 1739-1742, 1993.

67. Hainaut, P., Rolley, N., Davies, M., and Milner, J. Modulation by copper of p53 conformation and sequence-specific DNA binding: role for Cu(II)/Cu(I) redox mechanism. *Oncogene*, *10*: 27-32, 1995.
68. Goebeler, M., Roth, J., Brocker, E. B., Sorg, C., and Schulze-Osthoff, K. Activation of nuclear factor-kappa B and gene expression in human endothelial cells by the common haptens nickel and cobalt. *J Immunol*, *155*: 2459-2467, 1995.
69. Leonard, S. S., Harris, G. K., and Shi, X. Metal-induced oxidative stress and signal transduction. *Free Radic Biol Med*, *37*: 1921-1942, 2004.
70. Durnam, D. M. and Palmiter, R. D. Transcriptional regulation of the mouse metallothionein-I gene by heavy metals. *J Biol Chem*, *256*: 5712-5716, 1981.
71. Foulkes, E. C. Renal tubular transport of cadmium-metallothionein. *Toxicol Appl Pharmacol*, *45*: 505-512, 1978.
72. Courgeon, A. M., Maisonhaute, C., and Best-Belpomme, M. Heat shock proteins are induced by cadmium in *Drosophila* cells. *Exp Cell Res*, *153*: 515-521, 1984.
73. Goering, P. L., Kish, C. L., and Fisher, B. R. Stress protein synthesis induced by cadmium-cysteine in rat kidney. *Toxicology*, *85*: 25-39, 1993.
74. Liu, J., Corton, C., Dix, D. J., Liu, Y., Waalkes, M. P., and Klaassen, C. D. Genetic background but not metallothionein phenotype dictates sensitivity to cadmium-induced testicular injury in mice. *Toxicol Appl Pharmacol*, *176*: 1-9, 2001.
75. Zheng, H., Liu, J., Choo, K. H., Michalska, A. E., and Klaassen, C. D. Metallothionein-I and -II knock-out mice are sensitive to cadmium-induced liver mRNA expression of c-jun and p53. *Toxicol Appl Pharmacol*, *136*: 229-235, 1996.
76. Jin, P. and Ringertz, N. R. Cadmium induces transcription of proto-oncogenes c-jun and c-myc in rat L6 myoblasts. *J Biol Chem*, *265*: 14061-14064, 1990.
77. Goldwasser, E., Jacobson, L. O., Fried, W., and Plzak, L. Mechanism of the erythropoietic effect of cobalt. *Science*, *125*: 1085-1086, 1957.
78. Ladoux, A. and Frelin, C. Cobalt stimulates the expression of vascular endothelial growth factor mRNA in rat cardiac cells. *Biochem Biophys Res Commun*, *204*: 794-798, 1994.

79. Semenza, G. L., Roth, P. H., Fang, H. M., and Wang, G. L. Transcriptional regulation of genes encoding glycolytic enzymes by hypoxia-inducible factor 1. *J. Biol. Chem.*, 269: 23757-23763, 1994.
80. Salnikow, K., Donald, S. P., Bruick, R. K., Zhitkovich, A., Phang, J. M., and Kasprzak, K. S. Depletion of intracellular ascorbate by the carcinogenic metals nickel and cobalt results in the induction of hypoxic stress. *J Biol Chem*, 2004.
81. Haddad, G. G. a. L., G. Tissue Oxygen Deprivation : From Molecular to Integrated Function, 1 edition, Vol. 1, p. 1085. New York: Marcel Dekker, 1996.
82. Lopez-Barneo, J., Pardal, R., and Ortega-Saenz, P. Cellular mechanism of oxygen sensing. *Annu Rev Physiol*, 63: 259-287, 2001.
83. Michiels, C. Physiological and pathological responses to hypoxia. *Am J Pathol*, 164: 1875-1882, 2004.
84. Post, J. M., Hume, J. R., Archer, S. L., and Weir, E. K. Direct role for potassium channel inhibition in hypoxic pulmonary vasoconstriction. *Am J Physiol*, 262: C882-890, 1992.
85. Dart, C. and Standen, N. B. Activation of ATP-dependent K<sup>+</sup> channels by hypoxia in smooth muscle cells isolated from the pig coronary artery. *J Physiol*, 483 ( Pt 1): 29-39, 1995.
86. Rubin, L. J. Pathology and pathophysiology of primary pulmonary hypertension. *Am J Cardiol*, 75: 51A-54A, 1995.
87. Archer, S. L., Weir, E. K., Reeve, H. L., and Michelakis, E. Molecular identification of O<sub>2</sub> sensors and O<sub>2</sub>-sensitive potassium channels in the pulmonary circulation. *Adv Exp Med Biol*, 475: 219-240, 2000.
88. Peers, C. and Kemp, P. J. Acute oxygen sensing: diverse but convergent mechanisms in airway and arterial chemoreceptors. *Respir Res*, 2: 145-149, 2001.
89. Cutz, E., Speirs, V., Yeger, H., Newman, C., Wang, D., and Perrin, D. G. Cell biology of pulmonary neuroepithelial bodies--validation of an in vitro model. I. Effects of hypoxia and Ca<sup>2+</sup> ionophore on serotonin content and exocytosis of dense core vesicles. *Anat Rec*, 236: 41-52, 1993.
90. Shweiki, D., Itin, A., Soffer, D., and Keshet, E. Vascular endothelial growth factor induced by hypoxia may mediate hypoxia-initiated angiogenesis. *Nature*, 359: 843-845, 1992.

91. Leung, D. W., Cachianes, G., Kuang, W. J., Goeddel, D. V., and Ferrara, N. Vascular endothelial growth factor is a secreted angiogenic mitogen. *Science*, **246**: 1306-1309, 1989.
92. Prentice, T. C. and Mirand, E. A. Effect of hypoxia on plasma erythropoietin in the rabbit. *Proc Soc Exp Biol Med*, **106**: 501-502, 1961.
93. DeGowin, R. L. and Johnson, S. Effect of endogenous erythropoiein on replicating hemopoietic stem cells. *Proc Soc Exp Biol Med*, **126**: 442-446, 1967.
94. Stenmark, K. R., Fagan, K. A., and Frid, M. G. Hypoxia-induced pulmonary vascular remodeling: cellular and molecular mechanisms. *Circ Res*, **99**: 675-691, 2006.
95. Preston, I. R., Hill, N. S., Warburton, R. R., and Fanburg, B. L. Role of 12-lipoxygenase in hypoxia-induced rat pulmonary artery smooth muscle cell proliferation. *Am J Physiol Lung Cell Mol Physiol*, **290**: L367-374, 2006.
96. Kourembanas, S. and Bernfield, M. Hypoxia and endothelial-smooth muscle cell interactions in the lung. *Am J Respir Cell Mol Biol*, **11**: 373-374, 1994.
97. Chen, Y. F. and Oparil, S. Endothelin and pulmonary hypertension. *J Cardiovasc Pharmacol*, **35**: S49-53, 2000.
98. Keith, I. M. The role of endogenous lung neuropeptides in regulation of the pulmonary circulation. *Physiol Res*, **49**: 519-537, 2000.
99. Ten, V. S. and Pinsky, D. J. Endothelial response to hypoxia: physiologic adaptation and pathologic dysfunction. *Curr Opin Crit Care*, **8**: 242-250, 2002.
100. Rafii, S. and Lyden, D. Therapeutic stem and progenitor cell transplantation for organ vascularization and regeneration. *Nat Med*, **9**: 702-712, 2003.
101. Yoon, C. H., Hur, J., Oh, I. Y., Park, K. W., Kim, T. Y., Shin, J. H., Kim, J. H., Lee, C. S., Chung, J. K., Park, Y. B., and Kim, H. S. Intercellular adhesion molecule-1 is upregulated in ischemic muscle, which mediates trafficking of endothelial progenitor cells. *Arterioscler Thromb Vasc Biol*, **26**: 1066-1072, 2006.
102. Romanic, A. M., Burns-Kurtis, C. L., Gout, B., Berrebi-Bertrand, I., and Ohlstein, E. H. Matrix metalloproteinase expression in cardiac myocytes following myocardial infarction in the rabbit. *Life Sci*, **68**: 799-814., 2001.

103. Hochachka, P. W. Defense strategies against hypoxia and hypothermia. *Science*, 231: 234-241, 1986.
104. Tinton, S., Tran-Nguyen, Q. N., and Buc-Calderon, P. Role of protein-phosphorylation events in the anoxia signal-transduction pathway leading to the inhibition of total protein synthesis in isolated hepatocytes. *Eur J Biochem*, 249: 121-126, 1997.
105. Buttgereit, F. and Brand, M. D. A hierarchy of ATP-consuming processes in mammalian cells. *Biochem J*, 312 ( Pt 1): 163-167, 1995.
106. Boutilier, R. G. and St-Pierre, J. Surviving hypoxia without really dying. *Comp Biochem Physiol A Mol Integr Physiol*, 126: 481-490, 2000.
107. Hue, L. and Rider, M. H. Role of fructose 2,6-bisphosphate in the control of glycolysis in mammalian tissues. *Biochem J*, 245: 313-324, 1987.
108. Marsin, A. S., Bertrand, L., Rider, M. H., Deprez, J., Beauloye, C., Vincent, M. F., Van den Berghe, G., Carling, D., and Hue, L. Phosphorylation and activation of heart PFK-2 by AMPK has a role in the stimulation of glycolysis during ischaemia. *Curr Biol*, 10: 1247-1255, 2000.
109. Minchenko, A., Leshchinsky, I., Opentanova, I., Sang, N., Srinivas, V., Armstead, V., and Caro, J. Hypoxia-inducible factor-1-mediated expression of the 6-phosphofructo-2-kinase/fructose-2,6-bisphosphatase-3 (PFKFB3) gene. Its possible role in the Warburg effect. *J Biol Chem*, 277: 6183-6187., 2002.
110. Kemp, B. E., Mitchelhill, K. I., Stapleton, D., Michell, B. J., Chen, Z. P., and Witters, L. A. Dealing with energy demand: the AMP-activated protein kinase. *Trends Biochem Sci*, 24: 22-25, 1999.
111. Hardie, D. G. and Hawley, S. A. AMP-activated protein kinase: the energy charge hypothesis revisited. *Bioessays*, 23: 1112-1119, 2001.
112. Ramaiah, A., Hathaway, J. A., and Atkinson, D. E. Adenylate as a Metabolic Regulator. Effect on Yeast Phosphofructokinase Kinetics. *J Biol Chem*, 239: 3619-3622, 1964.
113. Hardie, D. G. Metabolic control: a new solution to an old problem. *Curr Biol*, 10: R757-759, 2000.
114. Bartley, W., Clegg, E. J., and Butler, V. M. Enzyme changes in mice under hypoxic conditions. *Biochem J*, 109: 48P, 1968.
115. Wang, G. L. and Semenza, G. L. General involvement of hypoxia-inducible factor 1 in transcriptional response to hypoxia. *Proc. Natl. Acad. Sci. USA*, 90: 4304-4308, 1993.

116. Wang, G. L. and Semenza, G. L. Characterization of hypoxia-inducible factor 1 and regulation of DNA binding activity by hypoxia. *J. Biol. Chem.*, 268: 21513-21518, 1993.
117. Hogenesch, J. B., Chan, W. C., Jackiw, V. H., Brown, R. C., Gu, Y.-Z., Pray-Grant, M., Perdew, G. H., and Bradfield, C. A. Characterization of a subset of the basic-helix-loop-helix-PAS superfamily that interact with components of the dioxin signaling pathway. *J. Biol. Chem.*, 272: 8581-8593, 1997.
118. Pongratz, I., Antonsson, C., Whitelaw, M. L., and Poellinger, L. Role of the PAS domain in regulation of dimerization and DNA binding specificity of the dioxin receptor. *Molecular & Cellular Biology*, 18: 4079-4088, 1998.
119. He, Q., Cheng, P., Yang, Y., Wang, L., Gardner, K. H., and Liu, Y. White collar-1, a DNA binding transcription factor and a light sensor. *Science*, 297: 840-843, 2002.
120. Crews, S. T. and Fan, C. M. Remembrance of things PAS: regulation of development by bHLH-PAS proteins. *Curr Opin Genet Dev*, 9: 580-587, 1999.
121. Ryan, H. E., Lo, J., and Johnson, R. S. HIF-1 alpha is required for solid tumor formation and embryonic vascularization. *EMBO Journal*, 17: 3005-3015, 1998.
122. Kozak, K. R., Abbott, B., and Hankinson, O. ARNT-deficient mice and placental differentiation. *Developmental Biology*, 191: 297-305, 1997.
123. Jiang, B. H., Zheng, J. Z., Leung, S. W., Roe, R., and Semenza, G. L. Transactivation and inhibitory domains of hypoxia-inducible factor 1alpha. Modulation of transcriptional activity by oxygen tension. *Journal of Biological Chemistry*, 272: 19253-19260, 1997.
124. Jiang, B. H., Rue, E., Wang, G. L., Roe, R., and Semenza, G. L. Dimerization, DNA binding, and transactivation properties of hypoxia-inducible factor 1. *Journal of Biological Chemistry*, 271: 17771-17778, 1996.
125. Ruas, J. L., Poellinger, L., and Pereira, T. Functional analysis of hypoxia-inducible factor-1 alpha-mediated transactivation. Identification of amino acid residues critical for transcriptional activation and/or interaction with CREB-binding protein. *J Biol Chem*, 277: 38723-38730, 2002.
126. Salceda, S. and Caro, J. Hypoxia-inducible factor 1alpha (HIF-1alpha) protein is rapidly degraded by the ubiquitin-proteasome system under normoxic conditions. Its stabilization by hypoxia depends on redox-induced changes. *J Biol Chem*, 272: 22642-22647, 1997.

127. Huang, L. E., Gu, J., Schau, M., and Bunn, H. F. Regulation of hypoxia-inducible factor 1alpha is mediated by an O<sub>2</sub>-dependent degradation domain via the ubiquitin-proteasome pathway. *Proc. Natl. Acad. Sci. USA*, 95: 7987-7992, 1998.
128. Kallio, P. J., Wilson, W. J., S., O. B., Makino, Y., and Poellinger, L. Regulation of the hypoxia-inducible transcription factor 1alpha by the ubiquitin-proteasome pathway. *J. Biol. Chem.*, 274: 6519-6525, 1999.
129. Stiehl, D. P., Jelkmann, W., Wenger, R. H., and Hellwig-Burgel, T. Normoxic induction of the hypoxia-inducible factor 1alpha by insulin and interleukin-1beta involves the phosphatidylinositol 3-kinase pathway. *FEBS Lett*, 512: 157-162, 2002.
130. Richard, D. E., Berra, E., and Pouyssegur, J. Nonhypoxic pathway mediates the induction of hypoxia-inducible factor 1alpha in vascular smooth muscle cells. *J Biol Chem*, 275: 26765-26771, 2000.
131. Thornton, R. D., Lane, P., Borghaei, R. C., Pease, E. A., Caro, J., and Mochan, E. Interleukin 1 induces hypoxia-inducible factor 1 in human gingival and synovial fibroblasts. *Biochem J*, 350 Pt 1: 307-312, 2000.
132. Arsham, A. M., Plas, D. R., Thompson, C. B., and Simon, M. C. Phosphatidylinositol 3-kinase/Akt signaling is neither required for hypoxic stabilization of HIF-1 alpha nor sufficient for HIF-1-dependent target gene transcription. *J Biol Chem*, 277: 15162-15170., 2002.
133. Gomez-Manzano, C., Fueyo, J., Jiang, H., Glass, T. L., Lee, H. Y., Hu, M., Liu, J. L., Jasti, S. L., Liu, T. J., Conrad, C. A., and Yung, W. K. Mechanisms underlying PTEN regulation of vascular endothelial growth factor and angiogenesis. *Ann Neurol*, 53: 109-117, 2003.
134. Laughner, E., Taghavi, P., Chiles, K., Mahon, P. C., and Semenza, G. L. HER2 (neu) signaling increases the rate of hypoxia-inducible factor 1alpha (HIF-1alpha) synthesis: novel mechanism for HIF-1-mediated vascular endothelial growth factor expression. *Mol Cell Biol*, 21: 3995-4004, 2001.
135. Liu, Y., Christou, H., Morita, T., Laughner, E., Semenza, G. L., and Kourembanas, S. Carbon monoxide and nitric oxide suppress the hypoxic induction of vascular endothelial growth factor gene via the 5' enhancer. *Journal of Biological Chemistry*, 273: 15257-15262, 1998.
136. Wang, G. L. and Semenza, G. L. Desferrioxamine induces erythropoietin gene expression and hypoxia-inducible factor 1 DNA-binding activity: implications for models of hypoxia signal transduction. *Blood*, 82: 3610-3615, 1993.

137. Epstein, A. C., Gleadle, J. M., McNeill, L. A., Hewitson, K. S., O'Rourke, J., Mole, D. R., Mukherji, M., Metzen, E., Wilson, M. I., Dhanda, A., Tian, Y. M., Masson, N., Hamilton, D. L., Jaakkola, P., Barstead, R., Hodgkin, J., Maxwell, P. H., Pugh, C. W., Schofield, C. J., and Ratcliffe, P. J. C. *C. elegans* EGL-9 and mammalian homologs define a family of dioxygenases that regulate HIF by prolyl hydroxylation. *Cell*, *107*: 43-54., 2001.
138. Bruick, R. K. and McKnight, S. L. A conserved family of prolyl-4-hydroxylases that modify HIF. *Science*, *294*: 1337-1340., 2001.
139. Ryle, M. J. and Hausinger, R. H. Non-heme iron oxygenases. *Curr. Opin. Chem. Biol*, *6*: 193-201, 2002.
140. Lando, D., Peet, D. J., Gorman, J. J., Whelan, D. A., Whitelaw, M. L., and Bruick, R. K. FIH-1 is an asparaginyl hydroxylase enzyme that regulates the transcriptional activity of hypoxia-inducible factor. *Genes Dev*, *16*: 1466-1471, 2002.
141. Pereira, T., Zheng, X., Ruas, J. L., Tanimoto, K., and Poellinger, L. Identification of residues critical for regulation of protein stability and the transactivation function of the hypoxia-inducible factor-1alpha by the von Hippel-Lindau tumor suppressor gene product. *J Biol Chem*, *278*: 6816-6823, 2003.
142. Kallio, P. J., Okamoto, K., S., O. B., Carrero, P., Makino, Y., Tanaka, H., and Poellinger, L. Signal transduction in hypoxic cells: inducible nuclear translocation and recruitment of the CBP/p300 coactivator by the hypoxia-inducible factor-1alpha. *EMBO Journal*, *17*: 6573-6586, 1998.
143. Takahata, S., Sogawa, K., Kobayashi, A., Ema, M., Mimura, J., Ozaki, N., and Fujii-Kuriyama, Y. Transcriptionally active heterodimer formation of an Arnt-like PAS protein, Arnt3, with HIF-1a, HLF, and clock. *Bioch. Biophys. Res. Comm.*, *248*: 789-794, 1998.
144. Freedman, S. J., Sun, Z. Y., Poy, F., Kung, A. L., Livingston, D. M., Wagner, G., and Eck, M. J. Structural basis for recruitment of CBP/p300 by hypoxia-inducible factor-1 alpha. *Proc Natl Acad Sci U S A*, *99*: 5367-5372, 2002.
145. Dames, S. A., Martinez-Yamout, M., De Guzman, R. N., Dyson, H. J., and Wright, P. E. Structural basis for Hif-1 alpha /CBP recognition in the cellular hypoxic response. *Proc Natl Acad Sci U S A*, *99*: 5271-5276, 2002.
146. Sang, N., Fang, J., Srinivas, V., Leshchinsky, I., and Caro, J. Carboxyl-terminal transactivation activity of hypoxia-inducible factor 1 alpha is governed by a von Hippel-Lindau protein-independent, hydroxylation-regulated association with p300/CBP. *Mol Cell Biol*, *22*: 2984-2992, 2002.

147. Arany, Z., Huang, L. E., Eckner, R., Bhattacharya, S., Jiang, C., Goldberg, M. A., Bunn, H. F., and Livingston, D. M. An essential role for p300/CBP in the cellular response to hypoxia. *Proceedings of the National Academy of Sciences of the United States of America*, 93: 12969-12973, 1996.
148. Hewitson, K. S., McNeill, L. A., Riordan, M. V., Tian, Y. M., Bullock, A. N., Welford, R. W., Elkins, J. M., Oldham, N. J., Bhattacharya, S., Gleadle, J. M., Ratcliffe, P. J., Pugh, C. W., and Schofield, C. J. Hypoxia-inducible Factor (HIF) Asparagine Hydroxylase Is Identical to Factor Inhibiting HIF (FIH) and Is Related to the Cupin Structural Family. *J Biol Chem*, 277: 26351-26355., 2002.
149. McNeill, L. A., Hewitson, K. S., Gleadle, J. M., Horsfall, L. E., Oldham, N. J., Maxwell, P. H., Pugh, C. W., Ratcliffe, P. J., and Schofield, C. J. The use of dioxygen by HIF prolyl hydroxylase (PHD1). *Bioorg Med Chem Lett*, 12: 1547-1550., 2002.
150. Lee, C., Kim, S. J., Jeong, D. G., Lee, S. M., and Ryu, S. E. Structure of human FIH-1 reveals a unique active site pocket and interaction sites for HIF-1 and von Hippel-Lindau. *J Biol Chem*, 278: 7558-7563, 2003.
151. Koivunen, P., Hirsila, M., Gunzler, V., Kivirikko, K. I., and Myllyharju, J. Catalytic properties of the asparaginyl hydroxylase (FIH) in the oxygen sensing pathway are distinct from those of its prolyl 4-hydroxylases. *J Biol Chem*, 279: 9899-9904, 2004.
152. Richard, D. E., Berra, E., Gothie, E., Roux, D., and Pouyssegur, J. p42/p44 mitogen-activated protein kinases phosphorylate hypoxia-inducible factor 1alpha (HIF-1alpha) and enhance the transcriptional activity of HIF-1. *J Biol Chem*, 274: 32631-32637., 1999.
153. Sodhi, A., Montaner, S., Miyazaki, H., and Gutkind, J. S. MAPK and Akt act cooperatively but independently on hypoxia inducible factor-1alpha in rasV12 upregulation of VEGF. *Biochem Biophys Res Commun*, 287: 292-300, 2001.
154. Gradin, K., Takasaki, C., Fujii-Kuriyama, Y., and Sogawa, K. The transcriptional activation function of the HIF-like factor requires phosphorylation at a conserved threonine. *J Biol Chem*, 277: 23508-23514., 2002.
155. Mylonis, I., Chachami, G., Samiotaki, M., Panayotou, G., Paraskeva, E., Kalousi, A., Georgatsou, E., Bonanou, S., and Simos, G. Identification of MAPK phosphorylation sites and their role in the localization and activity of hypoxia-inducible factor-1alpha. *J Biol Chem*, 281: 33095-33106, 2006.
156. Jeong, J. W., Bae, M. K., Ahn, M. Y., Kim, S. H., Sohn, T. K., Bae, M. H., Yoo, M. A., Song, E. J., Lee, K. J., and Kim, K. W. Regulation and

- destabilization of HIF-1 $\alpha$  by ARD1-mediated acetylation. *Cell*, 111: 709-720., 2002.
157. Fisher, T. S., Etages, S. D., Hayes, L., Crimin, K., and Li, B. Analysis of ARD1 Function in Hypoxia Response Using Retroviral RNA Interference. *J. Biol. Chem.*, 280: 17749-17757, 2005.
  158. Kim, S. H., Park, J. A., Kim, J. H., Lee, J. W., Seo, J. H., Jung, B. K., Chun, K. H., Jeong, J. W., Bae, M. K., and Kim, K. W. Characterization of ARD1 variants in mammalian cells. *Biochem Biophys Res Commun*, 340: 422-427, 2006.
  159. Wang, G. L. and Semenza, G. L. Molecular basis of hypoxia-induced erythropoietin expression. *Current Opinion in Hematology*, 3: 156-162, 1996.
  160. Forsythe, J. A., Jiang, B. H., Iyer, N. V., Agani, F., Leung, S. W., Koos, R. D., and Semenza, G. L. Activation of vascular endothelial growth factor gene transcription by hypoxia-inducible factor 1. *Mol. Cell. Biol.*, 16: 4604-4613, 1996.
  161. Nguyen, S. V. and Claycomb, W. C. Hypoxia regulates the expression of the adrenomedullin and HIF-1 genes in cultured HL-1 cardiomyocytes. *Biochem Biophys Res Co*, 265: 382-386., 1999.
  162. Feldser, D., Agani, F., Iyer, N. V., Pak, B., Ferreira, G., and Semenza, G. L. Reciprocal positive regulation of hypoxia-inducible factor 1 $\alpha$  and insulin-like growth factor 2. *Cancer Res*, 59: 3915-3918, 1999.
  163. Wykoff, C. C., Beasley, N. J., Watson, P. H., Turner, K. J., Pastorek, J., Sibtain, A., Wilson, G. D., Turley, H., Talks, K. L., Maxwell, P. H., Pugh, C. W., Ratcliffe, P. J., and Harris, A. L. Hypoxia-inducible expression of tumor-associated carbonic anhydrases. *Cancer Res*, 60: 7075-7083, 2000.
  164. Ebert, B. L., Firth, J. D., and Ratcliffe, P. J. Hypoxia and Mitochondrial Inhibitors Regulate Expression of Glucose Transporter-1 via Distinct Cis-acting Sequences. *J. Biol. Chem.*, 270: 29083-29089, 1995.
  165. Semenza, G. L. Targeting HIF-1 for cancer therapy. *Nat Rev Cancer*, 3: 721-732, 2003.
  166. Sowter, H. M., Ratcliffe, P. J., Watson, P., Greenberg, A. H., and Harris, A. L. HIF-1-dependent regulation of hypoxic induction of the cell death factors BNIP3 and NIX in human tumors. *Cancer Res*, 61: 6669-6673., 2001.

167. Shoshani, T., Faerman, A., Mett, I., Zelin, E., Tenne, T., Gorodin, S., Moshel, Y., Elbaz, S., Budanov, A., Chajut, A., Kalinski, H., Kamer, I., Rozen, A., Mor, O., Keshet, E., Leshkowitz, D., Einat, P., Skaliter, R., and Feinstein, E. Identification of a novel hypoxia-inducible factor 1-responsive gene, RTP801, involved in apoptosis. *Mol Cell Biol*, 22: 2283-2293, 2002.
168. Vande Velde, C., Cizeau, J., Dubik, D., Alimonti, J., Brown, T., Israels, S., Hakem, R., and Greenberg, A. H. BNIP3 and genetic control of necrosis-like cell death through the mitochondrial permeability transition pore. *Mol Cell Biol*, 20: 5454-5468, 2000.
169. Kubasiak, L. A., Hernandez, O. M., Bishopric, N. H., and Webster, K. A. Hypoxia and acidosis activate cardiac myocyte death through the Bcl-2 family protein BNIP3. *Proc Natl Acad Sci U S A*, 99: 12825-12830, 2002.
170. Kubasiak, L. A., Hernandez, O. M., Bishopric, N. H., and Webster, K. A. Hypoxia and acidosis activate cardiac myocyte death through the Bcl-2 family protein BNIP3. *Proc Natl Acad Sci USA*, 99: 12825-12830, 2002.
171. Cifone, M. A., Myhr, B., Eiche, A., and Bolcsfoldi, G. Effect of pH shifts on the mutant frequency at the thymidine kinase locus in mouse lymphoma L5178Y TK+/- cells. *Mutat Res*, 189: 39-46, 1987.
172. Yuan, J., Narayanan, L., Rockwell, S., and Glazer, P. M. Diminished DNA repair and elevated mutagenesis in mammalian cells exposed to hypoxia and low pH. *Cancer Res*, 60: 4372-4376, 2000.
173. Murdoch, C. and Lewis, C. E. Macrophage migration and gene expression in response to tumor hypoxia. *Int J Cancer*, 117: 701-708, 2005.
174. Weinmann, M., Belka, C., and Plasswilm, L. Tumour hypoxia: impact on biology, prognosis and treatment of solid malignant tumours. *Onkologie*, 27: 83-90, 2004.
175. Li, C. and Jackson, R. M. Reactive species mechanisms of cellular hypoxia-reoxygenation injury. *Am J Physiol Cell Physiol*, 282: C227-241, 2002.
176. Erecinska, M. and Silver, I. A. Tissue oxygen tension and brain sensitivity to hypoxia. *Respir Physiol*, 128: 263-276, 2001.
177. Biagas, K. Hypoxic-ischemic brain injury: advancements in the understanding of mechanisms and potential avenues for therapy. *Curr Opin Pediatr*, 11: 223-228, 1999.
178. Bhatia, G., Sosin, M., Leahy, J. F., Connolly, D. L., Davis, R. C., and Lip, G. Y. Hibernating myocardium in heart failure. *Expert Rev Cardiovasc Ther*, 3: 111-122, 2005.

179. Buja, L. M. Myocardial ischemia and reperfusion injury. *Cardiovasc Pathol*, **14**: 170-175, 2005.
180. Kloner, R. A. and Jennings, R. B. Consequences of brief ischemia: stunning, preconditioning, and their clinical implications: part 2. *Circulation*, **104**: 3158-3167, 2001.
181. Braunwald, E. and Kloner, R. A. The stunned myocardium: prolonged, postischemic ventricular dysfunction. *Circulation*, **66**: 1146-1149, 1982.
182. Ryan, H. E., Poloni, M., McNulty, W., Elson, D., Gassmann, M., Arbeit, J. M., and Johnson, R. S. Hypoxia-inducible factor-1alpha is a positive factor in solid tumor growth. *Cancer Res*, **60**: 4010-4015, 2000.
183. Aebbersold, D. M., Burri, P., Beer, K. T., Laissue, J., Djonov, V., Greiner, R. H., and Semenza, G. L. Expression of hypoxia-inducible factor-1alpha: a novel predictive and prognostic parameter in the radiotherapy of oropharyngeal cancer. *Cancer Res*, **61**: 2911-2916, 2001.
184. Wiesener, M. S. and Eckardt, K. U. Erythropoietin, tumours and the von Hippel-Lindau gene: towards identification of mechanisms and dysfunction of oxygen sensing. *Nephrol Dial Transplant*, **17**: 356-359, 2002.
185. Dachs, G. U. and Tozer, G. M. Hypoxia modulated gene expression: angiogenesis, metastasis and therapeutic exploitation. *Eur J Cancer*, **36**: 1649-1660, 2000.
186. Sondergaard, K. L., Hilton, D. A., Penney, M., Ollerenshaw, M., and Demaine, A. G. Expression of hypoxia-inducible factor 1alpha in tumours of patients with glioblastoma. *Neuropathol Appl Neurobiol*, **28**: 210-217, 2002.
187. Talks, K. L., Turley, H., Gatter, K. C., Maxwell, P. H., Pugh, C. W., Ratcliffe, P. J., and Harris, A. L. The expression and distribution of the hypoxia-inducible factors HIF-1alpha and HIF-2alpha in normal human tissues, cancers, and tumor-associated macrophages. *Am J Pathol*, **157**: 411-421, 2000.
188. Zhong, H., De Marzo, A. M., Laughner, E., Lim, M., Hilton, D. A., Zagzag, D., Buechler, P., Isaacs, W. B., Semenza, G. L., and Simons, J. W. Overexpression of hypoxia-inducible factor 1alpha in common human cancers and their metastases. *Cancer Res*, **59**: 5830-5835, 1999.
189. Wartenberg, M., Ling, F. C., Muschen, M., Klein, F., Acker, H., Gassmann, M., Petrat, K., Putz, V., Hescheler, J., and Sauer, H. Regulation of the multidrug resistance transporter P-glycoprotein in multicellular tumor spheroids by hypoxia-inducible factor (HIF-1) and reactive oxygen species. *Faseb J*, **17**: 503-505, 2003.

190. Finkel, T. Oxygen radicals and signaling. *Curr Opin Cell Biol*, 10: 248-253, 1998.
191. Palmer, H. J. and Paulson, K. E. Reactive oxygen species and antioxidants in signal transduction and gene expression. *Nutr Rev*, 55: 353-361, 1997.
192. Sies, H. Strategies of antioxidant defense. *Eur J Biochem*, 215: 213-219, 1993.
193. Byrne, J. A., Grieve, D. J., Cave, A. C., and Shah, A. M. Oxidative stress and heart failure. *Arch Mal Coeur Vaiss*, 96: 214-221, 2003.
194. Brand, M. D., Affourtit, C., Esteves, T. C., Green, K., Lambert, A. J., Miwa, S., Pakay, J. L., and Parker, N. Mitochondrial superoxide: production, biological effects, and activation of uncoupling proteins. *Free Radic Biol Med*, 37: 755-767, 2004.
195. Turrens, J. F. Mitochondrial formation of reactive oxygen species. *J Physiol*, 552: 335-344, 2003.
196. Madesh, M. and Hajnoczky, G. VDAC-dependent permeabilization of the outer mitochondrial membrane by superoxide induces rapid and massive cytochrome c release. *J Cell Biol*, 155: 1003-1015, 2001.
197. Mello Filho, A. C. and Meneghini, R. In vivo formation of single-strand breaks in DNA by hydrogen peroxide is mediated by the Haber-Weiss reaction. *Biochim Biophys Acta*, 781: 56-63, 1984.
198. Imlay, J. A., Chin, S. M., and Linn, S. Toxic DNA damage by hydrogen peroxide through the Fenton reaction in vivo and in vitro. *Science*, 240: 640-642, 1988.
199. Zhang, L., Yu, L., and Yu, C. A. Generation of superoxide anion by succinate-cytochrome c reductase from bovine heart mitochondria. *J Biol Chem*, 273: 33972-33976, 1998.
200. Starkov, A. A., Fiskum, G., Chinopoulos, C., Lorenzo, B. J., Browne, S. E., Patel, M. S., and Beal, M. F. Mitochondrial alpha-ketoglutarate dehydrogenase complex generates reactive oxygen species. *J Neurosci*, 24: 7779-7788, 2004.
201. Cadenas, E. and Davies, K. J. Mitochondrial free radical generation, oxidative stress, and aging. *Free Radic Biol Med*, 29: 222-230, 2000.
202. Touati, D. Iron and oxidative stress in bacteria. *Arch Biochem Biophys*, 373: 1-6, 2000.

203. Leonard, S., Gannett, P. M., Rojanasakul, Y., Schwegler-Berry, D., Castranova, V., Vallyathan, V., and Shi, X. Cobalt-mediated generation of reactive oxygen species and its possible mechanism. *J Inorg Biochem*, 70: 239-244, 1998.
204. Salnikow, K., Blagosklonny, M. V., Ryan, H., Johnson, R., and Costa, M. Carcinogenic nickel induces genes involved with hypoxic stress. *Cancer Research*, 60: 38-41, 2000.
205. Shi, X., Dalal, N. S., and Kasprzak, K. S. Generation of free radicals from model lipid hydroperoxides and H<sub>2</sub>O<sub>2</sub> by Co(II) in the presence of cysteinyl and histidyl chelators. *Chem Res Toxicol*, 6: 277-283, 1993.
206. O'Brien, T., Xu, J., and Patierno, S. R. Effects of glutathione on chromium-induced DNA crosslinking and DNA polymerase arrest. *Mol Cell Biochem*, 222: 173-182, 2001.
207. Kasprzak, K. S. Oxidative DNA and protein damage in metal-induced toxicity and carcinogenesis. *Free Radic Biol Med*, 32: 958-967, 2002.
208. Chin, T. A. and Templeton, D. M. Protective elevations of glutathione and metallothionein in cadmium-exposed mesangial cells. *Toxicology*, 77: 145-156, 1993.
209. Hussain, T., Shukla, G. S., and Chandra, S. V. Effects of cadmium on superoxide dismutase and lipid peroxidation in liver and kidney of growing rats: in vivo and in vitro studies. *Pharmacol Toxicol*, 60: 355-358, 1987.
210. Filipic, M. and Hei, T. K. Mutagenicity of cadmium in mammalian cells: implication of oxidative DNA damage. *Mutat Res*, 546: 81-91, 2004.
211. Lesnefsky, E. J. and Hoppel, C. L. Ischemia-reperfusion injury in the aged heart: role of mitochondria. *Arch Biochem Biophys*, 420: 287-297, 2003.
212. Lesnefsky, E. J., Gallo, D. S., Ye, J., Whittingham, T. S., and Lust, W. D. Aging increases ischemia-reperfusion injury in the isolated, buffer-perfused heart. *J Lab Clin Med*, 124: 843-851, 1994.
213. Vanden Hoek, T. L., Becker, L. B., Shao, Z., Li, C., and Schumacker, P. T. Reactive oxygen species released from mitochondria during brief hypoxia induce preconditioning in cardiomyocytes. *Journal of Biological Chemistry*, 273: 18092-18098, 1998.
214. Nelson, D. R., Zeldin, D. C., Hoffman, S. M., Maltais, L. J., Wain, H. M., and Nebert, D. W. Comparison of cytochrome P450 (CYP) genes from the mouse and human genomes, including nomenclature recommendations for genes, pseudogenes and alternative-splice variants. *Pharmacogenetics*, 14: 1-18, 2004.

215. Jezek, P. and Hlavata, L. Mitochondria in homeostasis of reactive oxygen species in cell, tissues, and organism. *Int J Biochem Cell Biol*, 37: 2478-2503, 2005.
216. Schrader, M. and Fahimi, H. D. Mammalian peroxisomes and reactive oxygen species. *Histochem Cell Biol*, 122: 383-393, 2004.
217. Cappola, T. P., Kass, D. A., Nelson, G. S., Berger, R. D., Rosas, G. O., Kobeissi, Z. A., Marban, E., and Hare, J. M. Allopurinol improves myocardial efficiency in patients with idiopathic dilated cardiomyopathy. *Circulation*, 104: 2407-2411, 2001.
218. Babior, B. M. The NADPH oxidase of endothelial cells. *IUBMB Life*, 50: 267-269, 2000.
219. Yu, B. P. Cellular defenses against damage from reactive oxygen species. *Physiol Rev*, 74: 139-162, 1994.
220. Ames, B. N., Gold, L. S., and Willett, W. C. The causes and prevention of cancer. *Proc Natl Acad Sci U S A*, 92: 5258-5265, 1995.
221. Beckman, K. B. a. A., B.N. Oxidants, Antioxidants and Aging. *In: J. G. Scandalios (ed.), Oxidative Stress and Molecular Biology of Antioxidant Dfenses*, Vol. 1, pp. 46. New York: Cod Spring Harbor Laboratory Press, 1997.

## CHAPTER 1

Vengellur, Ajith, Phillips, Jennifer M., Hogenesch, John B., Lapres, John J. (2005). Gene Expression Profiling of Hypoxia Signaling in Human Hepatocellular Carcinoma Cells. Physiological Genomics, 22: 308-318.

## **Abstract**

Cellular, local, and organismal responses to low oxygen availability occur during processes such as anaerobic metabolism, wound healing, and pathological conditions such as stroke and cancer. These responses include increases in glycolytic activity, vascularization, breathing and red blood cell production, and they are mediated in part by the hypoxia inducible factors (HIFs), which receive information on O<sub>2</sub> levels from a group of iron and oxygen-dependent hydroxylases. Hypoxia mimics, such as cobalt chloride, nickel chloride, and deferoxamine, act to simulate hypoxia by altering the iron status of these hydroxylases. To determine if these mimics are appropriate substitutes for lower oxygen tension evoked naturally, we compared transcriptional responses of a Hep3B cell line using high-density oligonucleotide arrays. A battery of core genes was identified that was shared by all four treatments (hypoxia, cobalt, nickel and deferoxamine) including glycolytic enzymes, cell cycle regulators and apoptotic genes. Importantly, cobalt, nickel and deferoxamine influenced transcription of distinct sets of genes that were not affected by cellular hypoxia. These global responses to hypoxia indicate a balancing act between adaptation and programmed cell death, and suggest caution in the use of hypoxia mimics as a substitute for low O<sub>2</sub> tension that occurs *in vivo*.

## **Introduction**

Cells, tissues, and organisms are said to be hypoxic when they receive less than normal levels of oxygen. Given the central role of oxygen in the production of adenosine triphosphate (ATP) through oxidative phosphorylation, it is critical for cells and tissue to respond rapidly to hypoxia. The importance of hypoxia signaling is further highlighted by its essential role in mammalian development, and several pathological conditions such as cardiovascular disease and cancer (1). This response is regulated by a family of transcription factors called the hypoxia inducible factors (HIFs). HIFs are members of the bHLH-PAS (basic-helix-loop-helix-PER, ARNT, SIM) family of transcription factors (2). For a detailed description of the pathway and its regulation see the “introduction” chapter. Under normoxic conditions, HIF1 $\alpha$  is ubiquitously transcribed, translated, and subsequently degraded. Under hypoxic conditions, however, HIF1 $\alpha$  protein becomes stabilized (3-5). This oxygen-dependent degradation of the HIF1 $\alpha$  protein is primarily controlled by a family of non-heme oxygenases called prolyl hydroxylase domain containing proteins (PHDs, also known as HIF prolyl hydroxylase) (6, 7). The iron-dependent activity of the PHD enzymes may help explain the ability of iron chelators and divalent metals to promote a hypoxic-like response. In fact, cobalt chloride and nickel chloride, transition metals capable of competing with iron at binding sites; and deferoxamine (DFO), an iron chelator, are widely used hypoxia mimics. The appropriateness of these hypoxia mimics has not been thoroughly tested. These current studies were performed to characterize the battery of hypoxia regulated genes and to test the

hypothesis that cobalt chloride, nickel chloride, and DFO were capable of modulating a similar battery of genes and act as true hypoxia mimics. To address these goals, the hepatocellular carcinoma cell line, Hep3B, was exposed to hypoxia, cobalt chloride, nickel chloride or DFO, total RNA extracted, and transcriptional responses were evaluated using high density oligonucleotide arrays. Comparisons among the four treatments suggest that there is substantial overlap; however, there is also a large set of genes that are specific for the individual treatments.

## **Materials and Methods**

*Cell culture:* Hep3B cells were maintained in MEM (Invitrogen) supplemented with 10% fetal bovine serum (Hyclone, Logan, UT), 20 mM L-glutamine, 1 mM MEM non-essential amino acids, 100 mM HEPES (pH=7.4), 1,000 units/ml penicillin G and 1,000  $\mu$ g/ml streptomycin sulfate (Invitrogen). They were approximately 70% confluent at the time of treatment. Cells were maintained at 37°C, 5% CO<sub>2</sub> and 21% O<sub>2</sub> prior to treatment. Hypoxia treatment (1% O<sub>2</sub>) was performed in oxygen-regulated incubator (Precision-NAPCO 7000, Winchester, VA) at 37°C and 5% CO<sub>2</sub>. Cobalt chloride (100  $\mu$ M), nickel chloride (100  $\mu$ M) and deferoxamine (100  $\mu$ M) treatments were performed at 37°C, 5% CO<sub>2</sub> and 21% O<sub>2</sub>.

*RNA extraction:* RNA was extracted by homogenization (Polytron, Kinematica, Lucerne, Switzerland) in TRIzol reagent (GIBCO/BRL) (added to cell pellet) at maximum speed for 90-120 sec. The homogenate was allowed to incubate for five minutes at room temperature, a 1/5 volume of chloroform was added, the tube was vortexed, and finally subjected to centrifugation at 12,000 x g for 15 minutes. The aqueous phase was isolated, and a half volume of isopropanol was added to precipitate the RNA. Following this initial isolation, a secondary purification was performed with the Qiagen RNeasy Total RNA isolation kit according to manufacturer's specifications. The purified total RNA was finally eluted in 10  $\mu$ L of DEPC treated H<sub>2</sub>O, and quantity and integrity were characterized using a Beckman DU640 UV spectrophotometer and Agilent Bioanalyzer 2100.

*RNA labeling:* Briefly, 5  $\mu$ g total RNA from separate biological replicates was used to make first strand cDNA using the Superscript Choice system (Gibco BRL) and a T7 promotor/oligodT primer (Gibco). Second strand cDNA was also made with the Superscript Choice system. The resulting cDNA was subjected to phenol:chloroform purification and ammonium acetate precipitation, and used as a template to make biotinylated amplified antisense cRNA using T7 RNA polymerase (Enzo kit, Affymetrix). Twenty micrograms cRNA was fragmented to a range of 20 to 100 bases in length using fragmentation buffer (200 mM Tris-acetate, pH 8.1, 500 mM KOAc, 150 mM MgOAc) and heating for 35 minutes at

94 °C. The quality of cRNA and size distribution of fragmented cRNA was examined by both agarose and polyacrylamide gel electrophoresis.

*Hybridization:* 20 µg of cRNA was hybridized to a U95A version 1 gene chip (Affymetrix) in with 1 X MES hybridization buffer using standard protocols outlined in the Gene Chip® Expression Analysis Technical Manual (Affymetrix). Hybridization was conducted in a GeneChip Hybridization Oven for 16 hours at 45 °C. Following hybridization, the arrays were washed on a Genechip Fluidics Station 400 according to manufacturer's instructions (Affymetrix). The arrays were finally scanned using a Hewlett Packard 2500A Gene Array Scanner and the raw images were analyzed using the MAS4 Software Suite (Affymetrix). Finally, quality of cRNA was assessed by examining 3'/5' ratios for GAPDH oligonucleotides present on the arrays.

*Data Analysis:* CEL files were condensed using the GCRMA algorithm in R ([www.r-project.org](http://www.r-project.org)) (8-10). Pair-wise comparisons between control and treatment conditions were conducted using a Students T-Test, two sample, equal variance on log<sub>2</sub> transformed data. Fold change calculations were performed in Excel on data that was median-scaled to a global intensity target value of 100. For each treatment vs. control condition, genes that changed were assigned based on a t-test value of <0.05 and a fold change value of > 2.

*Relative Real-Time PCR analysis:* Changes in gene expression observed by microarray analyses were verified by real-time PCR, performed on an Applied Biosystems Prism 7000 Sequence detection System (Foster City, CA) as described (11). Briefly, cDNA was synthesized from total RNA (1 µg per sample per treatment, n=6) in a reverse transcriptase reaction in 20 µl of 1X First Strand Synthesis buffer (Invitrogen, Carlsbad, CA) containing 1 µg oligo (5'-T<sub>21</sub>VN-3'), 0.2 mM dNTPs, 10 mM DTT, and 200 IU of Superscript II reverse transcriptase (Invitrogen). The reaction mixture was incubated at 42 °C for 60 min, and stopped by incubation at 75 °C for 15 min. Amplification of cDNA (1/20) was performed using SYBR Green PCR buffer (1x AmpliTaq™ Gold PCR Buffer, 0.025 U/µl AmpliTaq™ Gold (Perkin-Elmer, Wellesley, MA), 0.2 mM dNTPs, 1 ng/µl 6-carboxy-X-rhodamine, 1:40,000 diluted SYBR® Green Dye and 3% DMSO) and 0.1 µM primers. The thermal cycling parameters were 95°C for 10 min followed by 40 cycles of 95°C for 15 seconds and 60°C for 60 seconds. The mRNA expression for each gene was determined by comparing it with a standard curve of known quantities of the specific target. This measurement was controlled for RNA quality, quantity, and RT efficiency by normalizing it to the expression level of the hypoxanthine guanine phosphoribosyl transferase (HPRT) gene. HPRT was used as a control gene because it was shown to be unaffected by any treatment used. Each primer set produced a single product as determined by melt-curve analysis and amplicons were of correct size as analyzed by agarose gel electrophoresis. Statistical significance was determined using normalized fold changes and student *t*-test.

Primers were designed using the web based application Primer3 ([http://www-genome.wi.mit.edu/cgi-bin/primer/primer3\\_www.cgi](http://www-genome.wi.mit.edu/cgi-bin/primer/primer3_www.cgi)) biasing towards the 3' end of the transcript to maximize the likelihood of giving a gene specific product. The settings used in Primer3 were 125 bp amplicon, 20mers, 60°C melting temperatures and all other as defaults. Primer sequences were analyzed by BLAST. Gene names, accession numbers, and forward and reverse primer sequences are listed in Table 2.

## **Results**

Gene expression measurements were generated following 24 hour exposure to each of the five treatments, normoxia, hypoxia, cobalt, nickel and deferoxamine, in Hep3b cells. To examine the global relatedness of each of these stimuli, we performed hierarchal clustering on the entire data set. These results indicated that there is considerable similarity among the four stimuli (data not shown). To compare directly the effects of these treatments on the complete data set, an analysis of variance (ANOVA) was performed. The results showed that greater than 38% (3,404/12,626 probe sets) were significantly ( $p < 0.05$ ) influenced by treatment. These results suggest that hypoxia and hypoxia mimics have profound effects on cellular homeostasis and that there is considerable similarity among the four hypoxia treatments.

**Table 2.** Primers used in qRT-PCR

Gene	Accession #	Forward	Reverse
HPRT	NM_000194	gaccagtaacaggggacat	cctgaccaaggaaagcaaaag
VEGF	AF024710	tctcacaccattgaaacca	gattcctgccctgtctctcg
HumIP (IP30)	BC031020	tgcataattccaacaagggtgga	gccaggcaatagtgccagactt
SLC6A8	NM_005629	ctggaacatctgtcccctgt	cagcgggtggtaaaaggact
PK1	NM_002610	tctggatcagtgaaagctctg	accaaatgaaacggatggctg
Carb. Amh. (MaTu)	NM_001216	acttcagccgctactccaa	agaggggtgggagcgtctta
IL8	M28130	tagccaggattccaacagtc	gcttcacatgtccacaa
HGFAL	NM_004132	ctctcttaaccctcccacag	cgctggatataacagctctc
Inhibin	NM_002193	aaggacacaaccctcagag	tttagccccctctctctcc
MAOA	NM_000240	acataaaggagttgcccgata	agcatttcccaaaagggtg
MCT3	NM_004207	acaacactggactggctcaagg	ctctcggaaatgacacggctcc
15-PGDH	NM_000860	tgggtaaaactctttgcaagc	agctgggaggtctggagta
Cyp1a1	NM_000499	cttcgcacactctctctcg	ggattgctgcaccctggttt

A direct comparison of each treatment was also performed to identify subsets of genes that were shared, and those that were unique, among treatment groups. Genes that showed significant changes in expression ( $p < 0.05$  and greater than 2 fold change) were compared. At these significance levels, hypoxia (1% O<sub>2</sub>) influenced 451 different probe sets. These sets of responsive genes included well known hypoxia-regulated genes such as glyceraldehydes-3-phosphate dehydrogenase (GAPDH), vascular endothelial growth factor (VEGF), insulin growth factor II (IGFII), carbonic anhydrase, and plasminogen activator inhibitor I (PAI I) (12), (13) (Table 3). This list of hypoxia responsive genes also included several genes that had not previously been demonstrated to be modulated by low oxygen tension. For example, pyruvate dehydrogenase kinase 1 (PDK1) and the creatine transporter, SLC6A8 were upregulated 4.7 and 5.7 fold respectively. In addition, the NAD<sup>+</sup>-dependent 15 hydroxyprostaglandin dehydrogenase and prohibitin genes were significantly down-regulated following hypoxia exposure. These results confirm the appropriateness of our data analysis and suggest that a more complete set of hypoxia responsive genes were identified.

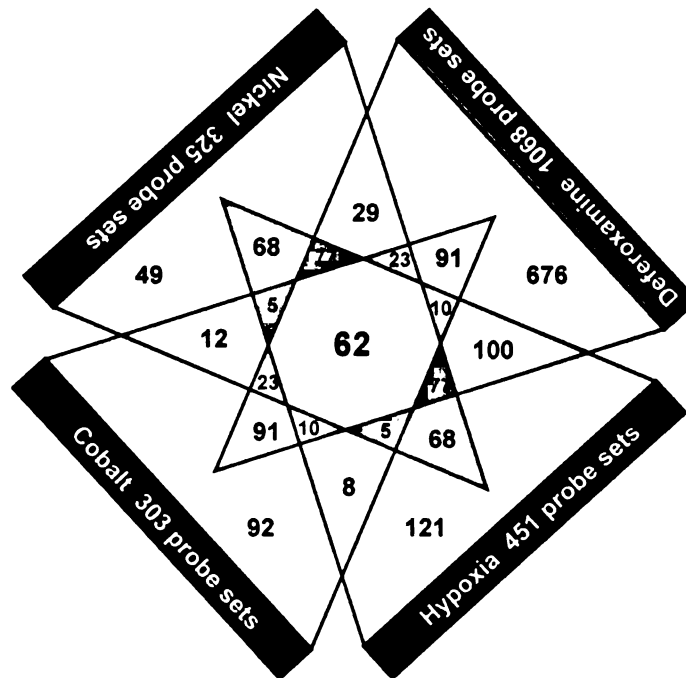
The other three treatments, cobalt, DFO and nickel, also had profound effects on the cells. Cobalt exposure (100  $\mu$ M, 24 hours) led to the significant change ( $p < 0.05$  and greater than 2 fold) in transcription of 303 probe sets (Figure 5). Of these 303 probes sets, 85 (28%) overlapped with the hypoxia responsive subset. Nickel exposure altered the expression of a similar number of genes as cobalt (325 probe sets), however, a higher percentage overlapped with the hypoxia

**Table 3. Top 20 hypoxia up and down-regulated probe sets**

Probe Set	FOLD CHANGE				Descriptions
	HYP	COB	DFO	NICK	
39352_at	-13.1	-1.9	2.5	-6.7	thyroid-stimulating hormone alpha subunit
1025_g_at	-10.2	-5.9	-14.7	-8.2	HSCYP450 Human gene for cytochrome P(1)-450
32570_at	-6.9	-5.8	-7.3	-5.4	15 hydroxyprostaglandin dehydrogenase (PGDH)
742_at	-5.0	-9.6	-4.4	-11.4	Human mRNA for HGF activator like protein
40588_r_at	-4.7	1.0	-4.8	-2.9	p18 protein
41363_at	-4.7	-1.7	-6.4	-2.6	survival of motor neuron protein interacting protein 1
39382_at	-4.5	-1.5	-3.4	-2.2	mRNA for KIAA0517 gb=AB011089
36592_at	-4.5	-1.5	-8.3	-2.6	prohibitin
38680_at	-4.4	-1.4	-1.6	-2.0	Alu repeats, region 5 to the SNRP E gene
39355_at	-4.3	-1.4	-6.5	-2.6	2-5A binding protein
31880_at	-4.1	-1.4	-6.6	-3.5	N9 Rep-8 gb=D83767
36636_at	-4.0	1.0	1.1	-1.9	ornithine aminotransferase
41772_at	-4.0	-2.2	-4.7	-2.9	monoamine oxidase A
38323_at	-4.0	1.1	-7.1	-2.8	BAC clone RG113D17 gb=AC005162
33791_at	-3.9	1.9	-2.6	-2.3	leukemia associated gene 1
38372_at	-3.9	-1.1	-1.7	-2.6	U66042:Human clone 191B7
40788_at	-3.9	1.0	-1.3	-2.6	adenylate kinase 2A (AK2A)
1969_s_at	-3.8	-1.0	-1.8	-2.9	CDK activating kinase
41246_at	-3.7	-1.4	1.8	-3.9	Homo sapiens gb=AI743134
37297_at	-3.7	-1.4	-3.7	-2.4	Homo sapiens DKFZp586A191
37758_s_at	4.6	-1.1	4.8	4.5	Homo sapiens gb=W28479
39827_at	4.7	4.4	4.7	6.8	Homo sapiens gb=AA522530
36386_at	4.7	10.8	14.9	3.9	pyruvate dehydrogenase kinase isoenzyme 1
40790_at	4.9	4.0	8.0	4.2	DEC1
36101_s_at	5.0	3.6	7.2	4.1	vascular endothelial growth factor
38545_at	5.2	2.5	12.1	4.0	testicular inhibin beta-B-subunit
40926_at	5.8	12.1	25.5	6.7	creatine transporter (SLC6A8)
38125_at	6.3	10.6	22.8	7.9	plasminogen activator inhibitor I
HUMGAPDH	6.5	-1.0	2.9	2.7	glyceraldehyde-3-phosphate dehydrogenase
40888_f_at	6.6	-1.3	3.6	3.3	Homo sapiens gb=W28170
34777_at	6.8	33.1	39.4	3.9	adrenomedullin precursor
32588_s_at	7.0	-2.5	1.3	8.5	ERF-2
40309_at	8.1	39.4	39.9	5.7	Carbonic anhydrases (MaTu MN)
31918_at	8.4	1.2	9.0	5.5	homeodomain protein (Prox 1)
34610_at	8.6	-1.0	1.6	3.1	Homo sapiens gb=W25845
1591_s_at	11.9	2.2	8.6	8.5	insulin-like growth factor II
36782_s_at	13.9	2.3	10.3	13.2	insulin-like growth factor II
672_at	14.2	7.4	13.5	3.3	plasminogen activator inhibitor-1
36933_at	79.9	127.7	241.0	61.5	RTP (N-myc downstream regulated gene 1)
2079_s_at	255.6	27.6	140.0	202.7	insulin-like growth factor (IGF-II)

**Figure 5 Venn diagrams representing genes whose expression was significantly influenced by treatment.**

Genes whose expression was influenced by the four hypoxia treatments are displayed as Venn diagrams. Total number of genes for each treatment group is listed at the bottom next to the treatment label. Each section that shares the same color and number represents the same subset of genes. (a) a complete list of these genes can be found in Table 4. (b) a partial list of these genes can be found in table 5. (c) a partial list of these genes can be found in table 6. (d) a partial list of these genes can be found in table 7, (e) a partial list of these genes can be found in table 8.



subset (65.2%, 212/325 probe sets) (Figure 5). DFO treatment led to altered expression of a much larger number of probe sets under these conditions (100  $\mu$ M, 24 hours). DFO exposure changed the expression of 1068 different probe sets and 23.3% (249/1068 probe sets) were shared with the hypoxia subset (Figure 5). These data suggest that there is a core set of genes that are responsive to hypoxia and hypoxia mimics but a larger population may be unique to each treatment.

To understand more thoroughly this core set of genes, a comprehensive analysis of those genes that were shared among all four treatment groups was performed. This analysis led to the identification of a core set of 62 probe sets, representing 55 different genes (Table 4). This list contains a large group of previously characterized hypoxia responsive genes, including IGF II, n-myc downstream regulated (also known as NDR1, RTP, AND CAP43), PAI 1, VEGF and several glycolytic enzyme genes. The list also contained several genes that had not been characterized as hypoxia responsive. These include pyruvate dehydrogenase kinase 1, PDGH, MAOA, inhibin and SLC6A8.

To verify the expression of some of the novel hypoxia regulated genes, as well as some of the conventional hypoxia target, qRT-PCR was performed. The genes verified included VEGF and carbonic anhydrase as controls for the hypoxia treatments. These genes are known hypoxia genes and qRT-PCR and

**Table 4. The 62 probe sets representing the overlap between all four treatments**

Probe Set	FOLD CHANGE				NICK	Descriptions
	HYP	COB	DFO	DFI		
1025_g_at	-10.21	-5.86	-14.71	-8.23		HSCYP450 Human gene for cytochrome P(1)-450
32570_at	-6.89	-5.82	-7.28	-5.38		NAD+-dependent 15-hydroxyprostaglandin dehydrogenase (PGDH)
742_at	-4.99	-9.59	-4.44	-11.42		HUMHGFL Human mRNA for HGF activator-like protein
41772_at	-4.00	-2.18	-4.68	-2.90		monoamine oxidase A (MAOA)
36687_at	-3.45	-2.13	-2.86	-2.86		cDNA DKFZp566D193 (from clone DKFZp566D193) gb=AL050051
37322_s_at	37322_s_at	-3.44	-4.30	-2.98	-2.53	15-hydroxy prostaglandin dehydrogenase
34297_at	-3.29	-5.82	-4.78	-3.78		putative endothelin receptor type B-like protein
34721_at	-3.07	-2.93	-3.72	-2.29		54 kDa progesterone receptor-associated immunophilin FKBP54
HUMISGF3A	-2.90	-2.35	-2.27	-2.52		transcription factor ISGF-3
31843_at	-2.76	-3.88	-3.51	-3.30		mRNA for KIAA0832 protein, gb=AB020639
925_at	-2.63	-2.05	-6.13	-2.41		HUMIIP Human gamma-interferon-inducible protein (IP-30)
32859_at	-2.59	-2.23	-2.49	-2.55		transcription factor ISGF-3 mRNA
37944_at	-2.44	-3.47	-2.79	-2.74		GTP cyclohydrolase 1 mRNA
41574_at	-2.21	-2.15	-3.79	-2.50		MEMA protein, gb=Y09703
286_at	-2.20	-2.24	-3.12	-2.24		histone H2A.2 mRNA
34308_at	-2.19	-2.30	-17.01	-2.34		histone 2A-like protein (H2A1)
35343_at	-2.02	-2.06	-3.64	-2.42		cytosolic aspartate aminotransferase
32001_s_at	2.02	3.86	5.97	2.35		subtilisin-like protein (PACE4)
41485_at	2.04	2.44	3.07	2.19		lactate dehydrogenase-A
34478_at	2.04	2.14	2.04	2.32		YPT3 mRNA, gb=X79780
39366_at	2.07	5.73	5.12	2.03		protein phosphatase 1, regulatory subunit (PPP1R3C)
34378_at	2.11	3.17	3.02	2.06		adipophilin
40049_at	2.25	2.03	2.51	2.64		DAP-kinase
38970_s_at	2.35	3.02	6.14	2.68		HIV-1, Nef-associated factor 1 beta (Naf1 beta)
32210_at	2.36	5.39	13.08	2.80		phosphoglucosyltransferase 1 (PGMT1)
35780_at	2.46	3.25	7.21	2.82		Homo sapiens clone Z3584 gb=AF035292
38010_at	2.47	13.15	10.00	2.58		E1B 19k/Bc1-2-binding protein Nip3 mRNA
39008_at	2.50	4.46	3.05	2.71		ceruloplasmin (ferroxidase)
32336_at	2.52	3.08	4.70	3.24		aldolase A
32622_at	2.59	2.07	3.84	3.01		dynamitin (DNM) mRNA

**Table 4. The 62 probe sets representing the overlap between all four treatments (continued)**

Probe Set	HYP	COB	DFO	Nick	Descriptions
1519_at	2.60	4.89	5.04	2.85	erythroblastosis virus oncogene homolog 2 (ets-2)
32538_at	2.67	2.94	3.11	3.52	transferrin
37639_at	2.83	2.34	2.69	3.04	serine protease hepsin
1826_at	2.92	2.04	8.87	3.06	Human ras-related rho
33113_at	2.97	3.48	5.55	3.22	msg1-related gene 1 (mrg1)
35703_at	3.02	2.52	2.15	3.57	platelet-derived growth factor PDGF-A
34786_at	3.09	5.55	8.16	3.00	lumojii domain containing 1A
1232_s_at	3.13	10.01	26.64	2.97	Human insulin-like growth factor binding protein hIGFBP1
37037_at	3.23	13.37	18.70	3.92	proyl 4-hydroxylase
40448_at	3.44	4.51	8.06	3.61	zinc finger transcriptional regulator
34795_at	3.55	7.11	9.32	3.92	lysyl hydroxylase isoform 2 (PLOD2)
40837_at	3.94	2.47	4.15	3.77	transducin-like enhancer protein (TLE2)
36100_at	3.99	3.18	4.78	3.19	vascular endothelial growth factor
33251_at	4.04	8.73	5.48	4.43	mRNA for KIAA0779 protein gb=AB018322
41503_at	4.27	4.18	3.76	4.07	zinc fingers and homeoboxes 2
39436_at	4.40	11.61	30.92	3.48	BCL2/adenovirus E1B 19kDa-interacting protein 3a (NIX)
33143_s_at	4.44	5.41	16.85	3.31	monocarboxylate transporter (MCT3) (AKA: SLC16A3)
1953_at	4.47	2.92	4.86	3.32	vascular endothelial growth factor (VEGF)
39827_at	4.72	4.39	4.70	6.80	DNA-damage-inducible transcript 4 (DDIT4)
36386_at	4.75	10.81	14.86	3.88	pyruvate dehydrogenase kinase isoenzyme 1 (PDK1)
40790_at	4.88	4.03	8.02	4.21	DEC1
36101_s_at	5.04	3.60	7.25	4.13	vascular endothelial growth factor
38545_at	5.16	2.48	12.07	4.03	testicular inhibin beta-B-subunit
40926_at	5.79	12.05	25.49	6.74	creatine transporter (SLC6A8)
38125_at	6.30	10.63	22.79	7.93	beta-migrating plasmineogen activator inhibitor 1
34777_at	6.77	33.13	39.45	3.87	adrenomedullin precursor
40309_at	8.05	39.37	39.90	5.70	Carbonic anhydrases (MatTu MN)
1591_s_at	11.93	2.19	8.58	8.53	insulin-like growth factor II
36782_s_at	13.92	2.28	10.26	13.20	insulin-like growth factor II
36933_at	79.94	127.74	241.04	61.55	RTP (N-myc downstream regulated gene 1)
2079_s_at	265.59	27.64	140.03	202.67	insulin-like growth factor (IGF-II)

microarray data were in good agreement. In addition, four other genes (PDK1, SLC6A8, inhibin and MCT3) that were upregulated in all four treatments and had not been characterized as hypoxia regulated were also verified. Each of the four treatments led to the upregulation of the PDK1 and SLC6A8 genes in the microarray and qRT-PCR analysis (Figure 6A). In addition, the qRT-PCR expression pattern of inhibin correlated with the microarray data in three of the four treatments, while MCT3 only verified in the DFO treatment group (Figure 6A).

There were also several down-regulated genes that were verified by qRT-PCR (Figure 6B). Cyp1A1 was down-regulated in all four treatments in both the microarray and q RT-PCR experiments and this is in good agreement with previously published reports (14, 15). IL8 was upregulated in three of the four treatments on the microarray and this pattern was verified in the qRT-PCR results. Finally, four genes (HGFAL, IP30, MAOA and 15-PGDH) were down-regulated in all four treatments on the microarray and this was confirmed on the qRT\_PCR, with one exception. Nickel induced a slight upregulation in the 15-PGDH gene in the qRT-PCR (Figure 6B).

A direct comparison of the microarray and qRT-PCR data was performed by compiling all of the values for all twelve genes under all four conditions and plotting them on a Log2 chart (Figure 7). The graph was further analyzed by linear regression and displayed a slope of 0.94 and an  $R^2$  value of 0.58. These

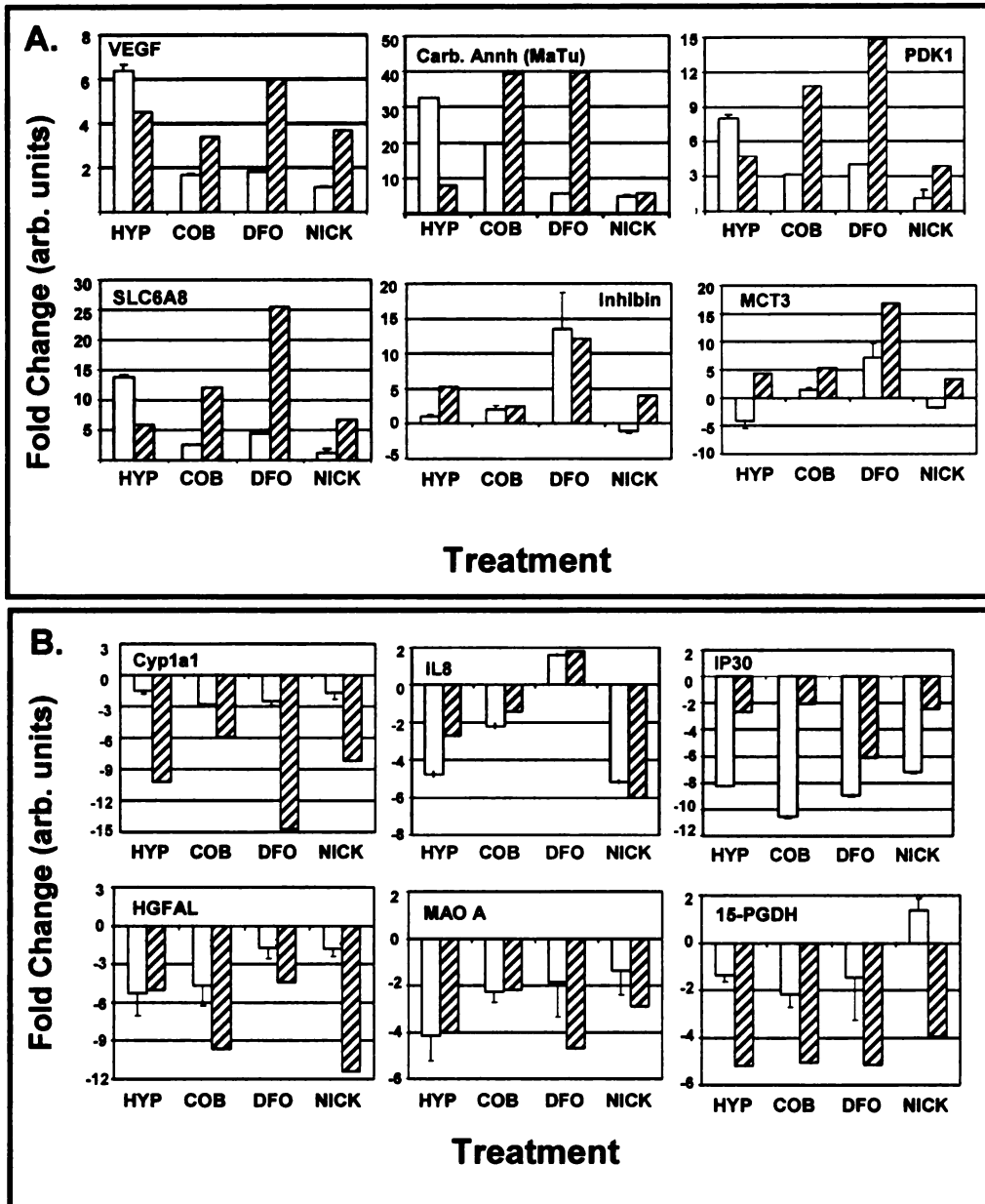


**Figure 6. qRT-PCR verification of 12 genes.**

The expression pattern for 6 upregulated genes (A) and 6 down-regulated genes (B) was verified by qRT-PCR using sybr green as a marker. The sybr green data (white bars) is directly compared to the microarray data (hatched bars). Gene names are listed at the top of each graph. HYP = 1% O<sub>2</sub>, COB = 100 μM CoCl<sub>2</sub>, DFO = 100 μM deferoxamine and NICK = 100 μM NiCl<sub>2</sub>

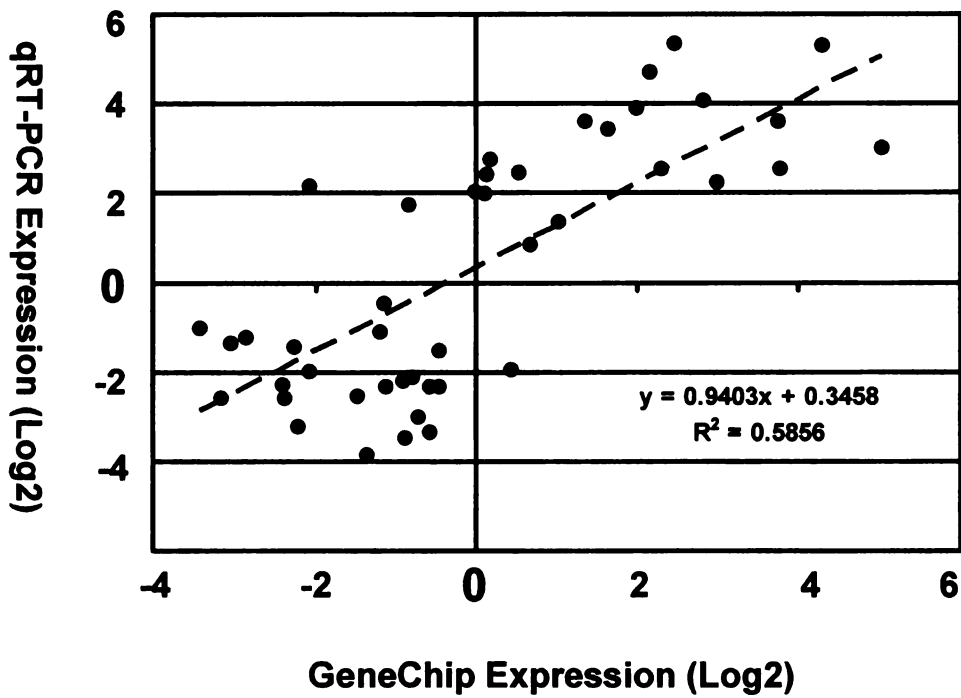


**Figure 7. Analytical comparison of qRT-PCR and microarray data.**

Fold change values from qRT-PCR and microarray results were Log2 transformed and plotted on a linear graph. Linear regression was performed and equation of the line and  $R^2$  values are listed.

results validate the microarray data analysis and suggest that there is very good correlation between the two assays.

The results suggest that there is considerable overlap between the various treatments; however, there is also a large subset of genes that were altered in a treatment specific manner. The expression of these genes passed significance and fold change cut-offs in only one treatment. For example, there were 121 probe sets that showed change in expression ( $p < 0.05$  and greater than 2 fold) following hypoxia treatment but were not significantly changed in the other three treatment groups (Figure 5, Table 5). This subset included probe sets for the guanine nucleotide binding protein, c-jun, MAP kinase phosphatase 1, ubiquitin-conjugating enzyme E2 and asparagine synthetase (Table 5). The role these genes play in the cellular response to hypoxia is currently being investigated.

There were also 92, 676 and 49 probes sets that were specific to cobalt, DFO and nickel, respectively (Figure 5). These subsets include growth factors (e.g. connective tissue growth factor, amphiregulin, and transforming growth factor-beta), structural proteins (e.g. desmocollin, spectrin and adducin), and genes for several important enzymes (e.g. glutathione-S-transferase, hepatic dihydrodiol dehydrogenase, and s-adenosylmethionine synthetase). In addition, each treatment altered the expression of various critical transcription factors and cell cycle regulators. For example, cobalt exposure led to the decreased expression of cyclin D1 (Table 6). Nickel altered the expression of the genes for

**Table 5. Top 20 up and down regulated genes specific to hypoxia (1% O<sub>2</sub>) exposure**

FOLD CHANGE					Descriptions
Probe Set	HYP	COB	DFO	NICK	
38680_at	-4.43	-1.37	-1.63	-2.05	Alu repeats in the small nuclear ribonucleoprotein E
36636_at	-4.00	1.03	1.09	-1.91	ornithine aminotransferase
36671_at	-3.43	-1.34	-1.52	-1.78	asparagine synthetase
40629_at	-3.05	1.15	-1.61	-1.29	GPI-H mRNA
40074_at	-3.05	-1.05	-1.31	-1.99	NAD-dependent methylene THF-DH cyclohydrolase
36604_at	-3.04	1.02	-1.66	-1.92	ubiquitin-conjugating enzyme E2
32777_at	-3.00	1.14	-1.80	-1.90	CHD5 protein
39983_at	-2.90	-1.88	-1.92	-2.76	FKBP-associated protein FAP48
38029_at	-2.80	-1.29	-1.07	-1.77	glycoprotein 4F2
41536_at	-2.75	1.27	-1.21	-1.77	AL022726 clone 625H18
34366_g_at	-2.75	1.10	-1.33	-1.76	cyclophilin-33B (CYP-33)
36857_at	-2.70	-1.30	-1.69	-1.90	DNA repair exonuclease (REC1)
38983_at	-2.69	-1.11	-1.85	-1.73	AI223047cDNA
33434_at	-2.62	1.46	-1.87	-1.52	Bet1p homolog (hbet1)
40250_at	-2.60	-1.46	-1.97	-2.51	Rev interacting protein Rip-1
402_s_at	-2.60	1.56	-1.08	-1.54	ICAM-3 mRNA
262_at	-2.58	-1.10	-1.42	-1.57	S-adenosylmethionine decarboxylase
40568_at	-2.56	-1.11	-1.50	-1.92	vacuolar H <sup>+</sup> -ATPase
34356_at	-2.54	1.23	-1.57	-1.80	polymerase II complex component SRB7
38725_s_at	-2.50	-1.81	-1.62	-1.86	N36295 cDNA
37657_at	2.01	-1.03	1.86	1.50	PALM gene
38586_at	2.03	-1.67	1.10	1.14	fatty acid binding protein (FABP)
41657_at	2.03	1.33	1.23	1.54	serine threonine kinase 11
40186_at	2.04	1.54	1.15	1.83	MAP kinase phosphatase 4
1443_at	2.04	1.50	1.42	2.78	HSMAPK4 MAP kinase phosphatase 4
41366_at	2.12	-1.04	-1.40	1.96	mRNA for KIAA1002
32583_at	2.13	1.51	1.81	1.70	c-jun proto oncogene (JUN)
38757_at	2.14	-1.14	1.42	1.87	PDGF associated protein
835_at	2.14	-1.89	1.71	1.87	PDGF associated protein
41061_at	2.17	-1.14	-1.15	1.61	huntingtin interacting protein 1
34303_at	2.21	1.23	1.75	1.86	AL049949 mRNA
40960_at	2.28	-1.02	1.75	1.79	beta-1,4-galactosyltransferase
HSAC07	2.31	-1.00	1.01	1.09	beta-actin
37880_at	2.33	1.25	1.33	1.67	L-alanine-glyoxylate aminotransferase
39385_at	2.41	-1.15	1.48	1.79	aminopeptidase N/CD13
38295_at	2.47	-1.00	1.53	1.87	PBX2 mRNA
hum_alu_at	2.55	-1.18	1.69	1.68	Alu-Sq subfamily
37884_f_at	2.66	4.75	2.50	1.81	AI375033 cDNA
41872_at	2.69	1.32	-1.37	1.72	nonsyndromic hearing impairment protein (DFNA5)
34610_at	8.57	-1.01	1.65	3.13	guanine nucleotide binding protein

**Table 6. Top 20 up and down regulated genes specific to CoCl<sub>2</sub> (100 μM) exposure**

Probe Set	FOLD CHANGE				Descriptions
	HYP	COB	DFO	NICK	
41320_s_at	1.56	-3.76	-1.57	-1.07	transcriptional repressor (GCF2)
2017_s_at	1.90	-3.75	1.13	1.29	Human cyclin D (cyclin D1)
37637_at	-1.20	-3.73	-1.52	-1.34	RGP3 mRNA
867_s_at	1.31	-3.58	1.36	1.26	thrombospondin-1
36638_at	-1.27	-3.47	1.11	-1.74	connective tissue growth factor
1143_s_at	-1.26	-3.41	-1.89	-1.68	Fibroblast Growth Factor Receptor K-Sam
38418_at	-1.07	-3.10	-1.53	-1.23	PRAD1 mRNA for cyclin
33436_at	-1.42	-2.95	-1.12	-1.26	SOX9 mRNA
34517_at	1.31	-2.90	-1.20	1.18	HMG-CoA-synthase
2020_at	-1.31	-2.86	-1.86	-1.20	bcl-1 mRNA
33389_at	-1.24	-2.75	-1.76	-1.26	cytochrome P450 (CYP51)
38686_at	-1.42	-2.64	-1.26	-1.27	vacuolar proton ATPase
31521_f_at	-1.64	-2.60	-2.00	-1.51	H4/e gene for H4 histone
1787_at	-1.08	-2.60	-1.30	-1.71	Cdk-inhibitor p57KIP2
34213_at	-1.17	-2.57	1.20	-1.58	mRNA for KIAA0869 protein
404_at	-1.17	-2.54	-1.92	-1.32	interleukin 4 receptor
1970_s_at	-1.09	-2.48	-1.85	-1.34	FGFR2 mRNA
866_at	-1.24	-2.43	-1.70	-1.23	thrombospondin-1
33369_at	1.05	-2.42	-1.95	1.44	AI535653 cDNA
40841_at	-1.04	-2.37	1.12	-1.33	TACC1 (TACC1) mRNA
35284_f_at	-1.63	2.83	-1.72	-1.78	W28620 cDNA
37002_at	1.33	2.91	1.12	1.32	biliverdin-IXbeta reductase I
38825_at	1.06	2.95	1.02	-1.06	fibrinogen alpha chain gene
1962_at	1.66	2.95	1.04	1.74	liver arginase
40838_at	1.56	3.11	1.46	1.31	mRNA for KIAA0530 protein
35214_at	-1.57	3.32	-1.21	1.73	UDP-glucose dehydrogenase (UGDH)
38876_at	-1.29	3.70	-1.06	1.34	AL080091 cDNA
31850_at	-1.41	3.89	1.26	1.27	gamma-glutamylcysteine synthetase
35724_at	-1.23	4.11	-1.46	1.50	Pirin, isolate 1
32664_at	-1.16	4.62	2.07	1.56	RNase 4
35686_s_at	-1.42	4.82	2.03	-1.34	MTCP1 gene
39365_i_at	1.19	4.95	1.70	1.12	protein phosphatase 1 (PPP1R5)
35194_at	1.12	5.05	1.00	1.05	glutathione peroxidase-like protein
748_s_at	1.20	5.79	3.44	1.35	Mxi1 protein
34342_s_at	1.16	6.93	1.01	1.07	osteopontin mRNA
39120_at	-1.32	9.41	-1.32	-1.49	AA224832 cDNA
37399_at	1.11	9.57	1.00	1.03	mRNA for KIAA0119 gene
38379_at	1.16	11.24	1.02	1.07	NMB mRNA
32805_at	-1.30	64.02	-1.95	-1.60	hepatic dihydrodiol dehydrogenase
32392_s_at	1.13	80.74	1.01	1.19	bilirubin UDP-glucuronosyltransferase isozyme 2

the transcription factors E2A and SL1 (Table 8). DFO had the largest unique set of genes and it contained the transcription factors, c-fos, activating transcription factor 3 and the farnesol receptor HRR-1 (Table 7). These results suggest that each of these treatments has different functional consequences on cellular homeostasis which distinguishes them from hypoxia exposure.

## **Discussion**

Several dozen genes responded to both cellular hypoxia and its mimics. These genes included known hypoxia regulated genes, such as IGFII, VEGF and carbonic anhydrase, but also many previously uncharacterized genes that were altered by all four treatments. Several genes were involved in the processes of adaptation and cell death, indicating a delicate balance between these processes under hypoxic stress. Adaptive genes included the previously known glycolytic enzymes and carbonic anhydrase, but also the creatine transporter, SLC6A8, through which creatine may function to regulate the ATP supply within the cell (16). Another gene induced by hypoxia and its mimics, PDK1, is responsible for inactivating the pyruvate dehydrogenase (PDH) complex and thus regulating the amount of glucose that is ultimately converted to acetyl-CoA. The upregulation of PDK1 and subsequent inactivation of the PDH complex may act to divert pyruvate to other metabolic pathways to cope with the hypoxic environment.

Conversely, apoptotic or cell death-promoting genes and cell proliferation inhibitors were also found to be regulated by all three hypoxic stimuli. These

**Table 7. Top 20 up and down regulated genes specific to Deferoxamine (100  $\mu$ M) exposure**

Probe Set	FOLD CHANGE				Descriptions
	HYP	COB	DFO	NICK	
38519_at	-1.40	-1.92	-27.06	-1.18	farnesol receptor HRR-1
527_at	-1.89	-1.64	-10.50	-1.33	centromere protein-A (CENP-A)
1647_at	-1.21	-1.81	-7.84	-1.22	RasGAP-related protein (IQGAP2)
40238_at	-1.56	-1.33	-7.31	-2.03	AI674208 cDNA
1599_at	-1.91	-1.62	-6.45	-1.76	protein tyrosine phosphatase (CIP2)
34851_at	-1.56	-1.12	-6.30	-1.29	serine/threonine kinase (BTAK)
37173_at	-1.96	-2.12	-6.22	-1.73	CENP-E mRNA
37649_at	-1.98	-1.22	-6.03	-1.61	hydroxymethylbilane synthase gene
38099_r at	-1.30	-1.67	-5.99	-1.33	acyl-CoA synthetase 4 (ACS4)
38717_at	1.61	-1.27	-5.91	1.77	AL050159 cDNA
40508_at	-2.00	1.35	-5.77	-1.53	glutathione S-transferase A4-4 (GSTA4)
33701_at	-1.63	-1.83	-5.68	-1.51	phenylalanine hydroxylase (PAH)
41211_at	-1.29	-1.19	-5.64	-1.03	mRNA for KIAA0765 protein
34852_g at	-1.43	-1.10	-5.60	-1.26	serine/threonine kinase (BTAK)
1945_at	-1.75	-1.48	-5.56	-1.63	cyclin B
41352_at	1.19	1.26	-5.51	1.58	beta-galactoside alpha-2,6-sialyltransferase
37302_at	-1.76	-1.86	-5.48	-1.75	mitosin mRNA
38824_at	-1.86	1.49	-5.41	-1.39	Tat-interacting protein TIP30
903_at	-1.12	-1.93	-5.31	-1.54	phosphatase 2A B56-alpha (PP2A)
37235_g at	-1.78	-1.81	-5.24	-1.40	alpha-2-thiol proteinase inhibitor
39279_at	1.07	-1.03	6.44	1.02	transforming growth factor-beta
35174_i at	1.30	1.13	6.61	1.45	elongation factor 1 alpha-2
38790_at	1.03	1.94	6.69	1.29	p53/HEH epoxide hydrolase (EPHX)
38457_at	1.49	1.02	6.70	1.09	troponin I fast-twitch isoform mRNA
36543_at	1.56	-1.28	6.86	1.07	Coagulation factor III
1890_at	1.62	1.58	7.18	1.15	TGF-beta superfamily protein
1733_at	1.16	1.01	7.66	1.08	transforming growth factor-beta
39302_at	1.04	2.91	8.02	-1.10	desmocollins type 2a and 2b
35617_at	1.63	1.28	8.21	1.73	BMK1 alpha kinase
37111_g at	1.35	1.48	8.51	1.35	fructose-6-phosphate,2-kinase
32899_s at	1.32	1.13	9.05	1.11	orphan hormone nuclear receptor RORalpha1
1113_at	-1.03	-1.39	10.03	-1.52	bone morphogenetic protein 2A
1915_s at	1.28	1.05	10.25	1.06	cellular oncogene c-fos
287_at	1.02	-1.05	11.22	-1.09	activating transcription factor 3
40367_at	1.09	-1.23	11.28	-1.10	morphogenetic protein 2A
41038_at	1.47	3.58	11.46	-1.49	neutrophil oxidase factor (p67-phox)
39248_at	-1.26	1.53	11.71	1.22	N74607cDNA
34661_at	-1.03	-1.30	17.11	1.68	mRNA for KIAA0350
33127_at	1.20	1.71	21.51	1.09	lysyl oxidase-related protein (WS9-14)
1916_s at	1.37	1.12	29.73	1.12	cellular oncogene c-fos

**Table 8. Top 20 up and down regulated genes specific to NiCl<sub>2</sub> (100 μM) exposure**

Probe Set	FOLD CHANGE				Descriptions
	HYP	COB	DFO	NICK	
34898_at	-2.16	-1.75	1.75	-2.92	amphiregulin (AR)
37701_at	-1.97	-1.61	-1.34	-2.88	helix-loop-helix basic phosphoprotein (G0S8)
35803_at	-2.91	-1.62	1.25	-2.61	RhoE=26 kda GTPase homolog
41662_at	-4.46	1.10	1.00	-2.49	AL050272 cDNA
39351_at	-1.85	-1.98	-1.29	-2.46	transmembrane protein (CD59)
36191_at	-2.92	-1.32	-1.99	-2.45	mitochondrial transcription factor 1
36079_at	-2.63	-1.96	-1.49	-2.33	Pig3 (PIG3)
38678_at	-1.62	-1.12	-1.78	-2.28	AA733050 cDNA
32088_at	-1.78	1.04	-1.40	-2.28	basic-leucine zipper nuclear factor (JEM-1)
35842_at	-1.75	-1.19	-1.10	-2.20	AL049265 cDNA
40269_at	-2.08	-1.35	-2.00	-2.13	hPrp18 mRNA
35006_at	-1.47	-1.51	-1.61	-2.11	transcription factor SL1
32102_at	-1.56	-1.21	-1.04	-2.11	AB018273 mRNA
39506_at	-1.37	1.05	-1.04	-2.09	AA933984 cDNA
39224_at	-1.24	-1.24	-1.33	-2.08	AB011152 mRNA
1536_at	-1.19	1.09	-1.34	-2.07	Cdc6-related protein (HsCDC6)
1119_at	-2.07	-1.24	-1.43	-2.06	Human replication protein A
38381_at	-1.49	-1.55	-1.63	-2.06	syntaxin 3
39533_at	-1.81	1.14	1.14	-2.05	D87432 mRNA
339_at	-1.96	-1.15	1.49	-2.05	caveolin-2
31431_at	1.71	1.19	1.24	2.06	IgG Fc receptor
1047_s_at	1.41	1.05	1.09	2.09	hepatocyte growth factor-like protein gene
41725_at	1.78	1.17	1.81	2.09	casein kinase I gamma 2
36784_at	2.40	-1.03	1.96	2.11	growth hormone and chorionic somatomammotropin
38406_f_at	1.96	1.12	1.19	2.12	AI207842 cDNA
39358_at	1.61	1.28	1.54	2.12	silencing mediator of retinoid and thyroid hormone
35154_at	1.63	1.57	1.55	2.13	W68046 cDNA
33630_s_at	1.34	1.01	-1.09	2.13	beta III spectrin (SPTBN2)
1218_at	1.76	1.24	1.42	2.13	v-erbA related ear-2
32146_s_at	2.01	1.58	2.24	2.18	alpha adducin
1374_g_at	1.62	1.82	1.29	2.22	transcription factor (E2A)
39372_at	1.88	-1.50	-1.14	2.28	W26480 cDNA
38789_at	1.48	1.80	1.13	2.29	transketolase
40850_at	1.96	1.67	1.68	2.29	FK-506 binding protein homologue (FKBP38)
446_at	1.85	-1.09	1.93	2.37	casein kinase I gamma 2
32800_at	1.88	1.04	1.29	2.53	retinoid X receptor alpha mRNA
1373_at	1.84	1.30	1.70	2.57	transcription factor (E2A)
39560_at	1.55	1.64	1.00	2.73	H10776 cDNA
32571_at	1.10	-1.08	-1.92	2.73	S-adenosylmethionine synthetase
35547_at	5.15	1.19	3.27	6.25	monocarboxylate transporter 2 (hMCT2)

include the known hypoxic targets BCL2/adenovirus E1B 19kDa-interacting protein 3 $\alpha$  (NIX), that can promote apoptosis or necrosis, depending on cell type and circumstances and DEC1 (deleted in esophageal cancers 1) an anti-proliferation and putative tumor suppressor gene (17-20). This list also included the RTP801 (also known as DDIT4 and N-myc downstream regulated gene 1). RTP801 (up regulated 80 fold by hypoxia) was previously described as a hypoxia-inducible gene that plays a complex role in cellular viability (21). Under certain conditions, it can act in a protective manner, however, under most standard conditions, overexpression of RTP801 leads to cell death. Collectively, these results indicate that hypoxia and its mimics induce a complex interplay between adaptive and pro-apoptotic responses that ultimately dictate cell survival.

Several genes that were identified and verified suggest a complex cellular response to hypoxia. There is an initial upregulation of the glycolytic enzymes as a way of coping with an inability to produce ATP through oxidative phosphorylation. This upregulation may also be important to the maintenance of critical cellular metabolites (22). This adaptive response is supported by other cellular processes, such as creatine transport (SLC6A8) that may allow the cell to survive in the hypoxic environment. The decrease in Cyp1A1 may be an attempt to control oxygen usage in side reactions or partial limits due to aryl hydrocarbon nuclear translocator (ARNT) availability. HGFAL (also known as GILT) is a serine protease involved in cellular adhesion and down-regulated in all four

treatments. A putative tumor suppressor gene, inhibin  $\beta$  was also down-regulated. Inhibin  $\beta$  is capable of inhibiting follicle-stimulating hormone when bound to inhibin  $\alpha$ . Finally, IP30 (also known as gamma-interferon-inducible protein (GILT)) is a lysosomal thiol reductase involved in disulfide bond reduction at low pH and is down-regulated under all four conditions (23). The role these proteins play in the adaptive or cell death response to hypoxia is currently unknown.

Current genomic technology has begun to unravel the various signaling networks that are influenced, both directly and indirectly, by hypoxia. Recent publications have used HIF1 $\alpha$  *-/-* cells to identify hypoxia-inducible genes using hypoxia and hypoxia mimics such as cobalt and nickel chloride (11, 24). A direct comparison between these genomic screens and those presented in this manuscript is difficult due to limited published information and the differences in the gene expression platforms. However, several points can be made: hypoxia and hypoxia mimics (i.e. nickel, cobalt and deferoxamine) alter the expression of glycolytic enzymes, apoptotic genes and several hydroxylases. The hydroxylases include EGLN1 (also known as PHD2, HPH2), an enzyme responsible for regulating HIF1 $\alpha$  stability. In addition, the transcription factor Jun B is represented by two different probe sets on the U95 chip (32786\_AT and 2049\_S\_AT), and both were significantly influenced by hypoxia and DFO treatment but were unaffected by exposure to either metal (data not shown). In Salnikow et al., Jun B was influenced in a HIF1 $\alpha$ -independent mechanism (24).

In contrast to Salnikow et al., we could detect no significant change for ATM or focal adhesion kinase, perhaps because these genes were not detectably expressed in Hep3B cells, not induced by the mimics employed in this manuscript, or due to platform issues.

A direct comparison to the cDNA microarray results from our previously published report and the current genomic screen is difficult due to platform, species and cell type differences; however, several interesting points can be made. First, when a direct comparison of Table 4 of this manuscript and table 3 (active genes from wild type fibroblasts under hypoxia and cobalt) of the previous report was performed there were 4 genes that were common to both tables. These include lactate dehydrogenase, prolyl 4 hydroxylase, aldolase and NIX. The limited overlap is primarily due to platform and cell type differences. Second, when a comparison of the 24 hour treatment times between the two experiments is made, approximately 18% of the clones regulated by hypoxia in the WT mouse embryonic fibroblasts are also influenced in the Hep3B cells (51 of 287 clones). Third, most of these clones were known hypoxia target genes, including the glycolytic enzymes and the apoptotic gene E1B 19K/Bcl-2-binding protein Nip3 (BNIP3) (11, 25). Fourth, the list also included some novel hypoxia targets, such as 17-beta-hydroxysteroid dehydrogenase. The 11-beta hydroxysteroid dehydrogenase gene has previously been shown to be a target of hypoxia mediated down-regulation and the addition of this family member may

suggest a global down regulation of steroid synthesis under hypoxic conditions (26).

The genomic screen most similar to the one reported here was performed in HepG2 cells and utilized the same platform (27). Of the 62 probe sets listed in Table 4, 22 could be found in the Sonna et al. report. (27). Interestingly, only one of these was a down-regulated gene (IP30, 925\_at). When the analysis is extended to the complete list of genes influenced by hypoxia at the 24 hour time point (data not shown) and the Sonna et al. there was approximately 10% overlap (47/452). These shared genes fell within the 95 confidence interval reported in the Sonna et al. tables. Again, this overlap was weighted towards upregulated genes (36 of 47 probe sets) even though a higher proportion was down-regulated (314 of 452). There were some known hypoxia- regulated genes found in the 24 hour chart not included in the Sonna et al. For example, the hydroxylase genes, PLOD2 and P4H, were not mentioned by Sonna et al. but were significantly altered in all four hypoxia treatments in this report (28, 29). There were also several known hypoxia genes not included in Table 4 that were found in the Sonna et al., including GAPDH and the glucose transporters. Though each of these was influenced in one or more treatments, they did not pass the significance and fold change cut-off in all four treatments. These results suggest that there is a core set of hypoxia inducible genes in all cell types and that each also harbors the ability to mount specific responses to low oxygen availability.

In a recent publication, serial analysis of gene expression (SAGE) was used to identify genes that showed changes in gene expression by the loss of the Von Hippel Lindau (VHL protein) (30). VHL plays an essential role in regulating hypoxia signaling by recognizing the hydroxylated form of the HIF and recruiting the ubiquitination machinery necessary for its degradation. Therefore, we hypothesized significant overlap between our results and those derived from their SAGE experiments (30). Indeed, there was extensive overlap, as 30 of the probe sets in table 4 were found in at least one supplemental data table from the VHL paper (30). These genes include plasminogen activator inhibitor, BNIP3 and IP30. As expected, these results suggest that there is considerable overlap between the loss of VHL and changes in hypoxia signaling. There were also considerable differences, possibly stemming from the different techniques, cell types and/or methodology, or underlying biology.

Adaptive responses to hypoxia involve a complex network of signaling pathways and are necessary for cell and organismal survival. Current study of hypoxia relies heavily on mimics such as cobalt chloride and DFO, which presumably function by inhibiting the iron-dependent hydroxylases that regulate HIF1 $\alpha$  stability. However, the possibility that cobalt and DFO have other activities that may complicate analysis of these experiments has not been fully addressed. Our results indicate that the overlap between these mimics and hypoxia is limited, and suggests caution in their use. In addition, we show that many genes are

induced by all three stimuli including glycolytic enzymes and other survival genes (i.e. SLC6A8), hydroxylases and apoptotic genes. A detailed mechanistic understanding of how cells respond to low oxygen, cobalt, and desferoxamine, including their transcriptional programmes, will ultimately be required for a more complete understanding of hypoxia- mediated signaling and how it relates to critical processes of development and cancer.

### **Acknowledgements**

We acknowledge Jennifer Villasenor and Mimmi Hayakawa for technical assistance, John Walker for help with data processing and analysis, Dr. Christopher Bradfield for his support during the initial phases of these experiments.

## References

1. Bunn, H. F. and Poyton, R. O. Oxygen sensing and molecular adaptation to hypoxia. *Phys. Rev.*, 76: 839-885, 1996.
2. Gu, Y.-Z., Hogenesch, J., and Bradfield, C. The PAS superfamily: Sensors of environmental and developmental signals. *In: Annu. Rev. Pharmacol. Toxicol.*, Vol. 40, pp. 519-561: Academic Press, 2000.
3. Iyer, N. V., Kotch, L. E., Agani, F., Leung, S. W., Laughner, E., Wenger, R. H., Gassmann, M., Gearhart, J. D., Lawler, A. M., Yu, A. Y., and Semenza, G. L. Cellular and developmental control of O<sub>2</sub> homeostasis by hypoxia-inducible factor 1 alpha. *Genes Dev*, 12: 149-162, 1998.
4. Blanchard, K. L., Acquaviva, A. M., Galson, D. L., and Bunn, H. F. Hypoxic induction of the human erythropoietin gene: cooperation between the promoter and enhancer, each of which contains steroid receptor response elements. *Mol Cell Biol*, 12: 5373-5385, 1992.
5. Semenza, G. L., Nejfelt, M. K., Chi, S. M., and Antonarakis, S. E. Hypoxia-inducible nuclear factors bind to an enhancer element located 3' to the human erythropoietin gene. *Proc. Natl. Acad. Sci. USA*, 88: 5680-5684, 1991.
6. Bruick, R. K. and McKnight, S. L. A conserved family of prolyl-4-hydroxylases that modify HIF. *Science*, 294: 1337-1340., 2001.
7. Epstein, A. C., Gleadle, J. M., McNeill, L. A., Hewitson, K. S., O'Rourke, J., Mole, D. R., Mukherji, M., Metzen, E., Wilson, M. I., Dhanda, A., Tian, Y. M., Masson, N., Hamilton, D. L., Jaakkola, P., Barstead, R., Hodgkin, J., Maxwell, P. H., Pugh, C. W., Schofield, C. J., and Ratcliffe, P. J. C. *C. elegans* EGL-9 and mammalian homologs define a family of dioxygenases that regulate HIF by prolyl hydroxylation. *Cell*, 107: 43-54., 2001.
8. Wu, Z., Irizarry, R. A., Gentleman, R., Murillo, F. M., and Spencer, F. A Model Based Background Adjustment for Oligonucleotide Expression Arrays. <http://www.bioinformatica.unito.it/downloads/complexity/gcpaper.pdf> 1-29, 2004.
9. Ihaka, R. and Gentleman, R. R: A Language for Data Analysis and Graphics. *J. Comp. Graph. Stats*, 5: 299-314, 1996.
10. Gentleman, R. C., Carey, V. J., Bates, D. M., Bolstad, B., Dettling, M., Dudoit, S., Ellis, B., Gautier, L., Ge, Y., Gentry, J., Hornik, K., Hothorn, T., Huber, W., Iacus, S., Irizarry, R., Leisch, F., Li, C., Maechler, M., Rossini,

- A. J., Sawitzki, G., Smith, C., Smyth, G., Tierney, L., Yang, J. Y., and Zhang, J. Bioconductor: open software development for computational biology and bioinformatics. *Genome Biol*, 5: R80, 2004.
11. Vengellur, A., Woods, B. G., Ryan, H. E., Johnson, R. S., and LaPres, J. J. Gene expression profiling of the hypoxia signaling pathway in hypoxia inducible factor 1 null mouse embryonic fibroblasts. *Gene Expression*, 11: 181-197, 2003.
  12. Semenza, G. L., Roth, P. H., Fang, H. M., and Wang, G. L. Transcriptional regulation of genes encoding glycolytic enzymes by hypoxia-inducible factor 1. *J. Biol. Chem.*, 269: 23757-23763, 1994.
  13. Levy, A. P., Levy, N. S., Wegner, S., and Goldberg, M. A. Transcriptional regulation of the rat vascular endothelial growth factor gene by hypoxia. *J Biol Chem*, 270: 13333-13340, 1995.
  14. Fradette, C., Bleau, A. M., Pichette, V., Chauret, N., and Du Souich, P. Hypoxia-induced down-regulation of CYP1A1/1A2 and up-regulation of CYP3A6 involves serum mediators. *Brit. J. Pharm.*, 137: 881-891, 2002.
  15. Fradette, C. and Du Souich, P. Effect of hypoxia on cytochrome P450 activity and expression. *Curr. Drug Metab.*, 5: 257-271, 2004.
  16. Salomons, G. S., van Dooren, S. J., Verhoeven, N. M., Cecil, K. M., Ball, W. S., Degrauw, T. J., and Jakobs, C. X-linked creatine-transporter gene (SLC6A8) defect: a new creatine-deficiency syndrome. *Amer J Hum Genet*, 68: 1497-1500, 2001.
  17. Sowter, H. M., Ferguson, M., Pym, C., Watson, P., Fox, S. B., Han, C., and Harris, A. L. Expression of the cell death genes BNip3 and NIX in ductal carcinoma in situ of the breast; correlation of BNip3 levels with necrosis and grade. *J Pathol*, 201: 573-580, 2003.
  18. Wykoff, C. C., Pugh, C. W., Maxwell, P. H., Harris, A. L., and Ratcliffe, P. J. Identification of novel hypoxia dependent and independent target genes of the von Hippel-Lindau (VHL) tumour suppressor by mRNA differential expression profiling. *Oncogene*, 19: 6297-6305., 2000.
  19. Nishiwaki, T., Daigo, Y., Kawasoe, T., and Nakamura, Y. Isolation and mutational analysis of a novel human cDNA, DEC1 (deleted in esophageal cancer 1), derived from the tumor suppressor locus in 9q32. *Gene Chromosome Canc*, 27: 169-176, 2000.
  20. Guo, K., Searfoss, G., Krolikowski, D., Pagnoni, M., Franks, C., Clark, K., Yu, K. T., Jaye, M., and Ivashchenko, Y. Hypoxia induces the expression of the pro-apoptotic gene BNIP3. *Cell Death Differ.*, 8: 367-376, 2001.

21. Shoshani, T., Faerman, A., Mett, I., Zelin, E., Tenne, T., Gorodin, S., Moshel, Y., Elbaz, S., Budanov, A., Chajut, A., Kalinski, H., Kamer, I., Rozen, A., Mor, O., Keshet, E., Leshkowitz, D., Einat, P., Skaliter, R., and Feinstein, E. Identification of a novel hypoxia-inducible factor 1-responsive gene, RTP801, involved in apoptosis. *Mol. Cell. Biol.*, 22: 2283-2293, 2002.
22. Griffiths, J. R., McSheehy, P. M., Robinson, S. P., Troy, H., Chung, Y. L., Leek, R. D., Williams, K. J., Stratford, I. J., Harris, A. L., and Stubbs, M. Metabolic changes detected by in vivo magnetic resonance studies of HEPA-1 wild-type tumors and tumors deficient in hypoxia-inducible factor-1beta (HIF-1beta): evidence of an anabolic role for the HIF-1 pathway. *Cancer Research*, 62: 688-695, 2002.
23. Luster, A. D., Weinshank, R. L., Feinman, R., and Ravetch, J. V. Molecular and biochemical characterization of a novel gamma-interferon-inducible protein. *J. Biol. Chem.*, 263: 12036-12043, 1988.
24. Salnikow, K., Davidson, T., Kluz, T., Chen, H., Zhou, D., and Costa, M. GeneChip analysis of signaling pathways effected by nickel. *J Environ Monitor*, 5: 206-209, 2003.
25. Vengellur, A. and LaPres, J. J. The Role of Hypoxia Inducible Factor 1a in Cobalt Chloride Induced Cell Death in Mouse Embryonic Fibroblasts. *Tox. Sci.*, 82: 638-646, 2004.
26. Heiniger, C. D., Kostadinova, R. M., Rochat, M. K., Serra, A., Ferrari, P., Dick, B., Frey, B. M., and Frey, F. J. Hypoxia causes down-regulation of 11 beta-hydroxysteroid dehydrogenase type 2 by induction of Egr-1. *FASEB Journal*, 17: 917-919, 2003.
27. Sonna, L. A., Cullivan, M. L., Sheldon, H. K., Pratt, R. E., and Lilly, C. M. Effect of hypoxia on gene expression by human hepatocytes (HepG2). *Physiol Genomics*, 12: 195-207, 2003.
28. Hofbauer, K. H., Gess, B., Lohaus, C., Meyer, H. E., Katschinski, D., and Kurtz, A. Oxygen tension regulates the expression of a group of procollagen hydroxylases. *Eur J Biochem*, 270: 4515-4522, 2003.
29. Takahashi, Y., Takahashi, S., Shiga, Y., Yoshimi, T., and Miura, T. Hypoxic induction of prolyl 4-hydroxylase alpha (I) in cultured cells. *J Biol Chem*, 275: 14139-14146., 2000.
30. Jiang, Y., Zhang, W., Kondo, K., Klco, J. M., St Martin, T. B., Dufault, M. R., Madden, S. L., Kaelin, W. G., Jr., and Nacht, M. Gene Expression Profiling in a Renal Cell Carcinoma Cell Line: Dissecting VHL and Hypoxia-Dependent Pathways. *Mol Cancer Res*, 1: 453-462., 2003.

## CHAPTER 2

Vengellur, Ajith., Woods, Barbara G., Ryan Heather E., Johnson, Randall .S., LaPres, John J. (2003) Gene Expression Profiling of the Hypoxia Signaling Pathway in Hypoxia-inducible Factor 1  $\alpha$  Null Mouse Embryonic Fibroblasts. Gene Expression 11: 181-197.

## **Abstract**

Hypoxia is defined as a deficiency of oxygen reaching the tissues of the body and it plays a critical role in development and pathological conditions, such as cancer. Once tumors outgrow their blood supply, their central portion becomes hypoxic and the tumor stimulates angiogenesis through the activation of the hypoxia inducible factors (HIFs). HIFs are transcription factors that are regulated in an oxygen-dependent manner by a group of prolyl hydroxylases (known as PHDs or HPHs). Our understanding of hypoxia signaling is limited by our incomplete knowledge of HIF target genes. cDNA microarrays and a cell line lacking a principal HIF protein, HIF1 $\alpha$ , were used to identify hypoxia regulated genes. The microarrays identified a group of 286 clones that were significantly influenced by hypoxia, and 54 of these were coordinately regulated by cobalt chloride. The expression profile of HIF1 $\alpha$  *-/-* cells also identified a group of down-regulated genes encoding enzymes involved in protecting cells from oxidative stress, offering an explanation for the increased sensitivity of HIF1 $\alpha$  *-/-* cells to agents that promote this type of response. The microarray studies confirmed the hypoxia induced expression of the HIF regulating prolyl hydroxylase, PHD2. An analysis of the members of the PHD family revealed that they are differentially regulated by cobalt chloride and hypoxia. These results suggest that HIF1 $\alpha$  is the predominant  $\alpha$  HIF isoform in fibroblasts and that it regulates a wide battery of genes critical for normal cellular function and survival under various stresses.

## Introduction

Hypoxia is defined as a state in which oxygen tension drops below the normal limits of 30 - 60mm Hg found in tissue beds (1). Hypoxia plays a central role in tumorigenesis but also has profound implications in normal cellular processes and development (2). Organisms have developed a programmed response to oxygen deprivation because of the critical role oxygen plays in energy production and survival (3). Central to an organism's response to hypoxia is the transcriptional upregulation of genes capable of stimulating glycolysis, angiogenesis and erythropoiesis (4-6) (see chapter "introduction"). Understanding hypoxia signaling, its transcriptional control and a complete assessment of target genes is critical to our ability to influence this signaling cascade and thereby treat or prevent illness that results in decreases in available oxygen. The HIF1 $\alpha$ :ARNT dimer is the most widely studied hypoxia signaling factor. The HIF1 $\alpha$  null animal is embryonic lethal due to vascularization defects, severely limiting its use for *in vivo* studies (7). Recently, a conditional null animal was created for HIF1 $\alpha$  using the Cre-LoxP system (8). Subsequently, an immortal mouse embryonic fibroblast (MEFs) cell line was established from this mouse model (8). The conditional animal and cell line make it possible to understand the role of HIF1 $\alpha$  *in vivo* at various developmental time points, tissues, and under various conditions.

We used cDNA microarrays and the HIF1 $\alpha$  null MEF cell line to study global gene expression pattern under hypoxia. Our results demonstrate that HIF1 $\alpha$  is

the primary mediator of hypoxia signaling in MEFs. The microarray experiments have detailed several groups of HIF1 $\alpha$  dependent genes. Among these HIF1 $\alpha$  dependent genes are the glycolytic enzymes and several pro-apoptotic factors. Most have been previously identified as hypoxia regulated, however some of these had not been previously characterized as HIF driven genes. Among the novel HIF1 $\alpha$  dependent genes identified in the microarray experiments and confirmed by relative real time PCR (rRT-PCR) was PHD2. In addition, PHD3 also showed HIF1 $\alpha$  dependent regulation. Overexpression of the PHDs was also shown to lead to a decrease in hypoxia induced gene transcription. The microarray study also gave some insight into the role of HIF1 $\alpha$  in cellular homeostasis. The direct comparison of untreated wild type and HIF1 $\alpha$   $-/-$  cells identified a group of genes influenced by the loss of the HIF1 $\alpha$  protein. These included genes that encode for proteins involved in protection against oxidative stress. These results suggest that the HIF1 $\alpha$  protein regulates a wide variety of genes and may be partially regulated by feedback inhibition.

### **Materials and methods**

*Materials:* Tissue culture media, supplements and fetal bovine serum were obtained from Invitrogen, Inc, Carlsbad, CA. The synthesis of oligonucleotides was performed by the macromolecular facility, Michigan State University, East Lansing, MI. SYBR Green Dye and 6-carboxy-X-rhodamine were purchased from Molecular Probes, Eugene, OR. AmpliTaq<sup>TM</sup> Gold PCR buffer and AmpliTaq<sup>TM</sup> Gold DNA polymerase were purchased from Perkin-Elmer,

Wellesley, MA. All other chemicals were reagent grade and obtained from Sigma-Aldrich Chemicals, St. Louis, MO.

*Cell culture, nuclear extracts and Western blotting:* Mouse embryonic fibroblast cell lines were maintained in DMEM media (10% heat inactivated FBS, penicillin-streptomycin (10 U/ml), non-essential amino acid (10  $\mu$ g/ml), L-glutamine (2mM)) and grown at 37°C in 5% CO<sub>2</sub>. Hypoxia treatments were performed in an oxygen-regulated incubator (Precision, Winchester, VA) or simulated by treating the cells with 100  $\mu$ M of CoCl<sub>2</sub> (dissolved in H<sub>2</sub>O).

Wild type and HIF1 $\alpha$  -/- cells were grown under control (20% O<sub>2</sub>), or hypoxic (1% O<sub>2</sub>) conditions or in the presence of 100  $\mu$ M CoCl<sub>2</sub> for 6 hours. Nuclear extracts were prepared as described previously with minor modifications (9). Briefly, cells were washed with cold PBS (4°C) and removed from surface by scraping in cell lysis buffer (10 mM Tris-HCl, pH 8.0, 1 mM EDTA, 150 mM NaCl, 1  $\mu$ g/mL each of Aprotinin, Leupeptin, Pepstatin A and 1 mM PMSF) and homogenized. The nuclei were removed by centrifugation (4000 rpm, 15 min) and the supernatant was saved. The nuclei were lysed upon addition of nuclei lysis buffer (20 mM HEPES, pH 7.9, 400 mM NaCl, 1 mM EDTA, and 1 mM DTT, 1  $\mu$ g/mL each of Aprotinin, Leupeptin, Pepstatin A and 1 mM PMSF). Insoluble matter was removed by centrifugation (10000 x g, 15 min). The protein concentration of the supernatant was determined by standard colorimetric assay via manufacturer's instructions (Bio-Rad™, Hercules, CA). Equal amounts of protein for each

sample were separated by SDS-PAGE, and Western blotting was performed with a HIF1 $\alpha$  specific antibody (Novus Biologicals, Littleton, CO). A horseradish peroxidase conjugated secondary antibody was used to facilitate detection. The blot was stripped and reprobed with a  $\beta$ -actin specific antibody (a generous gift from Dr. John Wang, Michigan State University). The blots were exposed using a chemiluminescent assay kit (Amersham Biosciences, Piscataway, NJ).

*cDNA microarray production:* The National Institute of Aging 15K clone set was used for the production of the microarray (10, 11). The NIA 15K set was supplemented with an additional 96 clones to bring the total number of clones to 15,360. Each clone was PCR amplified with modified M13 forward and reverse primers (Table 9). Each primer was modified on the 5' end with an amino linker to facilitate linkage to the aldehyde-modified glass substrate. Amplicons were precipitated and the size and quality verified by agarose gel electrophoresis, then resuspended in 3X SSC. The full 15K set was printed on Telechem<sup>TM</sup> Superaldehyde slides (Telechem International Inc., Sunnyvale, CA) using an OmniGrid<sup>TM</sup> robot (GenMachines®, San Carlos, CA) with Chipmaker 2 microarray pins (Telechem International Inc).

*Microarray experimental design:* The microarray experiments were performed using a “Loop” design (12) (Figure 8). This design was chosen to increase the statistical strength of the model, to allow for effective comparison among treatments and cell types and to facilitate the long-term goals of the project.

**Table 9. Primers for microarray production and RT-PCR**

Gene	Accession#	Forward	Reverse
M13		CTGCAAGGCGATTAAAGTTGGG	CTGCAAGGCGATTAAAGTTGGGTAAC
HPRT	NM_013556	AAGCCTAAGATGAGCGCAAG	TTACTAGGCAGATGCCACA
GAPDH	M32599	ACCCAGAAAGACTGGATGG	TTTAGCTGGGATGACCTT
P4H	NM_011031	CTGTTGTGGCCGAGTAAAT	GAAGTCGAAAGTGCGGTTTCAT
PHD1	AF453879	GGAAACCACATGAGGTGAAG	AACACCTTCTGTCCCCGATG
PHD2	XM_134453	GAACTGGGCAACTACAGGA	CATGTCAAGCATCTTCCATC
PHD3	NM_028133	AAGTTACACGGAGGGGTCT	GGCTGGACTTCATGTGGATT
SOD1	BC002066	GAGACTGGGCAATGTACT	TTGTTTCTCATGGACCACCA
SOD2	BC018173	AACTCAGGTGGCTTCAGC	GCTTGATAGCCCTCCAGCAAC
Catalase	NM_009804	CCAGTTGGCAAAGTGGTTTT	GCCCTGAAAGCTTTTTGTGACG
GST- $\mu$	NM_0010358	CACAAGATCACCCAGAGCAA	GGTGTCCATGACCTGGTTCT

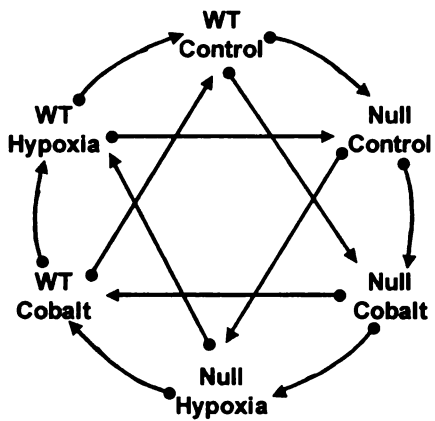


**Figure 8. Experimental Design of Loop**

Graphical representation of the 2V loop experimental design. Each arrow represents a single microarray slide. The arrowhead represents the sample labeled with Cy5 and the arrow tail represents sample labeled with Cy3. Since the loop was performed twice, each treatment group sample was labeled in 8 separate reactions, 4 with Cy3 and 4 with Cy5

Total RNA from two independent 10 cm tissue culture plates (approximately  $1 \times 10^7$  cells) within each treatment were labeled. Each RNA sample was labeled four times, twice with Cy3 and twice with Cy5. Two complete loops were performed; therefore, four independent cultures were labeled twice, once with each dye, equaling a total of eight individual labeling reactions per treatment group. It is important to note that the loop design does not utilize the calculation of expression intensity ratios but relies on the averaged expression within each treatment over all of the labeling reactions (in this case 8). Expression patterns are then statistically analyzed to determine those genes for which expression is significantly changed (below). Ratios can be calculated for each treatment by direct comparison of the averaged expression between the treatments of interest.

*RNA extraction and cDNA microarray probe labeling and hybridization:* RNA extraction was performed using Trizol reagent (Invitrogen) via the manufacturer's instructions and quantitated spectrophotometrically. 30  $\mu$ g of total RNA from wild type or HIF1 $\alpha$  *-/-* cells grown for 24 hours under control (20% O<sub>2</sub>) or hypoxic (1% O<sub>2</sub>) conditions or in the presence of 100  $\mu$ M CoCl<sub>2</sub> was used to generate probes as follows: Total RNA was incubated with 6  $\mu$ g anchored oligo-dT primers (5'-T<sub>21</sub>VN-3'). The reverse transcription was performed using Superscript™ II RNase H- Reverse Transcriptase (400 U, Invitrogen) in the presence of aminoallyl dUTP (aa-dUTP) (Amersham Biosciences, Piscataway, NJ), dTTP, dATP, dCTP and dGTP (final dNTPs = 0.5 mM). The ratio of aa-dUTP to dTTP was 2:1. The unincorporated nucleotides were removed using the QIAquick™ PCR purification

kit (Qiagen Inc., Valencia, CA) according to the manufacturer's instructions, after substituting the wash buffer with phosphate wash buffer (5mM KPO<sub>4</sub>, pH = 8.0 in 80% ethanol), and eluted with 4 mM KPO<sub>4</sub> (pH = 8.5). The probes were dried under vacuum centrifugation and resuspended in 0.1 M Na<sub>2</sub>CO<sub>3</sub> (pH = 9.0) and conjugated to monoreactive Cy3 and Cy5 dyes (Amersham Biosciences). Unincorporated dyes were removed using the QIAquick™ nucleotide removal kit (QIAGEN Inc.). Microarrays were prehybridized in pre-hyb buffer (5X SSC, 0.1 % w/v SDS, 1 % w/v BSA) for 2 hours at 42°C. Cy3 and Cy5 labeled probes were resuspended in hybridization buffer (50% formamide, 5X SSC, 0.1% SDS, 20 µg Cot1 DNA, and 20 µg Poly (A)-DNA) and denatured at 95°C for 3 minutes. The probes were hybridized for at least 20 hours to the microarrays at 42°C under Lifter slips™ (Erie Scientific Company, Portsmouth, NH). Slides were washed as follows: 1) brief wash with 1x SSC and 0.2% SDS at 42°C to remove the cover slips; 2) 4 min in 1x SSC and 0.2% SDS at 42°C; 3) 4 min in 0.1x SSC and 0.2% SDS at room temperature; and 4) twice for 2.5 min each in 0.1x SSC at room temperature. Slides were dried and scanned immediately.

*Microarray data analysis:* Slides were scanned with an Affymetrix™ 428 scanner (Affymetrix™, Santa Clara, CA) at 532 nm (Cy3) and 635 nm (Cy5). The images were analyzed using GenePix™ Version 3.0 software (Axon™ Instruments Inc., Union City, CA) and output files were analyzed using GP3 (<http://www.bch.msu.edu/~zacharet/microarray/gp3.html>) (13). GP3 automatically flags spots with intensities below background levels, corrects for

background signal, and normalizes the two channels using a z-score method. The GP3 output values were normalized within the loop using the Centralizer program (14) (<http://cartan.gmd.de/~zien/centralization/>). Genes differentially expressed between treatments were identified by t-test (two tailed, unequal variance,  $p \leq 0.05$  cut-off). All genes called present (signal > [background + 2 standard deviations of background]) were hierarchically clustered using GeneSpring™, v 4.2.1 (Silicon Genetics, Redwood City, CA).

*Relative Real-Time PCR analysis:* Changes in gene expression observed by microarray analyses were verified by real-time PCR, performed on an Applied Biosystems Prism 7000 Sequence detection System (Foster City, CA) (for detailed protocol see chapter 1 methods section). Gene names, accession numbers, forward and reverse primer sequences are listed in Table 9.

*Transient Transfection of Hep3B cells:* Hep3B cells were maintained in DMEM + 5% FBS (growth media). Prior to transfection, cells were washed twice with serum free medium (DMEM). Cells were transfected using lipofectamine (Invitrogen, Carlsbad, CA) via manufacturer's instructions using 5 ul of lipofectamine (LF) with an incubation time of 6 hours prior to addition of growth media. Cells were transfected with an HRE-driven luciferase reporter, a  $\beta$ -galactosidase ( $\beta$ GAL) expression vector for control of transfection efficiency and the various PHD expression vectors (A generous gift of Dr. Peter Ratcliff, University of Oxford, United Kingdom). All transfections were normalized for

DNA content with an empty expression vector. DNA was incubated with rehydrated LF for 15 minutes prior to transfection. Cells were then treated with DNA:LF mix for 6 hours. Following this, incubation medium was removed and replaced with growth media and placed into control (20% O<sub>2</sub>) or hypoxia (1% O<sub>2</sub>) incubator. Cells were incubated for 18 hours and assayed for luciferase and  $\beta$ -Gal activity via standard assays (Promega, Madison, WI). Luciferase values were normalized to  $\beta$ Gal activity in each well and untreated empty expression vector within experiments.

## **Results**

*Verification of the MEF cell line phenotype:* A Western blot was performed on the cell lines used in our microarray experiments to verify their phenotype. Wild type and HIF1 $\alpha$  -/- cells were exposed to CoCl<sub>2</sub> (100  $\mu$ M) or hypoxia (1% O<sub>2</sub>) for 6 hrs. Nuclear extracts were prepared from treated and untreated cells and analyzed using a HIF1 $\alpha$  specific antibody (Novus Biologicals, Littleton, CO). As expected, HIF1 $\alpha$  was only detectable in the wild type cells. A very small amount was observed in untreated cells but greatly increased following exposure to cobalt or hypoxia (Figure 9). There was also a migratory shift in these treated fractions suggesting a protein modification. The blot was reprobbed with an antibody specific to  $\beta$ -actin to verify loading (Figure 9).

*Hierarchical Cluster analysis of microarray data:* cDNA microarrays have given researchers an opportunity to understand signaling networks as they relate to

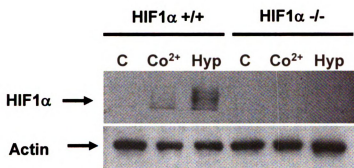


**Figure 9. HIF1 $\alpha$  Western Blot**

Wild type (HIF1 $\alpha$  +/+) and Null (HIF1 $\alpha$  -/-) cells were exposed to CoCl<sub>2</sub> (Co<sup>2+</sup>, 100  $\mu$ M) or Hypoxia (Hyp, 1% O<sub>2</sub>) for 6 hours or left untreated (C). Nuclear extracts were prepared and proteins were separated by SDS-PAGE, transferred to nitrocellulose membrane and probed with a HIF1 $\alpha$  specific antibody (**upper panel**). Blot was reprobbed with  $\beta$ -actin to verify equal loading (**lower panel**).

global changes in gene expression. Here microarrays were used to characterize hypoxia signaling and the role of HIF1 $\alpha$  in this process. Two cell lines were used, the wild type and the HIF1 $\alpha$   $-/-$  MEFs. Each cell line was left untreated (Control, 20% O<sub>2</sub>) or treated with hypoxia (1% O<sub>2</sub>) or cobalt chloride (100  $\mu$ M) for 24 hours. Cobalt has been extensively used as a hypoxia mimic and has been shown to inhibit the activity of the PHDs (15). The microarray experiments were performed in a “loop” design as described above (Figure 8) and statistically analyzed (16).

Hierarchical cluster analysis of microarray data along treatments and genes creates relationships between groups based on expression patterns observed in the gene set as a whole. Here we used cluster analysis to identify combinations of treatments and genotype that were similar at the gene expression level and to identify groups of genes responding in a similar manner among the various treatment and genotype combinations. As expected, results from CoCl<sub>2</sub> and hypoxia treatments in the wild type cells clustered together (Figure 10). This similarity in gene expression between these two treatments did not extend to the null MEFs. These results suggest that CoCl<sub>2</sub> and hypoxia are driving expression of a similar gene cluster and that HIF1 $\alpha$  is essential for this regulation. Interestingly, the HIF1 $\alpha$   $-/-$  cells under hypoxic conditions behaved most like the null control cells (Figure 10). The loss of hypoxia signaling and comparable expression pattern between hypoxia and control suggests that HIF1 $\alpha$  is central to hypoxia mediated signaling in these cells.

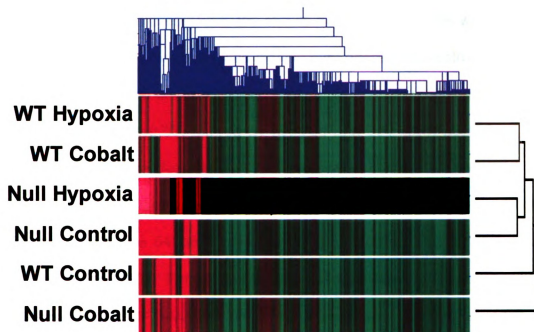


**Figure 10. Hierarchical Cluster diagram of entire data set**

The microarray data was filtered to remove genes for which expression was determined to be insignificant (signal < {background + 2 st. dev. Background}). Expression results from the filtered data were clustered by treatment and gene. The relationships are represented as a dendrogram in both directions. Red represents a high level of expression and green represents low expression.

*Statistical comparison of hypoxia and cobalt treatment in WT cells:* The major focus of these microarray studies was to identify a more complete battery of hypoxia regulated genes. This was accomplished first by statistical assessment of expression patterns within the data. Stringent criteria were set to minimize the possibility of false positives. First, the results from wild type cells were screened for all genes whose expression was significantly altered by treatment ( $p < 0.05$  compared to untreated control). The results show that expression of 286 clones was significantly ( $p \leq 0.05$ ) altered by hypoxia and 252 were altered by cobalt (Figure 11). Next, we determined the overlap within these two sets and found that there were 54 clones representing 49 different genes that were in both of these groups. These 54 clones were then analyzed for function and grouped accordingly (Table 10). Finally, we determined how many of these genes were also altered in the HIF1 $\alpha$ -/- cells under the same conditions. None of these 49 genes were altered in both hypoxia and cobalt in the null cells. However, seven of the 49 genes in table 10 were significantly altered in the HIF1 $\alpha$  -/- cells in either cobalt or hypoxia treatment. The genes for metallothionein (clone A-2031) and transglutaminase (clone H3137C06) were influenced in the HIF1 $\alpha$  -/- cells by cobalt. The HIF1 $\alpha$  independent increase in metallothionein is most likely due to its regulation by the metal transcription factor (17). Five of the 49 genes were shown to be significantly influenced by hypoxia in the null cells. These genes were pyruvate kinase 3 (clones H3030D10 and H3030D11), cathepsin L (clone H3028F03), galectin 3 (clone H3016D10), tissue specific transplantation antigen P35B (clone H3147H11) and one gene with unknown function (clone H3116A06).

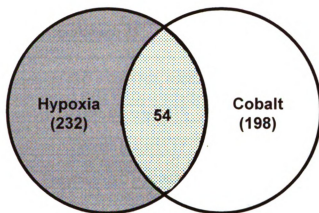


**Figure 11. Analysis of  $\text{CoCl}_2$  and hypoxia treatment in wild type cells**

The Venn diagram represents total number of genes unique to each treatment group (in parentheses) and the number of genes shared between the two treatments.

**Table 10. Significantly influenced genes in WT cells treated with hypoxia or cobalt**

ID	Gene Name	Abbr.	Fold Changes			
			W-Co	W-H	N-Co	N-H
<b>Extracellular (GO= 0005615, 0005576, 0005578)</b>						
H3003D12	proline 4-hydroxylase	P4ha2	1.29	2.61	0.97	1.05
H3011E02	chorionic somatomammotropin hormone 1	Csh1	0.67	0.80	0.81	0.82
H3027D05	lymphocyte antigen 6 complex, locus E	Ly6e	0.78	1.26	0.88	0.84
H3028F03	cathepsin L	Ctsl	2.17	1.54	1.28	2.92
H3058D07	matrix metalloproteinase 23	Mmp23	0.71	1.43	0.49	0.55
H3109A05	CD24a antigen	Cd24a	0.71	0.67	0.59	0.62
H3115F11	Nidogen-2	Nid2	1.40	1.35	0.76	1.05
<b>Mitochondrial (GO = 0005762, 0005739, 0005743)</b>						
H3016D08	BCL2/adenovirus E1B 19kDa-interacting prote	Bnip3l	1.39	1.58	0.91	0.95
H3029D09	mitochondrial ribosomal protein S11	Mrps11	0.81	0.77	1.40	0.86
H3052D11	adenylate kinase 2	Ak2	0.74	0.74	0.93	0.96
H3137G05	mitochondrial ribosomal protein L17	Mrpl17	0.55	0.60	1.03	0.77
H3143D12	mitochondrial carrier homolog 1 (C. elegans)	Mtch1	1.45	1.55	1.05	1.21
<b>Glycolytic Enzymes (GO = 0006096)</b>						
H3012A11	glyceraldehyde-3-phosphate dehydrogenase	Gapd	1.36	1.63	0.79	0.82
H3019E08	glyceraldehyde-3-phosphate dehydrogenase	Gapd	1.45	1.75	0.90	0.86
H3023D06	phosphoglycerate kinase 1	Pgk1	2.31	3.67	0.69	0.93
H3023H12	lactate dehydrogenase 1, A chain	Ldh1	2.71	3.93	0.86	0.89
H3027E07	enolase 1, alpha non-neuron	Eno1	1.94	1.82	0.75	0.92
H3027E08	enolase 1, alpha non-neuron	Eno1	2.12	3.02	0.98	1.10
H3027E09	enolase 1, alpha non-neuron	Eno1	1.76	2.48	0.87	0.75
H3030D10	pyruvate kinase, muscle	Pkm2	1.62	2.02	0.86	0.69
H3030D11	pyruvate kinase, muscle	Pkm2	1.93	2.36	0.87	0.65
H3031D03	aldolase 1, A isoform	Aldo1	1.35	1.92	0.88	0.92
H3149C10	triosephosphate isomerase	Tpi	2.06	2.18	0.82	0.81
<b>Membrane Proteins (GO = 0016021)</b>						
H3022E01	membrane bound C2 domain containing prote	Mbc2	1.24	1.22	1.01	1.04
H3151C09	CD 81 antigen	Cd81	1.49	1.44	0.96	1.25
<b>Enzymes and Misc Function (Various GO)</b>						
H3016D10	lectin, galactose binding, soluble 3	Igal3	1.46	1.62	1.07	1.32
H3016G08	cask-interacting protein 2	Caskin2	1.64	1.82	1.17	1.28
H3019C07	macrophage migration inhibitory factor	Mif	1.69	1.95	1.21	1.05
H3020C02	metallothionein 1	Mt1	2.07	1.27	1.25	1.11
A-2031	metallothionein 1 (image 1052401)	Mt1	2.810	1.784	2.134	1.561
H3031B12	minichromosome main. Def. 3 assoc. protein	Mcm3a	1.42	1.33	0.92	0.96
H3137C06	transglutaminase 2, C polypeptide	Tgm2	0.63	0.85	0.56	0.88
H3147H11	tissue specific transplantation antigen P35B	Tsta3	1.73	1.47	1.26	1.45
H3016F05	Similar to translation initiation factor 3, subunit	Eif3s4	0.89	0.83	0.99	0.91
H3130A05	proteasome 26S subunit, non-ATPase, 2	Psm2	0.50	0.51	0.60	0.57
<b>Function Unknown (Various GO)</b>						
H3044B11	DNA segment, Chr 8		0.80	0.63	0.98	0.94
H3065C11	expressed sequence AU022848		0.61	0.70	0.80	0.90
H3118D07	DNA segment, Chr 11		0.77	0.90	1.01	0.97
H3128G06	expressed sequence AW215868		1.47	1.70	1.09	1.22
H3134C05	hypothetical protein LOC223886		0.67	0.54	0.71	0.53
H3142E06	RIKEN cDNA 1110031E24 gene		0.74	0.90	0.83	1.13
H3148A03	DNA segment, Chr 10		0.76	0.67	0.86	0.88

**Table 10. Significantly influenced genes in WT cells treated with hypoxia or cobalt (continued)**

ID	Gene Name	Abbr.	W-Co	W-H	N-Co	N-H
H3030G02	Neurophilin-like molecule		1.77	2.20	1.12	1.12
H3108H01	Human from clone RP11-494N1 on chromosome 9		0.80	0.73	1.08	0.99
H3116A06	Mus musculus, clone IMAGE:4024675, mRNA		1.24	1.35	1.08	1.30
H3132E05	Mouse from clone RP23-170G19 on chromosome X		1.31	0.79	0.87	0.81
	<b>Unknown (Various GO)</b>					
H3017G08			1.59	2.05	0.93	0.96
H3150A01			1.36	1.73	0.88	1.00
H3022E07			1.43	1.94	0.79	0.82
H3125B04			1.64	1.76	1.15	1.23
H3017D11			0.74	0.63	0.88	0.92
H3072E04			1.21	0.85	0.88	1.06
H3123A12			1.95	2.07	0.78	0.95
H3146H09			0.74	0.57	0.90	1.05

It should be noted that the pyruvate kinase 3 gene was significantly downregulated in the null cells while being significantly upregulated in the WT cells under hypoxia.

Only 12 of the 49 genes in Figure 11 and Table 10 had been previously associated with hypoxia signaling. The 54 clones were separated into 7 categories by ontology. The largest group that could be assigned a function consists of glycolytic enzymes (11 clones, 7 genes, Table 10). These enzymes are well known targets of the hypoxia signaling cascade. There were several genes in other groups that also had been identified as hypoxia targets. Most notably are proline-4-hydroxylase (P4H, clone H3003D12) and BCL2/adenovirus E1B 19 kDa-interacting protein 3-like (BNIP3L or NIX, clone H3016D08). There were also several groups that had not been previously identified as hypoxia targets. These include a large group of matrix remodeling genes and cellular antigens. The largest group included clones for which function has not yet been assigned (Table 10).

*Comparison of hypoxia and cobalt treatment in HIF1 $\alpha$  -/- cells:* As noted above, only a handful of genes identified in Figure 11 and Table 10 were significantly changed in null cells. None of these genes (metallothionein, pyruvate kinase, transglutaminase, cathepsin L and galectin 3) were influenced in both treatments in the null cells. To further clarify the HIF1 $\alpha$  independently regulated genes from the microarray studies, a comparison between cobalt and hypoxia treated HIF1 $\alpha$

-/- cells was performed. There were 376 clones significantly altered in these cells upon exposure to hypoxia (1%, 24 hours) and 349 clones significantly altered upon exposure to cobalt (100  $\mu$ M, 24 hours) (data not shown). There were 65 clones that were shared between these two lists (Figure 12A). Of these 65 clones, none were found in the list for the wild type cells (Table 10, Appendix data table 11). These 65 clones represented several different enzymes including subunits of ATPase and biliverdin reductase B (BLRVB). BLRVB is downstream of heme oxygenase 1 in the metabolism of heme. Heme oxygenase, a known hypoxia regulated gene, converts heme into carbon monoxide, biliverdin and free iron. BLRVB converts biliverdin into bilirubin (18-20). This suggests that the pathway for heme degradation is not coordinately regulated under hypoxic conditions. This group also contained a receptor for tumor necrosis factor and raises the possibility that hypoxia and hypoxic mimics influence the expression of the receptor of a factor known to play a role in hypoxia signaling (21, 22). These 65 clones presumably represent a subset of genes that can be influenced by hypoxia and cobalt in a HIF1 $\alpha$  independent manner and may involve HIF2 $\alpha$  or HIF3 $\alpha$  since both are expressed in these cells at a much lower level than that of HIF1 $\alpha$  (data not shown).

*Comparison of hypoxia treatment in wild type and HIF1 $\alpha$  -/- cells:* The comparison described in Figure 11 and 12A were done using those genes that were significantly changed by hypoxia and cobalt. To identify genes regulated in

a

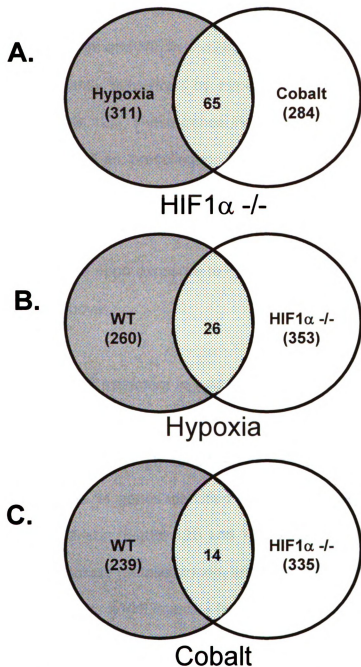


**Figure 12. Venn diagrams of various combinations of cell types and treatments**

Total number of genes unique to each treatment group (in parentheses) and the number of genes shared between the two treatments (central shaded area). **(A)** The Venn diagram representing genes significantly influenced by hypoxia and/or cobalt in HIF1 $\alpha$  -/- cells. **(B)** Comparison of WT and HIF1 $\alpha$  -/- cells following hypoxia treatment (1% O<sub>2</sub>, 24 hrs). **(C)** Comparison of WT and HIF1 $\alpha$  -/- cells following cobalt treatments (100  $\mu$ M, 24 hrs).

HIF1 $\alpha$  independent manner by hypoxia alone, a comparison between hypoxia treatments in wild type and HIF1 $\alpha$  *-/-* cells was performed. There were 26 genes that were significantly influenced by hypoxia in both cell types (Figure 12B, Appendix data table 12). These genes included those described above (Figure 11, Table 10), as well as, procollagen. Hypoxia-induced collagen synthesis has been previously described and may be critical to several disease states (23, 24). Interestingly, procollagen is upregulated in the wild type cells and down-regulated in the HIF1 $\alpha$  *-/-* cells upon exposure to hypoxia, similar to the pyruvate kinase 3 gene mentioned above.

*Comparison of cobalt treatment in wild type and HIF1 $\alpha$  *-/-* cells:* A comparison between wild type and HIF1 $\alpha$  *-/-* cells was also performed for genes significantly influenced by cobalt. Though cobalt is used as a hypoxia mimic, there is no overlap between the 14 genes identified in this comparison and those found for the hypoxia comparison (Figure 12B and 12C, Appendix data table 13). The 14 genes in this list include metallothionein and transglutaminase 2 (Tg2). Tg2 was previously identified as a VHL/hypoxia target gene (25).

*Comparison of WT ctrl and HIF1 $\alpha$  *-/-* ctrl cells:* Finally, a direct comparison between untreated WT and HIF1 $\alpha$  *-/-* cells was performed to determine the role of HIF1 $\alpha$  in cellular homeostasis. There were 234 genes influenced by the loss of HIF1 $\alpha$  (data not shown). Of these, H19 was significantly upregulated by the loss of the HIF protein. The three clones, H3144B07, H3144B06, H3140G12,

displayed a WT control/HIF1 $\alpha$  -/- control ratio of 0.067, 0.211 and 0.131 respectively (average 9 fold higher in HIF1 $\alpha$  -/- cells). H19 is an imprinted gene involved in development and not highly expressed following birth (26). The reason for its aberrant expression following loss of the HIF1 $\alpha$  protein is unknown. Another group of genes also stood out in this comparison of control cells. The HIF1 $\alpha$ -/- cells displayed a decreased expression level of genes involved in the cellular response to oxidative stress. These genes include glutathione S transferase- $\mu$  (GST- $\mu$ , clones = H3134F05, H3119G08, H3159G05), superoxide dismutase 1 (SOD1, clones = H3130B11, H3130B11), SOD2 (A-2062) and catalase (A-2049). This decreased level of these protective genes may explain why HIF1 $\alpha$  -/- cells are more sensitive to oxidative stress (27). In addition, this decrease adds to the growing evidence of the complex role hypoxia signaling plays in normal cellular homeostasis and tumorigenesis.

*The glycolytic cluster:* One hypothesis of expression profiling is that genes that cluster together are regulated in a similar manner. We wanted to identify novel genes that may also play a role in the cellular response to hypoxia, and our hypothesis was that they would behave similarly, at the expression level, to the glycolytic enzymes. The glycolytic enzymes are critical to a cell's response to low oxygen tension and are direct targets of HIF regulated transcription. We isolated a cluster of glycolytic genes from our microarray data and looked for functional information for several of the non-glycolytic genes (Figure 13). First, three genes involved in apoptosis were found within this cluster. Two are known

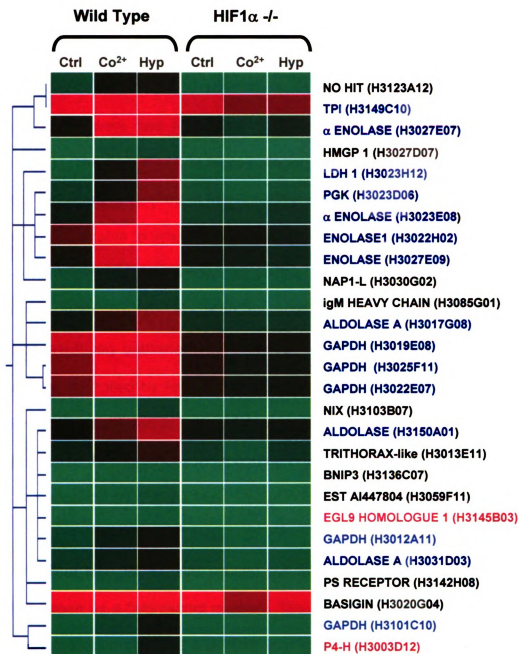


**Figure 13. Glycolytic enzyme cluster**

The cluster of glycolytic enzyme genes (Fig. 4) was further analyzed to identify novel hypoxia regulated genes. Four subsets of genes were identified; the glycolytic enzyme's genes (**blue**), apoptotic genes (**green**), hydroxylases (**red**) and others (**black**). Red represents a high level of expression and green represents low expression.

(BNIP3 and NIX) and one is a novel (PS receptor) hypoxia-regulated gene (28, 29). The role that these genes play in the downstream events following acute and chronic hypoxia is currently being investigated.

Second, there were two hydroxylases identified within this glycolytic cluster (Figure 13). The first, P4-H, is a pro-collagen prolyl 4-hydroxylase and a known hypoxia regulated gene (30). It functions in a similar manner to that of the PHDs, however, it is unable to influence HIF stability in *C. elegans* (15). The second is EGL-9 homologue 1, also known as PHD2. As mentioned earlier, the PHDs negatively influence HIF signaling by controlling HIF stability. This result confirms previously published data and supports the hypothesis that HIF1 $\alpha$  may be partially controlled by feedback inhibition (15, 31). It should be pointed out that PHD2 was not listed in Table 10 (genes altered by cobalt and hypoxia in WT cells) because the increase seen following cobalt exposure for this clone did not pass statistical cut off (Figure 14).

*Relative Real time PCR:* We verified our microarray data by rRT-PCR using SYBR<sup>®</sup> Green as a fluorescent marker. The glycolytic enzyme glyceraldehyde-3-phosphate dehydrogenase (GAPDH) is a known hypoxia regulated gene and acted as a positive control for our SYBR<sup>®</sup> Green protocol. GAPDH was also present on the microarray and shown to be regulated in a HIF1 $\alpha$ -dependent manner (Figure 11, 13 and Figure 14A). In addition, the loss of GAPDH regulation by hypoxia in the HIF1 $\alpha$  *-/-* suggests that HIF1 $\alpha$  is the primary

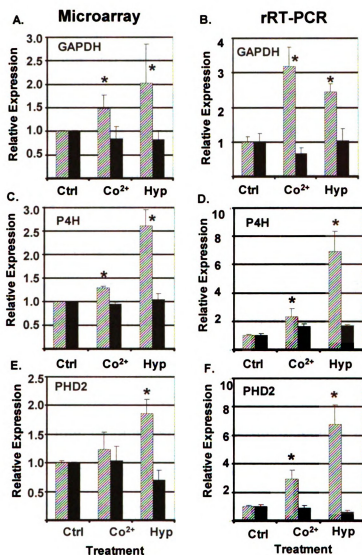


**Figure 14. Comparison of microarray and rRT-PCR results**  
 GAPDH (A, B), P4H (C, D) and PHD2 (E, F) were analyzed for expression levels in wild type (hatched bars) and HIF1 $\alpha$ <sup>-/-</sup> cells (solid bars) by microarray (A, C, E) and rRT-PCR (B, D, F) protocols. Each value was normalized to the control level in the corresponding cell line. Ctrl = untreated, Co<sup>2+</sup> = 100  $\mu$ M CoCl<sub>2</sub> and Hyp = 1% O<sub>2</sub> for 24 hours. Averaged expression within each treatment group was used to generate ratios (see experimental design). \* Represents  $p < 0.05$  when compared to corresponding control

mediator of hypoxia signaling in MEFs. These results were confirmed in the rRT-PCR. Six separate biological samples were analyzed for each separate treatment in the two cell lines. There was a significant increase in GAPDH message in the cobalt and hypoxia treated wild type cells when compared to the control. This increase did not extend to the HIF1 $\alpha$  *-/-* cell line (Figure. 14B). A similar HIF1 $\alpha$ -dependent expression pattern was seen on the microarray for P4-H (Figure 13 and 14C). This result was also verified on the rRT-PCR (Figure. 14D). The results for the cobalt treatment were not as pronounced as that following hypoxia exposure, though both were statistically significant. Finally, the expression pattern of PHD2 was also confirmed by rRT-PCR (Figure. 14E and 14F). There was only a modest increase in expression when the microarray was analyzed. The expression pattern among the treatment groups, however, was identical to that of other known hypoxia regulated genes in the cluster (i.e. increased in cobalt and hypoxia in wild type cells, no change in HIF1 $\alpha$  *-/-* cells). The rRT-PCR results confirmed that PHD2 transcription increased in response to cobalt (> 3 fold) and hypoxia (> 6 fold) when compared to the control treatment only in the wild type cells. These results suggest that HIF1 $\alpha$  may indirectly control its own stability by affecting the level of the prolyl hydroxylase that marks it for degradation. This data also show the level of data compression that is often seen in microarray data due to the dynamic range of the microarray scanner, normalization and other mathematical manipulation necessary for comparisons between multiple experiments and labelings (32). The difference in fold change in the microarray data is consistently underestimated. The relative compression

of the data for various genes ranged from 2 to 10 fold lower on the microarray compared to rRT-PCR.

Given the implications of hypoxia-regulated PHD expression we also analyzed the expression pattern of all three PHDs for their time and HIF1 $\alpha$  dependent expression by rRT-PCR. Wild type and HIF1 $\alpha$   $-/-$  cells were left untreated or exposed to hypoxia (1% O<sub>2</sub>) or cobalt (100  $\mu$ M) for 0.25, 2, 8, 24, 48 and 72 hours. PHD1 exhibited small but significant changes in expression at various times, however these changes did not follow a pattern and did not appear HIF1 $\alpha$  dependent (Figure 15). PHD2 was significantly upregulated in a HIF1 $\alpha$  dependent manner in the wild type cells as early as 15 minutes after exposure in both the hypoxia and cobalt treated cells. PHD3 showed a large increase (> 11-fold) in the wild type cells following hypoxia but not cobalt exposure (Figure 15). The time course of this induction was also notably different from that of PHD2. The mechanism that controls the expression differences between the various PHDs has not been determined. These results indicate that the PHD genes are regulated by hypoxia in different ways. In addition, the identification of PHD2 and PHD3 as hypoxia-regulated genes suggests that the hypoxia signaling cascade may be partially controlled by feedback inhibition.

Finally, the microarray data suggests that loss of HIF1 $\alpha$  leads to a down regulation of the basal levels of oxidative stress genes. The basal level of

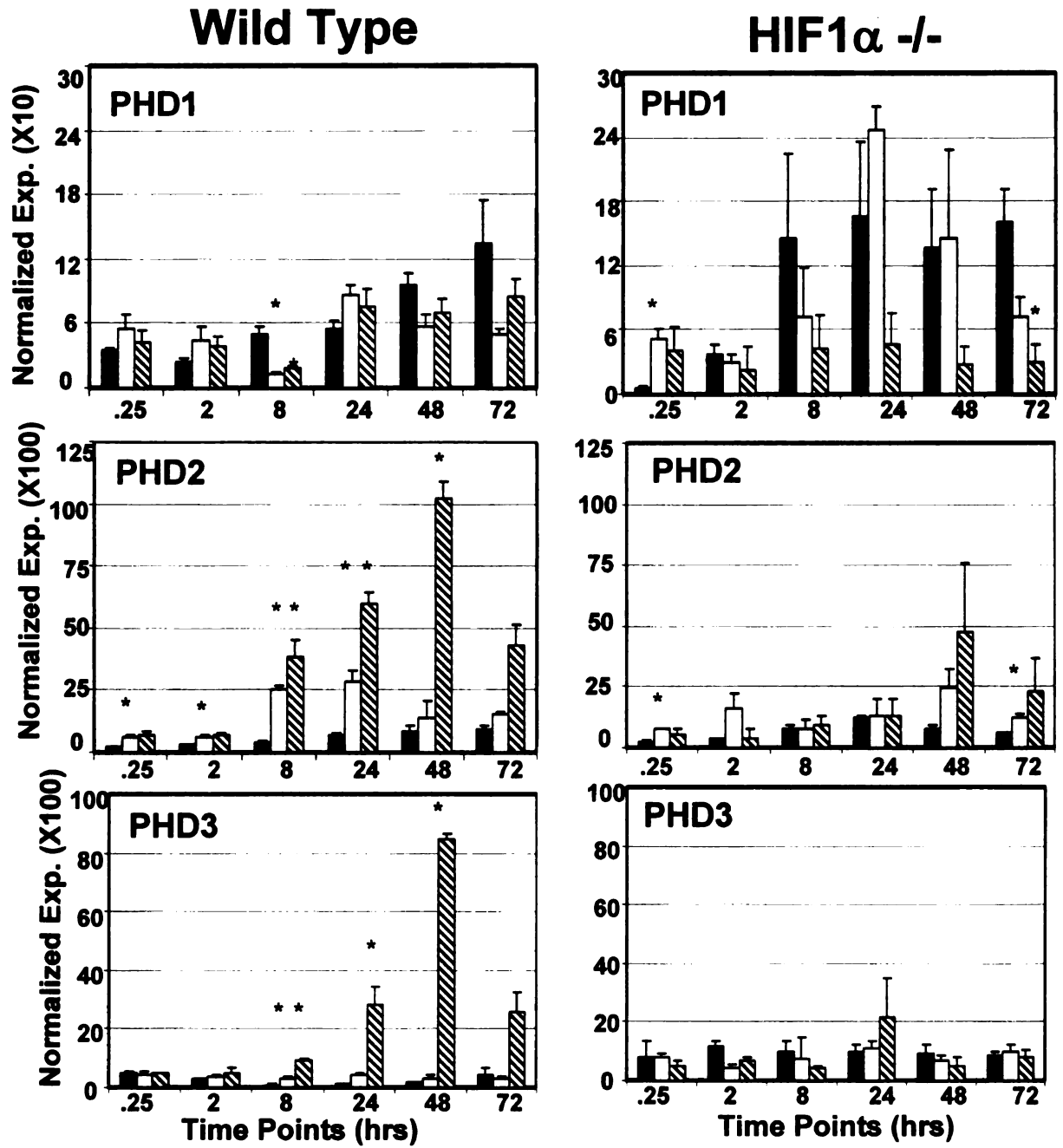


**Figure 15. Time course analysis of the PHDs by rRT-PCR**

The expression levels of the various PHDs were analyzed by rRT-PCR in wild type (left) and HIF1 $\alpha$  -/- (right) cells. Each bar represents an average value of 6 samples normalized to the expression level of the control gene and graphed as normalized expression. **Black bars** = untreated, **White bars** = 100  $\mu$ M CoCl<sub>2</sub> and **Hatched bars** = 1% O<sub>2</sub>. \* Represents p < 0.05 when compared to corresponding control.

expression of GST- $\mu$ , SOD1, SOD2 and catalase were verified by rRT-PCR. As seen in Figure 16, the basal levels of GST- $\mu$ , SOD1 and SOD2 were significantly repressed following loss of the HIF1 $\alpha$  proteins. Catalase was not influenced in this comparison. The decreased level of expression of these protective enzymes may explain why HIF1 $\alpha$   $-/-$  cells are more susceptible to oxidative stress induced damage (27).

*PHD effects on HIF mediated transcription:* The possibility that upregulation of the PHDs might lead to a feedback inhibition of HIF mediated signal was tested in transient transfection experiments. Hep3B cells were transfected with an HRE driven luciferase reporter and the various PHD expression plasmids. The cells were left at control (20% O<sub>2</sub>, ctrl) or hypoxia (1% O<sub>2</sub>) for 18 hours and analyzed for luciferase expression. PHD2 was capable of completely inhibiting HRE mediated luciferase expression (Figure 17). PHD3 was also capable of inhibiting this transactivation but to only 50% of controls (Figure 17). Finally, hypoxia mediated transcription displayed a 40% reduction in the presence of PHD1; however, this decrease was not significant. This supports the notion that these enzymes play a role in regulating the initial HIF signal and are also involved in attenuating the signal by feedback inhibition (15, 31, 33).

## **Discussion**

Hypoxia mediated signaling is critical to normal development and is strongly involved in several pathological conditions, including cancer and heart disease.

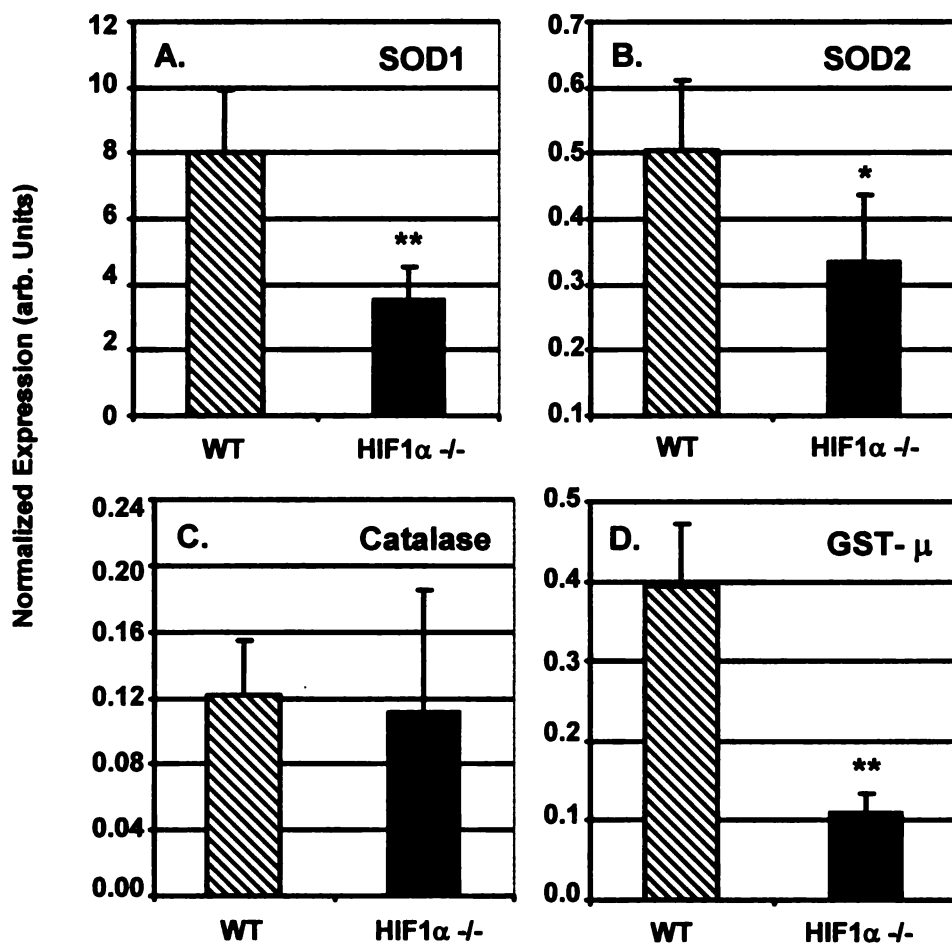


**Figure 16. Analysis of basal levels of GST- $\mu$ , SOD1, SOD2 and catalase by rRT-PCR**

The basal level of expression of genes involved in the cellular response to oxidative stress was analyzed by rRT-PCR. SOD1 (A), SOD2 (B), Catalase (C) and GST- $\mu$  (D) were analyzed in untreated control cells to determine their relative levels of expression in wild type (hatched bars) vs. HIF1 $\alpha$  -/- cells (solid bars). \*\* Represents p < 0.05, \* Represents p < 0.1.

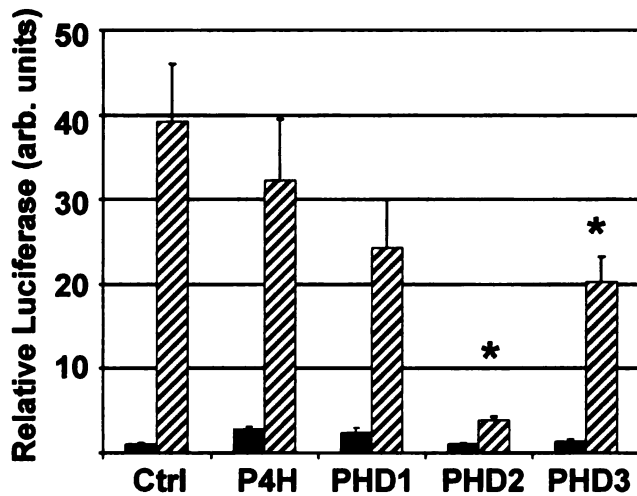


**Figure 17. Transient transfection of Hep3b cells**

Hep3b cells were transiently transfected with a HRE driven reporter and one of the PHDs or an empty expression vector as a control. Transfected cells were left untreated (**Dark Bars**) or exposed to hypoxia (1% O<sub>2</sub> for 18 hours, **Hatched Bars**) Luciferase levels were determined and normalized to co-transfected β-Gal activity and then to untreated control.

Characterizing the upstream and downstream events following onset of hypoxia is critical to our ability to treat and understand these conditions. Recent publications have increased our understanding of the upstream signals involved in HIF stabilization and the role that hydroxylation plays in mediating the HIF:VHL interaction (15, 34, 35). However, our understanding of the downstream events is not as complete. For example, we do not know the events and proteins involved in translocating HIFs into the nucleus. In addition, we do not know what, if any, protein is involved in controlling the ability of HIFs to interact with ARNT or ARNT2. Finally, we do not know the complete battery of hypoxia-regulated genes. The microarray is an excellent tool to address the latter knowledge gap. To this end we have used the NIA 15K gene set to identify novel hypoxia regulated genes.

Our microarray experiments confirmed the expression of several known hypoxia regulated genes, including glycolytic enzymes, pro-apoptotic genes and a prolyl hydroxylase (Figure 11 and 13 and Table 10). These act as positive controls to confirm that our treatments, microarray experiments and data processing are valid. In addition, it gave added confidence to the results that we observed for the novel hypoxia-regulated genes identified. To further validate the analysis a comparison of the 49 gene identified in Figure 11 and Table 10 was made with a recently published report that used serial analysis of gene expression (SAGE) to analyze the effect of VHL and hypoxia on normal and tumor derived renal cells (36). Given that the species and platforms are different, the extent of overlap will

be underestimated. However, of the 49 genes identified as hypoxia responsive in this study, 12 were found to be hypoxia responsive in the SAGE study (Appendix data table 14 and figure 3 of (36)). This number is most likely higher due to the nature of SAGE and the genes represented on the microarray. For example, GLUT1 and GLUT2 were shown to be hypoxia responsive via SAGE while GLUT4 was found in this study (Appendix data table 14). In addition, GLUT1 and GLUT2 are not represented in the NIA 15K.

The microarray confirmed that the hypoxic mimic,  $\text{CoCl}_2$ , increases a battery of genes similar to that of hypoxia. This overlap between expression patterns was only partial, suggesting differences in secondary signals or downstream signaling molecules. The exposure period was 24 hours and each treatment may initiate other pathways and distinct secondary responses that will be observed at this time point. It should also be pointed out that the results observed in these studies with respect to the PHDs are in agreement with previously published reports; however, the time course and differences seen between cobalt and hypoxia treatments had not been previously described (15, 37, 38). Finally, the microarray experiments suggest that HIF1 $\alpha$  is the primary cytoplasmic controller of hypoxia signaling in MEFs. The role of HIF2 $\alpha$  and HIF3 $\alpha$  has yet to be determined in these cells.

The identification of PHD2 and PHD3 as hypoxia-regulated genes implies that HIF1 $\alpha$  is subject to feedback inhibition (31). This feedback is not surprising when

considering the implications of overstimulation of the hypoxia-signaling cascade. For example, the VHL protein is thought to be a tumor suppressor in part because of its ability to mediate the degradation of HIF (39). Once the VHL gene is mutated, this ability is lost and HIF signaling goes unabated leading to the overproduction of a number of factors such as VEGF. This unchecked production of growth factors and other proteins may explain the hypervascularization of VHL  $-/-$  neoplasms (39). The control of the hypoxia-signaling cascade, both upstream and downstream, is therefore critical to normal cells and tissue homeostasis. We speculate that the feedback loop would limit the expression of the pro-apoptotic genes, thus giving the cell an alternative to programmed cell death. For example, the oxygen concentration of the cell at equilibrium may be "set" to limit damage due to small decreases in oxygen tension. Once these small fluctuations are encountered, the HIF protein is stabilized and the cell begins to transcribe the glycolytic, pro-apoptotic and PHD genes. As the level of the PHDs increases, the equilibrium between the available oxygen, PHDs and HIF stabilization is shifted in favor of HIF hydroxylation. The increase in available PHDs would compensate for the small decrease in available oxygen. However, at larger decreases in oxygen tension, the cell would not be able to compensate by overproduction of the PHDs and the pro-apoptotic gene transcription would continue until the cell began its programmed cell death. One other feature of this feedback loop is the level of the individual PHDs within any given tissue and cell type. PHD1 was not upregulated by cobalt or hypoxia so presumably it would not be able to participate in this type of regulation.

Therefore, tissues that only express this isoform of the hydroxylase would not exhibit feedback inhibition. This idea of tissue specific regulation and hydroxylase differences is supported by recent publications (37, 38, 40).

The role of HIF1 $\alpha$  in maintaining proper cellular function during development and normal function is often neglected. The comparison of untreated WT and HIF1 $\alpha$  -/- cells clearly showed that HIF1 $\alpha$  has an important role in normal homeostasis. A battery of protective genes, such as SOD1 and SOD2, calmodulin (clones H3019D01 and H3021E08) and genes encoding metal binding proteins (metallothionein, clone 1-2031 and CRIP1 clone H3108G04) were shown to be affected negatively by the loss of the HIF1 $\alpha$  protein (see Figure 16, data not shown). In addition, several genes were positively influenced by the loss of HIF1 $\alpha$ . These results suggest that a basal level of HIF1 $\alpha$  must be present to maintain transcriptional regulation for these genes. Alternatively, the loss of HIF1 $\alpha$  may upset the signaling balance within the cell and these changes are the result.

In summary, these observations suggest a role for the PHDs in the feedback inhibition of the hypoxia-signaling cascade. The results also support the idea that cobalt and hypoxia exposure lead to the increase in the transcription of a number of gene families, including hydroxylases, glycolytic enzymes and pro-apoptotic genes. The interplay among these families and the regulation of the downstream events may help to explain the role of hypoxia in mediating the

damage following several pathological conditions, such as stroke and cardiovascular disease.

### **Acknowledgements**

The authors wish to thank the Tim Zacharewski laboratory for their careful reading of this manuscript and the extensive bio-informatics support. We would especially like to acknowledge Kirsten Fertuck, Lyle Burgoon and Darrell Boverhof for their help in these endeavors.

## References

1. Vaupel, P., Schlenger, K., Knoop, C., and Hockel, M. Oxygenation of human tumors: evaluation of tissue oxygen distribution in breast cancers by computerized O<sub>2</sub> tension measurements. *Cancer Res*, *51*: 3316-3322., 1991.
2. Semenza, G. L. Regulation of mammalian O<sub>2</sub> homeostasis by hypoxia-inducible factor 1. *Ann. Rev. Cell Dev. Biol.*, *15*: 551-578, 1999.
3. Bunn, H. F. and Poyton, R. O. Oxygen sensing and molecular adaptation to hypoxia. *Phys. Rev.*, *76*: 839-885, 1996.
4. Li, H., Ko, H. P., and Whitlock, J. P. Induction of phosphoglycerate kinase 1 gene expression by hypoxia. Roles of Arnt and HIF1alpha. *J. Biol. Chem.*, *271*: 21262-21267, 1996.
5. Maltepe, E. and Simon, M. C. Oxygen, genes, and development: an analysis of the role of hypoxic gene regulation during murine vascular development. *J. Mol. Med.*, *76*: 391-401, 1998.
6. Semenza, G. L., Roth, P. H., Fang, H. M., and Wang, G. L. Transcriptional regulation of genes encoding glycolytic enzymes by hypoxia-inducible factor 1. *J. Biol. Chem.*, *269*: 23757-23763, 1994.
7. Ryan, H. E., Lo, J., and Johnson, R. S. HIF-1 alpha is required for solid tumor formation and embryonic vascularization. *EMBO Journal*, *17*: 3005-3015, 1998.
8. Ryan, H. E., Poloni, M., McNulty, W., Elson, D., Gassmann, M., Arbeit, J. M., and Johnson, R. S. Hypoxia-inducible factor-1alpha is a positive factor in solid tumor growth. *Cancer Res*, *60*: 4010-4015, 2000.
9. Jiang, B. H., Semenza, G. L., Bauer, C., and Marti, H. H. Hypoxia-inducible factor 1 levels vary exponentially over a physiologically relevant range of O<sub>2</sub> tension. *American Journal of Physiology*, *271*: C1172-1180, 1996.
10. Kargul, G. J., Dudekula, D. B., Qian, Y., Lim, M. K., Jaradat, S. A., Tanaka, T. S., Carter, M. G., and Ko, M. S. Verification and initial annotation of the NIA mouse 15K cDNA clone set. *Nat Genet*, *28*: 17-18., 2001.
11. Tanaka, T. S., Jaradat, S. A., Lim, M. K., Kargul, G. J., Wang, X., Grahovac, M. J., Pantano, S., Sano, Y., Piao, Y., Nagaraja, R., Doi, H., Wood, W. H., 3rd, Becker, K. G., and Ko, M. S. Genome-wide expression

- profiling of mid-gestation placenta and embryo using a 15,000 mouse developmental cDNA microarray. *Proc Natl Acad Sci U S A*, 97: 9127-9132., 2000.
12. Kerr, M. K. and Churchill, G. A. Statistical design and the analysis of gene expression microarray data. *Genet Res*, 77: 123-128., 2001.
  13. Fielden, M. R., Halgren, R. G., Dere, E., and Zacharewski, T. R. GP3: GenePix post-processing program for automated analysis of raw microarray data. *Bioinformatics*, 18: 771-773., 2002.
  14. Zien, A., Aigner, T., Zimmer, R., and Lengauer, T. Centralization: a new method for the normalization of gene expression data. *Bioinformatics*, 17: S323-331., 2001.
  15. Epstein, A. C., Gleadle, J. M., McNeill, L. A., Hewitson, K. S., O'Rourke, J., Mole, D. R., Mukherji, M., Metzen, E., Wilson, M. I., Dhanda, A., Tian, Y. M., Masson, N., Hamilton, D. L., Jaakkola, P., Barstead, R., Hodgkin, J., Maxwell, P. H., Pugh, C. W., Schofield, C. J., and Ratcliffe, P. J. C. *C. elegans* EGL-9 and mammalian homologs define a family of dioxygenases that regulate HIF by prolyl hydroxylation. *Cell*, 107: 43-54., 2001.
  16. Kerr, M. K., Martin, M., and Churchill, G. A. Analysis of variance for gene expression microarray data. *J Comput Biol*, 7: 819-837, 2000.
  17. Murphy, B. J., Andrews, G. K., Bittel, D., Discher, D. J., McCue, J., Green, C. J., Yanovsky, M., Giaccia, A., Sutherland, R. M., Laderoute, K. R., and Webster, K. A. Activation of metallothionein gene expression by hypoxia involves metal response elements and metal transcription factor-1. *Cancer Res*, 59: 1315-1322, 1999.
  18. Lee, P. J., Jiang, B. H., Chin, B. Y., Iyer, N. V., Alam, J., Semenza, G. L., and Choi, A. M. Hypoxia-inducible factor-1 mediates transcriptional activation of the heme oxygenase-1 gene in response to hypoxia. *J Biol Chem*, 272: 5375-5381, 1997.
  19. Dulak, J., Jozkowicz, A., Foresti, R., Kasza, A., Frick, M., Huk, I., Green, C. J., Pachinger, O., Weidinger, F., and Motterlini, R. Heme oxygenase activity modulates vascular endothelial growth factor synthesis in vascular smooth muscle cells. *Antioxid Redox Signal*, 4: 229-240., 2002.
  20. Yet, S. F., Melo, L. G., Layne, M. D., and Perrella, M. A. Heme oxygenase 1 in regulation of inflammation and oxidative damage. *Methods Enzymol*, 353: 163-176., 2002.
  21. Jung, Y., Isaacs, J. S., Lee, S., Trepel, J., Liu, Z. G., and Neckers, L. Hypoxia-inducible factor induction by tumour necrosis factor in normoxic

- cells requires receptor-interacting protein-dependent nuclear factor kappa B activation. *Biochem J*, 370: 1011-1017., 2003.
22. Lahat, N., Rahat, M. A., Ballan, M., Weiss-Cerem, L., Engelmayer, M., and Bitterman, H. Hypoxia reduces CD80 expression on monocytes but enhances their LPS-stimulated TNF-alpha secretion. *J Leukoc Biol*, 74: 197-205., 2003.
  23. Tajima, R., Kawaguchi, N., Horino, Y., Takahashi, Y., Toriyama, K., Inou, K., Torii, S., and Kitagawa, Y. Hypoxic enhancement of type IV collagen secretion accelerates adipose conversion of 3T3-L1 fibroblasts. *Biochim Biophys Acta*, 1540: 179-187., 2001.
  24. Falanga, V., Zhou, L., and Yufit, T. Low oxygen tension stimulates collagen synthesis and COL1A1 transcription through the action of TGF-beta1. *J Cell Physiol*, 191: 42-50., 2002.
  25. Wykoff, C. C., Pugh, C. W., Maxwell, P. H., Harris, A. L., and Ratcliffe, P. J. Identification of novel hypoxia dependent and independent target genes of the von Hippel-Lindau (VHL) tumour suppressor by mRNA differential expression profiling. *Oncogene*, 19: 6297-6305., 2000.
  26. Poirier, F., Chan, C. T., Timmons, P. M., Robertson, E. J., Evans, M. J., and Rigby, P. W. The murine H19 gene is activated during embryonic stem cell differentiation in vitro and at the time of implantation in the developing embryo. *Development*, 113: 1105-1114., 1991.
  27. Williams, K. J., Telfer, B. A., Airley, R. E., Peters, H. P., Sheridan, M. R., van der Kogel, A. J., Harris, A. L., and Stratford, I. J. A protective role for HIF-1 in response to redox manipulation and glucose deprivation: implications for tumorigenesis. *Oncogene*, 21: 282-290., 2002.
  28. Bruick, R. K. Expression of the gene encoding the proapoptotic Nip3 protein is induced by hypoxia. *Proc Natl Acad Sci U S A*, 97: 9082-9087., 2000.
  29. Sowter, H. M., Ratcliffe, P. J., Watson, P., Greenberg, A. H., and Harris, A. L. HIF-1-dependent regulation of hypoxic induction of the cell death factors BNIP3 and NIX in human tumors. *Cancer Res*, 61: 6669-6673., 2001.
  30. Takahashi, Y., Takahashi, S., Shiga, Y., Yoshimi, T., and Miura, T. Hypoxic induction of prolyl 4-hydroxylase alpha (I) in cultured cells. *J Biol Chem*, 275: 14139-14146., 2000.
  31. Berra, E., Richard, D. E., Gothie, E., and Pouyssegur, J. HIF-1-dependent transcriptional activity is required for oxygen-mediated HIF-1alpha degradation. *FEBS Lett*, 491: 85-90., 2001.

32. Kothapalli, R., Yoder, S. J., Mane, S., and Loughran, T. P., Jr. Microarray results: how accurate are they? *BMC Bioinformatics*, 3: 22., 2002.
33. Bruick, R. K. and McKnight, S. L. A conserved family of prolyl-4-hydroxylases that modify HIF. *Science*, 294: 1337-1340., 2001.
34. Jaakkola, P., Mole, D. R., Tian, Y. M., Wilson, M. I., Gielbert, J., Gaskell, S. J., Kriegsheim, A., Hebestreit, H. F., Mukherji, M., Schofield, C. J., Maxwell, P. H., Pugh, C. W., and Ratcliffe, P. J. Targeting of HIF- $\alpha$  to the von Hippel-Lindau ubiquitylation complex by O<sub>2</sub>-regulated prolyl hydroxylation. *Science*, 292: 468-472., 2001.
35. Hon, W. C., Wilson, M. I., Harlos, K., Claridge, T. D., Schofield, C. J., Pugh, C. W., Maxwell, P. H., Ratcliffe, P. J., Stuart, D. I., and Jones, E. Y. Structural basis for the recognition of hydroxyproline in HIF-1  $\alpha$  by pVHL. *Nature*, 417: 975-978., 2002.
36. Jiang, Y., Zhang, W., Kondo, K., Klco, J. M., St Martin, T. B., Dufault, M. R., Madden, S. L., Kaelin, W. G., Jr., and Nacht, M. Gene Expression Profiling in a Renal Cell Carcinoma Cell Line: Dissecting VHL and Hypoxia-Dependent Pathways. *Mol Cancer Res*, 1: 453-462., 2003.
37. Cioffi, C. L., Qin Liu, X., Kosinski, P. A., Garay, M., and Bowen, B. R. Differential regulation of HIF-1 $\alpha$  prolyl-4-hydroxylase genes by hypoxia in human cardiovascular cells. *Biochem Biophys Res Co*, 303: 947-953., 2003.
38. Lieb, M. E., Menzies, K., Moschella, M. C., Ni, R., and Taubman, M. B. Mammalian EGLN genes have distinct patterns of mRNA expression and regulation. *Biochem Cell Biol*, 80: 421-426, 2002.
39. Kaelin, W. G., Iliopoulos, O., Lonergan, K. M., and Ohh, M. Functions of the von Hippel-Lindau tumour suppressor protein. *Journal of Internal Medicine*, 243: 535-539, 1998.
40. Metzen, E., Berchner-Pfannschmidt, U., Stengel, P., Marxsen, J. H., Stolze, I., Klinger, M., Huang, W. Q., Wotzlaw, C., Hellwig-Burgel, T., Jelkmann, W., Acker, H., and Fandrey, J. Intracellular localisation of human HIF-1  $\alpha$  hydroxylases: implications for oxygen sensing. *J Cell Sci*, 116: 1319-1326., 2003.

## **CHAPTER 2 APPENDIX**

**This section contains the supplementary data tables described in the results and discussion sections of chapter 2.**

**Appendix Table 11:**  
**Genes significantly influenced by cobalt and hypoxia**  
**in HIF1 $\alpha$  -/- cells**

ID	Gene Name	Abbr
	<b>Nuclear (GO = 0005634)</b>	
H3014H11	DNA segment, Chr 15, ERATO Doi 417, expressed	
H3017F05	lamin A	Lmna
H3100G09	requiem	Req
H3110H03	Btg3 associated nuclear protein	Banp
H3118B02	prothymosin alpha	Ptma
H3135G01	myeloid ecotropic viral integration site-related gene 1	Mrg1
	<b>Membrane Proteins (GO = 0016021)</b>	
H3029C03	podocalyxin-like	Podxl
H3035F09	Ras and a-factor-converting enzyme 1 homolog	Rce1
H3090D12	mannose-P-dolichol utilization defect 1	Mpdu1
H3112F03	degenerative spermatocyte homolog (Drosophila)	Degs
H3140C05	tumor necrosis factor receptor superfamily	Tnfrsf12a
H3151H12	RIKEN cDNA 1110025J15 gene	
	<b>Enzymes (Various GO)</b>	
H3013B02	ATPase, H <sup>+</sup> transporting, V1 subunit B, isoform 2	Atp6v1b2
H3021E11	ATPase, H <sup>+</sup> transporting, V1 subunit A, isoform 1	Atp6v1a1
H3028F05	ornithine decarboxylase, structural	Odc
H3042F09	dual specificity phosphatase 19	Dusp19
H3048G11	biliverdin reductase B (flavin reductase (NADPH))	Blvrb
H3095F09	brain-specific ang. Inh. 1-associated protein 2	Baiap2
H3157A06	PET112-like (yeast)	Pet112l
H3157D12	microsomal glutathione S-transferase 3	Mgst3
	<b>Misc Functions (Various GO)</b>	
H3002F06	eukaryotic translation initiation factor 3	Eif3
H3003H10	actinin, alpha 1	Actn1
H3042H12	expressed sequence A1840044	
H3078C09	oxysterol binding protein-like 2	Osbpl2
H3108H07	cortactin	Cttn
H3138G07	vacuolar protein sorting 26 (yeast)	Vps26
H3151F07	procollagen, type VI, alpha 1	Col6a1
	<b>Function Unknown</b>	
H3008B08	RIKEN cDNA 6330411E07 gene	
H3014E12	signal recognition particle 72	Srp72
H3038G11	translocase of outer mitochondrial membrane	Tomm20
H3043F08	protein phosphatase 1, regulatory subunit 2	Ppp1r2
H3057G09	RIKEN cDNA 6030440G05 gene	
H3060C11	spermine oxidase	Smox
H3071D02	kelch domain containing 2	Klhd2
H3094E02	RIKEN cDNA A230106A15 gene	
H3098D04	RIKEN cDNA 1300004C11 gene	
H3103E10	Rho GTPase activating protein 18	Arhgap18
H3106H11	RIKEN cDNA 2400001E08 gene	
H3110E06	RIKEN cDNA 9130011E15 gene	
H3139F07	RIKEN cDNA 2410066K11 gene	
H3144B07	H19 fetal liver mRNA	H19
H3146A07	RIKEN cDNA C130083N04 gene	

**Appendix Table 11: (Continued)**  
**Genes significantly influenced by cobalt and hypoxia**  
**in HIF1 $\alpha$  -/- cells**

H3156C11	RIKEN cDNA 1700052N19 gene	
	Unknown	
H3010B02		
H3014F03		
H3014G11		
H3017C01		
H3017D04		
H3034H05		
H3049F11		
H3051E02		
H3056B11		
H3065B07		
H3094E01		
H3096C07		
H3098B01		
H3101A07		
H3101A11		
H3107B03		
H3111B07		
H3115G07		
H3118H04		
H3150D07		
H3154E06		
H3159A07		

**Appendix Table 12:**  
**Genes significantly influenced by hypoxia in Wild type and HIF1 $\alpha$  -/- cells**

ID	Name	Abbr.
H3003H10	Rattus norvegicus non-muscle alpha-actin	Actn1
H3016D10	lectin, galactose binding, soluble 3	Lgals3
H3024B04	Mus musculus chaperonin subunit 3 (gamma)	Cct3
H3028F03	Mus musculus cell-line LXB2 cathepsin L	Ctsl
H3030D10	Mus musculus pyruvate kinase, muscle	Pkm2
H3030D11	Mus musculus pyruvate kinase, muscle	Pkm2
H3045G06	translocated promoter region (TPR) NM_003292.1	
H3048G11	Similar to biliverdin reductase B	Blvrb
H3059H07	clone RP23-20N14 on chromosome 11	
H3067C04	Homo sapiens small nuclear ribonucleoprotein	Snrpb2
H3088G10	Similar to Absent in melanoma 1 protein	Mina
H3094E01	RP23-32O9 on chromosome 2	
H3103C03	Similar to R13F6.10.p [Caenorhabditis elegans]	
H3103G04	ras association (RalGDS/AF-6) domain family	Rassf1
H3116A06	Mus musculus, clone IMAGE:4024675	
H3118B01	Mouse mRNA for prothymosin alpha	Ptma
H3128C03	RIKEN cDNA 5430419M09 gene (5430419M09Rik)	
H3129G12	protease, serine, 15	Prss15
H3137C05	RAB14, member RAS oncogene family	Rab14
H3145H03	mitogen activated protein kinase 3	Mapk3
H3146D12	clone RP23-135F6 on chromosome 11	
H3147H11	tissue specific transplantation antigen P35B	Tsta3
H3148E03	capping protein (actin filament) muscle Z-line, beta	Capzb
H3151F07	procollagen, type VI, alpha 1 (Col6a1)	Col6a1
H3153B03	Mus musculus chromosome 8 clone RP24-324M11	
H3157D03	clone RP23-384K10 on chromosome 2	

**Appendix Table 13:  
Genes significantly influenced by cobalt treatment in  
Wild type and HIF1 $\alpha$  -/- cells**

<b>ID</b>	<b>Gene Name</b>	<b>Abbr.</b>
A-2031	Metallothionein-I (image 1052401)	Mt1
H3020E11	M.musculus mRNA for cyclin F	Ccnf
H3024G12	clone RP23-407M20 on chromosome 11	
H3028F05	Mouse kidney ornithine decarboxylase mRN	Odc
H3029B11	Mouse chromatin nonhistone high mobility	Hmga1
H3049F11	RIKEN cDNA 9930116P15 gene (9930116P15Rik)	
H3067E01	eukaryotic translation elongation factor 1 alpha 1	Eef1a1
H3098B01	Unknown	
H3131A07	Mus musculus peroxisomal/mitochondrial d	Ech1
H3132E03	Homo sapiens chromosome 17, clone hRPK.1	
H3137C06	Mouse transglutaminase (TGase) mRNA, com	Tgm2
H3140C11	Homo sapiens ATPase, H <sup>+</sup> transporting, ly	Atp6v0b
H3144B07	Mus musculus H19 and muscle-specific Nct	H19
H3151H12	NMDA receptor glutamate-binding subunit	Lag

**Appendix Table 14:**  
**Comparison of genes in Table 2 with those presented**  
**in Jiang et al. (ref.36)**

<b>Figure</b>	<b>Identical</b>	<b>Homologous</b>
<b>Fig 1A</b>	metallothionein	L26 (L17)
	p35 (H3147H11)	L15 (L17)
	eIF3	L29 (L17)
		L13 (L17)
<b>Fig 1B</b>	enolase	L21 (L17)
<b>Fig 1</b>		Chronic Sommatatropin2 (csh1)
		L13 (L17)
		L37 (L17)
		L22 (L17)
		L39 (L17)
		L41 (L17)
		L3 (L17)
		L12 (L17)
<b>Fig 2C</b>	fibronectin Receptor beta	Glut1 (Glut4)
	lactate dehydrogenase	eIF2 (eIF3)
	GAPDH	eIF1a (eIF3)
	P4H	MMP7 (MMP23)
	eIF3	L9 (L17)
		L21 (L17)
		L37 (L17)
		L13 (L17)
		L28 (L17)
		L41 (L17)
	L22 (L17)	
<b>Fig 2D</b>	lactate dehydrogenase	eIF1a (eIF3)
	fibronectin Receptor beta	eIF4 (eIF3)
	micropain 26S	eIF2 (eIF3)
		MMP28 (MMP23)
		MMP25 (MMP23)
		L13 (L17)
		L28 (L17)
		L20 (L17)
		L15 (L17)
		L18 (L17)
	L7 (L17)	
<b>Fig 2E</b>	enolase	L7 (L17)
	galactoside binding	L30 (L17)
	proline rich(H31116A06)	eIF2 (eIF3)
	eIF3	L5 (L17)
		L3 (L17)

**Appendix Table 14: (Continued)**  
**Comparison of genes in Table 2 with those presented**  
**in Jiang et al. (ref.36)**

<b>Fig 3F</b>		Chronic Sommatatropin2 (csh1)
		L22 (L17)
		L3 (L17)
		L12 (L17)
		L13 (L17)
		L37 (L17)
		L39 (L17)
		L21 (L17)
		L41 (L17)
<b>Fig 3G</b>	enolase	
<b>Fig 3</b>	cathepsin L	Glut1 (Glut4)
	pyruvate kinase	Glut2 (Glut4)
	p35 (H3147H11)	eIF1 (eIF3)
	GPI	eIF2 (eIF3)
	galctoside binding	eIF4 (eIF3)
	BNIP3	Adenylate kinase 3 (ADK2)
	BNIP3L	27a (L17)
	GAPDH	L12 (L17)
	aldolase	L29 (L17)
	P4H	L30 (L17)
	ADK2	L9 (L17)
	Transglutaminase 2	L10 (L17)
		L30 (L17)
		L27 (L17)
<b>Fig 4H</b>	enolase	lymphocyte ant 1 (lymA 3)
	MUM2	
	transglutaminase 2	
	micropain 26S	
		Chronic Sommatatropin2 (csh1)
<b>Fig 4</b>	enolase	L3 (L17)
	mitochondrial carrier	L12 (L17)
	GAPDH	L13 (L17)
		L37 (L17)
		L39 (L17)
		L21 (L17)
		L41 (L17)

## CHAPTER 3

Vengellur, Ajith., LaPres, John J. 2004. The Role of Hypoxia Inducible Factor 1alpha in Cobalt Chloride Induced Cell Death in Mouse Embryonic Fibroblasts. Toxicological Sciences. 82:638-46.

## **Abstract**

Cobalt has been widely used in the treatment of anemia and as a hypoxia mimic in cell culture and it is known to activate hypoxic signaling by stabilizing the hypoxia inducible transcription factor 1 $\alpha$  (HIF1 $\alpha$ ). However, cobalt exposure can lead to tissue and cellular toxicity. These studies were conducted to determine the role of HIF1 $\alpha$  in mediating cobalt-induced toxicity. Mouse embryonic fibroblasts (MEFs) that were null for the HIF1 $\alpha$  protein were used to show that HIF1 $\alpha$  protein plays a major role in mediating cobalt-induced cytotoxicity. Previous work from our laboratory and others has shown that two BH3 domain containing cell death genes, BNip3 and NIX, are targets of hypoxia signaling. These experiments document that BNip3 and NIX expression is HIF1 $\alpha$ -dependent, and cobalt induces their expression in a time and dose dependent manner. In addition, their expression is correlated with an increase in BNIP3 and NIX protein. Characteristically, the elevated level of BNIP3 was correlated with an increased presence of chromatin condensation, one marker for cell injury. Interestingly, this increased chromosomal condensation was not coupled to caspase-3 activation as usually seen in a typical apoptotic response. These results show that HIF1 $\alpha$  is playing a major role in mediating cobalt-induced toxicity in mouse embryonic fibroblasts and may offer a possible mechanism for the underlying pathology of injuries seen in workers exposed to environmental contaminants that can influence the hypoxia signaling system, such as cobalt.

## **Introduction**

Metals constitute a large percentage of the earth's crust and their biochemical and geochemical cycles have been drastically altered by human activities. Metals are stable and persistent environmental contaminants and tend to collect in soils and sediments. Many of these metals, such as cobalt, nickel and manganese are used in a wide variety of industrial applications, including the production of alloys, paints and batteries. Exposure to these metals often occurs in workers involved in these industrial processes. Environmental exposure has now become a cause for concern. Metal smelting and other industrial processes close to agricultural land and the use of bio-solids in the production of fertilizers has increased the possibility that these metals are entering our food supply in greater quantities (1). In addition, the recent approval of the gasoline additive, methylcyclopentadienyl manganese tricarbonyl (MMT), increases the risk of environmental contamination. Accordingly, understanding the underlying molecular mechanism(s) of metal-induced toxicity is of increasing importance.

Certain metals are also essential for human health. For example, cobalt plays a critical role in the synthesis of vitamin B12. In contrast, excessive exposure to cobalt is associated with several conditions, including asthma, pneumonia, and hematological abnormalities (2). In addition, nickel, cobalt, cadmium and other metals are known or suspected carcinogens (3). Despite numerous reports of metal-induced toxicity, the underlying mechanism remains unclear. Studies in various systems have shown that exposure to certain metals, such as cobalt,

promotes a response similar to hypoxia. Hypoxia is defined as a state when oxygen tension drops below normal limits and it plays a central role in development and several pathological conditions including stroke, cardiovascular disease and tumorigenesis (4). Due to oxygen's critical role in energy production, organisms have developed a programmed response to hypoxia that increases glucose utilization and stimulates erythropoiesis and angiogenesis to compensate for the decrease in available oxygen (5-8). The hypoxia inducible factors (HIFs) are a family of transcription factors that mediate the response to hypoxia by regulating the expression of genes capable of regulating glycolysis, angiogenesis and erythropoiesis, such as erythropoietin (EPO), vascular endothelial growth factor (VEGF), pyruvate kinase and many others (9-13).

Prolonged hypoxia can also induce genes involved in cell death (14). Cobalt and nickel can activate hypoxia-mediated signaling pathways aberrantly under normoxia by stabilizing the cytosolic hypoxia inducible factor 1 $\alpha$  (HIF1 $\alpha$ ) (15). For example, cobalt is thought to stabilize HIF1 $\alpha$  by inhibiting the prolyl hydroxylase domain- containing enzymes (PHDs), a family of enzymes that play a key role in oxygen dependent degradation of the transcription factor (16). The characterization of the PHD family of enzymes offers a direct link between metal exposure and HIF mediated signaling. This direct link and the overlap between gene expression patterns between hypoxia and cobalt exposure have led us to hypothesize that HIFs may be necessary to the toxic effects of cobalt (17). This hypothesis was tested using HIF1 $\alpha$   $-/-$  cells and several markers of toxicity. Our

results demonstrate that HIF1 $\alpha$  plays an important role in metal-induced toxicity. Among the HIF1 $\alpha$  dependent genes whose expression was altered by cobalt treatment are the pro-apoptotic factors, BNIP3 and NIX. Overall, these results suggest that cobalt-induced toxicity is dependent upon the HIF1 $\alpha$  protein and its ability to induce the expression of cell death promoting genes.

## **Methods**

*Materials* — Tissue culture media and supplements were obtained from Invitrogen, Inc. Cosmic calf serum was obtained from Hyclone. Oligonucleotide synthesis was performed at the Macromolecular Facility, Michigan State University, East Lansing, MI. SYBR Green <sup>TM</sup> real time PCR reagents were purchased from Applied Biosystems<sup>TM</sup>, CA. All other chemicals were reagent grade and obtained from Sigma<sup>TM</sup> Chemical Company, MO.

*Cell Culture and Toxicity assay* — Mouse embryonic fibroblast cell lines were maintained in modified DMEM media (10% heat inactivated FBS, penicillin-streptomycin (10 U/ml), non-essential amino acid (10  $\mu$ g/ml), L-glutamine (2mM)). The cells were treated with 0, 1, 10, and 100  $\mu$ M of CoCl<sub>2</sub> for 48 hours. Cells were trypsinized, counted with a hemacytometer and 10,000 cells were plated in 6 cm cell culture dishes. Cells were counted with a hemacytometer on 1, 2, 3, 4, and 5 days after plating.

**MTT Assay** — Cells were grown in 96 well plates and treated with 0, 50, 100, 150 and 200  $\mu\text{M}$  of  $\text{CoCl}_2$  for 72 hours. The MTT assay was performed by replacing the cobalt containing media with 100 $\mu\text{l}$  of media containing 5mg/ml of MTT (3-(4,5-dimethylthiazolyl-2)-2, 5-diphenyltetrazolium bromide). The plates were then incubated for 4 hours (37°C). Medium was then removed by aspiration and 200 $\mu\text{l}$  of solvent (1:1 DMSO:ethanol) was added and the formazan crystals solubilized with continuous agitation. OD measurements were taken at 550 and 630nm and the difference in OD relative to untreated controls was taken as a measure of cell viability (18). For the  $\text{CoCl}_2$  time course experiment cells were treated with 150  $\mu\text{M}$   $\text{CoCl}_2$  and MTT assay was performed on four consecutive days and values are represented as a percent of time matched controls within cell types.

**Protein Extraction and Western Blotting** — Wild type and HIF1 $\alpha$   $-/-$  cells were grown under control (20%  $\text{O}_2$ ), or hypoxic (1%  $\text{O}_2$ ) conditions (NAPCO 7000 incubator, NAPCO, VA) or in the presence of 100 $\mu\text{M}$  or 150 $\mu\text{M}$   $\text{CoCl}_2$  and protein extracts were prepared as described previously (19). Briefly, cells were washed with cold PBS (4°C) and removed from surface by scraping on cold PBS and collected by centrifugation. Soluble proteins were extracted with cell lysis buffer (25 mM HEPES, pH=7.6, 2 mM EDTA, 10 % glycerol, 1  $\mu\text{g}/\text{mL}$  of aprotinin, leupeptin, pepstatin A and 1 mM PMSF) and three rounds of sonication (5 secs., 4°C). Insoluble material was removed by centrifugation (16,000g, 1hour). Protein concentrations were determined using Bio-Rad™ Bradford assay kit and

BSA standards (20). An equal amount of protein was separated by SDS-PAGE, and Western blotting was performed with BNIP3 and NIX specific antibody (Sigma, MO and Exalpha Biologicals, MA respectively) using ECL chemiluminescent detection kit (Amersham Pharmacia). A  $\beta$ -actin specific antibody (a generous gift of Dr. John Wang, MSU) was used to verify equal loading.

*RNA Extraction and Reverse Transcription* — RNA extraction was performed using TriZol reagent (Invitrogen) via manufacturer's instruction. Briefly, cells were treated for the specific duration and washed in 1X PBS (4°C). Cells were removed by scraping in the presence of 1 mL of TriZol™ reagent. Phase separation was accomplished by addition of chloroform and centrifugation (16,000g, 15min). RNA was precipitated using isopropanol and was quantitated spectrophotometrically. 1  $\mu$ g total RNA was used in subsequent reverse transcription reaction using Superscript™ II RNase H- Reverse Transcriptase (Invitrogen) via manufacturer's instructions.

*Real-Time Quantitative PCR Analysis* — The measurement of BNip3 and NIX mRNA levels were performed using real-time PCR technology and SYBR® Green as a detector on an Applied Biosystems Prism 7000 Sequence detection System (Foster City, CA) (Table. 15). For detailed protocol see chapter 1 methods section.

<b>Gene</b>	<b>Accession</b>	<b>Forward</b>	<b>Reverse</b>
HPRT	NM 013556	AAGCCTAAGATGAGCGCAAG	TTACTAGGCAGATGGCCACA
BNip3	NM 009760	GGCGTCTGACAACCTCCACT	AACACCCCAAGGACCATGCTA
BNip3(L) (NIX)	NM 009761	GGAAGAGTGGAGCCATGAAG	GTGTGCTCAGTCGTTTTCCA

**Table 15. qRT-PCR primers**

***Cell Staining and Caspase Assay*** - Cells were left untreated or exposed to CoCl<sub>2</sub> (150 μM, 48 hrs) or staurosporine (1 μM, 3 hrs) and stained with Hoechst 33342 dye (1 μg/ml, 15 min.). Cells were viewed and photographed with fluorescent microscopy. The percentage of apoptotic nuclei were determined by counting the number of cells displaying a dense nuclear staining. At least 200 cells were counted in at least 3 separate fields for each treatment and values are displayed as a percent of total nuclei.

Caspase assays were performed using EnZChek caspase-3 assay kit #2 (Molecular Probes) via the manufacturer's instructions. Briefly, cells were left untreated or exposed to CoCl<sub>2</sub> (150 μM, 48 hrs) or Staurosporine (1 μM, 3 hrs). Cell extracts were obtained by scraping the cells in lysis buffer and cleared by centrifugation. The caspase-3 activity in the supernatant was analyzed spectrophotometrically (caspase activity in the cell lysate leads to the cleavage of the non-fluorescent substrate into a fluorescent product). The specificity of the caspase 3 activity was determined by the addition of a caspase-3 inhibitor (Ac-DEVD-CHO Inhibitor).

***Statistics*** - Statistical analysis was performed between treated and untreated or vehicle controls using t-test (two tailed, unequal variance, p <= 0.05 cut-off).

## Results

### *Growth Curve Analysis of wild type and HIF1 $\alpha$ -/- cells under CoCl<sub>2</sub> treatment:*

An equal number of untreated and cobalt exposed (100  $\mu$ M, 48 hrs) Wild type and HIF 1 $\alpha$  -/- cells were plated onto 6 cm cell culture dishes. The cells in each plate were counted on each of the subsequent 5 days. Wild types cells showed little or no growth following CoCl<sub>2</sub> (100 $\mu$ M) treatment (Figure 18). In contrast, HIF1 $\alpha$  -/- cells exposed to CoCl<sub>2</sub> were initially slow to grow compared to untreated controls, but had a much higher survival compared to wild type treated cells. Wild type cells showed a lower rate of cell proliferation and the total cell viability was lower than HIF1 $\alpha$  -/- cells under cobalt treatment even after 5 days. These results suggest that HIF1 $\alpha$  plays a role in mediating cobalt-induced growth inhibition.

*Cell Toxicity Assay of CoCl<sub>2</sub> treated cells using MTT Assay:* The growth curves described in figure 18 suggest that HIF1 $\alpha$  plays an important role in cobalt-induced growth arrest; however, it does not prove that HIF1 $\alpha$  is involved in cobalt-induced toxicity. To determine the role of HIF1 $\alpha$  in the cytotoxicity induced by CoCl<sub>2</sub>, wild type and HIF1 $\alpha$  -/- cells were treated with varying concentrations of cobalt (0, 50, 100, 150 and 200 $\mu$ M CoCl<sub>2</sub>) when cells had reached approximately 40% confluence. After incubation of 72 hours, cell viability was evaluated using the MTT assay. The cytotoxic effects of cobalt were significantly attenuated in the HIF1 $\alpha$  -/- cells when compared to the WT cells (Figure 19A). To determine the time course of cell injury, MTT assay was

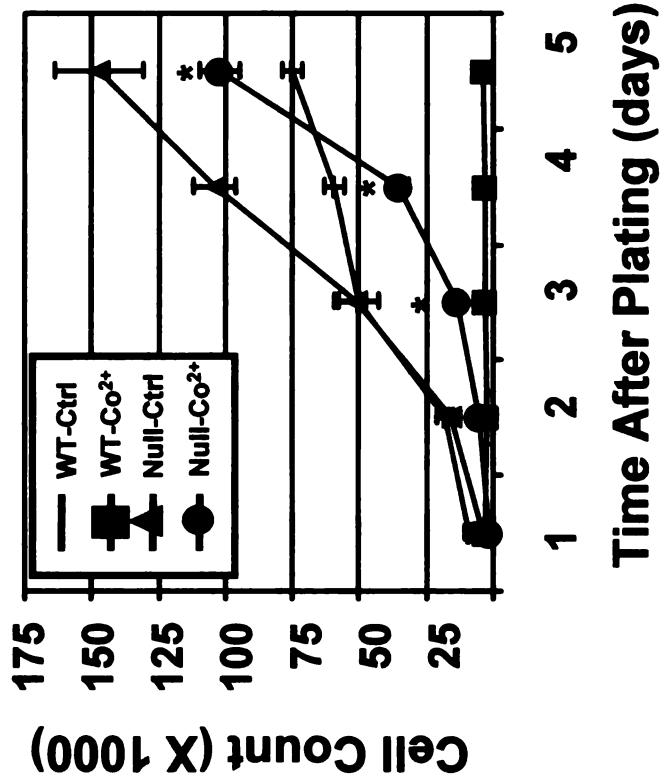


**Figure 18. Growth Curve**

Wild type (WT) and HIF1 $\alpha$  -/- cells were left untreated (Ctrl) or exposed to CoCl<sub>2</sub> (Co<sup>2+</sup>, 100  $\mu$ M) for 48 hrs. Following treatment, 10,000 cells were plated in triplicate and cell counts were recorded on subsequent days. Values were normalized to Day 1 values within cell type. \* Represents p < 0.05 when HIF1 $\alpha$  -/- cobalt treated cells were compared to WT cobalt treated cells

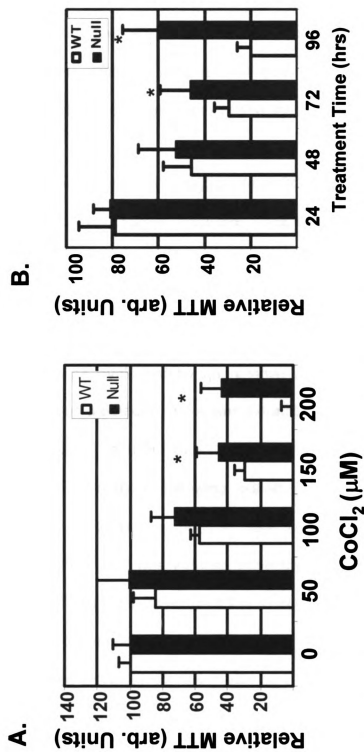


**Figure 19. Dose response and time course analysis of CoCl<sub>2</sub>-induced cytotoxicity**  
 A: Wild type (WT, white bars) and HIF1 $\alpha$ -/- (black bars) cells were exposed to various concentrations of CoCl<sub>2</sub> (50, 100, 150 and 200  $\mu$ M) or left untreated (Ctrl) for 72 hours. Cell viability was assayed using a standard MTT assay. Control values within cell type were set to 100%. B: Wild type (WT, white bars) and HIF1 $\alpha$ -/- (black bars) cells were exposed to 150 $\mu$ M CoCl<sub>2</sub> and cell viability was assayed using MTT assay after 24-96 hours. MTT values were normalized to time matched controls. \* Represents  $p < 0.05$  when the HIF1 $\alpha$ -/- and WT values were compared

performed on the wild type and HIF1  $\alpha$   $-/-$  cells following exposure to 150  $\mu$ M CoCl<sub>2</sub>. As shown in figure 19B, CoCl<sub>2</sub> exposure resulted in progressive increase in toxicity to wild type cells compared to HIF1 $\alpha$   $-/-$  cells. These results support the growth curve analysis presented in Figure 18 and suggest that HIF1 $\alpha$  plays an important role in cobalt-induced cytotoxicity.

*Quantitative Real-time PCR Analysis of the BCL2 family genes, BNip3 and NIX genes:* Our lab and others have described the regulation by hypoxia of two members of the BCL2 family, BNip3 and NIX (17, 21-23). Global expression analysis using cDNA microarrays of cobalt-induced genes in WT and HIF1 $\alpha$   $-/-$  cells has shown that this regulation is HIF1 $\alpha$  dependent (17). The expression of these genes was evaluated by quantitative real-time PCR (qRT-PCR) using SYBR<sup>®</sup> Green as a detector. RNA was extracted from untreated and hypoxia- or cobalt-exposed WT and HIF1 $\alpha$   $-/-$  cells. BNip3 was upregulated 8 fold in a HIF1 $\alpha$ -dependent manner following cobalt (100  $\mu$ M) or hypoxia (1% O<sub>2</sub>) exposure (Figure 20A). In addition, NIX also showed a HIF1 $\alpha$ -dependent expression pattern and was induced more than 12 fold after cobalt exposure (Figure 20B). These results suggest that cobalt upregulates BNip3 and NIX in a HIF1 $\alpha$ -dependent manner and are consistent with cobalt-induced activation of HIF1 $\alpha$ -regulated cell-death signaling pathways.

*Time course analysis of BNip3 mRNA levels under CoCl<sub>2</sub> or hypoxia treatment:* The time course of BNip3 upregulation by cobalt and hypoxia was also analyzed

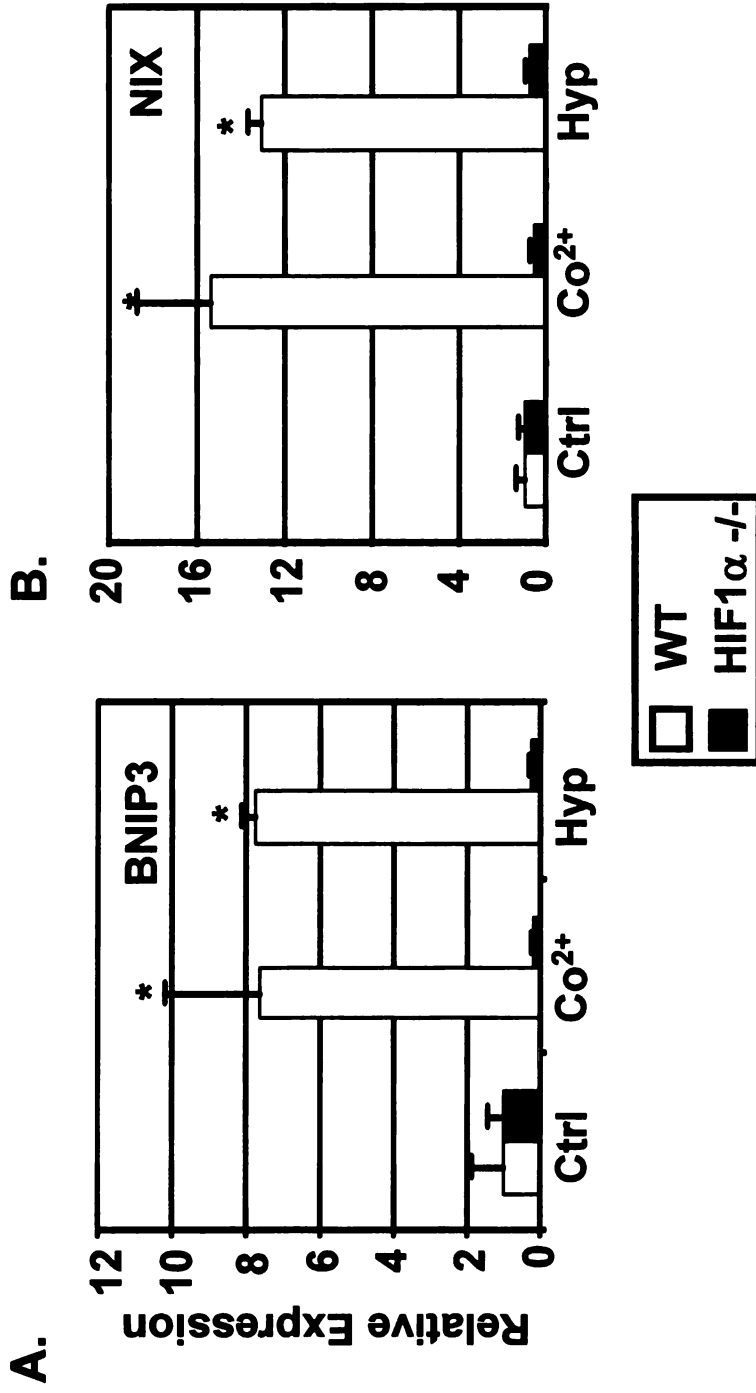


**Figure 20. qRT-PCR data for BNip3 and BNip3L**  
 BNip3 (A) and BNip3L (NIX) (B) expression levels were analyzed by qRT-PCR in wild type (WT, white bars) and HIF1 $\alpha$  -/- cells (black bars) as described in methods section. Each value was normalized to the control level in the corresponding cell line. Ctrl = untreated, Co<sup>2+</sup> = 100  $\mu$ M CoCl<sub>2</sub> and Hyp = 1% O<sub>2</sub> for 24 hours. \* Represents  $p < 0.05$  when compared to corresponding control.

by qRT-PCR. WT cells were left untreated or exposed to  $\text{CoCl}_2$  (100  $\mu\text{M}$ ) or hypoxia (1%  $\text{O}_2$ ). Total RNA was extracted at various time points (0.25 to 72 hours) after treatment and analyzed for BNip3 and HPRT expression. BNip3 expression levels reached maximum expression at 8 hours following exposure to  $\text{CoCl}_2$  (Figure 21A). This expression level remained stable for the duration of the time course. The BNip3 expression pattern following exposure to hypoxia in the WT cells gradually increased and reached a maximum after 48 hours of treatment (Figure 21A). BNip3 was not regulated by cobalt or hypoxia at any time point tested in the  $\text{HIF1}\alpha^{-/-}$  cells (data not shown).

*Dose response analysis of BNip3 mRNA levels under  $\text{CoCl}_2$ :* The regulation of BNip3 mRNA expression in cells was determined by qRT-PCR following exposure to 0, 50, 100, 150 and 200  $\mu\text{M}$   $\text{CoCl}_2$  for 24 hours. As shown in figure 21B, wild type cells showed marked upregulation of BNip3 mRNA at all doses tested with a maximum effect at 150 $\mu\text{M}$   $\text{CoCl}_2$ . The  $\text{HIF1}\alpha^{-/-}$  cells displayed no significant changes in Bnip3 transcript levels at any dose (Figure 21B). The Ct value and actual transcript levels of BNip3 in WT cells ranged from 18.1 to 22.6 and 9.2E05 to 4.5E04 respectively (data not shown). The expression level of the control gene HPRT was also analyzed and shown not to significantly change following exposure to any concentration of  $\text{CoCl}_2$  in either cell type (Figure 21B).

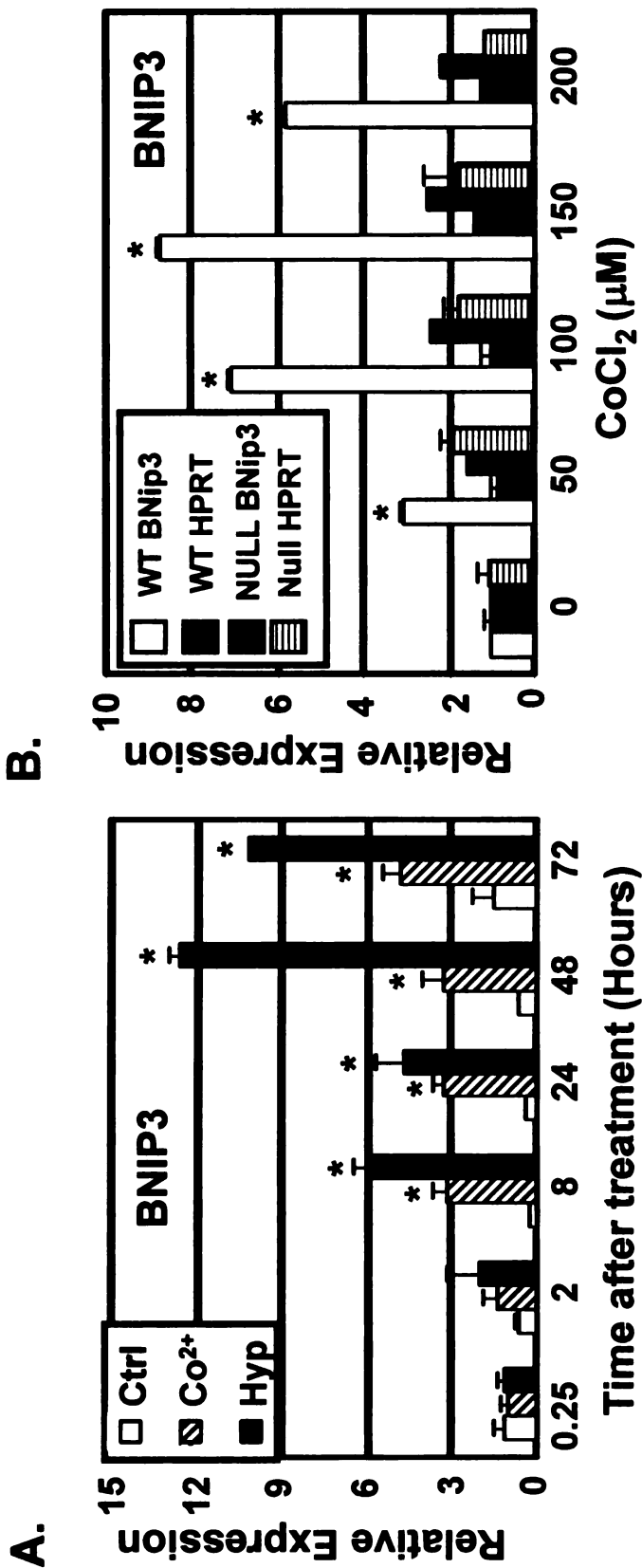


**Figure 21. qRT-PCR data for BNip3 expression under CoCl<sub>2</sub> and hypoxia time course in wild type cells**  
 A: BNip3 expression levels were analyzed by qRT-PCR in wild type cells left untreated (Ctrl, white bars) or following exposure to Co<sup>2+</sup> (100 μM, hatched bars) or, hypoxia (1% O<sub>2</sub>, black bars). RNA was extracted at 0.25, 2, 8, 24, 48 and 72 hours following 100μM CoCl<sub>2</sub> exposure. Each value was normalized to the untreated control level at 0.25 hours. B: BNip3 and HPRT expression levels were analyzed by qRT-PCR in wild type (WT, BNip3 white bars, HPRT gray bars) and HIF1α -/- cells (BNip3 black bars, HPRT hatched bars) left untreated or with 50, 100, 150 and 200μM CoCl<sub>2</sub> for 72 hours. BNip3 expression levels are calculated as explained in methods and normalized to respective controls. HPRT expression levels are absolute levels normalized to its respective control values. \* Represents p < 0.05 when compared to corresponding control.

**Western Blot Analysis of BNIP3 and NIX levels:** Western blot analysis was performed to determine the levels of BNIP3 and NIX proteins in CoCl<sub>2</sub> treated cells. Wild type and HIF1 $\alpha$  -/- cells were treated with cobalt (100 and 150  $\mu$ M) or hypoxia (1% O<sub>2</sub>) for 48 hours and total protein was extracted and separated by SDS-PAGE. There was a dramatic increase in BNIP3 levels following cobalt and hypoxia exposure and this increase was dependent upon the presence of HIF1 $\alpha$  (Figure 22, upper panel). The multiple bands represented in the BNIP3 Western blot are due to progressive proteolysis and has been previously reported to be indicative of cellular stress (24). NIX protein levels also showed a marginal increase in CoCl<sub>2</sub> and hypoxia treated wild type cells (Figure 22, middle panel). Both BNIP3 and NIX levels were unchanged in CoCl<sub>2</sub> treated HIF1 $\alpha$  -/- cells.  $\beta$ -actin was used to verify equal protein loading (Figure 22, lower panel).

**Cell Morphology:** The results suggest that cobalt may be promoting cell death by inducing HIF1 $\alpha$ -mediated upregulation of pro-apoptotic genes. Apoptosis is correlated with morphological and biochemical changes within the cell, such as nuclear condensation, DNA fragmentation, and caspase activation. However, BNIP3 overexpression has been shown to induce a necrosis-like, caspase-independent cell death (25). To determine if cobalt treated cells were undergoing classic apoptosis or something similar to BNIP3 induced necrotic cell death, chromosomal staining and caspase-3 assay were performed in the WT and HIF1 $\alpha$  -/- cells.

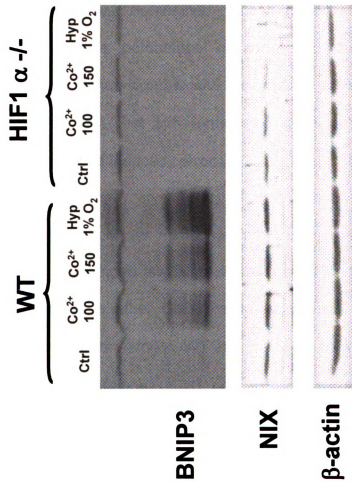


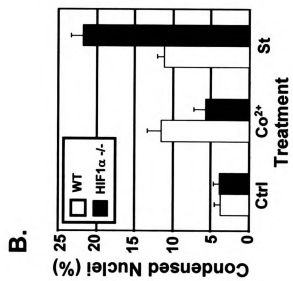
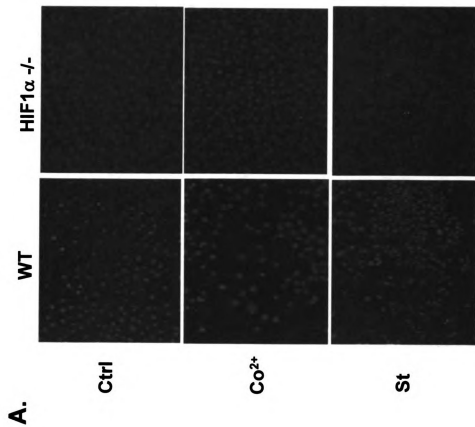
**Figure 22. BNIP3 and BNIP3L (NIX) Western Blot**  
 Wild type (WT) and HIF1 $\alpha$   $-/-$  cells were left untreated (Ctrl) or exposed to 100  $\mu$ M CoCl<sub>2</sub>, 150  $\mu$ M CoCl<sub>2</sub> or hypoxia (1% O<sub>2</sub>), for 48 hours. Total protein was extracted and separated by SDS-PAGE, transferred to nitrocellulose membrane and probed with a BNIP3 (upper panel) and NIX (middle panel) specific antibody. Blots were stripped and re-probed with  $\beta$ -actin to verify equal loading (lower panel).

Cells were left untreated or exposed to cobalt (150  $\mu$ M), or staurosporine (0.01 $\mu$ M) for 48 hours and stained with Hoechst33342 nuclear dye. Staurosporine is a known inducer of apoptosis and was used as a positive control (26). Cobalt induced a moderate level of chromatin condensation in the WT cells, while little, if any, was observed in the HIF1 $\alpha$   $-/-$  cells. In contrast, staurosporine treated WT and HIF1 $\alpha$   $-/-$  cells showed marked chromatin condensation (Figure 23A). The percentage of condensed nuclei in each treatment was also determined. Cobalt treated wild type cells induced a 3 fold increase in the percentage of condensed nuclei (Figure 23B). These experiments, taken together with the previous gene expression and Western blot results, suggest that HIF1 $\alpha$ -mediated gene activation may be involved in promoting cobalt-induced cell death.

*Caspase-3 Assay:* As mentioned previously, caspase-3 activation is another hallmark of apoptosis and is considered one of the final steps in the process (27). To determine whether CoCl<sub>2</sub> treatment causes activation of caspase-3 in a HIF1 $\alpha$ -dependent manner, WT and HIF1 $\alpha$   $-/-$  cells were exposed to cobalt (150  $\mu$ M) or staurosporine (1 $\mu$ M) and extracts were prepared (Figure 24A, B). Caspase-3 activity in the extracts was assessed by fluorimetric analysis in the presence and absence of a caspase-3 inhibitor (Ac-DEVD-CHO, Molecular Probes). WT as well as HIF1 $\alpha$   $-/-$  cells showed no significant increase in caspase-3 activity following CoCl<sub>2</sub> treatment. This was not due to a general lack of activity in the assay since the positive control, staurosporine, showed a

**Figure 23. Cell Morphology**

A: Wild type (WT) and HIF1 $\alpha$  -/- cells were left untreated (Ctrl) or exposed to 150  $\mu$ M CoCl $_2$  (Co $^{2+}$ ) or 0.01 $\mu$ M staurosporine (St) for 48 hours. Cell morphology was observed using Hoechst33342 DNA binding dye using florescent microscope. White arrows denote cells with morphology consistent with chromatin condensation. B: Percentage of condensed nuclei in wild type (WT, white bars) and HIF1 $\alpha$  -/- cells (black bars) left untreated (Ctrl) or exposed to 150  $\mu$ M CoCl $_2$  (Co $^{2+}$ ) or 0.01 $\mu$ M staurosporine (St) for 48 hours. \* Represents p < 0.05 when compared to corresponding control.



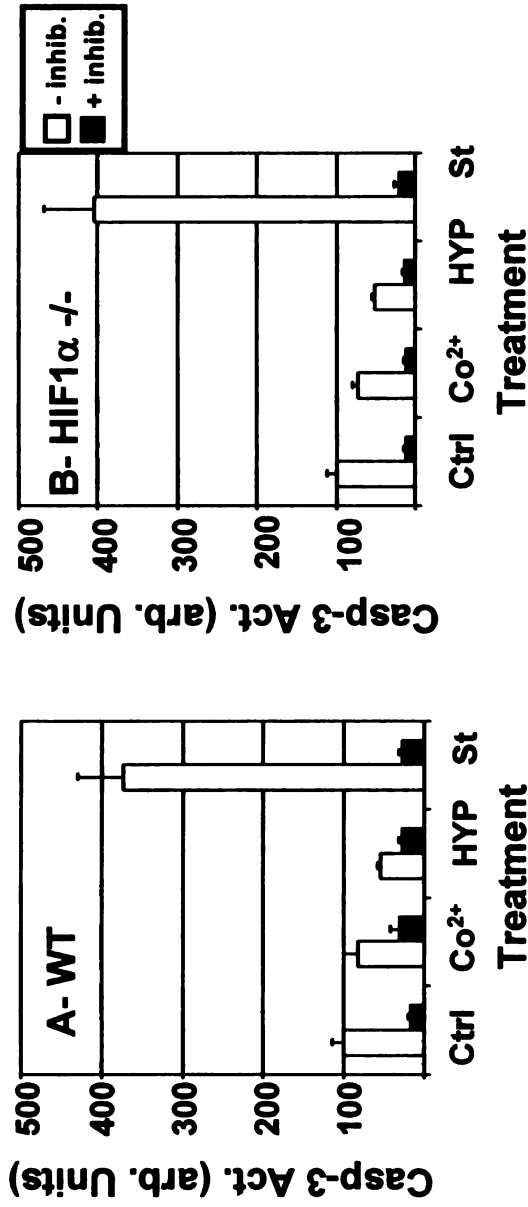


**Figure 24. Caspase-3 assay**  
 (A) Wild type (WT) and (B) HIF1 $\alpha$  -/- cells were left untreated (Ctrl) or exposed to CoCl<sub>2</sub> (Co<sup>2+</sup>, 150 $\mu$ M, 48 hours), Hypoxia (HYP, 1% O<sub>2</sub>, 48 hours) or staurosporine (St, 1  $\mu$ M, 4 hours). Caspase3 activity was measured using EnZChek caspase-3 assay kit #2 (Molecular Probes). Assay was performed in the presence of either control (DMSO – white bars) or a caspase inhibitor (black bars).

marked activation of caspase-3 in the WT and HIF1 $\alpha$  *-/-* cells. This activity was abolished in the presence of the caspase-3 inhibitor confirming the specificity of the assay (Figure 24). These results suggest that cobalt induced cytotoxicity involves HIF1 $\alpha$ -dependent upregulation of BNIP3 or NIX leading to a caspase-independent necrosis-like cell death.

## **Discussion**

Hypoxia is a characteristic feature of a number of pathophysiological conditions such as cancer, stroke, cardiac ischemia etc. (28). Cobalt chloride has been widely used as a hypoxia mimic in both *in vivo* and *in vitro* studies (29). However, the role of aberrant hypoxic signaling in cobalt-induced toxicity has not been addressed. Previous work has shown that on a global gene expression level, both cobalt and hypoxia regulate a similar group of genes (17). The observed similarity in gene expression appears to be dependent upon a functional HIF1 $\alpha$  protein (17, 30). The experiments described here characterized the mechanism of action of cobalt chloride-induced cell death and determine the role of HIF1 $\alpha$  in this process.

Cell viability and proliferation studies show that wild type cells are more susceptible to cobalt-induced toxicity when compared to HIF1 $\alpha$  *-/-* cells. Given that HIF1 $\alpha$  is a transcription factor, it seemed likely that this toxicity is dependent upon gene activation. Previous genomic screens and other reports have identified BNip3 and NIX as target genes of hypoxia signaling (14, 17, 23).

Expression of these pro-apoptotic factors was shown to be HIF1 $\alpha$  dependent and to occur at a dose and in a time frame similar to that of cobalt-induced cell damage (Figure 19 and 21). These results offer a direct link between the cobalt exposure, hypoxia signaling and activation of genes involved in cell injury. BNIP3 and NIX are BH3 domain-containing proteins belonging to the pro-apoptotic family of genes and their increased expression is correlated with increased cell death (31). Here we show that these mitochondrial proteins are not mediating cell death through the classical caspase-3 activation pathway. There have been earlier reports that increases in BNIP3 lead to caspase activation in primary cardiac myocytes undergoing hypoxia (22). However, in other cell types, BNIP3 induces a cell death similar to necrosis, which doesn't involve caspase activation (21). In addition, it has been shown that BNIP3 causes a necrosis-like cell death in cells through the mitochondrial permeability transition pore which involves the loss of mitochondrial potential but without caspase activation and cytochrome C release (25). This is not surprising, as there are alternate pathways of apoptosis that do not require caspase activation such as the AIF pathway (32). One important point is that caspase-dependent apoptosis is an energy requiring process. At least during hypoxia, ATP levels in the cell are low due to the inhibition of oxidative phosphorylation. Therefore, it is possible that the cells initiate an apoptotic process but resort to a necrotic pathway due to reduced ATP levels. At present it is not clear if ATP levels are reduced under cobalt treatment however, the morphological study of CoCl<sub>2</sub> treated cells show moderate chromatin condensation in the absence of caspase

3 activation. Taken together, it seems likely that the HIF1 $\alpha$ -dependent increase in BNIP3 and NIX leads to caspase-independent, necrotic-like cell death similar to what has been demonstrated in 293T, MCF7, other MEFs and various tumors (23, 25, 33).

Cobalt and nickel are known to activate hypoxic signaling, and nickel-induced transformation of fibroblasts requires a functional hypoxia signaling pathway (34, 35). The mechanism of action of CoCl<sub>2</sub> mediated stabilization of HIF1 $\alpha$  under normoxia is not completely elucidated. It is thought to inhibit the iron containing HIF prolyl hydroxylase enzyme, which plays a critical role in mediating the normal hypoxic signaling by modifying HIF1 $\alpha$  protein and targeting it for degradation. The chemical characteristics of cobalt also allow it to compete for iron at reactive sites of various enzymes, rendering these enzymes inactive. The first published reports of the PHD family of enzymes characterized this inhibition and helped explain the ability of cobalt to act as a hypoxic mimic (16). Recent reports also suggest that cobalt exposure may not displace iron at the catalytic site within the hydroxylase but may sequester the available ascorbate in the cell. Since ascorbate is necessary for the transition of iron between oxidation states, this would effectively inhibit PHD activity (36).

The hypoxic signaling pathway is known to activate cell survival genes involved in glycolysis, angiogenesis and erythropoiesis (8, 37, 38). In addition, in some cell types, cobalt and hypoxia exposure has been shown to inhibit apoptotic

pathways (39). Under chronic hypoxia, however, this pathway also activates genes involved in cell cycle arrest and death including pro-apoptotic genes (14). These reports and our current results suggest a complex and at times, contradictory picture for cobalt induced damage. The protective effects of cobalt were shown using a very different experimental paradigm and this may explain the differences in results. Piret et al exposed HepG2 cells to tert-butyl hydroperoxide (t-BHP) under serum-free conditions to characterize cobalt's inhibitory effects (39). In contrast, we utilized MEFs in the presence of serum and absence of outside apoptotic stimuli. Treatment time may have also been a factor since the HepG2 cell's cobalt exposure was limited to 8 hours in the serum containing controls. These differences highlight the complexity in metal-induced toxicity and suggest multiple pathways may be involved. For example, the observation that cobalt toxicity was only partially attenuated in the HIF1 $\alpha$  *-/-* cells suggests that cobalt-induced cell death involves HIF1 $\alpha$  dependent and independent mechanisms (Figure 18). HIF1 $\alpha$  independent mechanisms may be require other functioning HIFs in the MEFs or the possible disruption of one or more of the essential enzymes that require iron as a cofactor, which may ultimately affect cell viability. Also, the effect of oxidative stress due to the production of reactive oxygen species on various cell processes and integrity of cellular components such as proteins, DNA and lipid bi-layer cannot be underestimated. Consistent with this hypothesis, cobalt chloride treatment is known to induce stress responsive proteins such as metallothionein in wild type and HIF1 $\alpha$  *-/-* cells (17, 40).

In summary, WT and HIF1 $\alpha$  -/- cells were treated with cobalt chloride and toxicity was studied using cell count and MTT assays. Wild type cells showed a marked decrease in viability as well as cell proliferation compared to HIF1 $\alpha$  -/- cells. Wild type cells showed an increase in the expression of the cell death gene, BNip3 mRNA and protein upon CoCl<sub>2</sub> treatment. The cell death and expression of BNip3 mRNA overlapped in both the time course and dose response studies. This study shows that cobalt chloride exposure in mouse embryonic fibroblast leads to a necrosis-like cell death which is dependent on the presence of functional HIF1 $\alpha$  protein. This indicates that the pathology of cobalt-induced toxicity might be due to the activation of aberrant hypoxic signaling leading to the increase in the cell death promoting genes such as BNIP3 and NIX levels and subsequent necrosis.

### **Acknowledgements**

We are grateful to Dr. Randy Johnson and Heather Ryan for providing the wild type HIF1 $\alpha$  -/- mouse embryonic fibroblast cell line. We thank Barbara Woods, KangAe Lee and Darrell Boverhof for critical reading of the manuscript and Jane Maddox, Brad Upham and Joseph Frentzel for assistance with cell staining and caspase assays.

## References

1. Adamu, C. A., Bell, P. F., Mulchi, C., and Chaney, R. Residual metal concentrations in soils and leaf accumulations in tobacco a decade following Farmland application of municipal sludge. *Environ. Poll.*, 56: 113-126, 1989.
2. Lauwerys, R. and Lison, D. Health risks associated with cobalt exposure--an overview. *Sci Total Environ*, 150: 1-6, 1994.
3. Hayes, R. B. The carcinogenicity of metals in humans. *Cancer Causes & Control*, 8: 371-385, 1997.
4. Giaccia, A., Siim, B. G., and Johnson, R. S. HIF-1 as a target for drug development. *Nat Rev Drug Discov*, 2: 803-811, 2003.
5. Bunn, H. F. and Poyton, R. O. Oxygen sensing and molecular adaptation to hypoxia. *Phys. Rev.*, 76: 839-885, 1996.
6. Li, H., Ko, H. P., and Whitlock, J. P. Induction of phosphoglycerate kinase 1 gene expression by hypoxia. Roles of Arnt and HIF1alpha. *J. Biol. Chem.*, 271: 21262-21267, 1996.
7. Maltepe, E. and Simon, M. C. Oxygen, genes, and development: an analysis of the role of hypoxic gene regulation during murine vascular development. *J. Mol. Med.*, 76: 391-401, 1998.
8. Semenza, G. L., Roth, P. H., Fang, H. M., and Wang, G. L. Transcriptional regulation of genes encoding glycolytic enzymes by hypoxia-inducible factor 1. *J. Biol. Chem.*, 269: 23757-23763, 1994.
9. Wang, G. L. and Semenza, G. L. Purification and characterization of hypoxia-inducible factor 1. *J. Biol. Chem.*, 270: 1230-1237, 1995.
10. Sandner, P., Wolf, K., Bergmaier, U., Gess, B., and Kurtz, A. Induction of VEGF and VEGF receptor gene expression by hypoxia: divergent regulation in vivo and in vitro. *Kid. Int.*, 51: 448-453, 1997.
11. Krieg, M., Marti, H. H., and Plate, K. H. Coexpression of erythropoietin and vascular endothelial growth factor in nervous system tumors associated with von Hippel-Lindau tumor suppressor gene loss of function. *Blood*, 92: 3388-3393, 1998.
12. Forsythe, J. A., Jiang, B. H., Iyer, N. V., Agani, F., Leung, S. W., Koos, R. D., and Semenza, G. L. Activation of vascular endothelial growth factor

- gene transcription by hypoxia-inducible factor 1. *Mol. Cell. Biol.*, **16**: 4604-4613, 1996.
13. Gleadle, J. M. and Ratcliffe, P. J. Induction of hypoxia-inducible factor-1, erythropoietin, vascular endothelial growth factor, and glucose transporter-1 by hypoxia: evidence against a regulatory role for Src kinase. *Blood*, **89**: 503-509, 1997.
  14. Bruick, R. K. Expression of the gene encoding the proapoptotic Nip3 protein is induced by hypoxia. *Proc Natl Acad Sci U S A*, **97**: 9082-9087., 2000.
  15. Ho, V. T. and Bunn, H. F. Effects of transition metals on the expression of the erythropoietin gene: further evidence that the oxygen sensor is a heme protein. *Biochem. Biophys. Res. Comm.*, **223**: 175-180, 1996.
  16. Epstein, A. C., Gleadle, J. M., McNeill, L. A., Hewitson, K. S., O'Rourke, J., Mole, D. R., Mukherji, M., Metzen, E., Wilson, M. I., Dhanda, A., Tian, Y. M., Masson, N., Hamilton, D. L., Jaakkola, P., Barstead, R., Hodgkin, J., Maxwell, P. H., Pugh, C. W., Schofield, C. J., and Ratcliffe, P. J. C. *C. elegans* EGL-9 and mammalian homologs define a family of dioxygenases that regulate HIF by prolyl hydroxylation. *Cell*, **107**: 43-54., 2001.
  17. Vengellur, A., Woods, B. G., Ryan, H. E., Johnson, R. S., and LaPres, J. J. Gene expression profiling of the hypoxia signaling pathway in hypoxia inducible factor 1 null mouse embryonic fibroblasts. *Gene Expression*, **11**: 181-197, 2003.
  18. van de Loosdrecht, A. A., Nennie, E., Ossenkoppele, G. J., Beelen, R. H. J., and Langenhuijsen, M. Cell-mediated cytotoxicity against U-937 cells by human monocytes and macrophages in a modified colorimetric MTT assay - a methodological study. *J Immun Meth*, **141**: 15-22, 1991.
  19. LaPres, J. J., Glover, E., Dunham, E. E., Bunger, M. K., and Bradfield, C. A. ARA9 Modifies Agonist Signaling through an Increase in Cytosolic Aryl Hydrocarbon Receptor. *J Biol Chem*, **275**: 6153-6159, 2000.
  20. Lowry, O. H., Rosebrough, N. J., Farr, A. L., and Randall, R. J. Protein measurement with the Folin phenol reagent. *J Biol Chem*, **193**: 265-275, 1951.
  21. Kubasiak, L. A., Hernandez, O. M., Bishopric, N. H., and Webster, K. A. Hypoxia and acidosis activate cardiac myocyte death through the Bcl-2 family protein BNIP3. *Proc Natl Acad Sci USA*, **99**: 12825-12830, 2002.
  22. Regula, K. M., Ens, K., and Kirshenbaum, L. A. Inducible expression of BNIP3 provokes mitochondrial defects and hypoxia-mediated cell death of ventricular myocytes.[see comment]. *Circ. Res.*, **91**: 226-231, 2002.

23. Sowter, H. M., Ratcliffe, P. J., Watson, P., Greenberg, A. H., and Harris, A. L. HIF-1-dependent regulation of hypoxic induction of the cell death factors BNIP3 and NIX in human tumors. *Cancer Res*, *61*: 6669-6673., 2001.
24. Chen, G., Ray, R., Dubik, D., Shi, L., Cizeau, J., Bleackley, R. C., Saxena, S., Gietz, R. D., and Greenberg, A. H. The E1B 19K/Bcl-2-binding protein Nip3 is a dimeric mitochondrial protein that activates apoptosis. *J Exp Med*, *186*: 1975-1983, 1997.
25. Vande Velde, C., Cizeau, J., Dubik, D., Alimonti, J., Brown, T., Israels, S., Hakem, R., and Greenberg, A. H. BNIP3 and genetic control of necrosis-like cell death through the mitochondrial permeability transition pore. *Mol Cell Biol*, *20*: 5454-5468, 2000.
26. Tamaoki, T., Nomoto, H., Takahashi, I., Kato, Y., Morimoto, M., and Tomita, F. Staurosporine, a potent inhibitor of phospholipid/Ca<sup>++</sup>dependent protein kinase. *Biochem Biophys Res Commun*, *135*: 397-402, 1986.
27. Nicholson, D. W., Ali, A., Thornberry, N. A., Vaillancourt, J. P., Ding, C. K., Gallant, M., Gareau, Y., Griffin, P. R., Labelle, M., Lazebnik, Y. A., and et al. Identification and inhibition of the ICE/CED-3 protease necessary for mammalian apoptosis. *Nature*, *376*: 37-43, 1995.
28. Semenza, G. L., Agani, F., Feldser, D., Iyer, N., Kotch, L., Laughner, E., and Yu, A. Hypoxia, HIF-1, and the pathophysiology of common human diseases. *Adv Exp Med Biol*, *475*: 123-130, 2000.
29. Wang, G. L. and Semenza, G. L. Desferrioxamine induces erythropoietin gene expression and hypoxia-inducible factor 1 DNA-binding activity: implications for models of hypoxia signal transduction. *Blood*, *82*: 3610-3615, 1993.
30. Salnikow, K., Su, W., Blagosklonny, M. V., and Costa, M. Carcinogenic metals induce hypoxia-inducible factor-stimulated transcription by reactive oxygen species-independent mechanism. *Cancer Res*, *60*: 3375-3378, 2000.
31. Chen, G., Cizeau, J., Vande Velde, C., Park, J. H., Bozek, G., Bolton, J., Shi, L., Dubik, D., and Greenberg, A. Nix and Nip3 form a subfamily of pro-apoptotic mitochondrial proteins. *J. Biol. Chem.*, *274*: 7-10, 1999.
32. Lorenzo, H. K., Susin, S. A., Penninger, J., and Kroemer, G. Apoptosis inducing factor (AIF): a phylogenetically old, caspase-independent effector of cell death. *Cell Death Differ*, *6*: 516-524, 1999.

33. Sowter, H. M., Ferguson, M., Pym, C., Watson, P., Fox, S. B., Han, C., and Harris, A. L. Expression of the cell death genes BNip3 and NIX in ductal carcinoma in situ of the breast; correlation of BNip3 levels with necrosis and grade. *J Pathol*, 201: 573-580, 2003.
34. Salnikow, K., Wang, S., and Costa, M. Induction of activating transcription factor 1 by nickel and its role as a negative regulator of thrombospondin I gene expression. *Cancer Res*, 57: 5060-5066, 1997.
35. Salnikow, K., Davidson, T., Zhang, Q., Chen, L. C., Su, W., and Costa, M. The involvement of hypoxia-inducible transcription factor-1-dependent pathway in nickel carcinogenesis. *Cancer Res*, 63: 3524-3530, 2003.
36. Salnikow, K., Donald, S. P., Bruick, R. K., Zhitkovich, A., Phang, J. M., and Kasprzak, K. S. Depletion of intracellular ascorbate by the carcinogenic metals nickel and cobalt results in the induction of hypoxic stress. *J Biol Chem*, 2004.
37. Levy, A. P., Levy, N. S., Wegner, S., and Goldberg, M. A. Transcriptional regulation of the rat vascular endothelial growth factor gene by hypoxia. *J Biol Chem*, 270: 13333-13340, 1995.
38. Wang, G. L., Jiang, B. H., Rue, E. A., and Semenza, G. L. Hypoxia-inducible factor 1 is a basic-helix-loop-helix-PAS heterodimer regulated by cellular O<sub>2</sub> tension. *Proc. Natl. Acad. Sci. USA*, 92: 5510-5514, 1995.
39. Piret, J. P., Lecocq, C., Toffoli, S., Ninane, N., Raes, M., and Michiels, C. Hypoxia and CoCl<sub>2</sub> protect HepG2 cells against serum deprivation- and t-BHP-induced apoptosis: a possible anti-apoptotic role for HIF-1. *Exp Cell Res*, 295: 340-349, 2004.
40. Murphy, B. J., Andrews, G. K., Bittel, D., Discher, D. J., McCue, J., Green, C. J., Yanovsky, M., Giaccia, A., Sutherland, R. M., Laderoute, K. R., and Webster, K. A. Activation of metallothionein gene expression by hypoxia involves metal response elements and metal transcription factor-1. *Cancer Res*, 59: 1315-1322, 1999.

## **CHAPTER 4**

### **THE ROLE OF HIF1 $\alpha$ IN METAL-INDUCED TOXICITY IN MOUSE EMBRYONIC FIBROBLASTS**

## **Abstract**

Hypoxia inducible factor 1 $\alpha$  is a major transcription factor that mediates cellular response to hypoxia and is regulated by iron-dependent HIF prolyl hydroxylases (PHDs) which modify and target HIF1 $\alpha$  protein for degradation under normoxia. Divalent metal ions such as cobalt and nickel and iron chelators such as desferoxamine can stabilize HIF1 $\alpha$  under normoxia by inhibiting the PHDs. Previously, it was shown that cobalt's ability to stabilize HIF1 $\alpha$  is directly related to its toxicity. To determine the role of HIF1 $\alpha$  in the toxicity of other divalent metals, wild type and HIF1 $\alpha$  null MEF cells were assessed for cadmium-induced damage. Cobalt exposure leads to stabilization of HIF1 $\alpha$  and activation of gene transcription of pro-cell death BNip3 gene, leading to increased cell death in the wild type cells. In contrast, cadmium treatment does not affect the HIF1 transcriptional signaling but leads to caspase activation and apoptotic cell death, which is greater in the HIF1 $\alpha$  null cells. Cadmium exposure also leads to greater oxidative stress compared to cobalt exposure, which is again significantly higher in the HIF1 $\alpha$  null cells. Surprisingly, HIF1 $\alpha$  null cells have a greater basal level of reactive oxygen species compared to wild type cells and have reduced mRNA, protein and activity of Cu/Zn superoxide dismutase enzyme (SOD1). Moreover, HIF1 $\alpha$  null cells had higher total glutathione levels following cobalt and cadmium exposure compared to wild type cells, pointing to decreased capacity to cope with oxidative stress. Overall, our results suggest that cobalt-induced cell damage is promoted through HIF1 $\alpha$  stabilization and subsequent transcriptional activation of cell death genes. Cadmium-induced cytotoxicity is due to ROS

generation and the compromised nature of the ROS scavenging system in the HIF1 $\alpha$  -/- cells.

## **Introduction**

Metals ions are critical for many processes necessary for cellular homeostasis, including the function of almost one third of all enzymes (1). The reactive nature of these metal ions also makes it necessary for cells to maintain a tight regulation on their concentration and localization and any deviation from this normalcy can adversely affect life processes by reacting with other cellular components such as proteins, lipids and nucleic acids (2). Most living organisms require an aerobic environment for survival and have a well developed signaling system to adapt to any fluctuations in oxygen availability. Hypoxia inducible factor 1 $\alpha$  (HIF1 $\alpha$ ) is a major transcription factor that regulates the cellular and physiological response to decreases in oxygen concentrations (i.e. hypoxia) (see "Introduction" chapter).

Insults that mimic hypoxia such as cobalt or nickel exposure and iron chelators such as deferoxamine can activate HIF signaling by stabilizing HIF1 $\alpha$  (3). In the present study the effects of exposure to two divalent metals, cobalt and cadmium were compared in two strains of mouse embryonic fibroblasts (MEFs) to establish the role of HIF1 $\alpha$  in mediating these effects. We show that HIF1 $\alpha$  plays a protective role against cadmium-induced toxicity while promoting cobalt-induced toxicity. The results also indicate that basal expression of HIF1 $\alpha$  under normoxia plays a crucial role in maintaining the levels of cellular antioxidants such as SOD1 and SOD2 and glutathione levels.

## **Methods**

*Materials* — Tissue culture media and supplements were obtained from Invitrogen, Inc. Cosmic calf serum was obtained from Hyclone. Oligonucleotide synthesis was performed at the Macromolecular Facility, Michigan State University, East Lansing, MI. SYBR Green™ real time PCR reagents were purchased from Applied Biosystems™, CA. All other chemicals were reagent grade and obtained from Sigma™ Chemical Company, MO.

*Cell Culture and Toxicity assay* — Mouse embryonic fibroblast cell lines were maintained in modified DMEM media (10% heat inactivated FBS, penicillin-streptomycin (10 U/ml), non-essential amino acid (10 µg/ml), L-glutamine (2mM) and Hepes Buffer, pH 7.0 (10mM). Cells were grown in 96 well plates and treated with 0, 100, 150, and 200 µM of CoCl<sub>2</sub> for 72 hours or 0, 1, 2, 5 and 10µM CdCl<sub>2</sub> for 72 hours. MTT assays were performed (see chapter 3 methods section). For figure 27C wild type and HIF1α -/- cells were treated with CoCl<sub>2</sub>, CdCl<sub>2</sub> and menadione alone or with N-acetyl cysteine, Tempol or melatonin for 72 hours and MTT assay was performed.

*Protein Extraction and Western Blotting* — Wild type and HIF1α -/- cells were grown in normal medium or in the presence of 150µM CoCl<sub>2</sub> or 1, 5 or 10µM CdCl<sub>2</sub> or 150µM CoCl<sub>2</sub> and 5µM CdCl<sub>2</sub> and protein extracts were prepared (see chapter 2 methods). For BNIP3, SOD1, and SOD2 westerns, total cell lysate was used. Briefly, cells were washed with cold PBS (4°C) and removed from the surface by scraping in cold PBS and collected by centrifugation. Soluble proteins

were extracted with cell lysis buffer (25 mM HEPES, pH-7.6, 2 mM EDTA, 10 % glycerol, 1 µg/mL of aprotinin, leupeptin, pepstatin A and 1 mM PMSF) and sonication (5 secs., 4°C). Insoluble material was removed by centrifugation (18000g, 20 min.) and protein concentrations were determined using Bio-Rad™ Bradford assay kit and BSA standards (4). An equal amount of protein was separated by SDS-PAGE, and western blotting was performed with anti-HIF1α (Novus Biologicals, CO) and BNip3 and β-actin (Sigma) and SOD1 and SOD2 specific antibodies (Santacruz Biotech) using ECL chemiluminescent detection kit (Amersham Pharmacia).

*RNA Extraction and Reverse Transcription and Real-Time Quantitative PCR Analysis* — RNA extraction was performed using TriZol reagent (Invitrogen) via manufacturer's instruction. The measurement of BNip3, SOD1 and SOD2 mRNA levels was performed using real-time PCR, on an Applied Biosystems Prism 7000 Sequence detection System (Foster City, CA). For detailed protocol see chapter 1 methods section. Primers were designed using the web based application [Primer3](http://www-genome.wi.mit.edu/cgi-bin/primer/primer3_www.cgi) ([http://www-genome.wi.mit.edu/cgi-bin/primer/primer3\\_www.cgi](http://www-genome.wi.mit.edu/cgi-bin/primer/primer3_www.cgi)) biasing towards the 3' end of the transcript giving a gene-specific product (Table 16). The relative abundance of mRNA was calculated from the Ct values normalized to HPRT.

*Creation of stable BNip3 shRNA cells –*

**Table 16. qRT-PCR primers**

<b>Gene</b>	<b>Accession</b>	<b>Forward</b>	<b>Reverse</b>
HPRT	NM_013556	AAGCCTAAGATGAGCGC AAG	TTACTAGGCAGATGGCC ACA
BNip3	NM_009760	GCGCTCTGACAACCTTCC ACT	AACACCCAAGGACCATG CTA
SOD1	NM_011434.1	GAGACCTGGGCAATGTG ACT	TTGTTTCTCATGGACCAC CA
SOD2	NM_013671.3	AACTCAGGTCGCTCTTC AGC	GCTTGATAGCCTCCAGC AAC

**Table 17. shRNA Sequences**

<b>Gene</b>	<b>Accession</b>	<b>Sequence</b>
shCTRL		TGCGTCTTGTTTCATCTCCT
shBNip3 #1	NM_009760	GGCAGCCTGCGCCGCTCAGC
shBNip3 #2	NM_009760	TGCCATTGCTGAAGTGCAGC

Target sequences were obtained using Ambion's siRNA target finder ([http://www.ambion.com/techlib/misc/siRNA\\_finder.html](http://www.ambion.com/techlib/misc/siRNA_finder.html)) and were analyzed by BLAST to determine specificity (Table 17). Oligos were designed and PCR was performed to create a shRNA cassette carrying U6 promoter sequence, sense-loop-antisense sequence and terminator sequence. The shRNA cassettes were cloned into a lentiviral vector and packaged using 293T cells via transient transfection with helper plasmids to generate infectious virus (obtained from University of California, San Diego). GFP construct was used as a control. Wild type cells were plated at the density of  $2 \times 10^4$  cells per 6 cm tissue culture dish and were infected with the virus overnight. Cells were split and individual colonies were isolated and Puromycin-selected to create the stable shRNA expressing cells. Scrambled target sequence with no similarity to any known gene was also cloned and infected to use as shControl.

*Cell Staining and Caspase Assay* - Cells were left untreated or treated with  $5 \mu\text{M}$   $\text{CdCl}_2$  for 24 hours and stained with Hoechst33342 dye ( $1 \mu\text{g/ml}$ , 15 min.). Cells were viewed and photographed with fluorescent microscopy. Caspase assays were performed using EnZChek caspase-3 assay kit (Molecular Probes) using the manufacturer's instructions. Briefly, cells were left untreated or exposed to  $\text{CdCl}_2$  ( $5 \mu\text{M}$ , 24 hours) or Staurosporine ( $1 \mu\text{M}$ , 4 hrs). Cell extracts were obtained using the lysis buffer provided and the caspase-3 activity in the supernatant was analyzed spectrophotometrically.

*Determination of ROS levels* – Cells were left untreated or treated with 200 $\mu$ M CoCl<sub>2</sub> or 5 $\mu$ M CdCl<sub>2</sub> for 24 hours or 1mM H<sub>2</sub>O<sub>2</sub> for 1 hour. Cells were trypsinized, pelleted, and treated with 5 $\mu$ M CM-H<sub>2</sub>DCFDA (Molecular Probes, OR) for 30 minutes in serum free media. Cells were washed with PBS and re-suspended in PBS supplemented with 10% cosmic calf serum and analyzed on a BD FACSDiva<sup>®</sup> flow cytometer. Fluorescence intensity (490nm excitation and 520nm emission) of 1 x 10<sup>4</sup> cells for each sample were measured and experiments were performed in duplicate.

*Determination of superoxide dismutase activity* – Total cellular superoxide dismutase activity was measured using superoxide dismutase assay (Cayman Chemicals, MI) as per manufacturer's description. Briefly, treated cells were harvested, pelleted, and lysed by sonication in buffer containing 20mM Hepes (pH = 7.2), 1mM EGTA, 210mM mannitol and 70mM sucrose. Supernatant was collected after centrifuging at 1500g for 5 minutes, and an aliquot was used for performing the superoxide dismutase assay and enzyme activity was quantified using a standard curve. Mn-SOD levels in the sample were determined using 3 mM KCN to inhibit the activity of Cu/Zn-SOD activity.

*Determination of Glutathione levels* – Total glutathione levels were determined using spectrophotometric assay (Cayman chemicals, Ann Arbor, MI) as per manufacturer's instructions. Briefly, treated cells were harvested by scraping in ice cold PBS and pelleted by centrifugation (1000g, 5 minutes). Cells were

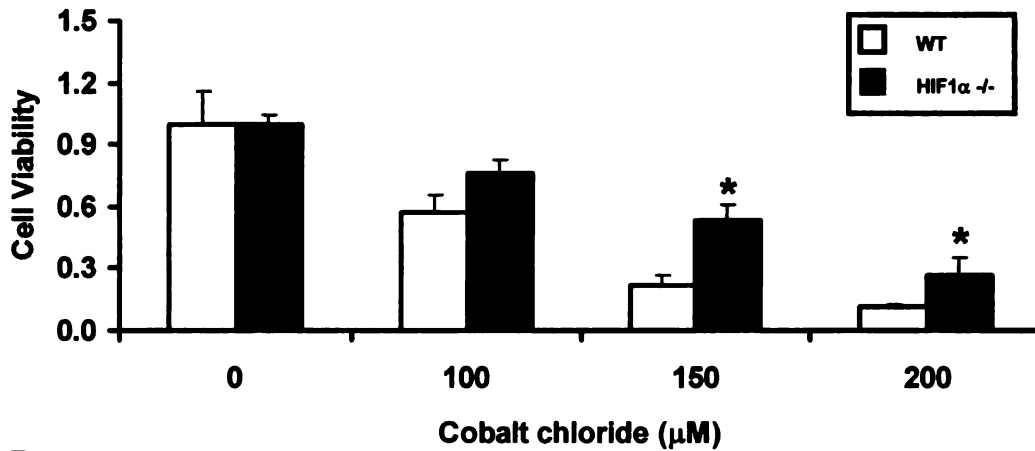
sonicated in 1X MES buffer and insoluble material was removed by centrifugation (5000g, 5 minutes). Supernatant was deproteinated by the addition of an equal volume of 10% metaphosphoric acid and neutralized by adding 4M triethanolamine. Glutathione concentration was determined by performing a coupled kinetic assay. In this assay, glutathione is used by glutathione reductase to convert a colorless tetrazolium salt into formazan which was measured spectrophotometrically. The results were normalized to total protein levels.

*Statistics* - Statistical analysis was performed between treated and untreated samples using t-test (two tailed, unequal variance,  $p \leq 0.05$ ).

## **Results**

*Cadmium and Cobalt Toxicity to MEFs* - Wild type and HIF1 $\alpha$  *-/-* mouse embryonic fibroblast (MEFs) cells were plated in 96 well plates and treated with 50, 100, 150 or 200 $\mu$ M CoCl<sub>2</sub> (Figure 25A) and 1, 2, 5 or 10 $\mu$ M CdCl<sub>2</sub> (Figure 25B) for 72 hours. Cell viability, determined by MTT assay, was markedly reduced in both wild type and HIF1 $\alpha$  *-/-* cell lines under cobalt and cadmium treatment in a dose dependent manner. However, cobalt-induced cytotoxicity was markedly higher in the wild type cells compared to HIF1 $\alpha$  *-/-* cells as we have reported earlier (5). In contrast, cadmium chloride treatment caused significantly greater cytotoxicity in the HIF1 $\alpha$  *-/-* cells compared to the wild type cells. The results indicate that HIF1 $\alpha$  might be playing different roles in cell survival following cobalt and cadmium exposure.

A.



B.

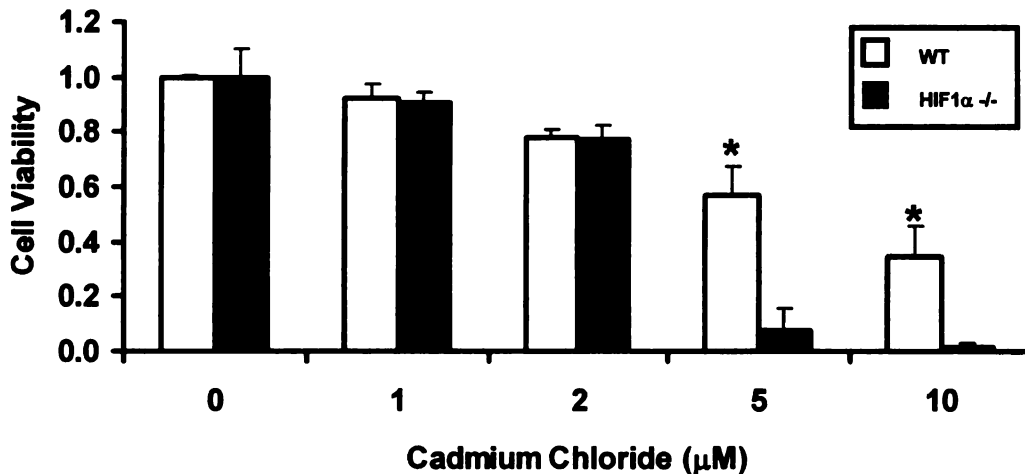


**Figure 25. Cytotoxicity of CoCl<sub>2</sub> and CdCl<sub>2</sub> to MEFs**

**A.** Wild type (WT, white bars) and HIF1α<sup>-/-</sup> (black bars) cells were left untreated (0) or exposed to 100, 150 or 200 µM CoCl<sub>2</sub> (100, 150, 200) for 72 hrs. Cell viability was assessed using a standard MTT assay. Control values within cell type were set to 1. \*, p < 0.05.

**B.** Wild type (WT, white bars) and HIF1α<sup>-/-</sup> (black bars) cells were left untreated (0) or exposed to 1, 2, 5, 10 µM CdCl<sub>2</sub> (1, 2, 5, 10) for 72 hrs. Cell viability was assayed using a standard MTT assay. Control values within cell type were set to 1. . \*, p < 0.05.

Previously, we reported that  $\text{CoCl}_2$ -induced cytotoxicity correlated with an increase in nuclear condensation; however, this condensation occurred in the absence of caspase-3 activation (5). To expand these findings, WT and  $\text{HIF1}\alpha$   $-/-$  MEFS were treated with  $\text{CdCl}_2$ , and nuclear morphology and caspase-3 activation was assessed. Wild type and  $\text{HIF1}\alpha$   $-/-$  cells showed significant levels of nuclear condensation characteristic of apoptosis following metal exposure, however, the null cells were more sensitive (Figure 26A). As seen in Figure 26B  $\text{HIF1}\alpha$   $-/-$  cells displayed a greater caspase-3 activation following cadmium exposure than the WT cells. This bias was not evident in the positive control, staurosporine treated samples (Figure. 26B).

*HIF1 $\alpha$  protein levels under cobalt and cadmium treatments* – Given that HIF1 is primarily regulated at the level of protein stability, the ability of both metals to stabilize HIF1 $\alpha$  was tested. Wild type cells were treated with various concentrations of metals, and HIF1 $\alpha$  protein levels were determined by western blot analysis (Figure 27A).  $\text{HIF1}\alpha$   $-/-$  cell extract treated with  $150\mu\text{M}$   $\text{CoCl}_2$  was used as a negative control. HIF1 $\alpha$  protein levels were detected only in the wild type cells under  $\text{CoCl}_2$  treatment. There were some non-specific bands present in all the lanes. In contrast to published reports in 293 cells exposed to hypoxia, cadmium co-treatment did not significantly reduce the HIF1 $\alpha$  protein levels in cobalt treated MEFs (Figure 27A) (6). These results suggest that the ability of WT to be refractory to cadmium-induced cytotoxicity is not mediated by metal-induced HIF1 $\alpha$  stabilization.

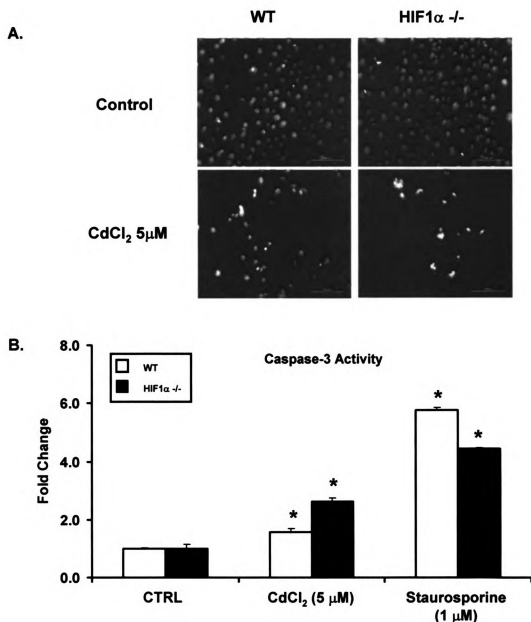


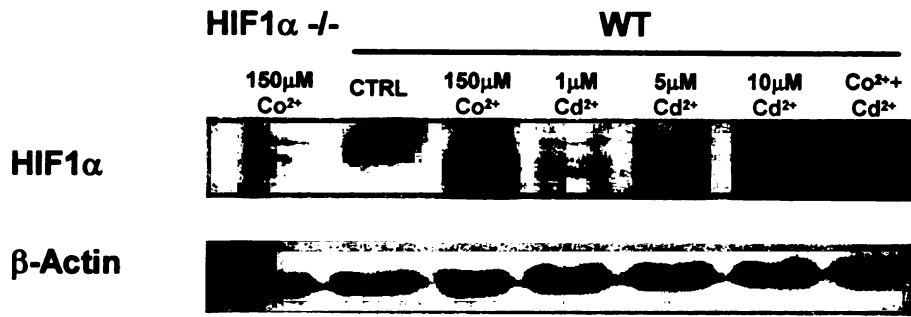
**Figure 26. Characterization of Cadmium-induced Cell Death.**

**A.** Wild type (WT) and HIF1 $\alpha$  -/- cells were left untreated (Control) or exposed to 5  $\mu$ M CdCl<sub>2</sub> for 24 hours and nuclear morphology was observed after staining with Hoechst 33342 dye using fluorescence microscopy. **B.** Wild type (WT, white bars) and HIF1 $\alpha$  -/- (black bars) cells were left untreated (CTRL) or exposed to CdCl<sub>2</sub> (CdCl<sub>2</sub> 5 $\mu$ M, 24 hours), or staurosporine (1  $\mu$ M, 4 hours). Caspase-3 activity was measured using EnZChek caspase-3 assay kit #2 (Molecular Probes). \*, p<0.05, n=4

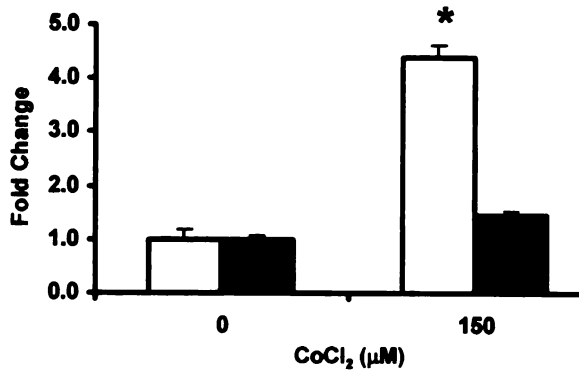
**Figure 27. Hypoxia signaling and cytotoxicity to CoCl<sub>2</sub> and CdCl<sub>2</sub>**

**A:** Wild type (WT) cells were left untreated (CTRL) or exposed to 150  $\mu$ M CoCl<sub>2</sub>, 1, 5 or 10  $\mu$ M CdCl<sub>2</sub> or 150  $\mu$ M CoCl<sub>2</sub> and 10  $\mu$ M CdCl<sub>2</sub> for 24 hours. HIF1 $\alpha$  -/- cells extract treated with 150 $\mu$ M CoCl<sub>2</sub> was used as a negative control. Nuclear protein was extracted and separated by SDS-PAGE, transferred to nitrocellulose membrane and probed with a HIF1 $\alpha$  (upper panel) or  $\beta$ -actin (lower panel) specific antibody. **B, C.** BNip3 mRNA expression levels were analyzed by qRT-PCR (SYBR Green) in wild type (WT, **white bars**) and HIF1 $\alpha$  -/- cells (**black bars**) as described in methods section. Cells were left untreated (**0**), 150 $\mu$ M CoCl<sub>2</sub> (**B, 150**) or 5 $\mu$ M CdCl<sub>2</sub> (**C, 5**) for 24 hours. Each value was normalized to the control level in the corresponding cell line. \*, p<0.05 compared to control within the cell type, n=4 **D.** BNip3 protein levels were determined in wild type (**1**), HIF1 $\alpha$  -/- (**2**), shControl (**3**), shBNip3 #1 (**4**), and shBNip3 #2 (**5**) after treatment with 150 $\mu$ M CoCl<sub>2</sub> or 5 $\mu$ M CdCl<sub>2</sub> for 24 hours using a BNip3 specific antibody and  $\beta$ -actin was used as a loading control (**Lower Panel**). **E.** Wild type (WT), HIF1 $\alpha$  -/-, shControl (**shCtrl**), shBNip3 #1 and shBNip3 #2 cells were exposed to 150 $\mu$ M CoCl<sub>2</sub> (**Co<sup>2+</sup>, white bars**) or 5 $\mu$ M CdCl<sub>2</sub> (**Cd<sup>2+</sup>, black bars**) for 72 hrs. Cell viability was assayed using a standard MTT assay. Control values within cell type were set to 1. \*, significant compared to wild type treatments, p<0.05, n=4.

A.



B.



C.

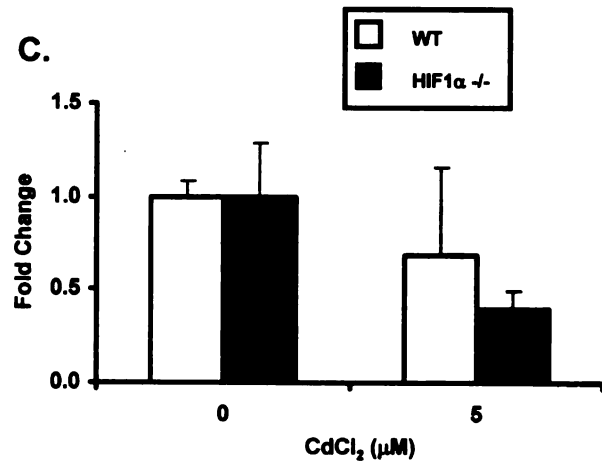
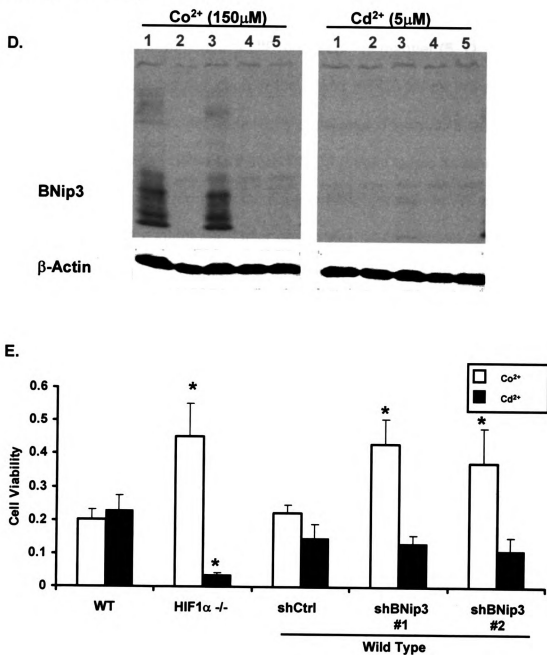


**Figure 27. Hypoxia signaling and cytotoxicity to CoCl<sub>2</sub> and CdCl<sub>2</sub> (continued)**



*BNip3 mRNA and protein expression following cobalt and cadmium treatments –*

Previously our group and others have shown that the mRNA and protein levels of BNip3, a BH3 domain containing, cell death promoting factor, are increased under cobalt chloride treatment in a HIF1 $\alpha$  dependent manner (5, 7). In contrast, CdCl<sub>2</sub> treatment caused a reduction in the BNip3 mRNA levels in wild type and HIF1 $\alpha$  -/- cells which was not statistically significant (Figure 27B and 27C). In addition, cadmium was unable to induce BNIP3 protein levels in either cell type, while cobalt treated cells led to an increase in BNIP3 protein in WT cells (Figure 27D). These results confirm our earlier observations and suggest that cadmium-induced cell damage is not mediated by BNIP3 (5, 7, 8).

To further characterize the role of BNIP3 in cobalt-induced toxicity, we created several cell strains with reduced BNIP3 expression levels using RNAi. WT cells were infected with a lentiviral vector expressing one of two independent shRNA constructs that specifically targeted BNip3 or a scrambled shRNA sequence as a negative control. Following selection of stable cell strains, BNIP3 protein levels were assessed by western blot analysis. The two independent BNip3 shRNAs showed greater than 80% reduction in the BNIP3 protein levels (Figure 27D). The cell lines were then treated with 150 $\mu$ M CoCl<sub>2</sub> for 72 hours and an MTT assay was performed to determine the role of BNip3 in cobalt-induced cytotoxicity. Both BNip3 shRNA expressing cell strains had reduced cobalt-induced cell death compared to the scrambled control. In fact, the results were comparable to HIF1 $\alpha$  -/- treated cells (Figure 27E). Moreover, knock-down of

BNIP3 levels in wild type cells did not influence the cell viability upon cadmium treatment significantly (Figure 27E). These results suggest that HIF1 $\alpha$ -induced BNIP3 protein expression plays a role in cobalt chloride induced toxicity but not in cadmium-induced toxicity in MEFs.

*Oxidative stress under cobalt and cadmium treatment* – Since HIF1 $\alpha$  activation and genes such as Bnip3 do not appear to play a role in cadmium induced toxicity, oxidative stress was characterized in the two cell lines. Cadmium and cobalt are known to produce reactive oxygen species (ROS) in various cell types (9, 10). To begin to characterize the role of oxidative stress in metal-induced cell death in the MEFs, the ROS levels were measured in WT and HIF1 $\alpha$  *-/-* cells following cobalt, cadmium, and hydrogen peroxide exposure. Cells were left untreated or treated with 150 $\mu$ M CoCl<sub>2</sub>, 5 $\mu$ M CdCl<sub>2</sub> or 1mM H<sub>2</sub>O<sub>2</sub> for 24 hours, and ROS were measured using flow cytometry and CH-H<sub>2</sub>DCFDA dye. Cadmium treatment caused a significant increase in ROS only in the HIF1 $\alpha$  *-/-* cells while cobalt was unable to alter the ROS profile in either cell type (Figure 28A). The lack of response in the WT cells from either metal was not due to any cell-specific mechanisms, as the positive control, H<sub>2</sub>O<sub>2</sub> treated WT displayed a marked increase in ROS generation. Interestingly, the HIF1 $\alpha$  *-/-* cells have a higher basal level of ROS compared to wild type cells (Figure 28B). These results suggest a possible mechanism for the specificity of cadmium-induced toxicity seen in the HIF1 $\alpha$  *-/-* cells and indicate that HIF1 $\alpha$  *-/-* cells are experiencing an increased ROS load under basal conditions.

**Figure 28. Oxidative stress in CoCl<sub>2</sub> and CdCl<sub>2</sub> mediated cytotoxicity.**  
**A.** Wild type (WT) and HIF1 $\alpha$  -/- cells were left untreated (CTRL), or exposed to 1mM H<sub>2</sub>O<sub>2</sub> (H<sub>2</sub>O<sub>2</sub>, 2hours), 200 $\mu$ M CoCl<sub>2</sub> (Co<sup>2+</sup>, 24 hours), or 5 $\mu$ M CdCl<sub>2</sub> (Cd<sup>2+</sup>, 24 hours). Reactive oxygen species generated in the cell were measured using the ROS sensitive dye CH-H<sub>2</sub>DCFDA and flow cytometry. **B.** Comparison of the levels of ROS generated in wild type (WT) and HIF1 $\alpha$  -/- cells untreated. **C.** Wild type and HIF1 $\alpha$  -/- cells were left treated with 150 $\mu$ M CoCl<sub>2</sub>, (Co<sup>2+</sup>), 150 $\mu$ M CoCl<sub>2</sub>, 5 $\mu$ M CdCl<sub>2</sub> (Cd<sup>2+</sup>) or 20 $\mu$ M menadione (MEN) alone or with 10mM N-acetyl cysteine (NAC), 1mM Tempol (TMP) or 1mM melatonin (MLT) for 72 hours and cell viability was measured using MTT assay. Control values within cell type were set to 1. \*, significant compared to single treatment, p<0.05, n=4



**Figure 28. Oxidative stress in  $\text{CoCl}_2$  and  $\text{CdCl}_2$  mediated cytotoxicity (continued)**

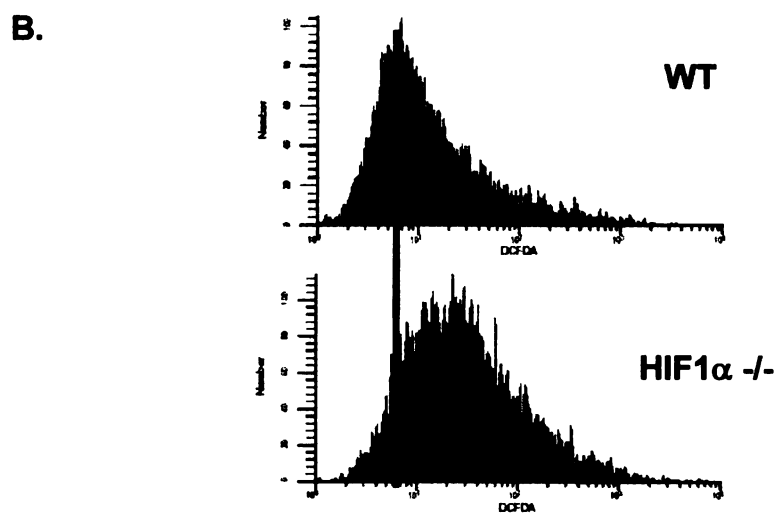
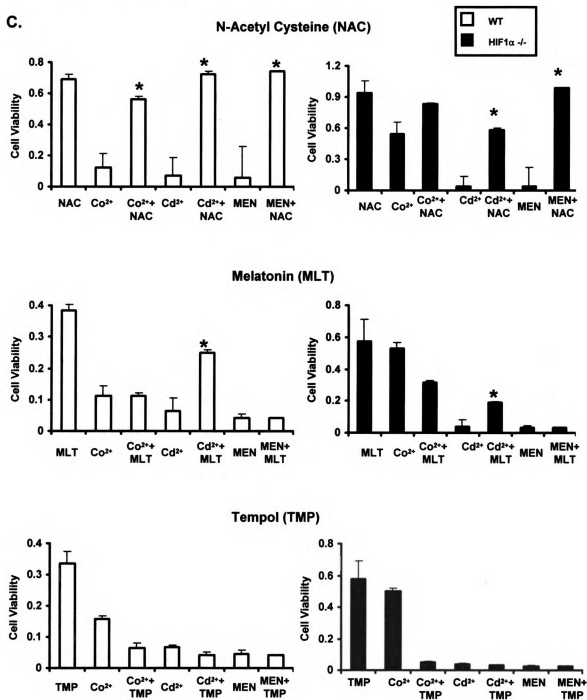


**Figure 28. Oxidative stress in  $\text{CoCl}_2$  and  $\text{CdCl}_2$  mediated cytotoxicity (continued)**

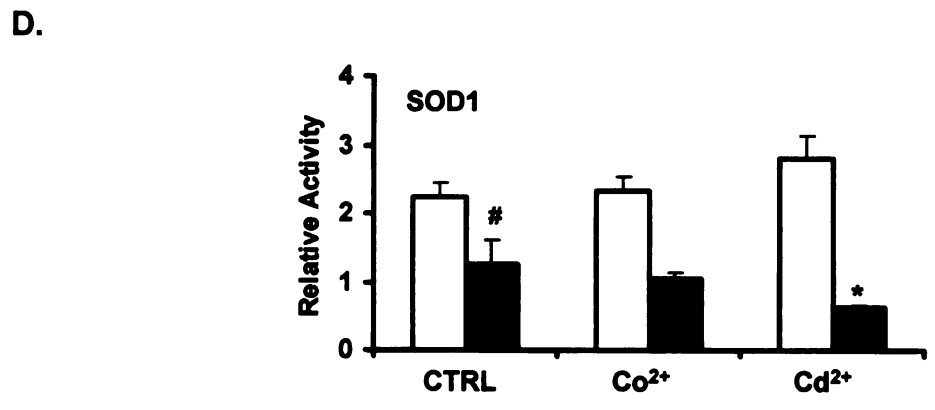
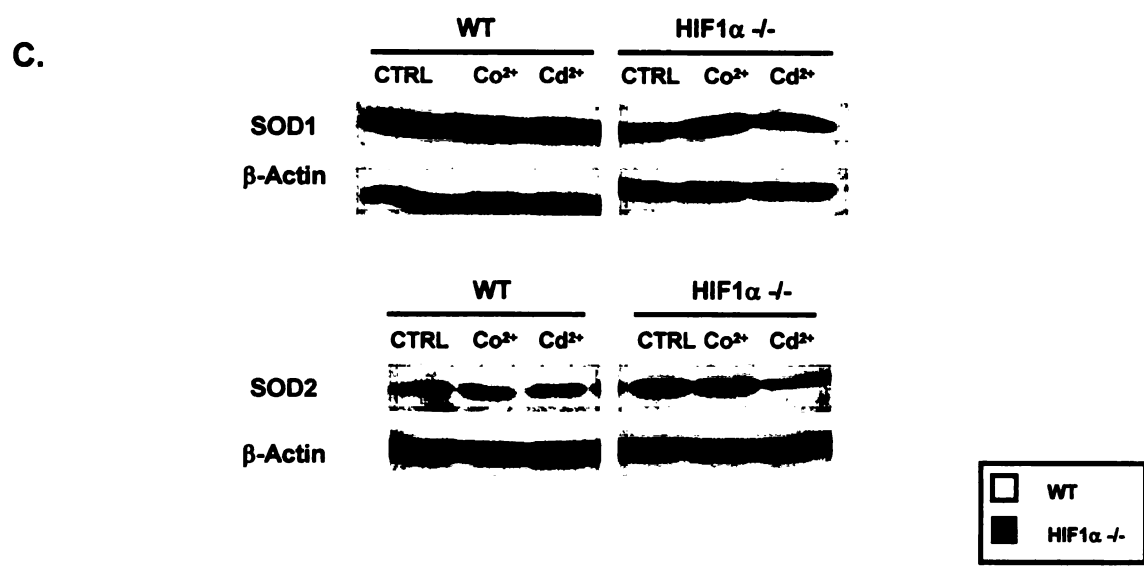
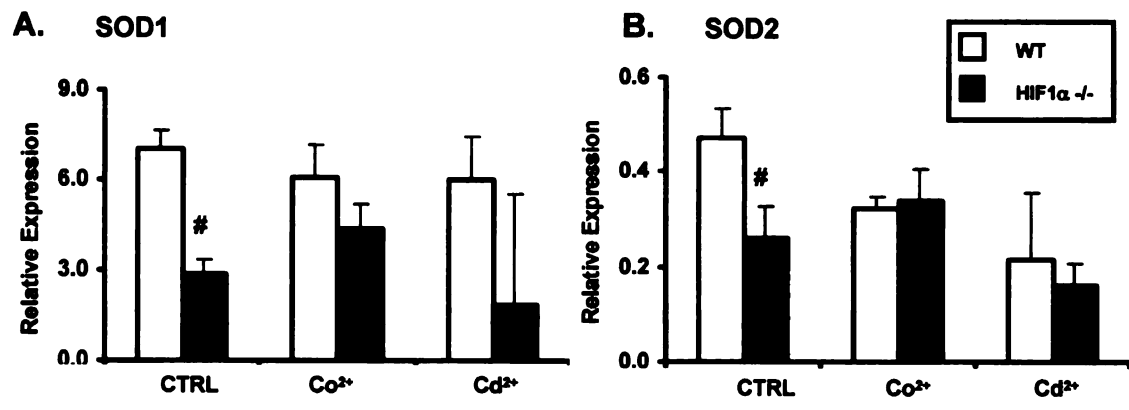


*Protection against toxicity by antioxidants* – Cadmium is known to create oxidative stress by sequestering the cellular glutathione pool through interactions with their sulfhydryl groups and effectively preventing their ability of to scavenge ROS. Cobalt is a well known Fenton metal that generates hydroxyl radicals by interacting with H<sub>2</sub>O<sub>2</sub> and superoxide (11, 12). N-acetyl cysteine (NAC), a known antioxidant, acts as a precursor for glutathione and can protect cells against oxidative injury caused by metals and other agents (13). Wild type and HIF1 $\alpha$  *-/-* cells were treated with CoCl<sub>2</sub>, or CdCl<sub>2</sub> in the presence and absence of NAC for 72 hours, and MTT assays were performed to assess cell viability. The results show that NAC prevented metal-induced cell damage in both cell types suggesting that ROS-mediated cobalt and cadmium-induced cytotoxicity. NAC also protected against menadione, a redox cycling agent known to generate oxidative stress in cells (Figure 28C) (14). . Among the other antioxidants tested, only melatonin at 1mM concentration showed any protection against cadmium exposure in wild type and HIF1 $\alpha$  *-/-* cells, and this effect was specific to cadmium-induced toxicity. Tempol, an SOD mimetic did not protect against either cobalt or cadmium exposure in either of the cells. Moreover, at 1mM concentration and even at 250 $\mu$ M concentration tempol reduced the cell viability in the control cells (Figure 28C, data not shown). These results suggest that oxidative stress plays a greater role in cadmium-induced toxicity compared to cobalt-induced toxicity.

*Superoxide dismutase levels in CoCl<sub>2</sub> and CdCl<sub>2</sub> treated cells* - Mammalian cells generate ROS as a result of several different metabolic processes and have evolved a variety of mechanisms for the efficient removal of these harmful species (15). For example, superoxide is generated as a by-product of ETC reactions due to incomplete electron transfer and is rapidly removed from the cellular space by superoxide dismutases (SODs), which convert the superoxide into oxygen and hydrogen peroxides (16). To determine if cobalt or cadmium altered SOD expression, the mRNA levels of SOD1 and SOD2 were analyzed by qRT-PCR. In agreement with our previously published report, SOD1 and SOD2 mRNA levels were significantly lower in the untreated HIF1 $\alpha$  *-/-* cells compared to WT cells (Figure 29A and B). CoCl<sub>2</sub> treatment did not change the expression of SOD1 and SOD2 in wild type or HIF1 $\alpha$  *-/-* cells. Although not statistically significant, CdCl<sub>2</sub> treatment caused a marginal reduction in SOD1 and SOD2 mRNA levels in HIF1 $\alpha$  *-/-* cells. To determine if these changes in mRNA expression correlated with changes in SOD protein levels, SOD1 and SOD2 were analyzed by western blot analysis. In agreement with the mRNA data, SOD1 protein levels were lower in the HIF1 $\alpha$  *-/-* control cells compared to wild type cells (Figure 29A). Metal exposure did not alter the levels of SOD1 in the wild type whereas cobalt exposure lead to increase in SOD1 protein levels in HIF1 $\alpha$  *-/-* cells (Figure 29C). In contrast, SOD2 protein levels were higher in the HIF1 $\alpha$  *-/-* cells compared to WT cells and CdCl<sub>2</sub> treatment caused a reduction in SOD2 protein levels. Finally, total SOD and SOD2 activity were determined and SOD1 activity was deduced by subtracting the latter from the former value. The

**Figure 29. Expression and activity of superoxide dismutases**

Transcript levels of SOD1 (A) and SOD2 (B) were determined using qRT-PCR in wild type (WT, white bars) and HIF1 $\alpha$  -/- cells (black bars) as described in methods section. Each value was normalized to the control level in the corresponding cell line. Cells were left untreated (CTRL) or treated with 150 $\mu$ M CoCl<sub>2</sub> (Co<sup>2+</sup>) or 5 $\mu$ M CdCl<sub>2</sub> (Cd<sup>2+</sup>) for 24 hours. C. Protein levels of both SOD1 (Top Upper panel) and SOD2 (Bottom Upper panel) were determined by Western blotting in wild type (WT) and HIF1 $\alpha$  -/- cells.  $\beta$ -actin levels (Top and Bottom lower panels) were used a loading control. Cells were treated as in A and B. (D) SOD1 enzyme activity in wild type (WT, white bars) and HIF1 $\alpha$  -/- (black bars) cells were determined as described in the methods. Cells were treated as in A and B. \*, significant compared to untreated cells within the cell type, p<0.05 n=4. #, significant compared to wild type cells, p<0.05, n=4.



results show that SOD1 activity is consistently lower in all HIF1 $\alpha$  *-/-* cell treatments compared to WT cells (Figure 29D). These results suggest that HIF1 $\alpha$  *-/-* cells have a reduced capacity to cope with superoxide stress compared to their WT counterparts and that cadmium exposure alters the SOD expression profile and activity in these null cells.

*Glutathione concentration in cells treated with CoCl<sub>2</sub> and CdCl<sub>2</sub>* – Glutathione plays a critical role in various detoxification reactions within the cell by acting as a reducing agent (17, 18). Cadmium is known to deplete the cellular glutathione pool by covalently binding to its sulfhydryl groups and compromises the cell's ability to protect against oxidative stress (12). To determine if metal exposure can alter the glutathione pool within the WT or HIF1 $\alpha$  *-/-* cells, total cellular glutathione was determined by a spectrophotometric assay (19). In contrast to the SOD activity, HIF1 $\alpha$  *-/-* cells showed higher total glutathione levels under control conditions compared to WT cells (Figure 30). Both cell types showed an increase in total glutathione following metal exposure and the absolute levels remained higher in the HIF1 $\alpha$  *-/-* cells under these conditions. These results suggest that HIF1 $\alpha$  modulates a cell's ability to regulate cellular glutathione

## **Discussion**

Divalent metal ions play a critical role in various cellular processes in all living things (1). Metals such as iron, manganese, magnesium, zinc, copper and cobalt are essential elements because of their critical role in the activity of various

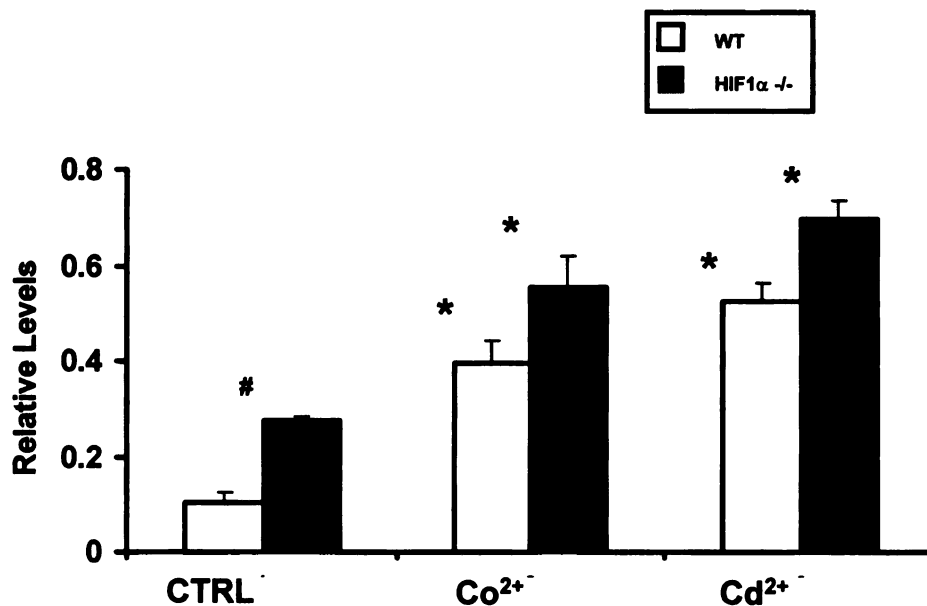


**Figure 30. Cellular Glutathione levels under CoCl<sub>2</sub> and CdCl<sub>2</sub> treatments**

**A.** Total cellular glutathione levels in wild type (WT, white bars) and HIF1 $\alpha$  -/- (black bars) cells were determined as described in the methods. Cells were left untreated (CTRL), with 150 $\mu$ M CoCl<sub>2</sub> (Co<sup>2+</sup>) or 5 $\mu$ M CdCl<sub>2</sub> (Cd<sup>2+</sup>) for 24 hours. \*, significant compared to respective controls, p<0.05, n=4. #, significant compared to wild type cells, p<0.05, n=4.

enzymes and metalloproteins (20). However, overabundance of metals can lead to imbalances in cellular processes due to their ability to form intra-molecular interactions and generate reactive intermediates (21). These cellular imbalances can lead to downstream effects and compromise a cell's ability to cope with oxidative stress. Hypoxia is a form of oxidative stress and the cellular response to decreases in oxygen availability are predominantly regulated by HIF1 $\alpha$ .

In this study we investigated the effect of two divalent metals, cobalt and cadmium, on their ability to interfere with the HIF1 $\alpha$  pathway. The results demonstrate that HIF1 $\alpha$  -/- cells are more sensitive to cadmium-induced toxicity. This is in contrast to the cobalt-induced toxicity, which is more toxic to wild type MEFs. Presumably, this difference is due, in part, to the two metal's ability to activate of HIF1 $\alpha$  pathway aberrantly (5). Cobalt is capable of stabilizing HIF1 $\alpha$  and promotes HIF1-mediated signaling; however, cadmium treatment does not cause HIF1 $\alpha$  stabilization and was unable to drive the expression of hypoxia-regulated genes. It was reported that cadmium treatment can cause a reduction in HIF1 $\alpha$  protein stabilized under hypoxia in 293T cells (6). This is in contrast to what was observed in MEFs, as cadmium was unable to inhibit CoCl<sub>2</sub>-induced HIF1 $\alpha$  stabilization. This difference is most likely due to cell specific factors and the differences in "hypoxia" treatment.

The aberrant activation of HIF1 $\alpha$  signaling by cobalt leads to increased expression of various adaptive and cell death promoting factors in the wild type

cells which are absent under cadmium exposure. For example, the pro-cell death factor BNip3 was induced only in wild type cells following cobalt exposure and this results in a caspase-independent necrotic cell death (5, 22). Under cadmium exposure, wild type and HIF1 $\alpha$   $-/-$  cells undergo apoptosis characterized by caspase activation and chromatin condensation but independent of BNip3 expression. Interestingly, cadmium-induced changes in caspase-3 activity and nuclear condensation were more pronounced in the HIF1 $\alpha$   $-/-$  cells. The experiments using shBNip3 clones showed that BNip3 activation is a major factor in the increased cell death under cobalt treatment in wild type cells. In contrast, BNip3 does not play any role in mediating cadmium induced cell death (Figure 27E). However, cadmium has been shown to modulate the expression of pro-apoptotic bax and cell cycle regulator p53 proteins in a variety of cell lines including alveolar type 2 cells promoting apoptotic cell death. The role these proteins play in MEFs is currently under investigation (23).

Another important characteristic of cadmium exposure was increased ROS levels in the HIF1 $\alpha$   $-/-$  cells compared to wild type cells. Redox active metals such as iron, cobalt and nickel are thought to produce ROS through Fenton-like reactions, while redox inactive metals such as mercury and cadmium are thought to deplete cellular sulfhydryl antioxidant reserves and interfere with cellular antioxidant enzymes such as glutathione transferases and glutathione peroxidases, leading to oxidative stress (12, 24). Although cobalt is a more direct ROS producer

compared to cadmium, under these experiments there was much higher ROS levels following cadmium treatment compared to wild type cells. This is consistent with earlier reports that suggests the need for a much higher dose of  $\text{CoCl}_2$  to generate any significant ROS generation (25). The most intriguing observation was that  $\text{HIF1}\alpha$   $-/-$  cells had a much higher level of ROS in the untreated cells compared to the wild type cells (Figure 28B). Similar results were observed by another group in MEF cells where they found increased production of  $\text{H}_2\text{O}_2$  in  $\text{HIF1}\alpha$   $-/-$  cells compared to wild type cells (26). Their data suggests that  $\text{HIF1}\alpha$   $-/-$  cells have lower levels of pyruvate dehydrogenase kinase1 (PDK1), a key inhibitory enzyme for the pyruvate dehydrogenase complex. This complex regulates the ability of pyruvate to enter the mitochondria, and the authors argue that increased carbon flux through the tricarboxylic acid cycle (TCA cycle) and subsequent electron flow through ETC in  $\text{HIF1}\alpha$   $-/-$  cells leads to increased oxidative stress. Our data also suggest that the most effective method to counter cadmium toxicity is to increase the glutathione reserves by treating with N-acetyl cysteine (NAC), a precursor for glutathione. This is consistent with many other studies (11, 13). NAC also marginally protected against  $\text{CoCl}_2$  mediated toxicity in both cell types. NAC is a well known cobalt chelator and the protection it offers against cobalt may primarily be due to the effective decrease in functional cobalt within the cell (27).

Oxidative stress can be a result of reduced elimination of reactive species. We have earlier reported that  $\text{HIF1}\alpha$   $-/-$  cells have a lower level of SOD1 and SOD2

mRNA compared to wild type cells (28)( Figure 29A, B). Overall levels of SOD1 protein and activity were also low in the HIF1 $\alpha$  -/- cells compared to their wild type counterparts. This might be a major factor in the increased oxidative stress in basal HIF1 $\alpha$  -/- cells and cadmium treatment might further increase the oxidative stress. The basal level of SOD1 is transcriptionally regulated by the binding of C/EBP $\alpha$ , SP1, EGR1 and WT1 proteins (29). YY1, a protein that binds to the upstream negative response element of SOD1 promoter, negatively regulates its expression (30). It is not known if any of these proteins are influenced by HIF1 $\alpha$  protein. The protein levels of the major mitochondrial SOD, SOD2 (Mn-SOD), were higher in the HIF1 $\alpha$  -/- cells, but activity levels were not significantly different compared to wild type cells.

Cellular glutathione pool shows a marked increase in wild type and HIF1 $\alpha$  -/- cells under CoCl<sub>2</sub> and CdCl<sub>2</sub> treatments. The higher glutathione levels in the HIF1 $\alpha$  -/- cells compared to wild type cells in all treatments studied may suggest an increased demand for glutathione for a cell under oxidative stress or an inability to utilize the available pool (Figure 30). We have shown earlier that mRNA levels of two major mitochondrial xenobiotic enzymes, GST $\mu$ 1 and GST $\alpha$ 1, are significantly lower in the HIF1 $\alpha$  -/- cells compared to wild type cells (28, 31)(data not shown). A reduction in the levels and activity of glutathione utilizing enzymes may result in an increased cellular glutathione pool. Also it is not known how much of the total glutathione pool is in the reduced form that is required for conjugation reactions.

We have performed a comparative analysis of the effect of two divalent metal ions cobalt and cadmium on HIF1 $\alpha$  signaling pathway. Taken together, our results suggest that cobalt-induced cell damage is promoted through HIF1 $\alpha$  stabilization and subsequent transcriptional regulation where, cadmium-induced cytotoxicity is due to ROS generation and the compromised nature of the ROS scavenging system in the HIF1 $\alpha$   $-/-$  cells. We show that HIF1 $\alpha$  plays a protective role against cadmium exposure putatively by its ability to maintain the activity of cellular antioxidant capacity whereas aberrant and constitutive activation of hypoxic signaling under cobalt exposure leads to cytotoxic effects by the activity of pro-cell death factors. This study points to the significant role played by HIF1 $\alpha$  in the presence of oxygen and its role in maintaining cellular homeostasis.

### **Acknowledgements**

We would like to thank Dr. Louis King of the MSU flow cytometry facility for help with the ROS detection procedures, Dr. KangAe Lee for help with the lentiviral infection procedures and Dr. Randall Johnson, UCSD for providing us with the wild type and HIF1 $\alpha$   $-/-$  MEF cell lines.

## References

1. Glusker, J. P. Structural aspects of metal liganding to functional groups in proteins. *Adv Protein Chem*, 42: 1-76, 1991.
2. Nelson, N. Metal ion transporters and homeostasis. *Embo J*, 18: 4361-4371, 1999.
3. Maxwell, P. H., Wiesener, M. S., Chang, G. W., Clifford, S. C., Vaux, E. C., Cockman, M. E., Wykoff, C. C., Pugh, C. W., Maher, E. R., and Ratcliffe, P. J. The tumour suppressor protein VHL targets hypoxia-inducible factors for oxygen-dependent proteolysis [see comments]. *Nature*, 399: 271-275, 1999.
4. Lowry, O. H., Rosebrough, N. J., Farr, A. L., and Randall, R. J. Protein measurement with the Folin phenol reagent. *J Biol Chem*, 193: 265-275, 1951.
5. Vengellur, A. and LaPres, J. J. The Role of Hypoxia Inducible Factor 1{alpha} in Cobalt Chloride Induced Cell Death in Mouse Embryonic Fibroblasts. *Toxicol. Sci.*, 82: 638-646, 2004.
6. Chun, Y. S., Choi, E., Kim, G. T., Choi, H., Kim, C. H., Lee, M. J., Kim, M. S., and Park, J. W. Cadmium blocks hypoxia-inducible factor (HIF)-1-mediated response to hypoxia by stimulating the proteasome-dependent degradation of HIF-1alpha. *European Journal of Biochemistry*, 267: 4198-4204, 2000.
7. Sowter, H. M., Ratcliffe, P. J., Watson, P., Greenberg, A. H., and Harris, A. L. HIF-1-dependent regulation of hypoxic induction of the cell death factors BNIP3 and NIX in human tumors. *Cancer Res*, 61: 6669-6673., 2001.
8. Kubasiak, L. A., Hernandez, O. M., Bishopric, N. H., and Webster, K. A. Hypoxia and acidosis activate cardiac myocyte death through the Bcl-2 family protein BNIP3. *Proc Natl Acad Sci USA*, 99: 12825-12830, 2002.
9. Waisberg, M., Joseph, P., Hale, B., and Beyersmann, D. Molecular and cellular mechanisms of cadmium carcinogenesis. *Toxicology*, 192: 95-117, 2003.
10. Leonard, S., Gannett, P. M., Rojanasakul, Y., Schwegler-Berry, D., Castranova, V., Vallyathan, V., and Shi, X. Cobalt-mediated generation of reactive oxygen species and its possible mechanism. *J Inorg Biochem*, 70: 239-244, 1998.

11. Im, J. Y., Paik, S. G., and Han, P. L. Cadmium-induced astroglial death proceeds via glutathione depletion. *J Neurosci Res*, **83**: 301-308, 2006.
12. Valko, M., Morris, H., and Cronin, M. T. Metals, toxicity and oxidative stress. *Curr Med Chem*, **12**: 1161-1208, 2005.
13. Shaikh, Z. A., Vu, T. T., and Zaman, K. Oxidative stress as a mechanism of chronic cadmium-induced hepatotoxicity and renal toxicity and protection by antioxidants. *Toxicol Appl Pharmacol*, **154**: 256-263., 1999.
14. Kukielka, E. and Cederbaum, A. I. NADPH- and NADH-dependent oxygen radical generation by rat liver nuclei in the presence of redox cycling agents and iron. *Arch Biochem Biophys*, **283**: 326-333, 1990.
15. Sies, H. Strategies of antioxidant defense. *Eur J Biochem*, **215**: 213-219, 1993.
16. Jezek, P. and Hlavata, L. Mitochondria in homeostasis of reactive oxygen species in cell, tissues, and organism. *Int J Biochem Cell Biol*, **37**: 2478-2503, 2005.
17. Pastore, A., Federici, G., Bertini, E., and Piemonte, F. Analysis of glutathione: implication in redox and detoxification. *Clin Chim Acta*, **333**: 19-39, 2003.
18. Rahman, Q., Abidi, P., Afaq, F., Schiffmann, D., Mossman, B. T., Kamp, D. W., and Athar, M. Glutathione redox system in oxidative lung injury. *Crit Rev Toxicol*, **29**: 543-568, 1999.
19. Baker, M. A., Cerniglia, G. J., and Zaman, A. Microtiter plate assay for the measurement of glutathione and glutathione disulfide in large numbers of biological samples. *Anal Biochem*, **190**: 360-365, 1990.
20. Lehninger, A. L. Role of metal ions in enzyme systems. *Physiol Rev*, **30**: 393-429, 1950.
21. Stohs, S. J. and Bagchi, D. Oxidative mechanisms in the toxicity of metal ions. *Free Radic Biol Med*, **18**: 321-336, 1995.
22. Vande Velde, C., Cizeau, J., Dubik, D., Alimonti, J., Brown, T., Israels, S., Hakem, R., and Greenberg, A. H. BNIP3 and genetic control of necrosis-like cell death through the mitochondrial permeability transition pore. *Mol Cell Biol*, **20**: 5454-5468, 2000.
23. Lag, M., Westly, S., Lerstad, T., Bjornsrud, C., Refsnes, M., and Schwarze, P. E. Cadmium-induced apoptosis of primary epithelial lung cells: involvement of Bax and p53, but not of oxidative stress. *Cell Biol Toxicol*, **18**: 29-42, 2002.

24. Ercal, N., Gurer-Orhan, H., and Aykin-Burns, N. Toxic metals and oxidative stress part I: mechanisms involved in metal-induced oxidative damage. *Curr Top Med Chem*, 1: 529-539, 2001.
25. Kotake-Nara, E., Takizawa, S., Quan, J., Wang, H., and Saida, K. Cobalt chloride induces neurite outgrowth in rat pheochromocytoma PC-12 cells through regulation of endothelin-2/vasoactive intestinal contractor. *J Neurosci Res*, 81: 563-571, 2005.
26. Kim, J. W., Tchernyshyov, I., Semenza, G. L., and Dang, C. V. HIF-1-mediated expression of pyruvate dehydrogenase kinase: a metabolic switch required for cellular adaptation to hypoxia. *Cell Metab*, 3: 177-185, 2006.
27. Llobet, J. M., Domingo, J. L., and Corbella, J. Comparison of antidotal efficacy of chelating agents upon acute toxicity of Co(II) in mice. *Research Communications in Chemical Pathology & Pharmacology*, 50: 305-308, 1985.
28. Vengellur, A., Woods, B. G., Ryan, H. E., Johnson, R. S., and LaPres, J. J. Gene expression profiling of the hypoxia signaling pathway in hypoxia inducible factor 1 null mouse embryonic fibroblasts. *Gene Expression*, 11: 181-197, 2003.
29. Chang, M. S., Yoo, H. Y., and Rho, H. M. Transcriptional regulation and environmental induction of gene encoding copper- and zinc-containing superoxide dismutase. *Methods Enzymol*, 349: 293-305, 2002.
30. Cho, J. S., Chang, M. S., and Rho, H. M. Transcriptional activation of the human Cu/Zn superoxide dismutase gene by 2,3,7,8-tetrachlorodibenzo-p-dioxin through the xenobiotic-responsive element. *Mol Genet Genomics*, 266: 133-141, 2001.
31. Raza, H., Robin, M. A., Fang, J. K., and Avadhani, N. G. Multiple isoforms of mitochondrial glutathione S-transferases and their differential induction under oxidative stress. *Biochem J*, 366: 45-55, 2002.

## **SUMMARY AND DISCUSSION**

The present studies were focused on understanding the relationship between environmental metals, such as cobalt and cadmium, and biological pathways that are essential in sustaining life. The prevalence of metals in our environment is a growing concern with the increase of “disposable” electronics, the EPA approved use of bio-metal-containing solids and industrial waste in the production of fertilizers and the industrial production necessary to expand the global economy. The wholesale release of these metals into the environment can lead to their large scale accumulation in soil and subsequently in the food chain. Therefore, understanding the toxicity of these metals is a growing environmental issue. Characterizing this toxicity is dependent upon comprehension of the basic biology involved in their signaling and this type of knowledge is critical if we are to understand the adverse effects metals have on human health. An attempt was made to understand the molecular mechanism of the metal induced toxicity using mouse fibroblasts as a model system.

Although certain metals are essential nutrients, excessive exposure to a wide range of metals can lead to a variety of toxic endpoints. Metals such as cobalt, nickel, and cadmium can interfere with several important pathways, one of which is the hypoxia signaling cascade. The hypoxia signaling pathway is activated under reduced levels of oxygen and helps the organism to maintain energy levels. Improper regulation of this pathway is involved in diseases such as

cardiac ischemia, stroke, and cancer. Cobalt and nickel exposure can mimic hypoxia by stabilizing HIF1 $\alpha$  protein. Global gene expression profiling using oligonucleotide array as described in chapter 2 showed that cobalt, hypoxia, and desferoxamine treatments resulted in similar patterns of gene expression in Hep3B cells. This suggested that a common signaling system was being induced under these conditions and we hypothesized that certain divalent metals might induce toxicity in cells by unnaturally activating HIF1 $\alpha$  signaling.

We were fortunate that engineered mouse embryonic fibroblasts (MEFs) were available to perform these experiments. Two MEF cell strains were used, a wild type (WT) cell that was genotypically normal and a HIF1 $\alpha$   $-/-$  cell that was identical to the WT cells except they lacked a functional HIF1 $\alpha$  locus. These cells enabled us to determine the role of HIF1 $\alpha$  in mediating metal-induced toxicity. As predicted, cobalt and hypoxia induced similar global changes in gene expression in the wild type cells and this overlap was not observed in the HIF1 $\alpha$  null cells. These results suggest that cobalt and hypoxia are working in a similar manner as observed in the Hep3B cells and indicated that HIF1 $\alpha$  is the major HIF $\alpha$  isoform in MEFs. Cobalt exposure induced the HIF1 $\alpha$ -dependent expression of genes involved in adaptive response, including glucose transport, glycolysis, angiogenesis, and erythropoiesis. There were also changes in non-adaptive genes, such as BNip3, a BH3 domain containing pro-cell death factor involved in apoptosis and necrosis in various cell types. BNip3 protein levels showed HIF1 $\alpha$ -, dose- and time-dependent increase upon cobalt exposure. Cell

morphology under cobalt exposure also displayed chromatin condensation in the absence of caspase-3 activation suggesting this increased expression of Bnip3 had functional consequence. Finally, cell lines that expressed shRNA targeting Bnip3 were partially protected against cobalt-induced damage and behaved like HIF1 $\alpha$  -/- following metal insult. This was a clear indication that metals like cobalt that are capable of aberrantly stabilizing HIF1 $\alpha$  and activating the hypoxic signaling cascade, can result in cellular damage through direct transcriptional regulation of cell death promoting factors.

The *in vivo* effect of cobalt exposure during cobalt treatment of anemia is characterized by polycythemia, an over-production of red blood cells. *In vivo*, the production of red blood cells is primarily regulated by erythropoietin (EPO), a growth factor produced by the kidney and liver and known HIF1 target gene. In the Hep3B cell culture model, cobalt was capable of increasing EPO expression and it is thought cobalt exposure, *in vivo*, would lead to a similar aberrant EPO expression, leading to the observed polycythemia. Gene expression under cobalt exposure in fibroblasts also suggests a potential role of various genes in mediating other *in vivo* effects. For example, chronic cobalt exposure through inhalation results in many pathological conditions, such as asthma, alveolitis and pulmonary fibrosis. Bnip3, a cobalt induced gene is known to be associated with tissue necrosis and might play a role in tissue necrosis under cobalt exposure eventually leading to fibrosis. The various genes expressed under cobalt exposure might also be playing a role in other symptoms such as allergic dermatitis and cardiomyopathy.

The fact that loss of HIF1 $\alpha$  protects against cobalt-induced toxicity establishes a role for the hypoxia signaling cascade in the cytotoxicity of hypoxic-mimicking metals, but what part, if any, does it play in the toxicity of divalent metals that do not stabilize HIF1 $\alpha$ , such as cadmium? The results were very different; HIF1 $\alpha$  null cells were more susceptible to cadmium-induced damage than their wild type counterparts. HIF1 $\alpha$  null cells exposed to cadmium exhibited chromatin condensation and caspase-3 activation characteristic of apoptotic cell death but lacked the expression of BNip3. Manipulation of Bnip3 levels by shRNA also did not affect the toxicity of cadmium. HIF1 $\alpha$  protein is thought to be degraded under normoxia without mediating any transcriptional activity. But it is clear that HIF1 $\alpha$  protein directly or indirectly affects cellular processes that lead to protection against cadmium in wild type cells. These results suggest that the HIF1 $\alpha$  protein has cellular functions under normoxia, either non-transcriptional or transcriptional.

Metals, by their nature can generate reactive intermediates causing oxidative stress in cells. Cobalt is a Fenton metal that produces hydroxyl radicals by reacting with hydrogen peroxide and superoxide. In contrast, cadmium depletes cellular glutathione levels interfering with the activity of various cellular antioxidant enzyme systems and generating oxidative stress indirectly. Cellular ROS measurements indicated that ROS levels are greater under cadmium treatment compared to cobalt exposure. Again HIF1 $\alpha$  null cells had much higher ROS levels under cadmium exposure compared to wild type cells suggesting a

possible explanation for increased cytotoxicity in those cells. Interestingly, there was a higher basal ROS levels in the HIF1 $\alpha$  null cells compared to wild type cells. There are two possible reasons for such an increase in ROS levels: increased ROS generation or decreased ROS scavenging activity. Recent data and results presented in this thesis suggest that HIF1 $\alpha$  regulates PDK1, the kinase responsible for regulating pyruvate's fate within the cell. It is possible that the loss of HIF1 $\alpha$  in the null cells results in increased pyruvate flux through TCA cycle due to dysregulation of PDK1, even under normoxia. This would result in more carbon moving into the mitochondria and the TCA cycle and lead to an increase in the activity of the electron transport chains. The increased ETC flux would tax the normal ROS maintenance machinery resulting in the change in basal levels in ROS observed in the HIF1 $\alpha$   $-/-$  cell. In addition, this increased oxidative stress would tax the cells in such a way that a metal capable of promoting further oxidative damage through direct competition of these same systems (e.g. glutathione), such as cadmium, would be more cytotoxic under these conditions.

Our data suggest another possible explanation for the increased ROS levels in the HIF1 $\alpha$  null cells. We observed differences in ROS scavenging enzymes, SOD1 and SOD2, and the antioxidant glutathione between HIF1 $\alpha$   $-/-$  and wild type cells. For example, SOD1, the major cytosolic dismutase, levels were low in cadmium treated HIF1 $\alpha$  null cells potentially compromising their ability to cope with the greater oxidative stress. These observations point to a potential role of

HIF1 $\alpha$  in the maintenance of cellular redox status. This maintenance happens in the absence of cellular stress and again suggests that HIF1 $\alpha$  has a role in cellular physiology outside of responding to hypoxic conditions. In fact, the results suggest that this “normoxic” role for HIF1 $\alpha$  in cellular homeostasis might be equally important to its role in hypoxia adaptation. The maintenance and possible surveillance role of HIF1 $\alpha$  for the redox state of the cell might actually establish its basal activity. For example, if ROS play a direct role in HIF1 $\alpha$  stability as has been proposed by various research groups, then the ability of HIF1 $\alpha$  to directly influence the basal expression level of genes, such as SOD1, which in turn controls the ROS levels within the cell would create a feedback circle to regulate oxidative stress.

Divalent metals, especially cobalt and cadmium are an important environmental contaminants and their presence will only increase over the coming years. Our dependence on disposable electronics and the ever increasing industrialization of our world will ensure that metals will become prominent environmental contaminants. Understanding the cellular and physiological response to these metals will help our understanding of the toxicological concerns that they pose. The research presented in this thesis also has implications outside of the field of toxicology and the environment. As mentioned above, hypoxia signaling is critical for several pathological conditions, as well as normal development and immune function. In addition, the cascade has now become a viable target for cancer chemotherapy due to its role tumorigenesis. We hope that the present

study will create a foundation for the analysis of this critical signaling pathway and will allow us to relate downstream effects to HIF1 $\alpha$  and other proteins involved in the hypoxia signaling network. This research will establish a basis for a systems biology approach to the study of hypoxia and its role in normal and stress mediated biology.

MICHIGAN STATE UNIVERSITY LIBRARIES



3 1293 02956 4170